(12) INTERNATIONAL APPLICATION PUBLISHED UNDER THE PATENT COOPERATION TREATY (PCT)

(19) World Intellectual Property Organization
International Bureau

(43) International Publication Date
7 April 2011 (07.04.2011)

PCT

(10) International Publication Number
WO 2011/039734 A2

(51) International Patent Classification: Not classified

(21) International Application Number:
PCT/IB2010/054470

(22) International Filing Date:
4 October 2010 (04.10.2010)

(25) Filing Language: English

(26) Publication Language: English

(30) Priority Data:
61/247,967 2 October 2009 (02.10.2009) US

(72) Inventor; and
(71) Applicant : **MEDICO, Enzo** [IT/IT]; Via Servais 200/E20, I-10146 Torino (IT).

(72) Inventors: **ISELLA, Claudio**; Via Borgo Dora, 38, I-10152 Torino (IT). **MIRA, Alessia**; Via Verbano, 2, I-20127 Ispra (VA) (IT).

(81) Designated States *(unless otherwise indicated, for every kind of national protection available)*: AE, AG, AL, AM, AO, AT, AU, AZ, BA, BB, BG, BH, BR, BW, BY, BZ, CA, CH, CL, CN, CO, CR, CU, CZ, DE, DK, DM, DO, DZ, EC, EE, EG, ES, FI, GB, GD, GE, GH, GM, GT, HN, HR, HU, ID, IL, IN, IS, JP, KE, KG, KM, KN, KP, KR, KZ, LA, LC, LK, LR, LS, LT, LU, LY, MA, MD, ME, MG, MK, MN, MW, MX, MY, MZ, NA, NG, NI, NO, NZ, OM, PE, PG, PH, PL, PT, RO, RS, RU, SC, SD, SE, SG, SK, SL, SM, ST, SV, SY, TH, TJ, TM, TN, TR, TT, TZ, UA, UG, US, UZ, VC, VN, ZA, ZM, ZW.

(84) Designated States *(unless otherwise indicated, for every kind of regional protection available)*: ARIPO (BW, GH, GM, KE, LR, LS, MW, MZ, NA, SD, SL, SZ, TZ, UG, ZM, ZW), Eurasian (AM, AZ, BY, KG, KZ, MD, RU, TJ, TM), European (AL, AT, BE, BG, CH, CY, CZ, DE, DK, EE, ES, FI, FR, GB, GR, HR, HU, IE, IS, IT, LT, LU, LV, MC, MK, MT, NL, NO, PL, PT, RO, RS, SE, SI, SK, SM, TR), OAPI (BF, BJ, CF, CG, CI, CM, GA, GN, GQ, GW, ML, MR, NE, SN, TD, TG).

**Declarations under Rule 4.17**:

— *as to applicant's entitlement to apply for and be granted a patent (Rule 4.17(ii))*

— *as to the applicant's entitlement to claim the priority of the earlier application (Rule 4.17(iii))*

— *of inventorship (Rule 4.17(iv))*

**Published**:

— *without international search report and to be republished upon receipt of that report (Rule 48.2(g))*

WO 2011/039734 A2

(54) **Title**: USE OF GENES INVOLVED IN ANCHORAGE INDEPENDENCE FOR THE OPTIMIZATION OF DIAGNOSIS AND TREATMENT OF HUMAN CANCER

(57) **Abstract**: The present invention discloses identification of GAB2-driven processes and anchorage independence associated with diagnosis, prognosis, metastasis, metastatic relapse, metastatic potential and prediction of response to treatment of cancers. In particular, a GAB2-signature based on anchorage independence is identified which can serve to define processes relevant to progression and response to treatment of human cancers.

# USE OF GENES INVOLVED IN ANCHORAGE INDEPENDENCE FOR THE OPTIMIZATION OF DIAGNOSIS AND TREATMENT OF HUMAN CANCER

## Related Application

This application takes priority from US Provisional application USSN 61/247,967 filed 02-OCT-2009, entitled "Use of genes involved in anchorage independence for the optimization of diagnosis and treatment of human cancer", and is incorporated herein in its entirety.

## Field of the Invention

The present invention is related to identification of GAB2-driven processes and anchorage independence associated with diagnosis, prognosis, metastasis, metastatic relapse, metastatic potential and prediction of response to treatment of cancers. In particular, a GAB2-signature based on anchorage independence is identified which can serve to define processes relevant to progression and response to treatment of human cancers.

## Background of the Invention

Normal epithelial cells integrate signals from soluble ligands, like growth factors (GFs), cytokines and hormones, with signals derived from the binding of transmembrane integrins to the extracellular matrix (ECM), to ensure that they only proliferate in the 'correct' social context (Berrier and Yamada 2007, J Cell Physiol, 213, 565-573). Joint integrin/GF signaling is required for cell proliferation and for optimal cell survival: cell adhesion enhances GF-dependent responses, like cell proliferation, migration and/or protection from apoptosis (Miranti and Brugge 2002, Nat Cell Biol, 4, E83-E90). Conversely, cell detachment results in cellular desensitization to GF receptor signaling (Schwartz and Baron 1999, Curr Opin Cell Biol, 11, 197-202). Moreover, signals evoked by integrins and GFs are widely integrated at the cellular level, since both impinge on an overlapping set of cytoplasmic signaling pathways (Berrier and Yamada 2007, J Cell Physiol, 213, 565-573). Dependence on this reciprocal cross-talk is progressively lost by transformed cells during formation and spread of tumors (Guo and Giancotti 2004, Nat Rev Mol Cell Biol, 5, 816-826), and the acquisition of anchorage-independence is considered to be a crucial step during cancer progression towards invasion and metastasis

(Tsatsanis and Spandidos 2004, Ann N Y Acad Sci, 1028, 168-175). Therefore, identification of genes or proteins promoting this step could provide novel targets or rationales for anti-cancer therapy. Among the possible ways for a genome-wide functional survey aimed at this scope are screenings based on the gain-of-function approach. Such screenings proved extremely valuable in the identification of genes involved in key cancer-related processes, like neoplastic transformation, resistance to apoptosis, or escape from senescence (Kitamura et al. 2003, Exp Hematol, 31, 1007-1014). As a screening model, we chose MCF10A cells, a spontaneously immortalized human breast line (Soule et al. 1990, Cancer Res, 50, 6075-6086) that relies on both GFs and anchorage to proliferate. When these cells are cultured in the absence of anchorage, for instance on polyhema-coated plates, they undergo growth arrest and detachment-induced apoptosis, also known as anoikis (Reginato et al. 2003). It was previously shown that the low transforming potential of these cells renders them well-suited to monitor the effects of genes conferring oncogenic properties (Debnath and Brugge 2005, Nat Rev Cancer, 5, 675-688). Therefore, MCF10A cells represent an ideal model to screen for genes conferring anchorage-independence. For the screening we exploited a novel approach, named "Xenoarray analysis", based on transduction of mammalian cells of a given species with an expression library from another species, followed by one-shot quantitative tracing with DNA microarrays of library-derived transcripts before and after a selective stress, to disclose genes conferring resistance to the selection (Martelli et al. 2008, BMC Genomics, 9, 254). After transduction with a mouse testis retroviral expression library, MCF10A cells were selected for growth in suspension and murine microarrays were used to compare signal intensities for the exogenous cDNAs before and after selection, to detect the enriched ones. Independent infection-selection experiments highlighted significant and reproducible enrichment for murine Gab2-encoding transcripts, suggesting a role of this gene in anchorage-independent growth. Through biochemical studies, cell-based assays and genomic analysis we found that Gab2 promotes anchorage-independent growth of normal and neoplastic cells, and drives a transcriptional program linked to metastatic progression of breast cancer.

**Summary of the invention:**

The invention provides identification of GAB2-driven processes and anchorage independence associated with diagnosis, prognosis, metastasis, metastatic relapse,

metastatic potential and prediction of response to treatment of cancers. Furthermore, a GAB2-signature based on anchorage independence is identified which can serve to define processes relevant to progression and response to treatment of human cancers.

In one aspect the invention provides a method for diagnosing or prognosing cancer in subjects comprising detecting expression of GAB2 and/or of its transcriptional target genes in the tumor tissue and/or in tumor cells isolated from the subject.
The method provides GAB2-signature genes of the invention useful for diagnosis or prognosis of any human cancer, especially breast cancer and myeloma, comprising detecting in the tumor tissue and/or in tumor cells isolated from the subject expression of at least two of GAB2-signature genes listed in Table 1, 2, 3, 4 or 5. The two genes can be selected from a single independent list (single table) or across the tables (more than one table).

In another aspect the invention provides a method for predicting metastasis or metastatic relapse or metastatic potential or response to treatment in cancer patients comprising detecting the expression of GAB2 and or its transcriptional target genes in the tumor tissue and/or in tumor cells isolated from the subject. The method provides GAB2-signature genes of the invention useful for diagnosis or prognosis of any human cancer, especially breast cancer and myeloma, comprising detecting in the tumor tissue and/or in tumor cells isolated from the subject expression of at least two of GAB2-signature genes listed in Table 1, 2, 3, 4 or 5. The two genes can be selected from a single independent list (single table) or across the tables (more than one table). The cancer treatment as provided herein encompasses all know cancer treatment including targeted drug therapy, chemotherapy, radiation therapy or a combination thereof.

In yet another aspect, the invention provides a method of treating a subject with cancer comprising the steps of:
a) obtaining blood or tissue sample from the subject with cancer;
b) screening said sample for the expression of a polypeptide encoded by a polynucleotide selected from a group consisting of GAB2-signature genes listed in Table 1, 2, 3, 4 and 5;
c) providing an antibody that reacts immunologically against said polypeptide; and
d) administering an effective amount of said antibody to the subject with cancer.

The invention also provides a method of treating a subject suffering from cancer comprising the steps of:

a) obtaining a sample of tissue from a subject suffering from cancer;

b) screening said sample for the expression of a polypeptide encoded by a polynucleotide selected from a group consisting of GAB2-signature genes listed in Table 1, 2, 3, 4 and 5;

c) providing an antisense DNA molecule that encodes an RNA molecule that binds to said polynucleotide;

d) providing said antisense DNA molecule in the form of a human vector containing appropriate regulatory elements for the production of said RNA molecule; and

e) administering an effective amount of said vector to the subject with cancer.

In another aspect, the invention provides a method of using *in vitro* anchorage independence model for deriving gene signature, the said signature comprising a set of genes associated with diagnosis, prognosis, metastasis and predicting response to treatment in cancer. The gene signature of the said method is GAB2-signature comprising at least two GAB2 and or its transcriptional target genes listed in Tables 1, 2, 3, 4 or 5. The two genes can be selected from a single independent list (single table) or across the tables (more than one table).

In yet another aspect of the invention, a method of predicting the grade of a tumor in a cancer patient, comprising detecting the expression of GAB2 and/or its transcriptional target genes in the tumor tissue and/or in tumor cells isolated from the subject is provided. This method encompasses detecting the expression of at least two of GAB2-signature genes listed in Table 1, 2, 3, 4 or 5. The two genes can be selected from a single independent list (single table) or across the tables (more than one table).

The invention also provides a GAB2-signature for diagnosing or prognosing human cancer, especially breast cancer or myeloma, in subjects comprising GAB2 and/or its transcriptional target genes in the tumor tissue and/or in tumor cells isolated from the subject as diagnostic or prognostic markers. The diagnosis or prognosis comprises detecting in the tumor tissue and/or in tumor cells isolated from the subject expression of at least two of GAB2-signature genes listed in Tables 1, 2, 3, 4 or 5. The two genes can

be selected from a single independent list (single table) or across the tables (more than one table).

In another aspect, the invention provides a GAB2-signature for predicting
metastasis; or
metastatic relapse; or
metastatic potential; or
response to treatment
in cancer patients including breast cancer and myeloma patients, comprising GAB2 and or its transcriptional target genes. The prediction of metastasis, metastatic relapse, metastatic potential or response to treatment is detected in tumor tissue and/or in tumor cells isolated from the patient expression of at least two of GAB2-signature genes listed in Tables 1, 2, 3, 4 or 5. The two genes can be selected from a single independent list (single table) or across the tables (more than one table). The cancer treatment as provided herein encompasses all know cancer treatment including targeted drug therapy, chemotherapy, radiation therapy or a combination thereof.

In yet another aspect, the invention provides an array comprising polynucleotides capable of specifically hybridizing to at least two genes listed in Table 1, 2, 3, 4 or 5.

The invention also encompasses kit comprising the array for diagnosing or prognosing cancer or predicting metastasis or metastatic relapse or metastatic potential of cancer cells in a subject by determining the expression of at least 2 genes listed in Table 1, 2, 3, 4 or 5. Furthermore, a kit for diagnosing or prognosing cancer cells or predicting metastasis or metastatic relapse or metastatic potential of cancer cells in a biological sample comprising a primer pair for amplifying a nucleic acid sequence selected from a group consisting of GAB2-signature genes listed in Table 1, 2, 3, 4 and 5 and containers for the primers is also provided.

In yet another aspect, a kit for diagnosing or prognosing cancer cells or predicting metastasis or metastatic relapse or metastatic potential of cancer cells in a biological sample comprising an oligonucleotide probe that binds under high stringency conditions to an isolated nucleic acid sequence selected from a group consisting of GAB2-signature

genes listed in Table 1, 2, 3, 4 and 5 and a container for the probe is also provided by the invention.

Furthermore, the invention provides a kit for diagnosing or prognosing cancer cells or predicting metastasis or metastatic relapse or metastatic potential of cancer cells in a biological sample comprising an antibody which binds immunologically to a protein having an amino acid sequence encoded by a polynucleotide selected from a group consisting of GAB2-signature genes listed in Table 1, 2, 3, 4 and 5 and a container for the probe.

**Brief Description of Drawings**

**Figure 1. Xenoarray analysis on MCF10A cells and acquisition of anchorage independence by library-transduced selected cells.**

(A) MTT growth assay on polyhema-selected populations after 48h and 72h in adhesion or suspension, as indicated. Cell growth is expressed as a ratio between library-transduced and GFP-transduced cells, after normalization to the amount of viable plated cells at day 0. The data represent the mean and standard error of triplicate values (Adhesion 48h $p<0.05$, Suspension 48h $p<0.01$, Suspension 72h $p<0.05$). (B) Soft agar assay on GFP- and library-transduced cells, unselected or selected on polyhema, as indicated. Phase-contrast images were captured by a BD Pathway microscopic station (BD biosciences) after 3 weeks in agar. (C) Dot plot of single colony sizes as calculated by the Attovision software (BD Biosciences, version 1.5) for the GFP-SEL and LIB-SEL populations grown in soft agar.

**Figure 2. Identification of enriched cDNAs in anchorage-independent, library-transduced MCF10A cells.**

(A) Real-time PCR validation of enriched transcripts in both selections. The y-axis represents the relative increase in abundance of the transcripts in selected cells compared to unselected cells. (B) Western blot analysis on GFP- and library-transduced cells before and after selection to detect Gab2 protein enrichment.

**Figure 3. Gab2 overexpression promotes anchorage-independent growth of**

**MCF10A cells.**

(A) Box-plot of an MTT growth assay on Mock- (M) or Gab2- (G) transduced MCF10A cells in adhesion or suspension, in the presence of complete medium or of starving medium (no EGF and 2% serum) for 48 hours. Cell vitality was normalized to the amount of cells in Mock-transduced, adherent cells in complete medium after 48 hours (CTRL) The data were obtained in triplicates, and t-test highlighted significant differences between G and M cells only in complete medium (* = $p<0.01$, ** = $p<0.0001$) (B) Dot plot of single colony sizes as calculated by the Attovision software (BD Biosciences, version 1.5) for the Mock and GAB2 cell populations grown in soft agar. (C) Flow cytometry analysis of apoptosis induction for Mock and Gab2-expressing MCF10A. Cell death was measured after 48h either in adhesion or suspension, by assessing the number of hypodiploid nuclei with the DNAcon3 kit. The percent of apoptotic cells is reported on the y-axis.

**Figure 4. Evaluation of the contribution of different signaling pathways to Gab2-mediated enhancement of cell growth.**

(A) Mock and GAB2-overexpressing (GAB2) MCF10A cells were incubated in adhesion (ADH) or suspension (SUSP) in the presence or absence of MEK inhibitor (PD98059, 40μM), PI3K inhibitor (LY294002, 50μM), Src inhibitor (PP2, 10μM), or JNK inhibitor (SP600125, 10μM). Cell vitality was assessed with the MTT assay after 24h from the treatment and the drug effect was expressed as percent growth inhibition (with respect to untreated cells). The data represent the mean and standard error of triplicate values from two independent experiments. (B) Boxplots of detailed analysis of the effects of Src inhibition by PP2 on cell growth in various conditions. Cell growth, measured by the MTT assay, is expressed as percent of untreated Mock, adherent cells. The data were obtained in triplicates, and t-test highlighted significant responses to PP2 in all cases except for mock cells in suspension (* = $p<0.05$, ** = $p<0.005$). (C) Western blot analysis on Mock and Gab2-expressing cells in adhesion or after 24h and 48h in suspension. Antibodies directed against the activated form of Src (phosphorylated at tyrosine 416) and Stat3 (phosphorylated at tyrosine 705), or total Src or Stat3 were used.

**Figure 5. Knock-down of endogenous Gab2 impairs MCF10A growth and anchorage-independent growth of human neoplastic cells.**

(A) MTT growth assay on wild-type MCF10A cells transduced with a scramble vector (CTRL) or a Gab2-shRNA in adhesion or suspension for 48h. Cell vitality was normalized to the amount of viable plated cells at time 0 and visualized independently for both cells by boxplots. The data were obtained in quintuplicate using two different GAB2-targeting shRNAs, and t-test highlighted significant differences between CTRL and GAB2-shRNA cells both in adhesion and suspension (* = $p<5x10^{-3}$, ** = $p<5x10^{-8}$). (B) MTT growth assay on MDA-MB-231 and MDA-MB-435 cells transduced with scramble vector (CTRL) or Gab2-shRNA in adhesion or suspension for 48h. Cell vitality was normalized to the amount of viable plated cells at time 0 and visualized independently for both cells by boxplots. The data were obtained in sextuplicate, and t-test highlighted modestly significant differences between CTRL and GAB2-shRNA cells in both MDA-MB-231 and MDA-MB-435 cells (* = $p<0.05$). (C) Soft agar growth of cells expressing Gab2 shRNA or scramble vector (CTRL). Phase-contrast images were captured by a BD Pathway microscopic station (BD biosciences) after 3 weeks in agar. (D) Western blot analysis of Src and Stat3 activation in control and GAB2 shRNA-transduced cells, as indicated.

**Figure 6. The GAB2-signature predicts breast cancer metastatic relapse.**

(A) Heatmap showing the expression of the two main gene functional modules in the NKI311 breast cancer dataset. The samples (columns) are ordered by decreasing GAB2-signature metastasis score (GAB2 MTS Score), which is graphically reported in the second row. The first row shows the occurrence of metastatic relapse within five year (white space = no relapse). The white vertical line crossing the heatmap indicates the 0 threshold value of metastasis score discriminating good and poor prognosis samples. White and black dots on the right highlight the genes annotated to the two functional modules, respectively downregulated and upregulated in poor prognosis samples. (B) Kaplan-Meier analysis of metastasis-free survival on a dataset of 198 breast cancer samples classified as good prognosis (green line) or poor prognosis (red line) by the GAB2-signature. (C) Kaplan-Meier analysis of disease-specific survival on a dataset of 236 breast cancer samples classified as good prognosis (GP) or poor prognosis (PP) by the GAB2-signature.

**Figure 7. The GAB2-signature is independent from existing clinical and genomic**

**breast cancer classifiers, and from estrogen receptor status.**

(A-F) Kaplan-Meier analysis on the 198-samples dataset subdivided in two prognostic subgroups (A,C,E = poor prognosis, B,D,F = good prognosis) by the Adjyvant!Online clinical score (A-B), the Veridex Index (C-D) and the Mammaprint classifier (E-F). Each subgroup is then further subdivided by the GAB2-signature in good prognosis (GP) or poor prognosis (PP) samples. (G-H) Kaplan-Meier analysis on the 198-samples dataset subdivided in ER-negative (G) and ER-positive (H) samples, then further subdivided by the GAB2-signature in good prognosis (GP) or poor prognosis (PP) samples.

**Figure 8. The GAB2-signature predicts prognosis in Estrogen Receptor-negative breast cancer.** Kaplan-Meier analysis of metastasis-free survival on a dataset of 175 Estrogen Receptor-negative breast cancer samples classified as good prognosis (GP) or poor prognosis (PP) by the GAB2-signature.

**Figure 9: The GAB2-signature predicts response of breast cancer to antineoplastic treatment.**

(A) Receptor-Operated Channel (ROC) analysis of the performance of the GAB2-signature Metastasis Score as a predictor of response to neoadjuvant treatment in the Hess dataset. AUC indicates the area under the Curve. (B) Dot plot analysis of the the GAB2-signature Metastasis score (x-axis) for the samples from patients showing pathological complete response (pCR) or residual disease (RD), as indicated.

**Figure 10. Microarrays and realtime PCR generate highly correlated diagnostic scores.** Dot plot showing the correlation between Metastasis Score calculated for 32 breast cancer samples from microarray data (x-axis) and from realtime PCR data (y-axis), using 15 genes of the GAB2 signature.

**Figure 11. The GAB2-signature is correlated to melanoma progression.** Heatmap showing Log2Ratio expression values for 83 Affymetrix probesets (rows) across tissue samples of different stages of melanoma progression (columns). The first row indicates the type of sample (from Normal Skin, black, to Metastatic Melanoma, white, as indicated). Samples have been subdivided, based on expression of the GAB2 genes, in four clusters of progressively increasing aggressiveness, from normal skin and benign nevi to metastatic melanoma.

**Detailed Description of the Invention**

The invention will now be described in detail in connection with certain preferred and optional embodiments, so that various aspects thereof may be more fully understood and appreciated.

**I. GAB2 is a key promoter of anchorage independence of human neoplastic cells**

***a. Gain-of-function screening for anchorage independence in MCF10A cells***

For the functional screening, MCF10A cells were transduced with a commercial mouse testis retroviral expression library (Stratagene) or with GFP as a control. To increase the screening robustness, infections were performed in duplicate (A and B), using an estimated multiplicity of infection of 1, to avoid multiple integrations in the same cell. To detect and quantify library-derived transcripts we performed Xenoarray analysis (Martelli et al. 2008, BMC Genomics, 9, 254), by extracting total RNA from the four cell populations and hybridizing the resulting cRNAs on murine expression arrays, to allow specific detection of library-derived transcripts of murine origin. Expression measurements obtained, for infections A and B, in GFP-transduced cells (x-axis) versus library-transduced cells were then compared. Both library-transduced populations clearly showed a consistent number of detectable murine transcripts (945 and 1125 probes in infection A and B, respectively, with a detection p-value <0.01). Conversely, very few probes (around 100) cross-hybridized to endogenous transcripts and were detected also in GFP-transduced cells. Based on our previous observations on Xenoarray analysis sensitivity (Martelli et al. 2008, BMC Genomics, 9, 254), we estimated that a selection-driven 20-fold enrichment of even a rare transcript, bringing it from 8 to 160 parts per million, should be enough to render it clearly detectable by Xenoarray analysis. A selective, anchorage-independence screening was then carried out by culturing GFP- or library-transduced MCF10A cells on polyhemacoated plates (polyhema does not allow the cells to attach to the substrate). The four transduced populations were each split in two sub-lines: one was grown in adherence, the other underwent six cycles of selection, each cycle consisting of 48h of culture on polyhema followed by 24h of recovery on regular plates. Cells recovered from GFP- and library-transduced cells after selection were named, respectively, “GFP-SEL” and “LIB-SEL”, and assayed for their ability to grow in the presence or absence of anchorage. LIB-SEL, but not GFP-SEL cells displayed

significantly higher growth rate than unselected cells, in both adherence and suspension (Figure 1A). Moreover, as shown in Figure 1B-C, only LIB-SEL cells could form large colonies in soft agar, an in vitro hallmark of cell transformation. These findings confirmed a "library effect" not explainable with insertional mutagenesis but likely deriving from the expression of advantageous exogenous transcripts. To identify library-derived transcripts promoting anchorage-independent growth, we conducted Xenoarray analysis on library-transduced cells, before and after selection. A significant number of probes displayed higher signal in selected cells, indicating that cells expressing the respective transcripts were enriched by the selection. To identify the genes that were reproducibly enriched in both selections we calculated, for each transcript, the Log(2) ratio of the signal before and after selection. Interestingly, the Gab2 transcript showed a strong enrichment in both selections (average enrichment = 14-fold). The enrichment was observed with 3 different probes, each designed in a different region of the Gab2 transcript. Other genes, including Ntrk3 and Cyp11a1, displayed a stronger enrichment in selection A (respectively, 41- and 49-fold in selection A, and 2- and 1.3-fold in selection B). Quantitative Real-Time PCR analysis with mouse-specific primers confirmed that Gab2 was the most enriched transcript, followed by Cyp11a1 and Ntrk3 (Figure 2A). Therefore, we focused on this gene and validated its enrichment also at the protein level (Figure 2B), thereby showing that the exogenous cDNA enriched after the selection actually encodes the full-length Gab2 protein. Exogenous Gab2 was found to be essential for anchorage-independent growth of the LIB-SEL population, as its downregulation by RNAi strongly reduced the growth advantage of LIB-SEL cells, in adhesion, in suspension and in soft agar.

***b. Validation and characterization of Gab2-driven anchorage-independence***

Gab2 is a scaffolding/docking protein involved in multiple signaling pathways downstream from membrane receptors (Nishida et al. 1999, Blood, 93, 1809-1816). To directly assess whether Gab2 may promote anchorage-independent growth, we transduced MCF10A cells with the human Gab2 coding sequence, cloned in a retroviral vector (Brummer et al. 2006). As shown in Figure 3A, adherent GAB2-overexpressing cells showed a significant increase in proliferation, which was further enhanced in the absence of anchorage. Notably, Gab2-driven growth advantage was almost totally lost when cells were kept in starving medium (no EGF, and serum lowered to 2%), indicating that Gab2

promotes proliferation independently from cell anchorage to the ECM, but dependently from the presence of GFs and/or serum. Accordingly, Gab2 overexpressing cells formed larger and more abundant colonies in soft agar, compared to wild-type cells (Figure 3B). To evaluate whether Gab2 promotes survival of detached cells, we estimated the fraction of dead cells after 48h of suspension culture. Surprisingly, after 48h of polyhema plating, we detected a comparable extent of cell death between wild-type and Gab2-expressing cells (Figure 3C). These data indicate that Gab2 is not involved in the protection of MCF10A cells from anoikis, but rather allows their proliferation in the absence of adhesion to the ECM.

Previous analyses have identified signaling molecules that can bind to Gab2 upon receptor activation, including the tyrosine phosphatase Ptpn11/Shp2, leading to activation of Erk and Jnk (Yu et al. 2006, J Biol Chem, 281, 28615-28626), the p85 subunit of PI3K, leading to Akt activation (Bouscary et al. 2001, Oncogene, 20, 2197-2204), and Src family kinases (Kong et al. 2003, J Biol Chem, 278, 5837-5844). Therefore, to dissect the signaling pathways downstream Gab2 that could mediate anchorage-independent growth, we examined the effects on cell vitality of a panel of small molecule inhibitors targeting the above mentioned signaling kinases (Figure 4A). The PI3K inhibitor was the most effective, but with no differential between anchorage-dependent and independent growth, or between control and Gab2expressing cells, showing a general requirement of this pathway for survival of MCF10A cells. A similar but less pronounced effect was observed for Mek inhibition. The Jnk inhibitor displayed modest effects in all conditions. Interestingly, the Src inhibitor PP2 displayed the highest specificity towards Gab2-expressing cells in suspension. A more detailed analysis of the effects of Src inhibition is shown in Figure 4B. According to these data, Gab2-driven anchorage independence requires Src, which typically is activated by integrins when cells are adherent and becomes inactivated upon detachment (Playford and Schaller 2004, Oncogene, 23, 7928-7946). Consistently, western blot analysis on cell lysates from control and Gab2-expressing cells cultured in adhesion or suspension confirmed Gab2-driven activation of Src and of one of its downstream targets, Stat3 (Figure 4C). In adhesion, Gab2-expressing cells displayed a stronger basal phosphorylation of Src. Active Src levels were reduced in cells kept in suspension, but while in control cells Src activation was completely abolished at 48h, Gab2expressing cells maintained some phosphorylation. Analysis of

Stat3 activation highlighted an even more pronounced response to Gab2 expression, indicating the capacity of Gab2 to sustain the activation of Stat3 also in the absence of a substratum consensus. Since many studies provided evidence for Stat3 involvement in Src-mediated oncogenesis (Yu et al. 1995, Science, 269, 81-83) and anchorage-independent growth (Laird et al. 2003, Mol Cancer Ther, 2, 461-469), these data indicate that Gab2 signals through Src and Stat3 to accomplish anchorage-independent growth.

***c. Endogenous Gab2 is essential for anchorage–independent growth of normal and neoplastic cells***

The data shown so far demonstrate that constitutive, exogenous expression of Gab2 promotes anchorage-independent growth. To verify if this effect is mirrored by physiologically controlled Gab2 expression, we silenced by RNAi the endogenous Gab2 in MCF10A and in human cancer cells. In MCF10A cells, Gab2 silencing markedly reduced their growth both in adhesion and in suspension (Figure 5A) while both MDA-MB-231 breast cancer cells and MDA-MB-435 melanoma cells responded to Gab2 silencing with a significant but modest reduction of proliferation (Figure 5B), indicating a minor role of Gab2 in the presence of attachment. Strikingly however, the ability of these cells to form colonies in soft agar was completely abrogated by Gab2 silencing (Figure 5C). In accordance with our previous western blot data, Gab2 loss determined a significant and concomitant decrease in Src and Stat3 activation (Figure 5D). Interestingly, the most evident reduction of Src-Stat3 phosphorylation was observed for MDA-MB 231 cells, which endogenously express the highest levels of Gab2 and most strongly reduce their soft agar growth upon Gab2 silencing. Altogether, these data confirmed the Gab2-Src-Stat3 axis as a key promoter of anchorage-independent growth of neoplastic cells, defining GAB2 as a potentially powerful diagnostic marker and therapeutic target for cancer treatment. While in the present invention we have used shRNA vectors as an example of a reagent that can be used to silence Gab2 and thus use it as a drug to treat cancer, a variety of other standard methods used to silence proteins or gene transcripts like monoclonal antibodies or diabodies or other protein neutralizing agents, antisense RNA and other nucleotide-based agents or small molecule inhibitors that can bind and to Gab2 or break its interaction with other proteins can also be easily employed as a therapeutic. The methods of preparation of these reagents are well known. A small molecule inhibitor can be identified through high-throughput screening methods

or through rational design or others methods typically used to identify such compounds. Anyone skilled in the art can develop these reagents to specifically abrogate the function of Gab2 and thus act as a drug for the treatment of solid cancers. Moreover, in Tables 1 to 5 we describe a series of genes that are transcriptional targets of GAB2 and/or are involved in anchorage independence. Such target genes are additional therapeutical targets against which inhibitors can be developed to treat breast cancer and other human neoplastic diseases.

**II. Definition of transcriptional signatures associated with GAB2, anchorage independence, cancer aggressiveness and response to treatment.**

***a. Definition of genomic signatures associated with GAB2 and with anchorage independence***

To gain further insights on Gab2-driven anchorage-independence, we performed gene expression profiling on MCF10A cells transduced with Gab2 and selected by growth in the absence of anchorage. As control, we used RNA extracted from GFP-transduced and selected cells. The selection was performed as described for the library-transduced cells. As further controls, GFP- and GAB2-transduced cells were profiled also before the selection, together with wild-type MCF10A cells and with Library-transduced selected cells (LIBSEL). Statistical analysis was applied to retrieve genes differentially expressed between GAB2transduced and GFP-transduced cells after the selection, highlighting 221 probes, corresponding to 205 independent genes: the "GAB2-signature" (Table 1). Other signatures were also derived, reflecting different aspects of GAB2 activity and of acquisition of anchorage independence in MCF10A cells: (i) the GAB2SEL vs GAB2UNS signature, composed of genes differentially expressed in GAB2-transduced cells before and after polyhema selection (Table 2); (ii) the GAB2UNS vs GFPUNS signature, composed of genes differentially expressed between GAB2-transduced and GFP-transduced cells before polyhema selection (Table 3); (iii) the GFPSEL vs GFPUNS signature, composed of genes differentially expressed in GFP-transduced cells before and after polyhema selection (Table 4); (iv) the LIBSEL vs GFPSEL signature, composed of genes differentially expressed in the above mentioned LIBSEL population described in the functional screening (Figure 1) and GFP-transduced cells after polyhema selection (Table 5). All these signatures, individually or altogether, capture various aspects of GAB2-driven processes and anchorage independence. This clearly demonstrates the use of the signatures in determining the metastatic potential of cancer cells. Metastatic

potential as meant in the current specification relates to the ability of a cancer cell to invade and to spread of cancer cells to other parts of the body. The same method that was used to derive the signatures in MCF10A cells transduced with GAB-2 or under different experimental conditions as described above can be easily replicated for a variety of cancers, in particular breast cancer, to determine their metastatic potential, the response to treatments and prognosis of the disease. In a diagnostic kit, one would use a micro-array seeded with probes that represent the signature that was derived in the above experiment and use it against a fluorescent, chemiluminescent or similar detection-capable tagged probes derived from tumor biopsies to determine their metastatic potential as well as the responsiveness to antineoplastic treatments, together with the general prognosis of the disease. Any alternative method for measuring expression of the signature genes, at the RNA or protein level, such as for example quantitative PCR in an array format or individually or immunohistochemistry using antibodies targeted to the proteins encoded by few or all of the signature genes, can be easily employed for the same task.

***b. The GAB2-signature is enriched in genes correlated to response to treatment and to metastatic propensity***

As an example of the clinical potential of the abovementioned signatures, we present here results obtained on the GAB2-signature. First of all, Probe identifiers contained in the annotation manifest provided by Illumina were loaded on the David Ease portal (Dennis G J et al, 2003, Genome Biology 4, P3) to generate a background list (all probes) and the GAB2-signature list. Enrichment in biological functions for the GAB2-signature genes was evaluated using the "functional annotation chart" function on the portal, and highlighted a strong enrichment in genes controlling proliferation. Subsequently, the signature was mapped on a gene expression dataset obtained on the NCI-60 panel of cell lines (Shankavaram et al. 2007, Mol Cancer Ther. 6, 820-832). Each line of the NCI-60 panel is annotated for sensitivity to a wide number of drugs. We concentrated on drugs affecting the Src-STAT3 axis downstream of GAB2, and found that the GAB2signature is significantly enriched in genes whose expression correlates to sensitivity to Resveratrol ($p=1x10^{-5}$), Piceatannol ($p=1x10^{-3}$) and SD-1029 ($p=1.2x10^{-4}$), small molecules that inhibit STAT3 activation by Src, Jak or other tyrosine kinases (Table 6). In another analysis conducted on a gene expression dataset obtained from human breast cancer cell lines (Huang et al., 2007), we found that the signature is also significantly enriched ($p<0.0023$)

in genes whose expression distinguishes Dasatinib-sensitive and resistant breast cancer cells. The genes and their differential expression between dasatinib-sensitive and resistant cells are listed in Table 7. Dasatinib is an oral small molecule inhibitor of Src-family kinases (Lombardo et al., 2004), currently employed for the treatment of leukemias. Recently, multiple clinical trials are assessing its efficacy on various solid tumors, including breast cancer and melanoma. These results confirm that the Src-STAT3 signaling axis plays a key role in GAB2-driven biological and transcriptional responses independently of tissue and cell type, and propose GAB2 and its transcriptional targets as predictors of sensitivity to targeted drugs blocking SRC and/or STAT3 activation. These studies also demonstrate the value of the assay in defining GAB2-driven signatures as predictor of many anti-cancer drugs whether singly or in combination and also response to other cytotoxic agents like radiation. Such signatures could be a powerful tool for determining prior to treatment for breast cancer or other cancers, which drug or combination of drugs (or radiation) would be most effective against the tumor of a particular patient. Such signature would also to a significant extent be able to identify the dose of the drug or combination of the drug would be most effective for treating the tumor of a particular patient. Practically, this would help the physician in avoiding using drugs or therapies that would not be expected to have any meaningful effect on the tumor of a particular patient and also identify the best drug or combination of drug and its dose that would be expected to have the most effect at the least doses.

To extend the value of the in-vitro model of Gab2-driven anchorage independence, we verified if the GAB2-signature could be associated to human breast cancer aggressiveness. To this aim, the signature was mapped on a 311-sample breast cancer dataset generated at the Netherland Cancer Institute on 2-color oligonucleotide microarrays (NKI dataset) and published in two works (van, V et al. 2002b; van, V et al. 2002a). After filtering for expression, the GAB2-signature was mapped to 150 probes. Interestingly, the signature resulted to be strongly enriched in genes discriminating breast cancer patients with or without metastatic recurrence within five years from the initial diagnosis ($p<10^{-8}$).

Determining the aggressiveness of cancer is a critical component of any treatment plan for cancer at present. This is typically done using histochemical assays of a section of the

tumor tissue derived from a biopsy and visually observing the difference in tissue architecture between normal tissue and the tumor tissue (level of differentiation) using a microscope. Based on the experience of the pathologist, a grade is assigned to the tumor -- higher the grade, the more aggressive the tumor. The physician makes important decisions on the treatment design from this score as to how to treat including whether to treat the disease aggressively or not. The main pitfall of determining the grade by this method is that the grade value derived by two pathologists could vary as much as 50% leading to the physician making the wrong treatment design. Use of molecular markers to make more accurate prediction of the grade (or level of aggressiveness) of a patient's tumor would have considerable value in making treatment decisions more accurately. The data presented in this application shows that GAB2-associated gene expression signatures can be used to determine the grade of a tumor even though additional clinical studies would be required to assign accurate grade of a patient's tumor with a particular GAB2-driven signature.

***c. A breast cancer classifier based on the GAB2-signature predicts metastatic relapse***

On the basis of the results mentioned above, using the nearest-mean classifier approach (Wessels et al. 2005, Bioinformatics, 21, 3755-3762), we built a classifier in the NKI dataset, based on the entire GAB2signature, which provides a "Metastasis Score", MS, discriminating patients with good and poor prognosis (Table 8). Data clustering and mining revealed two specific gene functional modules associated with prognosis: (i) a sizeable proliferation module positively correlated to metastatic progression, and (ii) an interesting module composed of negative regulators of cell-matrix interaction, migration and invasion, expressed at higher levels in good prognosis samples (Figure 6A and Table 9). To validate the classifier, we mapped it on two independent datasets of 198 and 236 samples, both obtained on Affymetrix microarrays and aimed at evaluating, respectively, metastasis-free survival and death of disease (Desmedt et al. 2007; Miller et al. 2005). In both cases the Gab2-signature classified patients with high accuracy, despite the change of microarray platform (Figure 6B-C). We then applied the Gab2-signature on the 198-sample dataset stratified by various clinical and genomic classifiers originally provided in the work. When samples were subdivided by their prognostic class according to the Adjuvant!Online score (Hess 2008, Am J Pathol, 174, 1524-1533), they could still be further subdivided in good- and poor-prognosis subgroups (GP and PP, respectively) by

the GAB2-signature (Fig. 7A-B). Similarly, the GAB-2 signature correctly re-classified also samples previously subdivided in good- and poor-prognosis subgroups by genomic classifiers such as the 76-gene "Veridex Index" (Desmedt et al. 2007) (Fig. 7C-D) and the 70-gene "Mammaprint" classifier (Buyse et al. 2006, J Natl Cancer Inst, 98, 1183-1192) (Fig. 7EF). These results show that the GAB2-signature predicts metastatic relapse of breast cancer independently of existing clinical and genomic classifiers. Such independence was further confirmed by univariate and multivariate statistics calculated, on the 198-sample dataset, for the Gab2 signature versus Adjuvant!online or three published genomic prognostic classifiers: Veridex index, MammaPrint and "Genomic Grade Index" (Sotiriou et al. 2006, J Natl Cancer Inst, 98, 262-272) (Table 10). Reciprocal significance impairment was only observed with the Mammaprint classifier, which, however, is obtained on a proprietary microarray platform, while the GAB2 signature can be directly tested on all publicly available Affymetrix microarray datasets. Finally, the GAB2-signature was found to maintain prognostic ability also in samples subdivided by estrogen receptor (ER) status (Fig. 7G-H). Intriguingly, a small fraction of the ER-negative samples was called "good-prognosis" with 100% precision, but with no statistical significance probably due to the limited number (64) of samples analyzed. We therefore added samples from two other datasets (Ivshina et al. 2006; Wang et al. 2005), reaching a total of 175 ER-negative samples, for which the GAB2-signature maintained 100% precision and reached statistical significance (Figure 8). Finally, we verified if the GAB2-signature metastasis score described above. These results confirm that the GAB2-signature is a powerful predictor of metastatic propensity, in breast cancer but likely in other human cancers. A similar complementary diagnostic potential would therefore be possessed by the other signatures herein described at Tables 2 to 5, all capturing traits of GAB2-driven processes and of anchorage independence. Moreover, being differentially expressed in aggressive vs. non-aggressive cancers, genes of the signatures represent also therapeutic targets for cancer treatment. Being based on a basic cellular process, the GAB2-signatures would present similar diagnostic and therapeutic properties also for other types of solid cancers, for which they can be used employing the same methodology and reagents.

***d. A breast cancer classifier based on the GAB2-signature predicts response to treatment***

To test if the classifier based on the GAB2-signature has the potential to also predict response of breast cancer to conventional chemotherapy, we mapped the classifier on a dataset of 133 samples, obtained on Affymetrix microarrays and aimed at evaluating response to preoperative treatment (Hess et al. 2006, J Clin Oncol, 24, 4236-4244). All samples were biopsies taken from the primary tumor before the start of neoadjuvant treatment with paclitaxel and fluorouracil, doxorubicin, and cyclophosphamide, and are annotated for the subsequent response of the patient. A pathological complete response (pCR) was observed in 34 patients, while the remaining had residual disease (RD) at surgery. We could therefore directly test the GAB2-signature metastasis score for its ability to discriminate responders from non-responders. Indeed, the GAB2-signature classifies patients with high accuracy, despite the fact that it is a prognostic classifier, as measured by ROC analysis (AUC>0.75; Figure 9A). The details of the classifier's performances are illustrated in Figure 9B. In this dot plot, it clearly emerges that the patients with low metastasis score are also those more unlikely to respond to the treatment. In clinical perspective, this result is very interesting because it would give two concomitant reasons to spare the patient from chemotherapy which has serious unwanted long-term and short-term side-effects: (i) unlikely to develop distant metastases; (ii) unlikely to respond to chemotherapy. Overall, these results confirm that the GAB2-signature is a powerful predictor of response to anticancer treatments, in breast cancer but likely in other human cancers. A similar and possibly complementary diagnostic potential is therefore likely to be possessed by the other signatures herein described at Tables 2 to 5, all capturing traits of GAB2-driven processes and of anchorage independence. Moreover, being differentially expressed in responsive vs. non-responsive cancers, genes of the signatures represents also therapeutic targets for cancer treatment. Being based on a basic cellular process, the GAB2-signatures are likely to present similar diagnostic and therapeutic properties also for other types of solid cancers, for which they can be used with the same methodology.

**Table 1: The GAB2-Signature in MCF10A Cells (GAB2SEL vs GFPSEL)**

| Illumina ID | Accession | Symbol | Gi Accession | GFP SEL A Log(2) Signal | GFP SEL B Log(2) Signal | GAB2 SEL A Log(2) Signal | GAB2 SEL B Log(2) Signal | GAB2 SEL / GFP SEL Log(2) Ratio |
|---|---|---|---|---|---|---|---|---|
| ILMN_856 | NM_172080.1 | CAMK2B | 26051209 | 4.797 | 5.100 | 9.506 | 9.305 | 4.457 |
| ILMN_22077 | NM_018584.4 | CAMK2N1 | 31324542 | 4.954 | 6.020 | 9.117 | 9.230 | 3.686 |
| ILMN_9421 | NM_003806.1 | HRK | 4504492 | 5.472 | 5.520 | 9.174 | 9.115 | 3.648 |
| ILMN_9653 | NM_139277.1 | KLK7 | 21327704 | 7.111 | 6.857 | 10.471 | 10.674 | 3.589 |
| ILMN_12238 | NM_206963.1 | RARRES1 | 46255042 | 5.501 | 5.433 | 8.953 | 9.110 | 3.564 |
| ILMN_8120 | NM_020037.1 | ABCC3 | 9955971 | 7.603 | 6.934 | 10.860 | 10.764 | 3.543 |
| ILMN_19268 | NM_001185.2 | AZGP1 | 38372939 | 5.396 | 6.066 | 9.044 | 9.430 | 3.506 |
| ILMN_17796 | NM_002274.2 | KRT13 | 24234693 | 5.511 | 5.109 | 8.697 | 8.784 | 3.431 |
| ILMN_4712 | NM_000624.3 | SERPINA5 | 34147643 | 8.145 | 8.330 | 11.474 | 11.658 | 3.329 |
| ILMN_24486 | NM_006105.3 | RAPGEF3 | 45269150 | 5.443 | 5.758 | 8.971 | 8.712 | 3.241 |
| ILMN_138267 | NM_000211.1 | ITGB2 | 4557885 | 5.644 | 5.624 | 8.798 | 8.674 | 3.103 |
| ILMN_5657 | NM_006762.1 | LAPTM5 | 5803055 | 5.845 | 5.403 | 8.616 | 8.679 | 3.023 |
| ILMN_4882 | NM_003246.2 | THBS1 | 40317625 | 6.029 | 6.051 | 9.139 | 8.960 | 3.009 |
| ILMN_14995 | NM_004460.2 | FAP | 16933539 | 5.675 | 5.652 | 8.539 | 8.789 | 3.000 |
| ILMN_14229 | NM_005630.1 | SLCO2A1 | 5032094 | 5.392 | 5.709 | 8.420 | 8.631 | 2.975 |
| ILMN_12486 | NM_005556.3 | KRT7 | 67782364 | 9.058 | 8.459 | 11.857 | 11.410 | 2.875 |
| ILMN_7403 | NM_001425.1 | EMP3 | 4503562 | 7.615 | 7.661 | 10.348 | 10.236 | 2.654 |
| ILMN_26451 | NM_001008540.1 | CXCR4 | 56790926 | 5.406 | 5.221 | 7.764 | 8.113 | 2.625 |
| ILMN_23474 | NM_144626.1 | TMEM125 | 21389442 | 6.192 | 5.961 | 8.635 | 8.758 | 2.620 |
| ILMN_12676 | NM_004454.1 | ETV5 | 4758315 | 5.485 | 6.092 | 8.589 | 8.113 | 2.563 |
| ILMN_10965 | NM_002888.2 | RARRES1 | 46255040 | 5.495 | 5.558 | 7.878 | 8.268 | 2.546 |
| ILMN_2486 | NM_001570.3 | IRAK2 | 58530885 | 5.823 | 5.545 | 8.111 | 8.299 | 2.521 |
| ILMN_138775 | XM_936314.1 | CAMK2B | 89025915 | 4.931 | 5.190 | 7.590 | 7.565 | 2.517 |
| ILMN_4070 | NM_002354.1 | TACSTD1 | 4505058 | 8.284 | 7.637 | 10.187 | 10.670 | 2.468 |
| ILMN_2939 | NM_004572.2 | PKP2 | 52630430 | 6.272 | 5.900 | 8.644 | 8.414 | 2.443 |
| ILMN_138896 | NM_001692.2 | ATP6V1B1 | 19913425 | 8.058 | 8.414 | 10.700 | 10.620 | 2.424 |
| ILMN_5800 | NM_006623.2 | PHGDH | 23308576 | 8.361 | 7.135 | 10.316 | 10.012 | 2.416 |
| ILMN_13615 | NM_004433.3 | ELF3 | 40255034 | 6.426 | 6.732 | 8.898 | 9.044 | 2.392 |
| ILMN_16665 | NM_018478.2 | C20orf35 | 56676381 | 8.997 | 8.527 | 11.023 | 11.222 | 2.361 |
| ILMN_23395 | NM_000170.1 | GLDC | 4504012 | 7.501 | 6.884 | 9.649 | 9.407 | 2.336 |
| ILMN_22286 | NM_005950.1 | MT1G | 10835229 | 6.498 | 6.564 | 8.729 | 8.959 | 2.313 |
| ILMN_23106 | NM_032501.2 | ACSS1 | 28416952 | 5.787 | 7.076 | 8.861 | 8.612 | 2.305 |
| ILMN_73404 | Hs.66187 | 0 | 2795905 | 5.833 | 5.919 | 7.965 | 8.369 | 2.291 |
| ILMN_8119 | NM_000667.2 | ADH1A | 11496886 | 6.338 | 6.621 | 8.592 | 8.847 | 2.240 |
| ILMN_12667 | NM_015621.2 | CCDC69 | 45935390 | 5.890 | 4.555 | 7.237 | 7.658 | 2.226 |
| ILMN_19983 | NM_001252.2 | TNFSF7 | 24119161 | 7.573 | 7.670 | 9.832 | 9.803 | 2.196 |
| ILMN_27148 | NM_007231.1 | SLC6A14 | 6005714 | 4.307 | 5.375 | 6.695 | 7.352 | 2.182 |
| ILMN_10592 | NM_000149.1 | FUT3 | 4503808 | 6.123 | 6.178 | 8.447 | 8.189 | 2.167 |
| ILMN_3057 | NM_080668.2 | CDCA5 | 34147481 | 6.641 | 6.648 | 8.614 | 8.949 | 2.137 |
| ILMN_21545 | NM_015864.2 | C6orf32 | 14277689 | 6.033 | 5.629 | 7.830 | 8.055 | 2.111 |
| ILMN_123833 | Hs.571652 | 0 | 13579761 | 4.591 | 4.781 | 6.471 | 7.080 | 2.089 |
| ILMN_4794 | NM_153750.1 | C21orf81 | 24371249 | 7.255 | 6.731 | 8.949 | 9.204 | 2.084 |
| ILMN_18673 | NM_002346.1 | LY6E | 4505048 | 10.127 | 9.887 | 12.074 | 12.103 | 2.081 |
| ILMN_29702 | NM_016448.1 | DTL | 7705575 | 6.375 | 6.879 | 8.594 | 8.787 | 2.063 |
| ILMN_20794 | NM_005564.2 | LCN2 | 38455401 | 6.829 | 6.542 | 8.549 | 8.927 | 2.052 |
| ILMN_22039 | NM_000934.1 | SERPINF2 | 11386142 | 6.770 | 6.493 | 8.634 | 8.707 | 2.039 |
| ILMN_5259 | NM_032432.2 | ABLIM2 | 40316949 | 6.013 | 6.119 | 7.966 | 8.196 | 2.015 |
| ILMN_18895 | NM_030928.2 | CDT1 | 19923847 | 6.759 | 6.711 | 8.893 | 8.594 | 2.008 |
| ILMN_9313 | NM_005130.3 | FGFBP1 | 49574208 | 7.822 | 6.469 | 9.081 | 9.214 | 2.002 |
| ILMN_24599 | NM_003809.2 | TNFSF12 | 23510442 | 5.714 | 6.284 | 7.873 | 8.085 | 1.980 |
| ILMN_43594 | XM_498969.2 | LOC441019 | 88974818 | 9.553 | 9.414 | 11.350 | 11.544 | 1.964 |

Table 1, continued

| | | | | | | | | |
|---|---|---|---|---|---|---|---|---|
| ILMN_28594 | NM_000900.2 | MGP | 49574513 | 5.450 | 5.267 | 6.954 | 7.679 | 1.958 |
| ILMN_24333 | NM_001025357.1 | LOC441376 | 70778888 | 5.174 | 5.725 | 7.146 | 7.652 | 1.950 |
| ILMN_25185 | NM_002982.3 | CCL2 | 56119169 | 5.963 | 5.585 | 7.480 | 7.965 | 1.948 |
| ILMN_16225 | NM_003155.2 | STC1 | 61676083 | 5.728 | 5.609 | 7.370 | 7.828 | 1.931 |
| ILMN_26854 | NM_016095.1 | Pfs2 | 7706366 | 6.370 | 6.217 | 8.257 | 8.188 | 1.929 |
| ILMN_16900 | NM_012485.1 | HMMR | 7108350 | 6.589 | 5.980 | 8.310 | 8.100 | 1.920 |
| ILMN_635 | NM_002281.2 | KRTHB1 | 15431319 | 12.938 | 12.058 | 14.562 | 14.269 | 1.918 |
| ILMN_138949 | NM_005672.2 | PSCA | 29893565 | 5.661 | 6.375 | 8.084 | 7.735 | 1.891 |
| ILMN_19849 | NM_001067.2 | TOP2A | 19913405 | 6.874 | 6.580 | 8.599 | 8.634 | 1.890 |
| ILMN_1375 | NM_152594.1 | SPRED1 | 22749220 | 7.360 | 7.465 | 9.390 | 9.211 | 1.888 |
| ILMN_16399 | NM_006086.2 | TUBB3 | 50592995 | 7.648 | 6.982 | 9.337 | 9.061 | 1.884 |
| ILMN_25781 | NM_003504.3 | CDC45L | 34335230 | 4.755 | 3.818 | 6.090 | 6.225 | 1.871 |
| ILMN_139316 | NM_054111.2 | IHPK3 | 55769529 | 5.667 | 5.561 | 7.419 | 7.545 | 1.868 |
| ILMN_21714 | NM_032814.1 | TMEM118 | 14249505 | 5.482 | 5.049 | 7.071 | 7.178 | 1.859 |
| ILMN_15264 | NM_080757.1 | C20orf127 | 50233782 | 9.726 | 8.978 | 11.181 | 11.235 | 1.856 |
| ILMN_12145 | NM_002742.1 | PRKD1 | 4506074 | 5.916 | 4.991 | 7.138 | 7.480 | 1.855 |
| ILMN_25474 | NM_178229.3 | IQGAP3 | 39753960 | 7.216 | 7.113 | 9.110 | 8.925 | 1.853 |
| ILMN_15159 | NM_207409.1 | UNQ3045 | 46409449 | 4.959 | 5.322 | 7.003 | 6.966 | 1.844 |
| ILMN_3512 | NM_015894.2 | STMN3 | 14670374 | 6.338 | 5.720 | 7.981 | 7.763 | 1.843 |
| ILMN_79597 | Hs.159264 | 0 | 1710274 | 4.921 | 5.104 | 6.609 | 7.093 | 1.838 |
| ILMN_23984 | NM_001338.3 | CXADR | 45827793 | 8.317 | 8.588 | 10.272 | 10.307 | 1.837 |
| ILMN_20465 | NM_003981.2 | PRC1 | 40807441 | 7.796 | 7.132 | 9.227 | 9.337 | 1.818 |
| ILMN_6398 | NM_181803.1 | UBE2C | 32967290 | 7.550 | 6.533 | 8.799 | 8.917 | 1.816 |
| ILMN_408 | NM_018136.2 | ASPM | 24211028 | 7.031 | 6.674 | 8.360 | 8.965 | 1.810 |
| ILMN_10261 | NM_012137.2 | DDAH1 | 31881756 | 5.100 | 5.240 | 6.705 | 7.255 | 1.809 |
| ILMN_138577 | NM_031311.2 | CPVL | 22027517 | 8.522 | 7.918 | 10.007 | 10.046 | 1.807 |
| ILMN_2929 | NM_001958.2 | EEF1A2 | 25453470 | 4.959 | 5.049 | 6.828 | 6.744 | 1.782 |
| ILMN_8234 | NM_013271.2 | PCSK1N | 20336240 | 5.739 | 5.252 | 7.167 | 7.386 | 1.781 |
| ILMN_10126 | NM_000527.2 | LDLR | 8051613 | 9.982 | 9.340 | 11.363 | 11.517 | 1.779 |
| ILMN_2142 | NM_002727.2 | PRG1 | 45935370 | 5.750 | 5.661 | 7.432 | 7.534 | 1.778 |
| ILMN_3335 | NM_006779.2 | CDC42EP2 | 30089963 | 5.883 | 5.624 | 7.481 | 7.534 | 1.754 |
| ILMN_4109 | NM_000755.2 | CRAT | 21618330 | 6.670 | 6.109 | 8.359 | 7.921 | 1.751 |
| ILMN_132978 | Hs.580797 | 0 | 12402397 | 9.327 | 9.174 | 10.721 | 11.267 | 1.743 |
| ILMN_3628 | NM_024094.1 | DCC1 | 13129095 | 5.766 | 5.830 | 7.446 | 7.634 | 1.742 |
| ILMN_15254 | NM_004701.2 | CCNB2 | 10938017 | 8.128 | 7.113 | 9.346 | 9.325 | 1.715 |
| ILMN_18800 | NM_001089.1 | ABCA3 | 4501848 | 6.119 | 5.692 | 7.707 | 7.530 | 1.713 |
| ILMN_8681 | NM_207362.1 | MGC42367 | 46409355 | 6.926 | 6.967 | 8.511 | 8.804 | 1.711 |
| ILMN_15358 | NM_001839.2 | CNN3 | 47080096 | 8.562 | 8.707 | 10.383 | 10.308 | 1.711 |
| ILMN_27289 | NM_002578.2 | PAK3 | 46249379 | 7.126 | 6.821 | 8.676 | 8.667 | 1.697 |
| ILMN_7092 | NM_003686.3 | EXO1 | 39995068 | 6.300 | 6.235 | 7.934 | 7.984 | 1.692 |
| ILMN_28552 | NM_032117.2 | GAJ | 38455411 | 4.838 | 5.579 | 6.910 | 6.884 | 1.689 |
| ILMN_915 | NM_020675.3 | SPBC25 | 23510353 | 3.700 | 4.217 | 5.807 | 5.479 | 1.684 |
| ILMN_12434 | NM_032918.1 | RERG | 14249703 | 4.186 | 4.828 | 6.002 | 6.379 | 1.684 |
| ILMN_12221 | NM_000204.1 | CFI | 4504578 | 7.656 | 7.384 | 9.159 | 9.239 | 1.679 |
| ILMN_7052 | NM_005727.2 | TSPAN1 | 21264577 | 6.489 | 6.320 | 8.012 | 8.155 | 1.679 |
| ILMN_8225 | NM_016343.3 | CENPF | 55770833 | 5.805 | 5.615 | 7.342 | 7.431 | 1.677 |
| ILMN_24855 | NM_021101.3 | CLDN1 | 21536297 | 9.320 | 9.696 | 11.129 | 11.240 | 1.676 |
| ILMN_90844 | Hs.430502 | 0 | 79239592 | 5.492 | 5.975 | 7.555 | 7.244 | 1.666 |
| ILMN_14069 | NM_000147.2 | FUCA1 | 24475878 | 7.250 | 6.843 | 8.577 | 8.845 | 1.665 |
| ILMN_20249 | NM_001006933.1 | TCEAL3 | 55749430 | 7.049 | 6.693 | 8.662 | 8.387 | 1.653 |
| ILMN_23549 | NM_199327.1 | SPRY1 | 40788000 | 5.202 | 5.594 | 6.891 | 7.209 | 1.653 |
| ILMN_18797 | NM_198282.1 | LOC340061 | 38093658 | 7.098 | 6.940 | 8.674 | 8.647 | 1.642 |
| ILMN_36990 | XM_930914.1 | LOC653108 | 89058118 | 5.909 | 5.664 | 7.262 | 7.588 | 1.638 |
| ILMN_6505 | NM_003282.2 | TNNI2 | 50593000 | 7.676 | 7.965 | 9.410 | 9.498 | 1.634 |
| ILMN_26085 | NM_003467.2 | CXCR4 | 56790928 | 5.820 | 5.304 | 7.051 | 7.333 | 1.630 |
| ILMN_24466 | NM_003641.2 | IFITM1 | 40254449 | 6.272 | 6.184 | 7.895 | 7.816 | 1.628 |
| ILMN_6876 | NM_003632.1 | CNTNAP1 | 4505462 | 6.127 | 5.825 | 7.673 | 7.527 | 1.624 |
| ILMN_3836 | NM_018367.3 | PHCA | 31543398 | 5.973 | 6.085 | 7.605 | 7.695 | 1.621 |

| Table 1, continued | | | | | | | | |
|---|---|---|---|---|---|---|---|---|
| ILMN_15608 | NM_005766.2 | FARP1 | 48928036 | 7.183 | 7.002 | 8.795 | 8.589 | 1.600 |
| ILMN_23044 | NM_052972.2 | LRG1 | 49574519 | 5.485 | 5.233 | 6.783 | 7.132 | 1.598 |
| ILMN_108776 | Hs.545615 | 0 | 2901934 | 6.309 | 6.520 | 7.919 | 8.100 | 1.594 |
| ILMN_25536 | NM_002386.2 | MC1R | 27477128 | 6.421 | 6.733 | 8.386 | 7.956 | 1.594 |
| ILMN_137805 | NM_004217.1 | AURKB | 4759177 | 6.036 | 6.106 | 7.727 | 7.571 | 1.578 |
| ILMN_5694 | NM_153322.1 | PMP22 | 24430164 | 5.307 | 5.650 | 7.142 | 6.959 | 1.572 |
| ILMN_25636 | NM_152666.1 | PLD5 | 22749352 | 6.104 | 5.274 | 7.234 | 7.278 | 1.567 |
| ILMN_30361 | NM_003896.2 | ST3GAL5 | 28373079 | 4.986 | 5.079 | 6.681 | 6.503 | 1.559 |
| ILMN_40146 | XM_496129.2 | LOC440349 | 89040448 | 6.227 | 6.075 | 7.466 | 7.941 | 1.553 |
| ILMN_16130 | NM_006997.2 | TACC2 | 45827751 | 11.174 | 11.047 | 12.627 | 12.697 | 1.552 |
| ILMN_27053 | NM_003637.3 | ITGA10 | 38569397 | 5.652 | 5.233 | 7.000 | 6.984 | 1.549 |
| ILMN_10005 | NM_031966.2 | CCNB1 | 34304372 | 6.759 | 6.498 | 8.045 | 8.309 | 1.549 |
| ILMN_19730 | NM_004091.2 | E2F2 | 34485718 | 6.020 | 5.591 | 7.336 | 7.365 | 1.545 |
| ILMN_3597 | NM_004431.2 | EPHA2 | 32967310 | 8.283 | 8.673 | 10.275 | 9.755 | 1.537 |
| ILMN_18617 | NM_031426.2 | C9orf58 | 50428929 | 9.093 | 8.994 | 10.673 | 10.417 | 1.501 |
| ILMN_13141 | NM_005480.2 | TROAP | 33438581 | 5.591 | 5.326 | 6.990 | 6.916 | 1.495 |
| ILMN_26277 | NM_024901.3 | DENND2D | 34147689 | 5.186 | 5.409 | 6.988 | 6.597 | 1.495 |
| ILMN_13533 | NM_016437.1 | TUBG2 | 7706750 | 7.764 | 7.606 | 9.198 | 9.147 | 1.488 |
| ILMN_9405 | NM_016445.1 | PLEK2 | 7706642 | 6.318 | 6.498 | 7.900 | 7.887 | 1.485 |
| ILMN_12351 | NM_001002876.1 | C22orf18 | 50845413 | 6.629 | 5.995 | 7.807 | 7.771 | 1.476 |
| ILMN_23620 | NM_022346.3 | HCAP-G | 50658080 | 7.019 | 6.695 | 8.368 | 8.296 | 1.475 |
| ILMN_9074 | NM_001175.4 | ARHGDIB | 56676392 | 8.266 | 8.078 | 9.624 | 9.665 | 1.472 |
| ILMN_1133 | NM_182776.1 | MCM7 | 33469921 | 9.595 | 9.620 | 11.093 | 11.045 | 1.461 |
| ILMN_6272 | NM_017823.3 | DUSP23 | 56786143 | 11.433 | 11.594 | 12.951 | 12.955 | 1.439 |
| ILMN_21136 | NM_014411.2 | NAG8 | 77404393 | 7.232 | 6.991 | 8.316 | 8.783 | 1.438 |
| ILMN_79861 | Hs.162734 | 0 | 2276759 | 6.508 | 6.508 | 7.830 | 8.055 | 1.434 |
| ILMN_11198 | NM_005953.2 | MT2A | 31543214 | 13.935 | 13.691 | 15.221 | 15.263 | 1.429 |
| ILMN_25046 | NM_006479.2 | RAD51AP1 | 19923778 | 5.463 | 5.888 | 7.066 | 7.141 | 1.428 |
| ILMN_20154 | NM_018728.1 | MYO5C | 9055283 | 8.291 | 7.854 | 9.523 | 9.466 | 1.422 |
| ILMN_138827 | NM_145810.1 | CDCA7 | 22027513 | 7.436 | 7.393 | 8.885 | 8.779 | 1.418 |
| ILMN_20107 | NM_006739.2 | MCM5 | 23510447 | 5.890 | 5.928 | 7.176 | 7.477 | 1.417 |
| ILMN_95224 | Hs.473191 | 0 | 21750193 | 7.355 | 7.324 | 8.722 | 8.766 | 1.405 |
| ILMN_22327 | NM_033412.1 | MCART1 | 15529971 | 12.615 | 12.944 | 14.243 | 14.121 | 1.403 |
| ILMN_21027 | NM_015651.1 | PHF19 | 58331160 | 6.772 | 6.533 | 8.102 | 7.954 | 1.375 |
| ILMN_12005 | NM_013282.2 | UHRF1 | 16507203 | 7.110 | 6.997 | 8.645 | 8.183 | 1.361 |
| ILMN_1733 | NM_198457.1 | ZNF600 | 39930584 | 6.592 | 6.490 | 7.892 | 7.894 | 1.351 |
| ILMN_25969 | NM_006845.2 | KIF2C | 13699832 | 5.763 | 5.456 | 7.094 | 6.810 | 1.342 |
| ILMN_14281 | NM_016359.2 | NUSAP1 | 59710089 | 7.704 | 7.807 | 9.139 | 9.051 | 1.339 |
| ILMN_12202 | NM_020127.1 | TUFT1 | 9910595 | 7.420 | 7.354 | 8.613 | 8.816 | 1.327 |
| ILMN_5047 | NM_152308.1 | MGC24665 | 24308244 | 6.079 | 6.096 | 7.319 | 7.500 | 1.322 |
| ILMN_16427 | NM_001237.2 | CCNA2 | 16950653 | 6.477 | 6.651 | 7.736 | 8.036 | 1.322 |
| ILMN_17477 | NM_032199.1 | ARID5B | 74136548 | 8.807 | 8.595 | 9.904 | 10.132 | 1.317 |
| ILMN_18194 | NM_021805.1 | SIGIRR | 11141876 | 6.154 | 6.064 | 7.453 | 7.341 | 1.288 |
| ILMN_21987 | NR_001568.1 | BCYRN1 | 34850482 | 9.587 | 9.520 | 10.871 | 10.809 | 1.287 |
| ILMN_6355 | NM_001010915.1 | PTPLAD2 | 58219057 | 9.790 | 10.076 | 11.178 | 11.249 | 1.280 |
| ILMN_6890 | NM_021034.1 | IFITM3 | 11995467 | 12.872 | 12.732 | 14.039 | 14.112 | 1.274 |
| ILMN_20682 | NM_004482.2 | GALNT3 | 9945386 | 6.947 | 6.969 | 8.191 | 8.260 | 1.267 |
| ILMN_6588 | NM_001613.1 | ACTA2 | 4501882 | 8.957 | 9.148 | 10.216 | 10.380 | 1.245 |
| ILMN_1091 | NM_024581.3 | C6orf60 | 40255142 | 5.797 | 6.049 | 7.165 | 7.143 | 1.231 |
| ILMN_10210 | NM_030666.2 | SERPINB1 | 20149554 | 8.976 | 8.964 | 10.174 | 10.226 | 1.229 |
| ILMN_37765 | XM_379668.3 | LOC286208 | 89029959 | 7.301 | 7.257 | 8.543 | 8.462 | 1.223 |
| ILMN_7673 | NM_024298.2 | LENG4 | 23308571 | 8.149 | 8.092 | 9.340 | 9.293 | 1.196 |
| ILMN_12918 | NM_022308.1 | ICA1 | 12545396 | 9.005 | 9.006 | 10.204 | 10.200 | 1.196 |
| ILMN_26916 | NM_004292.2 | RIN1 | 68989255 | 8.743 | 8.745 | 7.574 | 7.626 | -1.144 |
| ILMN_19302 | NM_032823.3 | C9orf3 | 24432057 | 8.423 | 8.535 | 7.311 | 7.313 | -1.167 |
| ILMN_22366 | NM_024617.2 | ZCCHC6 | 58331271 | 11.512 | 11.524 | 10.403 | 10.279 | -1.177 |
| ILMN_7864 | NM_016525.3 | UBAP1 | 22212941 | 10.120 | 9.984 | 8.809 | 8.839 | -1.228 |
| ILMN_9696 | NM_014872.1 | ZBTB5 | 7662073 | 7.985 | 8.136 | 6.645 | 6.955 | -1.260 |

| Table 1, continued | | | | | | | | |
|---|---|---|---|---|---|---|---|---|
| ILMN_5444 | NM_006285.2 | TESK1 | 66932998 | 8.705 | 8.709 | 7.468 | 7.401 | -1.273 |
| ILMN_71954 | Hs.25318 | 0 | 4406612 | 9.975 | 9.822 | 8.562 | 8.630 | -1.302 |
| ILMN_6140 | NM_174921.1 | LOC201895 | 28372538 | 10.256 | 10.467 | 8.902 | 9.138 | -1.342 |
| ILMN_12831 | NM_024302.3 | MMP28 | 73808269 | 7.725 | 7.603 | 6.468 | 6.168 | -1.346 |
| ILMN_13962 | NM_001752.2 | CAT | 60302919 | 10.147 | 10.092 | 8.744 | 8.802 | -1.347 |
| ILMN_25965 | NM_002202.1 | ISL1 | 4504736 | 7.464 | 7.408 | 5.986 | 6.154 | -1.366 |
| ILMN_28002 | NM_181353.1 | ID1 | 31317296 | 11.104 | 11.119 | 9.886 | 9.606 | -1.375 |
| ILMN_71591 | Hs.19339 | 0 | 34191392 | 9.050 | 9.362 | 7.756 | 7.901 | -1.377 |
| ILMN_25748 | NM_004432.1 | ELAVL2 | 4758261 | 6.796 | 7.146 | 5.652 | 5.482 | -1.403 |
| ILMN_87528 | Hs.363156 | 0 | 18204365 | 7.867 | 8.105 | 6.289 | 6.682 | -1.500 |
| ILMN_7334 | NM_152574.1 | C9orf52 | 22749190 | 8.734 | 8.928 | 7.296 | 7.329 | -1.518 |
| ILMN_10998 | NM_014899.2 | RHOBTB3 | 41281538 | 9.363 | 9.379 | 7.670 | 7.926 | -1.573 |
| ILMN_28967 | NM_001540.2 | HSPB1 | 4996892 | 15.340 | 15.213 | 13.665 | 13.742 | -1.573 |
| ILMN_29543 | NM_022165.2 | LIN7B | 56676320 | 7.506 | 7.491 | 5.670 | 6.075 | -1.626 |
| ILMN_19881 | NM_014214.1 | IMPA2 | 7657235 | 11.886 | 11.636 | 10.041 | 10.189 | -1.646 |
| ILMN_15434 | NM_012464.3 | TLL1 | 22547220 | 7.141 | 7.258 | 5.629 | 5.453 | -1.658 |
| ILMN_13399 | NM_001032278.1 | MMP28 | 73808270 | 9.191 | 9.401 | 7.563 | 7.657 | -1.686 |
| ILMN_28493 | NM_023944.1 | CYP4F12 | 13184045 | 8.332 | 7.791 | 6.306 | 6.320 | -1.749 |
| ILMN_491 | NM_021945.4 | C6orf85 | 48526515 | 9.805 | 10.136 | 8.218 | 8.188 | -1.768 |
| ILMN_12568 | NM_013281.2 | FLRT3 | 38202220 | 11.298 | 11.262 | 9.412 | 9.611 | -1.769 |
| ILMN_19665 | NM_198061.1 | CES2 | 37622886 | 12.511 | 12.583 | 10.726 | 10.811 | -1.778 |
| ILMN_20221 | NM_000896.1 | CYP4F3 | 4503240 | 9.989 | 9.289 | 7.637 | 8.071 | -1.785 |
| ILMN_14614 | NM_000104.2 | CYP1B1 | 13325059 | 9.757 | 9.954 | 7.779 | 8.316 | -1.808 |
| ILMN_16111 | NM_023938.4 | C1orf116 | 56550121 | 10.183 | 10.415 | 8.503 | 8.460 | -1.818 |
| ILMN_8954 | NM_001072.2 | UGT1A6 | 45827764 | 7.604 | 7.731 | 5.698 | 5.975 | -1.831 |
| ILMN_13999 | NM_001018109.1 | PIR | 66363696 | 11.156 | 10.976 | 9.006 | 9.424 | -1.851 |
| ILMN_18558 | NM_001512.2 | GSTA4 | 23065568 | 11.286 | 11.093 | 9.141 | 9.476 | -1.881 |
| ILMN_26717 | NM_006308.1 | HSPB3 | 5453687 | 6.670 | 7.335 | 5.450 | 4.787 | -1.884 |
| ILMN_17286 | NM_002304.1 | LFNG | 58696421 | 7.679 | 7.992 | 6.198 | 5.600 | -1.936 |
| ILMN_3066 | NM_000599.2 | IGFBP5 | 46094066 | 7.516 | 7.814 | 5.907 | 5.536 | -1.944 |
| ILMN_22744 | NM_004925.3 | AQP3 | 22165421 | 8.002 | 7.766 | 5.865 | 5.963 | -1.969 |
| ILMN_26240 | NM_001257.3 | CDH13 | 61676095 | 9.924 | 9.931 | 7.832 | 8.061 | -1.981 |
| ILMN_9965 | NM_033260.2 | FOXQ1 | 32526906 | 9.762 | 10.181 | 7.942 | 7.937 | -2.032 |
| ILMN_11871 | NM_003739.4 | AKR1C3 | 24497582 | 13.929 | 13.528 | 11.627 | 11.708 | -2.061 |
| ILMN_15343 | NM_153034.2 | ZNF488 | 40255102 | 8.810 | 9.439 | 6.988 | 7.102 | -2.080 |
| ILMN_15188 | NM_014689.1 | DOCK10 | 58037090 | 7.811 | 7.347 | 5.178 | 5.807 | -2.086 |
| ILMN_22014 | NM_001001548.1 | CD36 | 48375179 | 7.526 | 7.709 | 5.133 | 5.860 | -2.121 |
| ILMN_6390 | NM_000691.3 | ALDH3A1 | 22907048 | 12.978 | 12.009 | 10.311 | 10.379 | -2.148 |
| ILMN_26004 | NM_213600.2 | PLA2G4F | 67972428 | 7.237 | 7.156 | 5.463 | 4.632 | -2.149 |
| ILMN_6829 | NM_002167.2 | ID3 | 32171181 | 11.670 | 11.948 | 9.546 | 9.686 | -2.193 |
| ILMN_6827 | NM_001885.1 | CRYAB | 4503056 | 8.985 | 9.125 | 6.820 | 6.758 | -2.266 |
| ILMN_139156 | NM_001001669.1 | FLJ41603 | 48717281 | 9.598 | 10.022 | 7.669 | 7.382 | -2.285 |
| ILMN_92725 | Hs.444329 | 0 | 34365191 | 10.075 | 9.594 | 7.348 | 7.739 | -2.291 |
| ILMN_1890 | NM_000421.2 | KRT10 | 40354191 | 12.224 | 13.005 | 10.177 | 10.301 | -2.375 |
| ILMN_15305 | NM_006456.1 | ST6GALNAC2 | 5454091 | 9.604 | 10.207 | 7.223 | 7.524 | -2.532 |
| ILMN_20483 | NM_001005340.1 | GPNMB | 52694751 | 9.470 | 11.604 | 7.834 | 8.150 | -2.545 |
| ILMN_23211 | NM_002612.2 | PDK4 | 33589822 | 10.919 | 10.492 | 8.033 | 8.265 | -2.556 |
| ILMN_10249 | NM_205862.1 | UGT1A6 | 45827766 | 8.645 | 8.804 | 5.807 | 6.458 | -2.592 |
| ILMN_796 | NM_001218.3 | CA12 | 45935381 | 11.675 | 11.715 | 9.061 | 9.047 | -2.641 |
| ILMN_11770 | NM_005309.1 | GPT | 4885350 | 6.582 | 6.343 | 3.848 | 3.263 | -2.907 |
| ILMN_33314 | XM_927593.1 | ATP10B | 88986422 | 8.347 | 9.330 | 6.178 | 5.591 | -2.954 |
| ILMN_28481 | NM_002166.4 | ID2 | 33946335 | 9.044 | 9.557 | 6.094 | 6.564 | -2.972 |
| ILMN_30616 | XM_940680.1 | LOC648517 | 89061897 | 12.827 | 12.382 | 9.410 | 9.443 | -3.178 |
| ILMN_11333 | NM_014907.1 | FRMPD1 | 7662415 | 6.933 | 6.604 | 2.459 | 4.555 | -3.262 |

**Table 2: The GAB2-Selected vs GAB2-Unselected Signature in MCF10A Cells**

| Illumina ID | Accession | Symbol | Gi Accession | GAB2 UNS A Log(2) Signal | GAB2 UNS B Log(2) Signal | GAB2 SEL A Log(2) Signal | GAB2 SEL B Log(2) Signal | GAB2 SEL/ GAB2 UNS Log(2) Ratio |
|---|---|---|---|---|---|---|---|---|
| ILMN_13685 | NM_002638.2 | PI3 | 31657130 | 5.545 | 5.843 | 11.031 | 11.487 | 5.565 |
| ILMN_856 | NM_172080.1 | CAMK2B | 26051209 | 3.954 | 3.868 | 9.506 | 9.305 | 5.495 |
| ILMN_22039 | NM_000934.1 | SERPINF2 | 11386142 | 4.113 | 4.597 | 8.634 | 8.707 | 4.316 |
| ILMN_9057 | NM_006472.1 | TXNIP | 5454161 | 9.574 | 9.273 | 13.510 | 13.457 | 4.060 |
| ILMN_5259 | NM_032432.2 | ABLIM2 | 40316949 | 3.644 | 4.573 | 7.966 | 8.196 | 3.973 |
| ILMN_138170 | NM_001001873.2 | LOC283174 | 51036610 | 3.248 | 5.545 | 8.225 | 8.256 | 3.844 |
| ILMN_9653 | NM_139277.1 | KLK7 | 21327704 | 7.232 | 6.409 | 10.471 | 10.674 | 3.752 |
| ILMN_12238 | NM_206963.1 | RARRES1 | 46255042 | 5.274 | 5.912 | 8.953 | 9.110 | 3.438 |
| ILMN_8120 | NM_020037.1 | ABCC3 | 9955971 | 7.184 | 7.604 | 10.860 | 10.764 | 3.418 |
| ILMN_23106 | NM_032501.2 | ACSS1 | 28416952 | 5.182 | 5.469 | 8.861 | 8.612 | 3.411 |
| ILMN_28364 | NM_199161.1 | SAA1 | 40316909 | 8.207 | 7.863 | 11.480 | 11.369 | 3.390 |
| ILMN_19268 | NM_001185.2 | AZGP1 | 38372939 | 5.810 | 6.022 | 9.044 | 9.430 | 3.321 |
| ILMN_138896 | NM_001692.2 | ATP6V1B1 | 19913425 | 7.537 | 7.448 | 10.700 | 10.620 | 3.168 |
| ILMN_16107 | NM_001085.4 | SERPINA3 | 73858562 | 11.730 | 11.833 | 14.832 | 14.956 | 3.113 |
| ILMN_24486 | NM_006105.3 | RAPGEF3 | 45269150 | 6.131 | 5.561 | 8.971 | 8.712 | 2.996 |
| ILMN_13615 | NM_004433.3 | ELF3 | 40255034 | 6.164 | 5.865 | 8.898 | 9.044 | 2.957 |
| ILMN_12676 | NM_004454.1 | ETV5 | 4758315 | 5.202 | 5.603 | 8.589 | 8.113 | 2.949 |
| ILMN_2104 | NM_201553.1 | FGL1 | 42544201 | 3.018 | 4.926 | 6.800 | 6.938 | 2.897 |
| ILMN_19880 | NM_000636.2 | SOD2 | 67782304 | 5.142 | 5.443 | 7.916 | 8.399 | 2.866 |
| ILMN_2486 | NM_001570.3 | IRAK2 | 58530885 | 5.117 | 5.615 | 8.111 | 8.299 | 2.839 |
| ILMN_3897 | NM_001165.3 | BIRC3 | 33946283 | 7.422 | 7.272 | 10.042 | 10.274 | 2.811 |
| ILMN_10965 | NM_002888.2 | RARRES1 | 46255040 | 5.296 | 5.318 | 7.878 | 8.268 | 2.765 |
| ILMN_21166 | NM_005746.1 | PBEF1 | 5031976 | 7.596 | 7.272 | 10.049 | 10.208 | 2.694 |
| ILMN_29078 | NM_002089.1 | CXCL2 | 4504154 | 3.609 | 4.472 | 6.244 | 7.176 | 2.669 |
| ILMN_138775 | XM_936314.1 | CAMK2B | 89025915 | 4.766 | 5.100 | 7.590 | 7.565 | 2.645 |
| ILMN_8119 | NM_000667.2 | ADH1A | 11496886 | 6.285 | 6.031 | 8.592 | 8.847 | 2.561 |
| ILMN_17166 | NM_001511.1 | CXCL1 | 4504152 | 7.293 | 7.284 | 9.685 | 9.970 | 2.539 |
| ILMN_29321 | NM_001734.2 | C1S | 41393600 | 5.695 | 4.916 | 7.753 | 7.914 | 2.528 |
| ILMN_22286 | NM_005950.1 | MT1G | 10835229 | 6.615 | 6.083 | 8.729 | 8.959 | 2.495 |
| ILMN_21545 | NM_015864.2 | C6orf32 | 14277689 | 5.396 | 5.552 | 7.830 | 8.055 | 2.469 |
| ILMN_6890 | NM_021034.1 | IFITM3 | 11995467 | 11.655 | 11.562 | 14.039 | 14.112 | 2.467 |
| ILMN_14995 | NM_004460.2 | FAP | 16933539 | 5.914 | 6.514 | 8.539 | 8.789 | 2.450 |
| ILMN_12248 | NM_001710.4 | CFB | 67782357 | 8.138 | 8.504 | 10.572 | 10.920 | 2.425 |
| ILMN_32659 | XM_940668.1 | IGSF9B | 89035217 | 4.760 | 5.146 | 7.433 | 7.256 | 2.391 |
| ILMN_23395 | NM_000170.1 | GLDC | 4504012 | 7.184 | 7.106 | 9.649 | 9.407 | 2.383 |
| ILMN_19577 | NM_178868.3 | CMTM8 | 32130535 | 5.009 | 5.845 | 7.741 | 7.870 | 2.379 |
| ILMN_123833 | Hs.571652 | 0 | 13579761 | 4.104 | 4.711 | 6.471 | 7.080 | 2.368 |
| ILMN_16372 | NM_006291.2 | TNFAIP2 | 26051239 | 4.873 | 4.912 | 7.307 | 7.180 | 2.351 |
| ILMN_43594 | XM_498969.2 | LOC441019 | 88974818 | 9.170 | 9.081 | 11.350 | 11.544 | 2.322 |
| ILMN_135987 | Hs.583806 | 0 | 21177747 | 8.749 | 8.605 | 10.857 | 11.113 | 2.308 |
| ILMN_15973 | NM_012116.2 | CBLC | 20149595 | 4.931 | 4.766 | 7.180 | 7.120 | 2.302 |
| ILMN_10592 | NM_000149.1 | FUT3 | 4503808 | 5.739 | 6.309 | 8.447 | 8.189 | 2.294 |
| ILMN_14229 | NM_005630.1 | SLCO2A1 | 5032094 | 6.431 | 6.038 | 8.420 | 8.631 | 2.291 |
| ILMN_9112 | NM_003378.2 | VGF | 17136077 | 4.912 | 4.162 | 6.672 | 6.983 | 2.291 |
| ILMN_19619 | NM_018530.1 | GSDML | 8924175 | 4.413 | 4.912 | 7.047 | 6.746 | 2.234 |
| ILMN_4882 | NM_003246.2 | THBS1 | 40317625 | 6.830 | 6.807 | 9.139 | 8.960 | 2.231 |
| ILMN_15792 | NM_031415.1 | MLZE | 13899220 | 4.009 | 4.070 | 6.221 | 6.287 | 2.214 |
| ILMN_2247 | NM_000584.2 | IL8 | 28610153 | 3.548 | 4.079 | 6.100 | 5.928 | 2.201 |
| ILMN_24167 | NM_002658.2 | PLAU | 53729348 | 7.204 | 7.239 | 9.471 | 9.368 | 2.198 |
| ILMN_1025 | NM_001080.3 | ALDH5A1 | 25777719 | 5.315 | 5.236 | 7.541 | 7.401 | 2.195 |

| Table 2, continued | | | | | | | | |
|---|---|---|---|---|---|---|---|---|
| ILMN_12902 | NM_032793.2 | MFSD2 | 42713695 | 6.881 | 7.313 | 9.227 | 9.329 | 2.181 |
| ILMN_25923 | NM_001005619.1 | ITGB4 | 54607026 | 10.336 | 10.242 | 12.512 | 12.397 | 2.166 |
| ILMN_11856 | NM_207336.1 | ZNF467 | 46409309 | 7.417 | 7.527 | 9.788 | 9.486 | 2.165 |
| ILMN_19834 | NM_001733.4 | C1R | 66347874 | 6.042 | 6.081 | 7.989 | 8.428 | 2.146 |
| ILMN_16362 | NM_001005474.1 | NFKBIZ | 53832023 | 6.156 | 6.644 | 8.328 | 8.730 | 2.129 |
| ILMN_4328 | NM_018948.2 | ERRFI1 | 21314673 | 10.016 | 9.711 | 11.922 | 12.063 | 2.129 |
| ILMN_7980 | NM_138712.2 | PPARG | 62865852 | 5.514 | 5.687 | 7.840 | 7.615 | 2.127 |
| ILMN_22529 | NM_006169.2 | NNMT | 62953139 | 10.465 | 10.377 | 12.663 | 12.386 | 2.103 |
| ILMN_26715 | NM_006509.2 | RELB | 35493877 | 5.689 | 5.379 | 7.509 | 7.691 | 2.066 |
| ILMN_11116 | NM_016424.3 | CROP | 52426741 | 7.484 | 7.368 | 9.274 | 9.708 | 2.065 |
| ILMN_10642 | NM_000991.3 | RPL28 | 34486095 | 8.763 | 8.972 | 10.949 | 10.915 | 2.064 |
| ILMN_16665 | NM_018478.2 | C20orf35 | 56676381 | 9.103 | 9.013 | 11.023 | 11.222 | 2.064 |
| ILMN_28619 | NM_000336.1 | SCNN1B | 4506816 | 6.490 | 6.446 | 8.334 | 8.721 | 2.059 |
| ILMN_28190 | NM_005449.3 | FAIM3 | 34147517 | 5.482 | 5.711 | 7.548 | 7.724 | 2.039 |
| ILMN_35015 | XM_943094.1 | LOC162073 | 89040701 | 9.048 | 8.907 | 10.869 | 11.153 | 2.034 |
| ILMN_23984 | NM_001338.3 | CXADR | 45827793 | 8.318 | 8.205 | 10.272 | 10.307 | 2.028 |
| ILMN_22874 | NM_182565.2 | FAM100B | 34222379 | 7.864 | 8.094 | 10.108 | 9.898 | 2.024 |
| ILMN_25208 | NM_005534.2 | IFNGR2 | 47419933 | 9.877 | 9.556 | 11.743 | 11.731 | 2.021 |
| ILMN_25185 | NM_002982.3 | CCL2 | 56119169 | 5.263 | 6.192 | 7.480 | 7.965 | 1.995 |
| ILMN_23474 | NM_144626.1 | TMEM125 | 21389442 | 6.571 | 6.843 | 8.635 | 8.758 | 1.989 |
| ILMN_24488 | NM_024320.2 | ATAD4 | 34147376 | 7.725 | 8.161 | 9.948 | 9.884 | 1.973 |
| ILMN_1375 | NM_152594.1 | SPRED1 | 22749220 | 7.296 | 7.370 | 9.390 | 9.211 | 1.968 |
| ILMN_12497 | NM_002970.1 | SAT | 4506788 | 10.064 | 9.928 | 11.834 | 12.081 | 1.962 |
| ILMN_6000 | NM_000610.3 | CD44 | 48255934 | 5.031 | 5.296 | 6.857 | 7.392 | 1.961 |
| ILMN_17789 | NM_000418.2 | IL4R | 56788409 | 9.476 | 9.440 | 11.591 | 11.230 | 1.953 |
| ILMN_2205 | NM_020531.2 | C20orf3 | 41327713 | 9.319 | 9.260 | 11.260 | 11.218 | 1.949 |
| ILMN_775 | NM_207311.1 | CCDC64 | 46409267 | 9.599 | 9.663 | 11.584 | 11.571 | 1.946 |
| ILMN_6029 | NM_203379.1 | ACSL5 | 42794757 | 7.342 | 7.425 | 9.215 | 9.439 | 1.944 |
| ILMN_9407 | NM_004843.2 | IL27RA | 18379338 | 6.190 | 6.227 | 7.941 | 8.354 | 1.939 |
| ILMN_3488 | NM_003357.3 | SCGB1A1 | 39725696 | 5.508 | 4.945 | 6.862 | 7.430 | 1.919 |
| ILMN_22135 | NM_003900.3 | SQSTM1 | 46251280 | 9.180 | 9.234 | 11.309 | 10.939 | 1.917 |
| ILMN_20440 | NM_139314.1 | ANGPTL4 | 21536397 | 6.166 | 6.508 | 8.262 | 8.198 | 1.893 |
| ILMN_12288 | NM_020879.1 | KIAA1505 | 55741666 | 5.482 | 6.055 | 7.407 | 7.915 | 1.892 |
| ILMN_12372 | NM_014428.1 | TJP3 | 10092690 | 6.891 | 6.874 | 8.661 | 8.883 | 1.889 |
| ILMN_7322 | NM_002291.1 | LAMB1 | 4504950 | 9.341 | 9.374 | 11.117 | 11.365 | 1.884 |
| ILMN_3001 | NM_080591.1 | PTGS1 | 18104968 | 4.536 | 4.739 | 6.461 | 6.552 | 1.869 |
| ILMN_6876 | NM_003632.1 | CNTNAP1 | 4505462 | 5.661 | 5.802 | 7.673 | 7.527 | 1.869 |
| ILMN_18673 | NM_002346.1 | LY6E | 4505048 | 10.200 | 10.252 | 12.074 | 12.103 | 1.862 |
| ILMN_28594 | NM_000900.2 | MGP | 49574513 | 5.744 | 5.178 | 6.954 | 7.679 | 1.855 |
| ILMN_14234 | NM_016947.1 | C6orf48 | 8393383 | 7.583 | 7.655 | 9.595 | 9.339 | 1.847 |
| ILMN_24075 | NM_000428.2 | LTBP2 | 46389563 | 4.959 | 5.225 | 6.903 | 6.953 | 1.836 |
| ILMN_22221 | NM_152286.2 | C9orf111 | 38524588 | 6.601 | 6.501 | 8.470 | 8.296 | 1.832 |
| ILMN_4207 | NM_012329.2 | MMD | 52630444 | 6.589 | 6.809 | 8.371 | 8.672 | 1.823 |
| ILMN_25134 | NM_021809.4 | TGIF2 | 39777595 | 6.327 | 6.527 | 8.361 | 8.127 | 1.817 |
| ILMN_16420 | NM_021178.2 | CCNB1IP1 | 33519433 | 7.985 | 8.322 | 9.993 | 9.918 | 1.802 |
| ILMN_79597 | Hs.159264 | 0 | 1710274 | 4.959 | 5.154 | 6.609 | 7.093 | 1.794 |
| ILMN_21913 | NM_017420.2 | SIX4 | 61837500 | 6.358 | 6.781 | 8.361 | 8.365 | 1.793 |
| ILMN_36990 | XM_930914.1 | LOC653108 | 89058118 | 5.591 | 5.684 | 7.262 | 7.588 | 1.788 |
| ILMN_11739 | NM_002198.1 | IRF1 | 4504720 | 9.662 | 9.475 | 11.300 | 11.400 | 1.782 |
| ILMN_137046 | NM_000985.2 | RPL17 | 14591906 | 9.443 | 9.381 | 11.012 | 11.363 | 1.775 |
| ILMN_14011 | NM_004666.1 | VNN1 | 4759311 | 6.392 | 6.385 | 7.960 | 8.363 | 1.773 |
| ILMN_19983 | NM_001252.2 | TNFSF7 | 24119161 | 8.057 | 8.037 | 9.832 | 9.803 | 1.770 |
| ILMN_2142 | NM_002727.2 | PRG1 | 45935370 | 5.536 | 5.912 | 7.432 | 7.534 | 1.759 |
| ILMN_26705 | NM_006307.2 | SRPX | 21314639 | 7.438 | 7.288 | 8.970 | 9.271 | 1.757 |
| ILMN_4070 | NM_002354.1 | TACSTD1 | 4505058 | 8.618 | 8.724 | 10.187 | 10.670 | 1.757 |
| ILMN_15358 | NM_001839.2 | CNN3 | 47080096 | 8.545 | 8.636 | 10.383 | 10.308 | 1.755 |
| ILMN_14847 | NM_032421.1 | CYLN2 | 14702161 | 8.211 | 8.200 | 9.994 | 9.927 | 1.755 |

| Table 2, continued | | | | | | | | |
|---|---|---|---|---|---|---|---|---|
| ILMN_11198 | NM_005953.2 | MT2A | 31543214 | 13.561 | 13.416 | 15.221 | 15.263 | 1.754 |
| ILMN_2038 | NM_006435.1 | IFITM2 | 10835237 | 12.922 | 12.828 | 14.567 | 14.685 | 1.751 |
| ILMN_27583 | NM_198053.1 | CD3Z | 37595564 | 5.329 | 5.300 | 7.018 | 7.103 | 1.746 |
| ILMN_21293 | NM_005239.4 | ETS2 | 56119171 | 8.371 | 8.263 | 10.157 | 9.967 | 1.745 |
| ILMN_25961 | NM_001992.2 | F2R | 6031164 | 6.650 | 7.080 | 8.552 | 8.658 | 1.740 |
| ILMN_9525 | NM_181782.2 | NCOA7 | 42476174 | 9.509 | 9.252 | 10.975 | 11.261 | 1.737 |
| ILMN_14782 | NM_013363.2 | PCOLCE2 | 16904386 | 5.450 | 4.678 | 6.691 | 6.894 | 1.728 |
| ILMN_26866 | NM_030938.2 | TMEM49 | 20070348 | 7.198 | 7.029 | 8.738 | 8.912 | 1.712 |
| ILMN_28725 | NM_003714.2 | STC2 | 61676085 | 7.231 | 7.630 | 9.195 | 9.081 | 1.707 |
| ILMN_17046 | NM_080797.2 | DIDO1 | 71044476 | 6.963 | 7.009 | 8.682 | 8.665 | 1.687 |
| ILMN_16130 | NM_006997.2 | TACC2 | 45827751 | 11.101 | 10.880 | 12.627 | 12.697 | 1.671 |
| ILMN_1797 | NM_005946.2 | MT1A | 71274112 | 13.304 | 13.101 | 14.904 | 14.836 | 1.668 |
| ILMN_13004 | NM_016535.3 | ZNF581 | 50592985 | 10.139 | 10.070 | 11.820 | 11.723 | 1.667 |
| ILMN_28415 | NM_018234.2 | STEAP3 | 59853424 | 9.125 | 9.277 | 11.044 | 10.680 | 1.661 |
| ILMN_2929 | NM_001958.2 | EEF1A2 | 25453470 | 5.146 | 5.109 | 6.828 | 6.744 | 1.659 |
| ILMN_17834 | NM_006287.3 | TFPI | 40254845 | 9.324 | 9.425 | 10.988 | 11.077 | 1.658 |
| ILMN_2113 | NM_053000.1 | TIGA1 | 16506300 | 11.207 | 11.193 | 12.721 | 12.983 | 1.652 |
| ILMN_109653 | Hs.547824 | 0 | 13572203 | 6.981 | 6.484 | 8.457 | 8.303 | 1.648 |
| ILMN_10862 | NM_001017915.1 | INPP5D | 64085166 | 8.602 | 8.658 | 10.321 | 10.195 | 1.628 |
| ILMN_3809 | NM_148177.1 | FBXO32 | 22547143 | 8.644 | 8.478 | 10.171 | 10.204 | 1.627 |
| ILMN_29619 | NM_022154.5 | SLC39A8 | 59710105 | 8.170 | 8.316 | 9.638 | 10.095 | 1.624 |
| ILMN_1289 | NM_000930.2 | PLAT | 14702165 | 6.732 | 6.997 | 8.608 | 8.367 | 1.624 |
| ILMN_2840 | NM_003986.1 | BBOX1 | 4502368 | 8.822 | 8.749 | 10.343 | 10.470 | 1.621 |
| ILMN_23858 | NM_201525.1 | GPR56 | 41584197 | 7.644 | 7.718 | 9.332 | 9.270 | 1.619 |
| ILMN_12517 | NM_022746.2 | MOSC1 | 33285009 | 5.995 | 6.238 | 7.742 | 7.707 | 1.607 |
| ILMN_24466 | NM_003641.2 | IFITM1 | 40254449 | 6.387 | 6.144 | 7.895 | 7.816 | 1.590 |
| ILMN_137635 | NM_133646.1 | ZAK | 19526766 | 9.555 | 9.659 | 11.013 | 11.376 | 1.588 |
| ILMN_30361 | NM_003896.2 | ST3GAL5 | 28373079 | 4.700 | 5.311 | 6.681 | 6.503 | 1.586 |
| ILMN_23476 | NM_005980.2 | S100P | 45827727 | 8.725 | 8.574 | 10.232 | 10.216 | 1.575 |
| ILMN_11202 | NM_000481.2 | AMT | 44662837 | 6.966 | 6.825 | 8.480 | 8.461 | 1.575 |
| ILMN_15082 | NM_002012.1 | FHIT | 4503718 | 6.051 | 6.215 | 7.671 | 7.730 | 1.567 |
| ILMN_17682 | NM_000201.1 | ICAM1 | 4557877 | 5.194 | 5.426 | 6.784 | 6.966 | 1.565 |
| ILMN_26643 | NM_080489.2 | SDCBP2 | 38044113 | 6.265 | 6.317 | 7.897 | 7.789 | 1.552 |
| ILMN_25878 | NM_022817.1 | PER2 | 12707561 | 7.787 | 7.788 | 9.164 | 9.513 | 1.551 |
| ILMN_22093 | NM_016323.1 | HERC5 | 7705930 | 6.289 | 6.736 | 8.075 | 8.043 | 1.546 |
| ILMN_15059 | NM_013269.2 | CLEC2D | 52426785 | 10.826 | 10.913 | 12.253 | 12.563 | 1.538 |
| ILMN_23549 | NM_199327.1 | SPRY1 | 40788000 | 5.413 | 5.621 | 6.891 | 7.209 | 1.534 |
| ILMN_138827 | NM_145810.1 | CDCA7 | 22027513 | 7.118 | 7.481 | 8.885 | 8.779 | 1.533 |
| ILMN_17170 | NM_147161.2 | ACOT11 | 25777709 | 8.295 | 8.384 | 9.984 | 9.735 | 1.520 |
| ILMN_78206 | Hs.145444 | 0 | 10432759 | 5.858 | 6.140 | 7.541 | 7.493 | 1.518 |
| ILMN_10095 | NM_002350.1 | LYN | 4505054 | 8.297 | 8.312 | 9.733 | 9.894 | 1.509 |
| ILMN_17874 | NM_005178.2 | BCL3 | 20336471 | 6.208 | 5.986 | 7.711 | 7.491 | 1.504 |
| ILMN_138392 | NM_000997.3 | RPL37 | 60218902 | 8.574 | 8.615 | 10.010 | 10.185 | 1.504 |
| ILMN_22527 | NM_001031628.1 | LOC57228 | 76496484 | 5.304 | 5.392 | 6.695 | 6.989 | 1.494 |
| ILMN_32937 | XM_939583.1 | LOC650495 | 89056995 | 6.329 | 6.580 | 7.699 | 8.154 | 1.472 |
| ILMN_6704 | NM_001006623.1 | WDR33 | 55743158 | 5.615 | 5.771 | 7.025 | 7.304 | 1.471 |
| ILMN_28050 | NM_152705.1 | MGC9850 | 22749406 | 8.516 | 8.519 | 9.956 | 10.016 | 1.468 |
| ILMN_23535 | NM_001196.2 | BID | 37574724 | 7.568 | 7.575 | 8.954 | 9.124 | 1.467 |
| ILMN_21487 | NM_003012.3 | SFRP1 | 56117837 | 11.045 | 11.020 | 12.524 | 12.469 | 1.464 |
| ILMN_23042 | NM_001550.2 | IFRD1 | 55953128 | 7.379 | 7.445 | 8.895 | 8.851 | 1.461 |
| ILMN_5657 | NM_006762.1 | LAPTM5 | 5803055 | 7.131 | 7.249 | 8.616 | 8.679 | 1.457 |
| ILMN_14880 | NM_005384.2 | NFIL3 | 52630428 | 8.886 | 8.659 | 10.066 | 10.339 | 1.430 |
| ILMN_7434 | NM_033306.2 | CASP4 | 73622124 | 9.158 | 9.117 | 10.564 | 10.571 | 1.430 |
| ILMN_19002 | NM_000110.2 | DPYD | 4557874 | 6.961 | 6.920 | 8.188 | 8.553 | 1.430 |
| ILMN_37027 | XM_939368.1 | LOC654103 | 89028579 | 9.465 | 9.345 | 10.726 | 10.944 | 1.430 |
| ILMN_5773 | NM_004776.2 | B4GALT5 | 13929470 | 7.702 | 7.819 | 9.101 | 9.273 | 1.427 |
| ILMN_17950 | NM_024032.2 | C17orf53 | 31543178 | 7.394 | 7.397 | 8.839 | 8.799 | 1.424 |

| Table 2, continued | | | | | | | | |
|---|---|---|---|---|---|---|---|---|
| ILMN_30324 | NM_014062.1 | NOB1P | 7661531 | 7.573 | 7.569 | 8.930 | 9.050 | 1.419 |
| ILMN_2827 | NM_181077.2 | GOLGA8A | 66363690 | 6.350 | 6.453 | 7.604 | 8.032 | 1.417 |
| ILMN_38384 | XM_943699.1 | C6orf160 | 88999261 | 11.758 | 11.549 | 12.859 | 13.279 | 1.415 |
| ILMN_414 | NM_001007075.1 | KLHL5 | 55770879 | 7.973 | 7.633 | 9.108 | 9.324 | 1.413 |
| ILMN_32329 | XM_937528.1 | C10orf73 | 89031946 | 5.206 | 5.389 | 6.746 | 6.652 | 1.402 |
| ILMN_14285 | NM_174912.2 | FLJ31204 | 30410024 | 6.894 | 6.981 | 8.375 | 8.300 | 1.400 |
| ILMN_18682 | NM_025079.1 | ZC3H12A | 13376631 | 7.039 | 6.760 | 8.230 | 8.362 | 1.396 |
| ILMN_16445 | NM_002928.2 | RGS16 | 34452689 | 7.065 | 7.112 | 8.373 | 8.586 | 1.392 |
| ILMN_11237 | NM_021944.1 | C14orf93 | 11345485 | 9.046 | 9.021 | 10.461 | 10.368 | 1.381 |
| ILMN_14562 | NM_020744.2 | MTA3 | 50878291 | 8.186 | 8.154 | 9.611 | 9.471 | 1.371 |
| ILMN_20291 | NM_021212.1 | ZF | 10864024 | 7.147 | 7.252 | 8.444 | 8.667 | 1.358 |
| ILMN_28796 | NM_172027.1 | ABTB1 | 25777623 | 7.762 | 7.740 | 9.187 | 9.025 | 1.355 |
| ILMN_3780 | NM_013312.1 | HOOK2 | 7019410 | 7.131 | 7.531 | 8.832 | 8.538 | 1.354 |
| ILMN_17241 | NM_023009.4 | MARCKSL1 | 32401423 | 5.739 | 5.797 | 7.055 | 7.181 | 1.350 |
| ILMN_18617 | NM_031426.2 | C9orf58 | 50428929 | 9.185 | 9.207 | 10.673 | 10.417 | 1.349 |
| ILMN_30002 | NM_012427.3 | KLK5 | 22208993 | 6.685 | 6.800 | 8.063 | 8.111 | 1.345 |
| ILMN_1429 | NM_001032281.1 | TFPI | 73760408 | 8.019 | 7.995 | 9.248 | 9.449 | 1.341 |
| ILMN_10210 | NM_030666.2 | SERPINB1 | 20149554 | 8.917 | 8.801 | 10.174 | 10.226 | 1.341 |
| ILMN_30110 | NM_002342.1 | LTBR | 4505038 | 9.263 | 9.277 | 10.562 | 10.660 | 1.341 |
| ILMN_16803 | NM_172174.1 | IL15 | 26787983 | 6.267 | 6.556 | 7.855 | 7.648 | 1.340 |
| ILMN_3011 | NM_000386.2 | BLMH | 33591068 | 8.467 | 8.605 | 9.887 | 9.864 | 1.340 |
| ILMN_6563 | NM_005195.2 | CEBPD | 28872797 | 10.668 | 10.707 | 11.979 | 12.057 | 1.331 |
| ILMN_15496 | NM_001024668.1 | LETMD1 | 67089166 | 8.272 | 8.120 | 9.498 | 9.518 | 1.312 |
| ILMN_6835 | NM_198129.1 | LAMA3 | 38045909 | 9.868 | 9.903 | 11.261 | 11.118 | 1.304 |
| ILMN_16629 | NM_005952.2 | MT1X | 31543213 | 13.728 | 13.606 | 14.976 | 14.946 | 1.294 |
| ILMN_5772 | NM_001010853.1 | ACY1L2 | 58082084 | 7.136 | 7.165 | 8.350 | 8.538 | 1.294 |
| ILMN_74159 | Hs.91389 | 0 | 60552342 | 7.830 | 7.725 | 9.119 | 9.019 | 1.291 |
| ILMN_22701 | NM_138288.2 | C14orf147 | 46358345 | 9.450 | 9.287 | 10.713 | 10.578 | 1.277 |
| ILMN_17925 | NM_031477.3 | YPEL3 | 40255198 | 7.262 | 7.235 | 8.425 | 8.609 | 1.269 |
| ILMN_25787 | NM_024310.2 | PLEKHF1 | 31543411 | 5.469 | 5.347 | 6.764 | 6.573 | 1.260 |
| ILMN_5603 | NM_021242.3 | MID1IP1 | 39725681 | 7.904 | 7.873 | 9.168 | 9.124 | 1.257 |
| ILMN_15649 | NM_152221.2 | CSNK1E | 40549400 | 8.261 | 8.477 | 9.636 | 9.609 | 1.254 |
| ILMN_26929 | NM_004036.2 | ADCY3 | 10947058 | 9.792 | 9.764 | 11.007 | 10.991 | 1.221 |
| ILMN_17550 | NM_006963.3 | ZNF22 | 55775473 | 6.784 | 6.807 | 8.024 | 7.997 | 1.215 |
| ILMN_18913 | NM_005803.2 | FLOT1 | 6552331 | 7.912 | 7.890 | 9.155 | 9.071 | 1.212 |
| ILMN_6272 | NM_017823.3 | DUSP23 | 56786143 | 11.807 | 11.774 | 12.951 | 12.955 | 1.163 |
| ILMN_15537 | NM_001017971.1 | LOC92270 | 63003909 | 6.340 | 6.359 | 7.475 | 7.538 | 1.157 |
| ILMN_4354 | NM_024336.1 | IRX3 | 39930458 | 13.416 | 13.374 | 12.282 | 12.158 | -1.175 |
| ILMN_28967 | NM_001540.2 | HSPB1 | 4996892 | 15.104 | 14.844 | 13.665 | 13.742 | -1.271 |
| ILMN_28086 | NM_001005741.1 | GBA | 54607044 | 8.073 | 7.958 | 6.713 | 6.728 | -1.295 |
| ILMN_137303 | NM_006888.2 | CALM1 | 31377794 | 10.275 | 10.094 | 8.920 | 8.848 | -1.300 |
| ILMN_1475 | NM_018291.2 | FLJ10986 | 21361729 | 8.858 | 8.768 | 7.323 | 7.610 | -1.346 |
| ILMN_22825 | NM_201650.1 | LRRC23 | 42542395 | 8.422 | 8.428 | 7.049 | 7.106 | -1.348 |
| ILMN_26237 | NM_006082.2 | K-ALPHA-1 | 57013275 | 14.730 | 14.543 | 13.205 | 13.350 | -1.359 |
| ILMN_19382 | NM_002398.2 | MEIS1 | 45006902 | 8.093 | 8.103 | 6.654 | 6.802 | -1.370 |
| ILMN_16042 | NM_138463.2 | TLCD1 | 34147548 | 8.576 | 8.624 | 7.270 | 7.148 | -1.391 |
| ILMN_7061 | NM_013376.1 | SERTAD1 | 7019524 | 9.561 | 9.686 | 8.196 | 8.239 | -1.406 |
| ILMN_20854 | NM_014187.1 | HSPC171 | 7661829 | 9.525 | 9.526 | 8.138 | 8.067 | -1.423 |
| ILMN_36679 | XM_926231.1 | LOC642829 | 89037242 | 7.820 | 7.952 | 6.370 | 6.553 | -1.425 |
| ILMN_18658 | NM_001456.1 | FLNA | 4503744 | 8.422 | 8.650 | 7.083 | 7.082 | -1.453 |
| ILMN_7731 | NM_001013672.2 | LOC400566 | 62177143 | 7.199 | 7.354 | 5.802 | 5.838 | -1.456 |
| ILMN_21872 | NM_001956.2 | EDN2 | 31542584 | 7.743 | 7.933 | 6.213 | 6.542 | -1.460 |
| ILMN_2269 | NM_004924.3 | ACTN4 | 34452697 | 10.974 | 10.971 | 9.572 | 9.429 | -1.472 |
| ILMN_18040 | NM_000154.1 | GALK1 | 4503894 | 10.374 | 10.277 | 8.828 | 8.876 | -1.473 |
| ILMN_2565 | NM_001101.2 | ACTB | 5016088 | 12.978 | 12.768 | 11.369 | 11.418 | -1.480 |
| ILMN_991 | NM_001033030.1 | FAIM | 74271910 | 9.644 | 9.745 | 7.945 | 8.421 | -1.512 |
| ILMN_10133 | NM_020349.2 | ANKRD2 | 39812132 | 7.621 | 7.681 | 6.184 | 6.044 | -1.537 |

Table 2, continued

| | | | | | | | | |
|---|---|---|---|---|---|---|---|---|
| ILMN_26165 | NM_024684.2 | PTD015 | 34328078 | 9.608 | 9.607 | 8.039 | 8.086 | -1.545 |
| ILMN_8830 | NM_001002857.1 | ANXA2 | 50845385 | 10.850 | 10.697 | 9.243 | 9.193 | -1.555 |
| ILMN_10561 | NM_144653.3 | BTBD14A | 42716306 | 7.652 | 8.036 | 6.291 | 6.280 | -1.559 |
| ILMN_15343 | NM_153034.2 | ZNF488 | 40255102 | 8.533 | 8.721 | 6.988 | 7.102 | -1.582 |
| ILMN_1759 | NM_005175.2 | ATP5G1 | 50659067 | 8.500 | 8.683 | 7.109 | 6.909 | -1.582 |
| ILMN_6837 | NM_007150.1 | ZNF185 | 6005971 | 10.169 | 10.032 | 8.606 | 8.412 | -1.592 |
| ILMN_39336 | XM_927609.1 | LOC221710 | 88992498 | 8.253 | 8.077 | 6.571 | 6.567 | -1.596 |
| ILMN_111840 | Hs.554203 | 0 | 37547462 | 8.415 | 8.645 | 6.631 | 7.233 | -1.598 |
| ILMN_6827 | NM_001885.1 | CRYAB | 4503056 | 8.372 | 8.412 | 6.820 | 6.758 | -1.603 |
| ILMN_26449 | NM_152319.2 | C12orf54 | 34303924 | 6.296 | 6.064 | 4.322 | 4.792 | -1.623 |
| ILMN_16111 | NM_023938.4 | C1orf116 | 56550121 | 10.105 | 10.143 | 8.503 | 8.460 | -1.642 |
| ILMN_6623 | NM_005345.4 | HSPA1A | 26787973 | 11.687 | 11.878 | 9.956 | 10.315 | -1.647 |
| ILMN_37020 | XM_938141.1 | LOC647954 | 88988822 | 8.392 | 8.603 | 6.609 | 7.013 | -1.686 |
| ILMN_9690 | NM_198277.1 | SLC37A2 | 38093648 | 8.272 | 8.334 | 6.555 | 6.641 | -1.705 |
| ILMN_19792 | NM_153714.1 | C10orf67 | 24308459 | 5.977 | 5.426 | 3.536 | 4.372 | -1.748 |
| ILMN_27745 | NM_005853.4 | IRX5 | 47778932 | 9.486 | 9.535 | 7.592 | 7.929 | -1.751 |
| ILMN_25636 | NM_152666.1 | PLD5 | 22749352 | 9.151 | 9.006 | 7.234 | 7.278 | -1.823 |
| ILMN_24250 | NM_032319.1 | C2orf7 | 14150089 | 9.754 | 9.691 | 7.621 | 8.001 | -1.912 |
| ILMN_26204 | NM_001159.3 | AOX1 | 71773479 | 8.294 | 8.050 | 6.020 | 6.304 | -2.010 |
| ILMN_17578 | NM_003944.2 | SELENBP1 | 16306549 | 9.887 | 9.865 | 7.854 | 7.862 | -2.018 |
| ILMN_9547 | NM_000702.2 | ATP1A2 | 48762683 | 7.236 | 7.013 | 5.053 | 5.079 | -2.059 |
| ILMN_12568 | NM_013281.2 | FLRT3 | 38202220 | 11.762 | 11.485 | 9.412 | 9.611 | -2.112 |
| ILMN_42462 | XM_932354.1 | LOC644760 | 88984918 | 8.964 | 8.955 | 7.022 | 6.556 | -2.170 |
| ILMN_18735 | NM_153046.1 | TDRD9 | 42734387 | 8.453 | 8.369 | 6.018 | 6.350 | -2.227 |
| ILMN_29038 | NM_052862.2 | RCSD1 | 31377636 | 6.545 | 6.474 | 4.263 | 4.256 | -2.250 |
| ILMN_6575 | NM_152780.2 | FLJ14503 | 31343502 | 8.132 | 8.290 | 6.092 | 5.736 | -2.297 |
| ILMN_137325 | NM_031845.1 | MAP2 | 14195617 | 8.651 | 8.540 | 6.269 | 6.302 | -2.310 |
| ILMN_6829 | NM_002167.2 | ID3 | 32171181 | 12.029 | 12.000 | 9.546 | 9.686 | -2.399 |
| ILMN_1890 | NM_000421.2 | KRT10 | 40354191 | 12.888 | 12.509 | 10.177 | 10.301 | -2.460 |
| ILMN_17286 | NM_002304.1 | LFNG | 58696421 | 8.275 | 8.538 | 6.198 | 5.600 | -2.508 |
| ILMN_34738 | XM_945010.1 | LOC651913 | 89057548 | 10.900 | 10.601 | 8.143 | 8.277 | -2.541 |
| ILMN_28481 | NM_002166.4 | ID2 | 33946335 | 9.292 | 9.304 | 6.094 | 6.564 | -2.969 |

**Table 3: The GAB2UNS vs GFPUNS Signature in MCF10A Cells**

| Illumina ID | Accession | Symbol | Gi Accession | GFP UNS A Log(2) Signal | GFP UNS B Log(2) Signal | GAB2 UNS A Log(2) Signal | GAB2 UNS B Log(2) Signal | GAB2 UNS / GFP UNS Log(2) Ratio |
|---|---|---|---|---|---|---|---|---|
| ILMN_4712 | NM_000624.3 | SERPINA5 | 34147643 | 6.242 | 5.993 | 9.707 | 9.622 | 3.547 |
| ILMN_7403 | NM_001425.1 | EMP3 | 4503562 | 8.002 | 7.741 | 10.614 | 10.550 | 2.710 |
| ILMN_26085 | NM_003467.2 | CXCR4 | 56790928 | 5.036 | 4.848 | 7.576 | 7.441 | 2.567 |
| ILMN_26451 | NM_001008540.1 | CXCR4 | 56790926 | 5.579 | 5.472 | 8.053 | 7.857 | 2.429 |
| ILMN_9547 | NM_000702.2 | ATP1A2 | 48762683 | 5.138 | 4.661 | 7.236 | 7.013 | 2.226 |
| ILMN_138267 | NM_000211.1 | ITGB2 | 4557885 | 5.248 | 5.579 | 7.455 | 7.758 | 2.193 |
| ILMN_34738 | XM_945010.1 | LOC651913 | 89057548 | 8.577 | 8.598 | 10.900 | 10.601 | 2.163 |
| ILMN_11551 | NM_201548.3 | CERKL | 65301113 | 5.022 | 5.396 | 7.201 | 7.229 | 2.006 |
| ILMN_89562 | Hs.400256 | 0 | 21749338 | 5.961 | 6.404 | 8.172 | 8.163 | 1.985 |
| ILMN_10408 | NM_020351.2 | COL8A1 | 32895367 | 6.564 | 6.682 | 8.580 | 8.591 | 1.963 |
| ILMN_21136 | NM_014411.2 | NAG8 | 77404393 | 6.580 | 6.509 | 8.361 | 8.630 | 1.951 |
| ILMN_138577 | NM_031311.2 | CPVL | 22027517 | 7.307 | 7.570 | 9.341 | 9.404 | 1.934 |
| ILMN_17578 | NM_003944.2 | SELENBP1 | 16306549 | 8.163 | 7.772 | 9.887 | 9.865 | 1.909 |
| ILMN_20249 | NM_001006933.1 | TCEAL3 | 55749430 | 7.912 | 7.977 | 9.802 | 9.801 | 1.857 |
| ILMN_126586 | Hs.574405 | 0 | 10437775 | 5.789 | 5.632 | 7.422 | 7.674 | 1.837 |
| ILMN_22032 | NM_007168.2 | ABCA8 | 41327761 | 5.672 | 5.952 | 7.623 | 7.649 | 1.824 |
| ILMN_74694 | Hs.101003 | 0 | 27838294 | 6.728 | 6.464 | 8.377 | 8.429 | 1.807 |
| ILMN_5657 | NM_006762.1 | LAPTM5 | 5803055 | 5.396 | 5.413 | 7.131 | 7.249 | 1.786 |
| ILMN_82165 | Hs.210390 | 0 | 10435476 | 7.049 | 6.759 | 8.614 | 8.727 | 1.767 |
| ILMN_4794 | NM_153750.1 | C21orf81 | 24371249 | 6.358 | 6.359 | 8.042 | 8.208 | 1.767 |
| ILMN_27289 | NM_002578.2 | PAK3 | 46249379 | 6.940 | 6.721 | 8.581 | 8.595 | 1.757 |
| ILMN_42462 | XM_932354.1 | LOC644760 | 88984918 | 7.238 | 7.167 | 8.964 | 8.955 | 1.757 |
| ILMN_21872 | NM_001956.2 | EDN2 | 31542584 | 6.142 | 6.025 | 7.743 | 7.933 | 1.755 |
| ILMN_5489 | NM_152527.3 | SLC16A14 | 42415495 | 5.533 | 6.209 | 7.662 | 7.542 | 1.731 |
| ILMN_17796 | NM_002274.2 | KRT13 | 24234693 | 6.029 | 5.993 | 7.670 | 7.753 | 1.700 |
| ILMN_19777 | NM_182796.1 | MAT2B | 33519454 | 7.719 | 7.720 | 9.500 | 9.265 | 1.663 |
| ILMN_116404 | Hs.563578 | 0 | 1364286 | 5.213 | 5.190 | 6.580 | 7.084 | 1.631 |
| ILMN_16225 | NM_003155.2 | STC1 | 61676083 | 5.600 | 5.194 | 6.892 | 7.080 | 1.589 |
| ILMN_25536 | NM_002386.2 | MC1R | 27477128 | 6.589 | 6.416 | 8.165 | 8.002 | 1.581 |
| ILMN_29894 | NM_002975.2 | CLEC11A | 37595568 | 5.609 | 5.805 | 7.219 | 7.322 | 1.564 |
| ILMN_1896 | NM_001006937.1 | TCEAL4 | 55749458 | 11.234 | 11.339 | 12.873 | 12.782 | 1.541 |
| ILMN_124625 | Hs.572444 | 0 | 10437827 | 6.755 | 7.039 | 8.456 | 8.386 | 1.524 |
| ILMN_29854 | NM_153233.1 | FLJ36445 | 23397509 | 5.129 | 5.138 | 6.713 | 6.579 | 1.513 |
| ILMN_36989 | XM_936226.1 | LOC653879 | 89057119 | 7.107 | 7.473 | 8.698 | 8.907 | 1.512 |
| ILMN_19983 | NM_001252.2 | TNFSF7 | 24119161 | 6.751 | 6.414 | 8.057 | 8.037 | 1.464 |
| ILMN_18735 | NM_153046.1 | TDRD9 | 42734387 | 6.864 | 7.030 | 8.453 | 8.369 | 1.464 |
| ILMN_22373 | NM_001033523.1 | GUSBL1 | 75905496 | 6.450 | 6.794 | 8.264 | 7.895 | 1.457 |
| ILMN_79861 | Hs.162734 | 0 | 2276759 | 6.681 | 6.912 | 8.241 | 8.251 | 1.449 |
| ILMN_975 | NM_018945.3 | PDE7B | 57242789 | 5.527 | 5.695 | 6.965 | 7.154 | 1.448 |
| ILMN_111189 | Hs.552999 | 0 | 7023310 | 5.588 | 5.576 | 7.104 | 6.939 | 1.440 |
| ILMN_114516 | Hs.560896 | 0 | 73475707 | 5.800 | 6.029 | 7.402 | 7.287 | 1.430 |
| ILMN_27339 | NM_015642.2 | ZBTB20 | 52694664 | 6.343 | 6.318 | 7.779 | 7.705 | 1.411 |
| ILMN_33220 | XM_942936.1 | LOC648394 | 89066728 | 7.205 | 7.141 | 8.601 | 8.560 | 1.408 |
| ILMN_138785 | NM_078626.1 | CDKN2C | 17981698 | 7.113 | 7.094 | 8.341 | 8.638 | 1.386 |
| ILMN_1759 | NM_005175.2 | ATP5G1 | 50659067 | 7.258 | 7.180 | 8.500 | 8.683 | 1.372 |
| ILMN_3755 | NM_003087.1 | SNCG | 4507112 | 6.751 | 6.958 | 8.194 | 8.237 | 1.361 |
| ILMN_124068 | Hs.571887 | 0 | 10437525 | 6.796 | 6.514 | 7.954 | 8.061 | 1.353 |
| ILMN_90741 | Hs.427242 | 0 | 27831153 | 6.423 | 6.650 | 7.840 | 7.922 | 1.345 |
| ILMN_17250 | NM_004172.3 | SLC1A3 | 34222301 | 6.568 | 6.564 | 7.946 | 7.875 | 1.345 |
| ILMN_29462 | NM_014343.1 | CLDN15 | 7656980 | 7.016 | 7.062 | 8.395 | 8.335 | 1.326 |
| ILMN_108776 | Hs.545615 | 0 | 2901934 | 5.815 | 5.840 | 6.983 | 7.317 | 1.322 |

| Table 3, continued | | | | | | | | |
|---|---|---|---|---|---|---|---|---|
| ILMN_114910 | Hs.561493 | 0 | 27880608 | 5.970 | 5.838 | 7.150 | 7.295 | 1.318 |
| ILMN_22825 | NM_201650.1 | LRRC23 | 42542395 | 7.167 | 7.052 | 8.422 | 8.428 | 1.316 |
| ILMN_10248 | NM_003195.4 | TCEA2 | 38505154 | 7.343 | 7.228 | 8.656 | 8.541 | 1.313 |
| ILMN_16651 | NM_001976.2 | ENO3 | 16554590 | 6.695 | 6.610 | 7.895 | 8.025 | 1.307 |
| ILMN_37765 | XM_379668.3 | LOC286208 | 89029959 | 6.607 | 6.598 | 7.874 | 7.946 | 1.307 |
| ILMN_80530 | Hs.176498 | 0 | 51474918 | 8.170 | 8.015 | 9.272 | 9.336 | 1.211 |
| ILMN_23180 | NM_006332.3 | IFI30 | 29826337 | 9.149 | 9.134 | 10.308 | 10.366 | 1.195 |
| ILMN_12021 | NM_001407.1 | CELSR3 | 13325065 | 7.182 | 7.307 | 8.483 | 8.334 | 1.164 |
| ILMN_4354 | NM_024336.1 | IRX3 | 39930458 | 12.254 | 12.227 | 13.416 | 13.374 | 1.154 |
| ILMN_11901 | NM_012302.2 | LPHN2 | 57165356 | 9.209 | 9.252 | 8.127 | 7.995 | -1.169 |
| ILMN_19508 | NM_014878.3 | KIAA0020 | 33620772 | 9.937 | 10.048 | 8.847 | 8.795 | -1.171 |
| ILMN_5224 | NM_031412.2 | GABARAPL1 | 56676368 | 11.212 | 11.262 | 10.044 | 9.939 | -1.245 |
| ILMN_4452 | NM_003598.1 | TEAD2 | 20070102 | 9.571 | 9.445 | 8.247 | 8.215 | -1.277 |
| ILMN_23486 | NM_173354.2 | SNF1LK | 48762713 | 9.364 | 9.689 | 8.229 | 8.241 | -1.292 |
| ILMN_7334 | NM_152574.1 | C9orf52 | 22749190 | 8.313 | 8.663 | 7.139 | 7.240 | -1.299 |
| ILMN_5444 | NM_006285.2 | TESK1 | 66932998 | 8.513 | 8.576 | 7.248 | 7.205 | -1.318 |
| ILMN_4328 | NM_018948.2 | ERRFI1 | 21314673 | 11.118 | 11.288 | 10.016 | 9.711 | -1.340 |
| ILMN_14281 | NM_016359.2 | NUSAP1 | 59710089 | 10.471 | 10.591 | 9.150 | 9.232 | -1.340 |
| ILMN_14524 | NM_032899.4 | FAM83A | 46255015 | 10.557 | 10.633 | 9.364 | 9.132 | -1.347 |
| ILMN_14636 | NM_207006.1 | FAM83A | 46255016 | 8.831 | 8.809 | 7.362 | 7.571 | -1.354 |
| ILMN_6798 | NM_018474.2 | C20orf19 | 32189414 | 7.879 | 7.714 | 6.349 | 6.501 | -1.372 |
| ILMN_6776 | NM_016282.2 | AK3 | 19923436 | 11.967 | 11.938 | 10.655 | 10.494 | -1.378 |
| ILMN_13696 | NM_001011709.1 | PNLIPRP3 | 58743370 | 9.563 | 9.535 | 8.195 | 8.146 | -1.379 |
| ILMN_29031 | NM_025182.2 | KIAA1539 | 33636716 | 8.995 | 8.808 | 7.477 | 7.559 | -1.383 |
| ILMN_2937 | NM_004839.2 | HOMER2 | 46249348 | 8.573 | 8.453 | 7.075 | 7.184 | -1.383 |
| ILMN_26473 | NM_018404.1 | CENTA2 | 8923762 | 7.577 | 7.388 | 6.087 | 6.104 | -1.387 |
| ILMN_3344 | NM_152362.1 | TNFAIP8L1 | 22748780 | 8.151 | 8.260 | 6.823 | 6.796 | -1.396 |
| ILMN_23940 | NM_003979.3 | GPRC5A | 63252917 | 7.984 | 8.089 | 6.456 | 6.805 | -1.406 |
| ILMN_28045 | NM_003064.2 | SLPI | 15834622 | 12.860 | 12.883 | 11.456 | 11.440 | -1.423 |
| ILMN_137089 | NM_018304.1 | PRR11 | 8922831 | 8.056 | 7.756 | 6.354 | 6.583 | -1.437 |
| ILMN_16867 | NM_006328.2 | RBM14 | 50593004 | 10.543 | 10.643 | 9.231 | 9.078 | -1.439 |
| ILMN_6288 | NM_000196.2 | HSD11B2 | 31542940 | 7.925 | 7.937 | 6.350 | 6.624 | -1.444 |
| ILMN_16427 | NM_001237.2 | CCNA2 | 16950653 | 9.438 | 9.607 | 8.007 | 8.150 | -1.444 |
| ILMN_29273 | NM_023016.2 | C2orf26 | 54607076 | 10.224 | 10.547 | 8.988 | 8.867 | -1.458 |
| ILMN_6890 | NM_021034.1 | IFITM3 | 11995467 | 13.046 | 13.104 | 11.655 | 11.562 | -1.466 |
| ILMN_1770 | NM_006342.1 | TACC3 | 5454101 | 8.708 | 8.598 | 7.017 | 7.346 | -1.472 |
| ILMN_26449 | NM_152319.2 | C12orf54 | 34303924 | 7.485 | 7.821 | 6.296 | 6.064 | -1.473 |
| ILMN_13119 | NM_033397.2 | KIAA1754 | 47271452 | 9.922 | 9.959 | 8.593 | 8.338 | -1.475 |
| ILMN_17074 | NM_021220.2 | OVOL2 | 40807462 | 9.947 | 10.108 | 8.451 | 8.651 | -1.476 |
| ILMN_33860 | XM_926530.1 | LOC643161 | 89031545 | 7.408 | 7.183 | 5.870 | 5.763 | -1.479 |
| ILMN_10501 | NM_005213.3 | CSTA | 61743964 | 10.535 | 10.646 | 9.065 | 9.153 | -1.482 |
| ILMN_15718 | NM_001001788.1 | RAET1G | 49169824 | 10.365 | 10.637 | 8.877 | 9.069 | -1.528 |
| ILMN_19849 | NM_001067.2 | TOP2A | 19913405 | 10.080 | 10.069 | 8.384 | 8.705 | -1.530 |
| ILMN_8225 | NM_016343.3 | CENPF | 55770833 | 8.532 | 8.931 | 7.042 | 7.358 | -1.531 |
| ILMN_26240 | NM_001257.3 | CDH13 | 61676095 | 9.255 | 9.276 | 7.951 | 7.402 | -1.589 |
| ILMN_12902 | NM_032793.2 | MFSD2 | 42713695 | 8.775 | 8.603 | 6.881 | 7.313 | -1.591 |
| ILMN_15185 | NM_201631.1 | TGM5 | 42518071 | 6.564 | 6.908 | 4.807 | 5.476 | -1.594 |
| ILMN_25878 | NM_022817.1 | PER2 | 12707561 | 9.367 | 9.404 | 7.787 | 7.788 | -1.598 |
| ILMN_19035 | NM_007267.5 | TMC6 | 34222212 | 7.385 | 7.522 | 5.982 | 5.700 | -1.613 |
| ILMN_25474 | NM_178229.3 | IQGAP3 | 39753960 | 10.769 | 10.837 | 9.035 | 9.294 | -1.639 |
| ILMN_25582 | NM_017779.3 | DEPDC1 | 41282232 | 7.403 | 7.872 | 5.853 | 6.121 | -1.651 |
| ILMN_25445 | NM_174919.2 | LOC201175 | 31341379 | 7.807 | 7.919 | 6.188 | 6.229 | -1.654 |
| ILMN_23211 | NM_002612.2 | PDK4 | 33589822 | 10.123 | 10.171 | 8.558 | 8.418 | -1.659 |
| ILMN_10912 | NM_000361.2 | THBD | 40288292 | 7.267 | 7.435 | 5.675 | 5.689 | -1.668 |
| ILMN_136986 | NM_001024209.1 | SPRR2E | 66730572 | 6.509 | 6.729 | 4.954 | 4.931 | -1.677 |
| ILMN_11548 | NM_000088.2 | COL1A1 | 14719826 | 7.438 | 7.403 | 5.890 | 5.591 | -1.680 |
| ILMN_7864 | NM_016525.3 | UBAP1 | 22212941 | 10.401 | 10.401 | 8.595 | 8.846 | -1.680 |

| Table 3, continued | | | | | | | | |
|---|---|---|---|---|---|---|---|---|
| ILMN_20465 | NM_003981.2 | PRC1 | 40807441 | 11.103 | 11.093 | 9.228 | 9.595 | -1.687 |
| ILMN_23476 | NM_005980.2 | S100P | 45827727 | 10.268 | 10.405 | 8.725 | 8.574 | -1.687 |
| ILMN_9096 | NM_005168.3 | RND3 | 56676394 | 10.211 | 10.402 | 8.665 | 8.570 | -1.689 |
| ILMN_10853 | NM_016006.3 | ABHD5 | 33469972 | 9.680 | 9.992 | 8.290 | 8.000 | -1.691 |
| ILMN_13755 | NM_001307.3 | CLDN7 | 34222214 | 11.962 | 11.889 | 10.099 | 10.355 | -1.699 |
| ILMN_13141 | NM_005480.2 | TROAP | 33438581 | 8.529 | 8.408 | 6.714 | 6.818 | -1.703 |
| ILMN_22039 | NM_000934.1 | SERPINF2 | 11386142 | 6.027 | 6.140 | 4.113 | 4.597 | -1.728 |
| ILMN_9525 | NM_181782.2 | NCOA7 | 42476174 | 11.024 | 11.207 | 9.509 | 9.252 | -1.734 |
| ILMN_17166 | NM_001511.1 | CXCL1 | 4504152 | 8.896 | 9.170 | 7.293 | 7.284 | -1.745 |
| ILMN_26077 | NM_020211.1 | RGMA | 24308188 | 7.472 | 7.648 | 5.621 | 5.977 | -1.761 |
| ILMN_26025 | NM_024554.2 | PGBD5 | 25777747 | 7.445 | 7.490 | 5.629 | 5.779 | -1.763 |
| ILMN_25969 | NM_006845.2 | KIF2C | 13699832 | 8.811 | 8.633 | 6.854 | 7.060 | -1.765 |
| ILMN_12592 | NM_206833.1 | CTXN1 | 45592953 | 9.429 | 9.500 | 7.654 | 7.730 | -1.773 |
| ILMN_17961 | NM_001300.4 | KLF6 | 56550115 | 12.280 | 12.315 | 10.397 | 10.619 | -1.789 |
| ILMN_15305 | NM_006456.1 | ST6GALNAC2 | 5454091 | 9.237 | 9.115 | 7.333 | 7.428 | -1.796 |
| ILMN_16107 | NM_001085.4 | SERPINA3 | 73858562 | 13.628 | 13.578 | 11.730 | 11.833 | -1.822 |
| ILMN_2226 | NM_032413.2 | C15orf48 | 37694068 | 6.121 | 6.746 | 4.420 | 4.728 | -1.860 |
| ILMN_25992 | NM_003485.3 | GPR68 | 74316010 | 6.610 | 7.195 | 4.561 | 5.514 | -1.865 |
| ILMN_16399 | NM_006086.2 | TUBB3 | 50592995 | 10.431 | 10.369 | 8.433 | 8.632 | -1.868 |
| ILMN_29321 | NM_001734.2 | C1S | 41393600 | 7.199 | 7.177 | 5.695 | 4.916 | -1.882 |
| ILMN_5176 | NM_020428.2 | SLC44A2 | 31377726 | 10.051 | 10.083 | 8.059 | 8.305 | -1.885 |
| ILMN_15028 | NM_000359.1 | TGM1 | 4507474 | 11.618 | 11.694 | 9.833 | 9.700 | -1.890 |
| ILMN_16900 | NM_012485.1 | HMMR | 7108350 | 10.135 | 10.223 | 8.146 | 8.432 | -1.890 |
| ILMN_12381 | NM_001008490.1 | KLF6 | 56550082 | 9.155 | 9.264 | 7.155 | 7.470 | -1.897 |
| ILMN_112886 | Hs.557559 | 0 | 5438942 | 7.825 | 7.382 | 5.597 | 5.797 | -1.907 |
| ILMN_22415 | NM_020789.2 | IGSF9 | 34147342 | 7.733 | 7.707 | 5.667 | 5.954 | -1.910 |
| ILMN_6398 | NM_181803.1 | UBE2C | 32967290 | 11.120 | 11.232 | 9.042 | 9.412 | -1.949 |
| ILMN_9624 | NM_207381.2 | TNFAIP8L3 | 59709435 | 8.503 | 8.689 | 6.394 | 6.849 | -1.975 |
| ILMN_28547 | NM_002298.2 | LCP1 | 7382490 | 7.474 | 7.761 | 5.282 | 5.995 | -1.979 |
| ILMN_15188 | NM_014689.1 | DOCK10 | 58037090 | 7.493 | 7.926 | 6.013 | 5.413 | -1.996 |
| ILMN_4880 | NM_014750.3 | DLG7 | 21361644 | 9.360 | 9.495 | 7.345 | 7.497 | -2.006 |
| ILMN_29078 | NM_002089.1 | CXCL2 | 4504154 | 5.870 | 6.227 | 3.609 | 4.472 | -2.008 |
| ILMN_135987 | Hs.583806 | 0 | 21177747 | 10.660 | 10.715 | 8.749 | 8.605 | -2.011 |
| ILMN_24887 | NM_178448.2 | C9orf140 | 31341967 | 8.212 | 8.114 | 6.049 | 6.211 | -2.033 |
| ILMN_138896 | NM_001692.2 | ATP6V1B1 | 19913425 | 9.556 | 9.496 | 7.537 | 7.448 | -2.033 |
| ILMN_24167 | NM_002658.2 | PLAU | 53729348 | 9.262 | 9.340 | 7.204 | 7.239 | -2.079 |
| ILMN_11466 | NM_014911.2 | AAK1 | 29570779 | 6.821 | 6.248 | 4.926 | 3.982 | -2.081 |
| ILMN_28750 | NM_000067.1 | CA2 | 4557394 | 11.209 | 11.329 | 9.256 | 9.075 | -2.103 |
| ILMN_11693 | NM_002317.3 | LOX | 21264603 | 9.131 | 9.340 | 7.319 | 6.928 | -2.111 |
| ILMN_22827 | NM_003810.2 | TNFSF10 | 23510439 | 8.501 | 8.604 | 6.588 | 6.235 | -2.141 |
| ILMN_14995 | NM_004460.2 | FAP | 16933539 | 8.298 | 8.426 | 5.914 | 6.514 | -2.148 |
| ILMN_14100 | NM_005733.1 | KIF20A | 5032012 | 10.682 | 10.747 | 8.215 | 8.910 | -2.152 |
| ILMN_15254 | NM_004701.2 | CCNB2 | 10938017 | 10.973 | 11.049 | 8.723 | 8.972 | -2.163 |
| ILMN_15973 | NM_012116.2 | CBLC | 20149595 | 7.087 | 6.939 | 4.931 | 4.766 | -2.165 |
| ILMN_26343 | NM_004004.3 | GJB2 | 42558282 | 8.512 | 8.685 | 6.333 | 6.500 | -2.182 |
| ILMN_73498 | Hs.72010 | 0 | 13726849 | 7.012 | 7.188 | 5.213 | 4.536 | -2.225 |
| ILMN_9313 | NM_005130.3 | FGFBP1 | 49574208 | 10.762 | 10.873 | 8.505 | 8.661 | -2.235 |
| ILMN_19881 | NM_014214.1 | IMPA2 | 7657235 | 11.938 | 11.901 | 9.742 | 9.601 | -2.248 |
| ILMN_15792 | NM_031415.1 | MLZE | 13899220 | 6.231 | 6.385 | 4.009 | 4.070 | -2.268 |
| ILMN_3001 | NM_080591.1 | PTGS1 | 18104968 | 7.097 | 6.718 | 4.536 | 4.739 | -2.270 |
| ILMN_1127 | NM_005030.3 | PLK1 | 34147632 | 7.831 | 7.643 | 5.863 | 5.044 | -2.283 |
| ILMN_16362 | NM_001005474.1 | NFKBIZ | 53832023 | 8.688 | 8.724 | 6.156 | 6.644 | -2.306 |
| ILMN_20689 | NM_000076.1 | CDKN1C | 4557440 | 10.982 | 10.899 | 8.706 | 8.495 | -2.340 |
| ILMN_92725 | Hs.444329 | 0 | 34365191 | 9.439 | 9.683 | 7.229 | 7.210 | -2.342 |
| ILMN_23858 | NM_201525.1 | GPR56 | 41584197 | 9.969 | 10.120 | 7.644 | 7.718 | -2.363 |
| ILMN_10005 | NM_031966.2 | CCNB1 | 34304372 | 10.136 | 10.300 | 7.764 | 7.930 | -2.371 |
| ILMN_12497 | NM_002970.1 | SAT | 4506788 | 12.343 | 12.453 | 10.064 | 9.928 | -2.402 |

| Table 3, continued | | | | | | | | |
|---|---|---|---|---|---|---|---|---|
| ILMN_4602 | NM_005988.2 | SPRR2A | 46094054 | 7.543 | 7.723 | 4.818 | 5.638 | -2.405 |
| ILMN_22377 | NM_001333.2 | CTSL2 | 23110959 | 9.660 | 9.604 | 7.098 | 7.343 | -2.412 |
| ILMN_29470 | NM_015150.1 | RAFTLIN | 41872576 | 7.091 | 6.944 | 4.256 | 4.878 | -2.451 |
| ILMN_6390 | NM_000691.3 | ALDH3A1 | 22907048 | 12.593 | 12.426 | 10.059 | 10.029 | -2.465 |
| ILMN_11871 | NM_003739.4 | AKR1C3 | 24497582 | 13.157 | 13.113 | 10.627 | 10.690 | -2.477 |
| ILMN_10722 | NM_004062.2 | CDH16 | 16507958 | 7.670 | 7.401 | 4.505 | 5.603 | -2.481 |
| ILMN_22744 | NM_004925.3 | AQP3 | 22165421 | 8.699 | 8.321 | 5.907 | 6.117 | -2.498 |
| ILMN_26643 | NM_080489.2 | SDCBP2 | 38044113 | 8.787 | 8.804 | 6.265 | 6.317 | -2.505 |
| ILMN_20932 | NM_001964.2 | EGR1 | 31317226 | 9.528 | 9.425 | 7.062 | 6.810 | -2.540 |
| ILMN_6827 | NM_001885.1 | CRYAB | 4503056 | 10.924 | 10.977 | 8.372 | 8.412 | -2.558 |
| ILMN_491 | NM_021945.4 | C6orf85 | 48526515 | 9.687 | 9.541 | 7.102 | 6.970 | -2.578 |
| ILMN_7567 | NM_005558.3 | LAD1 | 32455232 | 13.139 | 13.213 | 10.660 | 10.484 | -2.604 |
| ILMN_30616 | XM_940680.1 | LOC648517 | 89061897 | 11.345 | 11.392 | 8.767 | 8.652 | -2.659 |
| ILMN_30002 | NM_012427.3 | KLK5 | 22208993 | 9.377 | 9.444 | 6.685 | 6.800 | -2.668 |
| ILMN_796 | NM_001218.3 | CA12 | 45935381 | 11.142 | 10.952 | 8.360 | 8.393 | -2.671 |
| ILMN_1768 | NM_001001414.1 | LOC342897 | 47825360 | 8.250 | 8.384 | 5.585 | 5.594 | -2.728 |
| ILMN_28364 | NM_199161.1 | SAA1 | 40316909 | 10.853 | 10.721 | 8.207 | 7.863 | -2.752 |
| ILMN_2247 | NM_000584.2 | IL8 | 28610153 | 6.451 | 6.792 | 3.548 | 4.079 | -2.808 |
| ILMN_14915 | NM_052815.1 | IER3 | 16554596 | 10.474 | 10.515 | 7.700 | 7.589 | -2.850 |
| ILMN_2266 | NM_002963.2 | S100A7 | 9845518 | 8.926 | 9.086 | 6.013 | 6.285 | -2.857 |
| ILMN_3781 | NM_001012632.1 | IL32 | 61658631 | 6.497 | 6.493 | 3.278 | 3.907 | -2.903 |
| ILMN_9653 | NM_139277.1 | KLK7 | 21327704 | 9.754 | 9.711 | 7.232 | 6.409 | -2.912 |
| ILMN_16252 | NM_001878.2 | CRABP2 | 6382069 | 9.793 | 10.069 | 6.739 | 7.280 | -2.922 |
| ILMN_1498 | NM_198538.1 | SBSN | 38348365 | 8.067 | 8.206 | 4.848 | 5.311 | -3.057 |
| ILMN_12614 | NM_024702.1 | FLJ13841 | 13375990 | 8.860 | 8.869 | 5.252 | 6.125 | -3.177 |
| ILMN_21964 | NM_002648.2 | PIM1 | 31543400 | 10.793 | 10.850 | 7.543 | 7.321 | -3.390 |
| ILMN_8892 | NM_181712.2 | ANKRD38 | 44917612 | 8.848 | 8.928 | 4.968 | 5.931 | -3.439 |
| ILMN_14466 | NM_002575.1 | SERPINB2 | 4505594 | 10.564 | 10.361 | 6.751 | 6.670 | -3.752 |
| ILMN_9057 | NM_006472.1 | TXNIP | 5454161 | 13.282 | 13.240 | 9.574 | 9.273 | -3.837 |
| ILMN_7664 | NM_005555.2 | KRT6B | 17505187 | 12.319 | 12.560 | 7.660 | 7.568 | -4.826 |
| ILMN_138240 | NM_003125.1 | SPRR1B | 4507186 | 10.904 | 10.825 | 5.760 | 5.888 | -5.040 |
| ILMN_13685 | NM_002638.2 | PI3 | 31657130 | 13.344 | 13.390 | 5.545 | 5.843 | -7.673 |

**Table 4: The GFPSEL vs GFPUNS Signature in MCF10A Cells**

| Illumina ID | Accession | Symbol | Gi Accession | GFP UNS A Log(2) Signal | GFP UNS B Log(2) Signal | GFP SEL A Log(2) Signal | GFP SEL B Log(2) Signal | GFP SEL / GFP UNS Log(2) Ratio |
|---|---|---|---|---|---|---|---|---|
| ILMN_20483 | NM_001005340.1 | GPNMB | 52694751 | 7.548 | 7.000 | 9.470 | 11.604 | 3.263 |
| ILMN_19880 | NM_000636.2 | SOD2 | 67782304 | 6.062 | 5.880 | 8.204 | 9.158 | 2.710 |
| ILMN_12248 | NM_001710.4 | CFB | 67782357 | 8.149 | 8.092 | 10.149 | 10.952 | 2.430 |
| ILMN_36989 | XM_936226.1 | LOC653879 | 89057119 | 7.107 | 7.473 | 9.380 | 9.952 | 2.375 |
| ILMN_3897 | NM_001165.3 | BIRC3 | 33946283 | 8.409 | 8.330 | 10.811 | 10.627 | 2.349 |
| ILMN_3297 | NM_000777.2 | CYP3A5 | 15147331 | 5.838 | 5.372 | 7.764 | 8.019 | 2.287 |
| ILMN_29078 | NM_002089.1 | CXCL2 | 4504154 | 5.870 | 6.227 | 8.215 | 8.407 | 2.262 |
| ILMN_17250 | NM_004172.3 | SLC1A3 | 34222301 | 6.568 | 6.564 | 8.675 | 8.812 | 2.178 |
| ILMN_16547 | NM_013261.2 | PPARGC1A | 29570796 | 5.850 | 5.446 | 7.307 | 7.737 | 1.873 |
| ILMN_14847 | NM_032421.1 | CYLN2 | 14702161 | 7.659 | 7.796 | 9.390 | 9.746 | 1.840 |
| ILMN_5682 | NM_000064.1 | C3 | 4557384 | 10.367 | 10.229 | 11.749 | 12.348 | 1.750 |
| ILMN_3319 | NM_015541.2 | LRIG1 | 54607117 | 4.350 | 4.440 | 5.865 | 6.190 | 1.633 |
| ILMN_28225 | NM_207397.1 | CD164L2 | 46409425 | 5.681 | 5.539 | 7.431 | 6.968 | 1.590 |
| ILMN_29321 | NM_001734.2 | C1S | 41393600 | 7.199 | 7.177 | 8.774 | 8.768 | 1.583 |
| ILMN_11739 | NM_002198.1 | IRF1 | 4504720 | 9.600 | 9.730 | 11.063 | 11.357 | 1.545 |
| ILMN_35526 | XM_935575.1 | LOC641825 | 89027574 | 3.807 | 4.027 | 5.385 | 5.530 | 1.541 |
| ILMN_2205 | NM_020531.2 | C20orf3 | 41327713 | 9.495 | 9.371 | 10.953 | 10.945 | 1.516 |
| ILMN_7322 | NM_002291.1 | LAMB1 | 4504950 | 9.214 | 9.260 | 10.746 | 10.689 | 1.480 |
| ILMN_19834 | NM_001733.4 | C1R | 66347874 | 7.036 | 7.045 | 8.321 | 8.713 | 1.476 |
| ILMN_20048 | NM_018370.1 | FLJ11259 | 8922957 | 6.695 | 6.552 | 7.926 | 8.223 | 1.451 |
| ILMN_5957 | NM_015187.1 | KIAA0746 | 39930348 | 9.031 | 8.995 | 10.452 | 10.434 | 1.430 |
| ILMN_15496 | NM_001024668.1 | LETMD1 | 67089166 | 8.077 | 8.102 | 9.429 | 9.604 | 1.427 |
| ILMN_71591 | Hs.19339 | 0 | 34191392 | 7.770 | 7.846 | 9.050 | 9.362 | 1.398 |
| ILMN_6029 | NM_203379.1 | ACSL5 | 42794757 | 7.387 | 7.575 | 8.691 | 9.051 | 1.390 |
| ILMN_29422 | NM_024101.4 | MLPH | 34222365 | 6.459 | 6.397 | 7.578 | 7.903 | 1.312 |
| ILMN_15035 | NM_000877.2 | IL1R1 | 27894331 | 6.404 | 6.642 | 7.984 | 7.679 | 1.308 |
| ILMN_138073 | NM_021255.1 | PELI2 | 10864062 | 5.443 | 5.638 | 6.853 | 6.805 | 1.288 |
| ILMN_23910 | NM_178349.1 | LCE1B | 30387655 | 5.853 | 5.810 | 7.150 | 7.044 | 1.266 |
| ILMN_9457 | NM_013262.3 | MYLIP | 38788242 | 7.470 | 7.525 | 8.580 | 8.888 | 1.237 |
| ILMN_7413 | NM_003594.3 | TTF2 | 40807470 | 9.111 | 9.085 | 7.837 | 8.007 | -1.176 |
| ILMN_103797 | Hs.538259 | 0 | 23273338 | 7.881 | 7.906 | 6.794 | 6.579 | -1.207 |
| ILMN_2476 | NM_006505.2 | PVR | 19923371 | 8.508 | 8.337 | 7.180 | 7.164 | -1.251 |
| ILMN_3629 | NM_182507.1 | LOC144501 | 32698852 | 7.521 | 7.684 | 6.198 | 6.468 | -1.270 |
| ILMN_7092 | NM_003686.3 | EXO1 | 39995068 | 7.607 | 7.493 | 6.300 | 6.235 | -1.283 |
| ILMN_6133 | NM_003173.1 | SUV39H1 | 4507320 | 8.678 | 8.714 | 7.457 | 7.338 | -1.298 |
| ILMN_16808 | NM_031423.2 | CDCA1 | 22027505 | 6.994 | 7.223 | 5.855 | 5.750 | -1.306 |
| ILMN_18637 | NM_001034.1 | RRM2 | 4557844 | 7.050 | 7.272 | 5.807 | 5.890 | -1.312 |
| ILMN_4220 | NM_002106.3 | H2AFZ | 53759146 | 13.394 | 13.355 | 12.102 | 11.936 | -1.356 |
| ILMN_12816 | NM_015703.3 | CGI-96 | 62751922 | 9.245 | 9.027 | 7.840 | 7.673 | -1.379 |
| ILMN_12332 | NM_001798.2 | CDK2 | 16936527 | 8.254 | 8.311 | 6.890 | 6.901 | -1.387 |
| ILMN_3344 | NM_152362.1 | TNFAIP8L1 | 22748780 | 8.151 | 8.260 | 6.736 | 6.896 | -1.389 |
| ILMN_1608 | NM_001070.3 | TUBG1 | 34222287 | 9.796 | 9.729 | 8.397 | 8.332 | -1.398 |
| ILMN_15944 | NM_001002799.1 | SMC4L1 | 50658066 | 9.871 | 10.053 | 8.558 | 8.556 | -1.405 |
| ILMN_9096 | NM_005168.3 | RND3 | 56676394 | 10.211 | 10.402 | 8.762 | 8.978 | -1.436 |
| ILMN_4289 | NM_001018.3 | RPS15 | 71284430 | 9.992 | 9.848 | 8.719 | 8.240 | -1.440 |
| ILMN_13450 | NM_012145.2 | DTYMK | 42544173 | 9.372 | 9.580 | 8.188 | 7.867 | -1.448 |
| ILMN_16938 | NM_017669.2 | FLJ20105 | 58331267 | 7.421 | 7.271 | 5.860 | 5.860 | -1.485 |
| ILMN_16948 | NM_030919.1 | C20orf129 | 24308304 | 9.180 | 9.191 | 7.772 | 7.617 | -1.491 |
| ILMN_28902 | NM_016240.2 | SCARA3 | 33598923 | 6.819 | 6.601 | 5.027 | 5.326 | -1.534 |

| Table 4, continued | | | | | | | | |
|---|---|---|---|---|---|---|---|---|
| ILMN_11313 | NM_001826.1 | CKS1B | 4502856 | 11.652 | 11.600 | 9.961 | 10.219 | -1.536 |
| ILMN_19331 | NM_152562.2 | CDCA2 | 44681483 | 6.921 | 7.198 | 5.396 | 5.635 | -1.544 |
| ILMN_20484 | NM_006397.2 | RNASEH2A | 38455390 | 8.356 | 8.222 | 6.768 | 6.714 | -1.548 |
| ILMN_11654 | NM_016639.1 | TNFRSF12A | 7706185 | 9.246 | 9.311 | 7.690 | 7.748 | -1.559 |
| ILMN_20327 | NM_001012271.1 | BIRC5 | 59859881 | 7.388 | 7.115 | 5.692 | 5.689 | -1.561 |
| ILMN_20107 | NM_006739.2 | MCM5 | 23510447 | 7.480 | 7.477 | 5.890 | 5.928 | -1.569 |
| ILMN_21369 | NM_003920.2 | TIMELESS | 52851463 | 8.974 | 8.911 | 7.452 | 7.290 | -1.572 |
| ILMN_1748 | NM_001005290.2 | PSRC1 | 73858557 | 7.963 | 8.087 | 6.640 | 6.256 | -1.578 |
| ILMN_3628 | NM_024094.1 | DCC1 | 13129095 | 7.514 | 7.253 | 5.766 | 5.830 | -1.585 |
| ILMN_26621 | NM_014865.2 | CNAP1 | 41281520 | 8.550 | 8.228 | 6.825 | 6.744 | -1.605 |
| ILMN_22415 | NM_020789.2 | IGSF9 | 34147342 | 7.733 | 7.707 | 6.324 | 5.907 | -1.605 |
| ILMN_138879 | NM_018193.1 | KIAA1794 | 42734338 | 8.317 | 8.354 | 6.677 | 6.785 | -1.605 |
| ILMN_12592 | NM_206833.1 | CTXN1 | 45592953 | 9.429 | 9.500 | 7.844 | 7.834 | -1.626 |
| ILMN_9870 | NM_003878.1 | GGH | 4503986 | 9.670 | 9.730 | 8.361 | 7.773 | -1.633 |
| ILMN_2930 | NM_052842.2 | BCL2L12 | 20336331 | 9.441 | 9.341 | 7.779 | 7.712 | -1.645 |
| ILMN_25046 | NM_006479.2 | RAD51AP1 | 19923778 | 7.313 | 7.340 | 5.463 | 5.888 | -1.651 |
| ILMN_18895 | NM_030928.2 | CDT1 | 19923847 | 8.468 | 8.317 | 6.759 | 6.711 | -1.657 |
| ILMN_15846 | NM_014264.2 | PLK4 | 21361432 | 8.244 | 8.233 | 6.541 | 6.621 | -1.658 |
| ILMN_23727 | NM_052886.1 | MAL2 | 16418396 | 11.709 | 11.826 | 10.159 | 10.052 | -1.662 |
| ILMN_14464 | NM_001012413.1 | SGOL1 | 60302878 | 6.430 | 6.302 | 4.728 | 4.644 | -1.680 |
| ILMN_22897 | NM_173608.1 | C14orf80 | 27734692 | 8.196 | 8.090 | 6.250 | 6.651 | -1.692 |
| ILMN_21947 | NM_024053.3 | C22orf18 | 50845412 | 7.299 | 7.319 | 5.675 | 5.552 | -1.696 |
| ILMN_13755 | NM_001307.3 | CLDN7 | 34222214 | 11.962 | 11.889 | 10.453 | 10.007 | -1.696 |
| ILMN_5134 | NM_018186.2 | C1orf112 | 40254930 | 8.266 | 8.137 | 6.568 | 6.428 | -1.703 |
| ILMN_11775 | NM_005563.3 | STMN1 | 44889961 | 8.284 | 8.333 | 6.600 | 6.609 | -1.704 |
| ILMN_18980 | NM_002130.4 | HMGCS1 | 54020719 | 10.053 | 9.978 | 8.500 | 8.114 | -1.708 |
| ILMN_23585 | NM_002105.2 | H2AFX | 52630339 | 8.856 | 8.935 | 7.128 | 7.241 | -1.711 |
| ILMN_9074 | NM_001175.4 | ARHGDIB | 56676392 | 9.941 | 9.878 | 8.266 | 8.078 | -1.737 |
| ILMN_11802 | NM_004856.4 | KIF23 | 20143965 | 8.213 | 8.311 | 6.576 | 6.459 | -1.745 |
| ILMN_24712 | NM_032737.2 | LMNB2 | 27436950 | 11.223 | 11.064 | 9.452 | 9.314 | -1.761 |
| ILMN_18676 | NM_019013.1 | FAM64A | 9506604 | 7.820 | 7.693 | 5.989 | 5.995 | -1.764 |
| ILMN_129103 | Hs.576922 | 0 | 27552801 | 7.093 | 7.597 | 5.463 | 5.687 | -1.770 |
| ILMN_138334 | NM_015675.1 | GADD45B | 9945331 | 8.361 | 8.307 | 6.613 | 6.513 | -1.771 |
| ILMN_8503 | NM_004523.2 | KIF11 | 13699823 | 8.519 | 8.570 | 6.709 | 6.824 | -1.778 |
| ILMN_137089 | NM_018304.1 | PRR11 | 8922831 | 8.056 | 7.756 | 6.229 | 6.027 | -1.778 |
| ILMN_29781 | NM_014875.1 | KIF14 | 7661877 | 7.725 | 8.220 | 6.406 | 5.933 | -1.803 |
| ILMN_10665 | NM_018455.3 | C16orf60 | 39725678 | 9.369 | 9.446 | 7.754 | 7.451 | -1.805 |
| ILMN_869 | NM_145061.3 | C13orf3 | 47419927 | 7.740 | 7.592 | 5.963 | 5.752 | -1.808 |
| ILMN_137325 | NM_031845.1 | MAP2 | 14195617 | 7.869 | 7.816 | 5.986 | 6.060 | -1.819 |
| ILMN_20794 | NM_005564.2 | LCN2 | 38455401 | 8.494 | 8.529 | 6.829 | 6.542 | -1.826 |
| ILMN_752 | NM_183049.2 | TMSL3 | 72255572 | 14.397 | 14.328 | 12.668 | 12.406 | -1.826 |
| ILMN_36910 | XM_927270.1 | LOC653400 | 88983843 | 7.504 | 7.947 | 6.174 | 5.624 | -1.827 |
| ILMN_15061 | NM_004237.2 | TRIP13 | 20149561 | 8.564 | 8.703 | 6.863 | 6.746 | -1.829 |
| ILMN_26148 | NM_018154.2 | ASF1B | 67782340 | 7.167 | 7.191 | 5.350 | 5.347 | -1.830 |
| ILMN_137482 | NM_017915.1 | C12orf48 | 8923595 | 9.092 | 9.101 | 7.426 | 7.097 | -1.835 |
| ILMN_23940 | NM_003979.3 | GPRC5A | 63252917 | 7.984 | 8.089 | 6.188 | 6.208 | -1.838 |
| ILMN_11038 | NM_145018.2 | FLJ25416 | 25072198 | 7.400 | 7.659 | 5.498 | 5.875 | -1.843 |
| ILMN_2026 | NM_014736.4 | KIAA0101 | 71773764 | 10.026 | 9.965 | 8.634 | 7.657 | -1.850 |
| ILMN_26854 | NM_016095.1 | Pfs2 | 7706366 | 8.260 | 8.036 | 6.370 | 6.217 | -1.854 |
| ILMN_14098 | NM_006101.1 | KNTC2 | 5174456 | 7.362 | 7.729 | 5.797 | 5.585 | -1.855 |
| ILMN_35948 | XM_935208.1 | LOC645625 | 89041729 | 8.978 | 9.107 | 6.890 | 7.443 | -1.876 |
| ILMN_1768 | NM_001001414.1 | LOC342897 | 47825360 | 8.250 | 8.384 | 6.691 | 6.180 | -1.882 |
| ILMN_16127 | NM_001790.2 | CDC25C | 12408659 | 7.499 | 7.513 | 5.440 | 5.807 | -1.883 |
| ILMN_36283 | XM_940001.1 | MGC40489 | 89042906 | 8.118 | 8.588 | 6.094 | 6.840 | -1.886 |
| ILMN_6827 | NM_001885.1 | CRYAB | 4503056 | 10.924 | 10.977 | 8.985 | 9.125 | -1.896 |
| ILMN_12202 | NM_020127.1 | TUFT1 | 9910595 | 9.234 | 9.385 | 7.420 | 7.354 | -1.922 |
| ILMN_21027 | NM_015651.1 | PHF19 | 58331160 | 8.497 | 8.662 | 6.772 | 6.533 | -1.927 |

| Table 4, continued | | | | | | | | |
|---|---|---|---|---|---|---|---|---|
| ILMN_12496 | NM_005542.3 | INSIG1 | 38327527 | 8.735 | 8.858 | 7.012 | 6.698 | -1.942 |
| ILMN_25582 | NM_017779.3 | DEPDC1 | 41282232 | 7.403 | 7.872 | 5.797 | 5.579 | -1.950 |
| ILMN_8372 | NM_005139.1 | ANXA3 | 4826642 | 9.626 | 9.674 | 7.700 | 7.697 | -1.952 |
| ILMN_30002 | NM_012427.3 | KLK5 | 22208993 | 9.377 | 9.444 | 7.372 | 7.526 | -1.962 |
| ILMN_15028 | NM_000359.1 | TGM1 | 4507474 | 11.618 | 11.694 | 9.746 | 9.632 | -1.967 |
| ILMN_10840 | NM_012310.2 | KIF4A | 7305204 | 7.840 | 7.754 | 5.585 | 6.060 | -1.974 |
| ILMN_2226 | NM_032413.2 | C15orf48 | 37694068 | 6.121 | 6.746 | 4.263 | 4.638 | -1.983 |
| ILMN_9421 | NM_003806.1 | HRK | 4504492 | 7.617 | 7.404 | 5.472 | 5.520 | -2.014 |
| ILMN_28723 | NM_013230.2 | CD24 | 73623396 | 11.260 | 11.177 | 9.096 | 9.245 | -2.048 |
| ILMN_28750 | NM_000067.1 | CA2 | 4557394 | 11.209 | 11.329 | 9.358 | 9.048 | -2.066 |
| ILMN_23985 | NM_002358.2 | MAD2L1 | 6466452 | 9.236 | 9.505 | 7.571 | 7.032 | -2.069 |
| ILMN_12005 | NM_013282.2 | UHRF1 | 16507203 | 9.082 | 9.190 | 7.110 | 6.997 | -2.083 |
| ILMN_19730 | NM_004091.2 | E2F2 | 34485718 | 8.000 | 7.782 | 6.020 | 5.591 | -2.085 |
| ILMN_21714 | NM_032814.1 | TMEM118 | 14249505 | 7.421 | 7.303 | 5.482 | 5.049 | -2.097 |
| ILMN_2839 | NM_007174.1 | CIT | 32698687 | 7.395 | 7.563 | 5.508 | 5.206 | -2.122 |
| ILMN_1127 | NM_005030.3 | PLK1 | 34147632 | 7.831 | 7.643 | 6.073 | 5.117 | -2.142 |
| ILMN_22926 | NM_020770.1 | CGN | 16262451 | 7.513 | 7.705 | 5.655 | 5.263 | -2.150 |
| ILMN_26449 | NM_152319.2 | C12orf54 | 34303924 | 7.485 | 7.821 | 5.495 | 5.508 | -2.151 |
| ILMN_15510 | NM_007085.3 | FSTL1 | 34304366 | 9.312 | 9.258 | 7.847 | 6.416 | -2.154 |
| ILMN_14702 | NM_001827.1 | CKS2 | 4502858 | 10.523 | 10.589 | 8.280 | 8.504 | -2.164 |
| ILMN_4549 | NM_018492.2 | PBK | 18490990 | 9.511 | 9.741 | 7.352 | 7.546 | -2.177 |
| ILMN_29470 | NM_015150.1 | RAFTLIN | 41872576 | 7.091 | 6.944 | 5.109 | 4.548 | -2.189 |
| ILMN_11844 | NM_001018115.1 | FANCD2 | 66528887 | 8.017 | 7.853 | 5.853 | 5.567 | -2.225 |
| ILMN_18200 | NM_007280.1 | OIP5 | 24307928 | 7.669 | 7.933 | 5.880 | 5.263 | -2.229 |
| ILMN_3162 | NM_003254.2 | TIMP1 | 73858576 | 14.517 | 14.557 | 12.579 | 11.988 | -2.253 |
| ILMN_20406 | NM_004669.2 | CLIC3 | 40288289 | 8.619 | 8.630 | 6.736 | 5.916 | -2.298 |
| ILMN_21964 | NM_002648.2 | PIM1 | 31543400 | 10.793 | 10.850 | 8.511 | 8.510 | -2.311 |
| ILMN_26237 | NM_006082.2 | K-ALPHA-1 | 57013275 | 14.750 | 14.928 | 12.733 | 12.304 | -2.320 |
| ILMN_12351 | NM_001002876.1 | C22orf18 | 50845413 | 8.632 | 8.648 | 6.629 | 5.995 | -2.328 |
| ILMN_13462 | NM_018101.2 | CDCA8 | 51593099 | 7.788 | 7.558 | 5.396 | 5.282 | -2.334 |
| ILMN_915 | NM_020675.3 | SPBC25 | 23510353 | 6.380 | 6.231 | 3.700 | 4.217 | -2.347 |
| ILMN_24472 | NM_003318.3 | TTK | 34303964 | 7.951 | 8.336 | 5.755 | 5.760 | -2.386 |
| ILMN_137805 | NM_004217.1 | AURKB | 4759177 | 8.514 | 8.402 | 6.036 | 6.106 | -2.387 |
| ILMN_12486 | NM_005556.3 | KRT7 | 67782364 | 11.280 | 11.079 | 9.058 | 8.459 | -2.421 |
| ILMN_14206 | NM_002266.2 | KPNA2 | 62388891 | 10.586 | 11.042 | 8.415 | 8.358 | -2.428 |
| ILMN_15300 | NM_001211.4 | BUB1B | 59814246 | 7.757 | 7.927 | 5.658 | 5.142 | -2.442 |
| ILMN_4602 | NM_005988.2 | SPRR2A | 46094054 | 7.543 | 7.723 | 5.698 | 4.638 | -2.465 |
| ILMN_24887 | NM_178448.2 | C9orf140 | 31341967 | 8.212 | 8.114 | 5.902 | 5.450 | -2.487 |
| ILMN_12352 | NM_198434.1 | STK6 | 38327565 | 9.397 | 9.457 | 7.036 | 6.707 | -2.555 |
| ILMN_11503 | NM_033379.2 | CDC2 | 27886643 | 10.133 | 10.317 | 7.602 | 7.687 | -2.580 |
| ILMN_23620 | NM_022346.3 | HCAP-G | 50658080 | 9.458 | 9.434 | 7.019 | 6.695 | -2.589 |
| ILMN_7509 | NM_001813.2 | CENPE | 71061467 | 8.148 | 8.361 | 6.044 | 5.256 | -2.604 |
| ILMN_8141 | NM_003784.1 | SERPINB7 | 4505148 | 7.127 | 7.405 | 4.392 | 4.912 | -2.614 |
| ILMN_10590 | NM_004336.2 | BUB1 | 56118215 | 8.700 | 8.853 | 6.049 | 6.154 | -2.675 |
| ILMN_10359 | NM_006461.3 | SPAG5 | 73623034 | 9.231 | 9.148 | 6.748 | 6.276 | -2.677 |
| ILMN_14995 | NM_004460.2 | FAP | 16933539 | 8.298 | 8.426 | 5.675 | 5.652 | -2.698 |
| ILMN_20208 | NM_012112.4 | TPX2 | 40354199 | 8.862 | 9.005 | 6.306 | 6.117 | -2.722 |
| ILMN_1770 | NM_006342.1 | TACC3 | 5454101 | 8.708 | 8.598 | 5.858 | 5.966 | -2.741 |
| ILMN_9653 | NM_139277.1 | KLK7 | 21327704 | 9.754 | 9.711 | 7.111 | 6.857 | -2.749 |
| ILMN_28483 | NM_152515.2 | FLJ40629 | 32526889 | 8.399 | 8.503 | 5.980 | 5.385 | -2.768 |
| ILMN_30154 | NM_003258.1 | TK1 | 4507518 | 8.703 | 8.212 | 5.916 | 5.459 | -2.769 |
| ILMN_635 | NM_002281.2 | KRTHB1 | 15431319 | 15.341 | 15.204 | 12.938 | 12.058 | -2.775 |
| ILMN_14281 | NM_016359.2 | NUSAP1 | 59710089 | 10.471 | 10.591 | 7.704 | 7.807 | -2.776 |
| ILMN_24793 | NM_001786.2 | CDC2 | 16306490 | 8.042 | 8.277 | 5.409 | 5.307 | -2.801 |
| ILMN_2266 | NM_002963.2 | S100A7 | 9845518 | 8.926 | 9.086 | 6.349 | 5.919 | -2.872 |
| ILMN_16427 | NM_001237.2 | CCNA2 | 16950653 | 9.438 | 9.607 | 6.477 | 6.651 | -2.959 |
| ILMN_18763 | NM_031299.3 | CDCA3 | 34147595 | 8.583 | 8.588 | 5.825 | 5.389 | -2.979 |

| Table 4, continued | | | | | | | | |
|---|---|---|---|---|---|---|---|---|
| ILMN_13141 | NM_005480.2 | TROAP | 33438581 | 8.529 | 8.408 | 5.591 | 5.326 | -3.010 |
| ILMN_8225 | NM_016343.3 | CENPF | 55770833 | 8.532 | 8.931 | 5.805 | 5.615 | -3.022 |
| ILMN_16252 | NM_001878.2 | CRABP2 | 6382069 | 9.793 | 10.069 | 6.878 | 6.910 | -3.037 |
| ILMN_3057 | NM_080668.2 | CDCA5 | 34147481 | 9.730 | 9.642 | 6.641 | 6.648 | -3.042 |
| ILMN_16399 | NM_006086.2 | TUBB3 | 50592995 | 10.431 | 10.369 | 7.648 | 6.982 | -3.085 |
| ILMN_22377 | NM_001333.2 | CTSL2 | 23110959 | 9.660 | 9.604 | 6.958 | 6.085 | -3.110 |
| ILMN_25969 | NM_006845.2 | KIF2C | 13699832 | 8.811 | 8.633 | 5.763 | 5.456 | -3.112 |
| ILMN_5449 | NM_001809.2 | CENPA | 4585861 | 8.489 | 8.635 | 5.863 | 4.986 | -3.137 |
| ILMN_8892 | NM_181712.2 | ANKRD38 | 44917612 | 8.848 | 8.928 | 5.888 | 5.594 | -3.147 |
| ILMN_20921 | NM_018685.2 | ANLN | 31657093 | 9.295 | 9.657 | 6.370 | 6.125 | -3.228 |
| ILMN_408 | NM_018136.2 | ASPM | 24211028 | 10.003 | 10.263 | 7.031 | 6.674 | -3.280 |
| ILMN_19849 | NM_001067.2 | TOP2A | 19913405 | 10.080 | 10.069 | 6.874 | 6.580 | -3.347 |
| ILMN_25636 | NM_152666.1 | PLD5 | 22749352 | 9.014 | 9.064 | 6.104 | 5.274 | -3.349 |
| ILMN_15254 | NM_004701.2 | CCNB2 | 10938017 | 10.973 | 11.049 | 8.128 | 7.113 | -3.390 |
| ILMN_14466 | NM_002575.1 | SERPINB2 | 4505594 | 10.564 | 10.361 | 7.073 | 7.027 | -3.413 |
| ILMN_10005 | NM_031966.2 | CCNB1 | 34304372 | 10.136 | 10.300 | 6.759 | 6.498 | -3.590 |
| ILMN_20465 | NM_003981.2 | PRC1 | 40807441 | 11.103 | 11.093 | 7.796 | 7.132 | -3.634 |
| ILMN_25474 | NM_178229.3 | IQGAP3 | 39753960 | 10.769 | 10.837 | 7.216 | 7.113 | -3.639 |
| ILMN_9313 | NM_005130.3 | FGFBP1 | 49574208 | 10.762 | 10.873 | 7.822 | 6.469 | -3.672 |
| ILMN_4880 | NM_014750.3 | DLG7 | 21361644 | 9.360 | 9.495 | 5.984 | 5.489 | -3.691 |
| ILMN_7664 | NM_005555.2 | KRT6B | 17505187 | 12.319 | 12.560 | 8.915 | 8.206 | -3.879 |
| ILMN_16900 | NM_012485.1 | HMMR | 7108350 | 10.135 | 10.223 | 6.589 | 5.980 | -3.895 |
| ILMN_6398 | NM_181803.1 | UBE2C | 32967290 | 11.120 | 11.232 | 7.550 | 6.533 | -4.134 |
| ILMN_14100 | NM_005733.1 | KIF20A | 5032012 | 10.682 | 10.747 | 7.064 | 6.083 | -4.141 |
| ILMN_13685 | NM_002638.2 | PI3 | 31657130 | 13.344 | 13.390 | 8.617 | 8.129 | -4.994 |

**Table 5: The LIBSEL vs GFPSEL Signature in MCF10A Cells**

| Illumina ID | Accession | Symbol | Gi Accession | GFP SEL A Log(2) Signal | GFP SEL B Log(2) Signal | LIB SEL A Log(2) Signal | LIB SEL B Log(2) Signal | LIB SEL / GFP SEL Log(2) Ratio |
|---|---|---|---|---|---|---|---|---|
| ILMN_3374 | NM_001901.1 | CTGF | 4503122 | 6.350 | 6.350 | 12.998 | 13.193 | 6.745 |
| ILMN_4882 | NM_003246.2 | THBS1 | 40317625 | 6.029 | 6.051 | 11.762 | 11.692 | 5.687 |
| ILMN_22077 | NM_018584.4 | CAMK2N1 | 31324542 | 4.954 | 6.020 | 11.551 | 10.601 | 5.589 |
| ILMN_12928 | NM_004419.3 | DUSP5 | 62865889 | 6.547 | 6.180 | 11.876 | 11.982 | 5.565 |
| ILMN_9851 | NM_005329.2 | HAS3 | 20302152 | 5.652 | 6.129 | 11.132 | 11.465 | 5.408 |
| ILMN_26343 | NM_004004.3 | GJB2 | 42558282 | 7.106 | 7.280 | 12.737 | 12.440 | 5.395 |
| ILMN_17599 | NM_000346.2 | SOX9 | 37704387 | 5.198 | 6.140 | 10.487 | 11.131 | 5.140 |
| ILMN_138322 | NM_007350.2 | PHLDA1 | 52486109 | 6.040 | 6.629 | 11.476 | 11.421 | 5.113 |
| ILMN_3542 | NM_002341.1 | LTB | 4505034 | 5.263 | 5.722 | 10.838 | 10.343 | 5.098 |
| ILMN_27148 | NM_007231.1 | SLC6A14 | 6005714 | 4.307 | 5.375 | 10.315 | 9.338 | 4.985 |
| ILMN_20440 | NM_139314.1 | ANGPTL4 | 21536397 | 9.084 | 8.306 | 13.970 | 13.372 | 4.976 |
| ILMN_9313 | NM_005130.3 | FGFBP1 | 49574208 | 7.822 | 6.469 | 11.868 | 12.213 | 4.895 |
| ILMN_12238 | NM_206963.1 | RARRES1 | 46255042 | 5.501 | 5.433 | 11.060 | 8.624 | 4.375 |
| ILMN_25111 | NM_000693.1 | ALDH1A3 | 4502040 | 7.726 | 8.703 | 12.706 | 12.358 | 4.318 |
| ILMN_21983 | NM_001554.3 | CYR61 | 34222286 | 6.702 | 6.505 | 11.184 | 10.599 | 4.289 |
| ILMN_18070 | NM_007272.2 | CTRC | 62526042 | 1.138 | 4.848 | 7.635 | 6.835 | 4.243 |
| ILMN_2266 | NM_002963.2 | S100A7 | 9845518 | 6.349 | 5.919 | 9.195 | 11.464 | 4.196 |
| ILMN_12202 | NM_020127.1 | TUFT1 | 9910595 | 7.420 | 7.354 | 11.397 | 11.696 | 4.159 |
| ILMN_124625 | Hs.572444 | 0 | 10437827 | 6.780 | 6.984 | 10.943 | 10.947 | 4.063 |
| ILMN_25104 | NM_004496.2 | FOXA1 | 24497500 | 6.592 | 6.250 | 10.204 | 10.723 | 4.042 |
| ILMN_13603 | NM_006732.1 | FOSB | 5803016 | 5.582 | 5.361 | 8.760 | 10.101 | 3.959 |
| ILMN_11654 | NM_016639.1 | TNFRSF12A | 7706185 | 7.690 | 7.748 | 11.704 | 11.586 | 3.926 |
| ILMN_28405 | NM_006186.2 | NR4A2 | 27894347 | 6.235 | 5.973 | 9.799 | 10.158 | 3.875 |
| ILMN_13328 | NM_000958.2 | PTGER4 | 38505196 | 5.368 | 5.083 | 9.007 | 9.179 | 3.868 |
| ILMN_7081 | NM_005415.3 | SLC20A1 | 31543629 | 8.991 | 9.226 | 13.119 | 12.778 | 3.840 |
| ILMN_24745 | NM_181339.1 | IL24 | 31317245 | 5.609 | 5.755 | 10.259 | 8.777 | 3.836 |
| ILMN_21866 | NM_002483.3 | CEACAM6 | 40255012 | 3.776 | 5.100 | 8.663 | 7.856 | 3.821 |
| ILMN_11736 | NM_013409.1 | FST | 7242221 | 4.823 | 5.621 | 8.668 | 9.274 | 3.749 |
| ILMN_15273 | NM_014391.2 | ANKRD1 | 38327521 | 4.524 | 4.644 | 8.926 | 7.720 | 3.740 |
| ILMN_2486 | NM_001570.3 | IRAK2 | 58530885 | 5.823 | 5.545 | 9.358 | 9.447 | 3.718 |
| ILMN_1289 | NM_000930.2 | PLAT | 14702165 | 7.612 | 7.698 | 11.186 | 11.486 | 3.681 |
| ILMN_29229 | NM_006919.1 | SERPINB3 | 5902071 | 6.389 | 6.154 | 9.315 | 10.533 | 3.653 |
| ILMN_24466 | NM_003641.2 | IFITM1 | 40254449 | 6.272 | 6.184 | 9.737 | 9.997 | 3.639 |
| ILMN_23395 | NM_000170.1 | GLDC | 4504012 | 7.501 | 6.884 | 11.329 | 10.284 | 3.614 |
| ILMN_25006 | NM_183247.1 | TMPRSS4 | 34304346 | 5.621 | 5.561 | 9.050 | 9.315 | 3.592 |
| ILMN_3597 | NM_004431.2 | EPHA2 | 32967310 | 8.283 | 8.673 | 12.069 | 12.040 | 3.577 |
| ILMN_8120 | NM_020037.1 | ABCC3 | 9955971 | 7.603 | 6.934 | 11.270 | 10.256 | 3.494 |
| ILMN_21872 | NM_001956.2 | EDN2 | 31542584 | 7.019 | 6.833 | 10.611 | 10.225 | 3.492 |
| ILMN_20794 | NM_005564.2 | LCN2 | 38455401 | 6.829 | 6.542 | 10.591 | 9.651 | 3.436 |
| ILMN_21154 | NM_004418.2 | DUSP2 | 12707563 | 5.150 | 5.403 | 8.687 | 8.646 | 3.390 |
| ILMN_138334 | NM_015675.1 | GADD45B | 9945331 | 6.613 | 6.513 | 9.654 | 10.116 | 3.322 |
| ILMN_28724 | NM_001955.2 | EDN1 | 21359861 | 7.120 | 7.180 | 10.022 | 10.921 | 3.321 |
| ILMN_6048 | NM_030758.3 | OSBP2 | 75905817 | 6.879 | 6.720 | 10.311 | 9.764 | 3.238 |
| ILMN_138591 | NM_138440.1 | SLITL2 | 39930520 | 6.111 | 5.850 | 9.976 | 8.306 | 3.161 |
| ILMN_24855 | NM_021101.3 | CLDN1 | 21536297 | 9.320 | 9.696 | 12.426 | 12.901 | 3.155 |
| ILMN_2127 | NM_005438.2 | FOSL1 | 34734076 | 5.902 | 6.140 | 8.694 | 9.516 | 3.084 |
| ILMN_5440 | NM_001946.2 | DUSP6 | 42764682 | 3.379 | 4.217 | 6.952 | 6.807 | 3.082 |
| ILMN_15041 | NM_003633.1 | ENC1 | 4505460 | 4.945 | 5.100 | 9.033 | 7.165 | 3.077 |
| ILMN_28902 | NM_016240.2 | SCARA3 | 33598923 | 5.027 | 5.326 | 8.190 | 8.283 | 3.060 |
| ILMN_15060 | NM_052901.2 | SLC25A25 | 56699400 | 6.983 | 6.855 | 9.050 | 10.826 | 3.019 |

| Table 5, continued | | | | | | | | |
|---|---|---|---|---|---|---|---|---|
| ILMN_5800 | NM_006623.2 | PHGDH | 23308576 | 8.361 | 7.135 | 11.015 | 10.500 | 3.009 |
| ILMN_16225 | NM_003155.2 | STC1 | 61676083 | 5.728 | 5.609 | 8.403 | 8.942 | 3.004 |
| ILMN_23221 | NM_145753.1 | PHLDB2 | 21955171 | 6.872 | 7.219 | 9.798 | 10.255 | 2.981 |
| ILMN_18970 | NM_012482.3 | ZNF281 | 40255235 | 8.863 | 8.865 | 11.805 | 11.871 | 2.974 |
| ILMN_7061 | NM_013376.1 | SERTAD1 | 7019524 | 8.844 | 8.838 | 11.934 | 11.673 | 2.963 |
| ILMN_23624 | NM_001453.1 | FOXC1 | 4503734 | 8.437 | 8.259 | 11.289 | 11.296 | 2.945 |
| ILMN_15271 | NM_133467.2 | CITED4 | 38455425 | 6.238 | 6.138 | 9.393 | 8.825 | 2.921 |
| ILMN_10965 | NM_002888.2 | RARRES1 | 46255040 | 5.495 | 5.558 | 9.484 | 7.389 | 2.910 |
| ILMN_79597 | Hs.159264 | 0 | 1710274 | 4.921 | 5.104 | 8.181 | 7.657 | 2.906 |
| ILMN_7087 | NM_178815.3 | ARL5B | 59858805 | 5.347 | 5.027 | 7.770 | 8.416 | 2.906 |
| ILMN_3319 | NM_015541.2 | LRIG1 | 54607117 | 5.865 | 6.190 | 9.089 | 8.713 | 2.874 |
| ILMN_7664 | NM_005555.2 | KRT6B | 17505187 | 8.915 | 8.206 | 10.619 | 12.175 | 2.836 |
| ILMN_17941 | NM_002974.1 | SERPINB4 | 28076868 | 5.706 | 5.476 | 8.192 | 8.644 | 2.827 |
| ILMN_107396 | Hs.543887 | 0 | 31808777 | 7.039 | 7.154 | 10.132 | 9.707 | 2.823 |
| ILMN_27517 | NM_003500.2 | ACOX2 | 51558754 | 5.641 | 5.773 | 7.989 | 9.033 | 2.804 |
| ILMN_2423 | NM_181726.1 | ANKRD37 | 32171200 | 6.724 | 6.567 | 9.312 | 9.586 | 2.803 |
| ILMN_11855 | NM_003311.3 | PHLDA2 | 57863296 | 7.120 | 6.890 | 9.504 | 10.111 | 2.802 |
| ILMN_23872 | NM_025090.2 | USP36 | 35250685 | 6.780 | 6.689 | 9.900 | 9.169 | 2.800 |
| ILMN_12736 | NM_004387.2 | NKX2-5 | 49574504 | 6.902 | 6.703 | 9.610 | 9.591 | 2.798 |
| ILMN_7637 | NM_018724.3 | IL20 | 50845426 | 6.176 | 6.140 | 9.127 | 8.748 | 2.780 |
| ILMN_12676 | NM_004454.1 | ETV5 | 4758315 | 5.485 | 6.092 | 8.666 | 8.421 | 2.755 |
| ILMN_856 | NM_172080.1 | CAMK2B | 26051209 | 4.797 | 5.100 | 7.440 | 7.906 | 2.725 |
| ILMN_9074 | NM_001175.4 | ARHGDIB | 56676392 | 8.266 | 8.078 | 11.000 | 10.742 | 2.699 |
| ILMN_20831 | NM_001450.3 | FHL2 | 42403584 | 9.708 | 9.774 | 12.665 | 12.210 | 2.696 |
| ILMN_9918 | NM_019605.2 | SERTAD4 | 19923818 | 5.567 | 5.229 | 8.235 | 7.937 | 2.688 |
| ILMN_4849 | NM_005574.2 | LMO2 | 6633806 | 7.022 | 6.839 | 9.755 | 9.461 | 2.677 |
| ILMN_11209 | NM_144497.1 | AKAP12 | 21493023 | 5.062 | 4.873 | 8.169 | 7.096 | 2.665 |
| ILMN_3512 | NM_015894.2 | STMN3 | 14670374 | 6.338 | 5.720 | 8.328 | 9.045 | 2.658 |
| ILMN_14021 | NM_139265.2 | EHD4 | 34147619 | 7.534 | 7.724 | 10.419 | 10.142 | 2.652 |
| ILMN_13668 | NM_015444.1 | RIS1 | 22001414 | 5.998 | 6.307 | 8.786 | 8.810 | 2.645 |
| ILMN_10606 | NM_018689.1 | KIAA1199 | 38638697 | 5.695 | 5.368 | 8.229 | 8.117 | 2.641 |
| ILMN_5947 | NM_031481.1 | SLC25A18 | 13899341 | 6.190 | 5.365 | 8.912 | 7.925 | 2.641 |
| ILMN_894 | NM_001553.1 | IGFBP7 | 4504618 | 9.117 | 9.211 | 11.980 | 11.613 | 2.632 |
| ILMN_29702 | NM_016448.1 | DTL | 7705575 | 6.375 | 6.879 | 9.258 | 9.238 | 2.621 |
| ILMN_22377 | NM_001333.2 | CTSL2 | 23110959 | 6.958 | 6.085 | 9.255 | 9.011 | 2.612 |
| ILMN_20142 | NM_001024912.1 | CEACAM1 | 68161540 | 4.991 | 5.450 | 8.004 | 7.656 | 2.610 |
| ILMN_6524 | NM_033027.2 | AXUD1 | 17136074 | 8.722 | 8.513 | 11.221 | 11.203 | 2.594 |
| ILMN_28765 | NM_014550.3 | CARD10 | 51093860 | 7.609 | 7.084 | 10.031 | 9.823 | 2.580 |
| ILMN_10912 | NM_000361.2 | THBD | 40288292 | 6.267 | 6.047 | 8.772 | 8.680 | 2.569 |
| ILMN_28610 | NM_002526.1 | NT5E | 4505466 | 5.000 | 5.240 | 7.827 | 7.532 | 2.560 |
| ILMN_9572 | NM_004684.2 | SPARCL1 | 21359870 | 5.361 | 4.892 | 7.151 | 8.219 | 2.558 |
| ILMN_16399 | NM_006086.2 | TUBB3 | 50592995 | 7.648 | 6.982 | 10.113 | 9.633 | 2.558 |
| ILMN_16665 | NM_018478.2 | C20orf35 | 56676381 | 8.997 | 8.527 | 11.358 | 11.280 | 2.557 |
| ILMN_15061 | NM_004237.2 | TRIP13 | 20149561 | 6.863 | 6.746 | 9.415 | 9.296 | 2.551 |
| ILMN_23792 | NM_138409.1 | C6orf117 | 24308441 | 5.113 | 4.912 | 7.434 | 7.669 | 2.539 |
| ILMN_23732 | NM_001001936.1 | KIAA1914 | 50897849 | 4.626 | 5.768 | 7.920 | 7.532 | 2.529 |
| ILMN_22299 | NM_003131.2 | SRF | 61743976 | 9.512 | 9.307 | 11.919 | 11.952 | 2.526 |
| ILMN_6398 | NM_181803.1 | UBE2C | 32967290 | 7.550 | 6.533 | 9.427 | 9.680 | 2.512 |
| ILMN_14948 | NM_002160.1 | TNC | 4504548 | 4.555 | 4.977 | 7.286 | 7.259 | 2.507 |
| ILMN_6339 | NM_144569.3 | SPOCD1 | 47271474 | 5.013 | 5.009 | 7.872 | 7.161 | 2.505 |
| ILMN_14373 | NM_004561.2 | OVOL1 | 38570157 | 5.186 | 5.062 | 7.208 | 8.045 | 2.502 |
| ILMN_6497 | NM_002205.2 | ITGA5 | 56237028 | 8.896 | 8.134 | 10.974 | 11.060 | 2.501 |
| ILMN_26854 | NM_016095.1 | Pfs2 | 7706366 | 6.370 | 6.217 | 8.838 | 8.740 | 2.495 |
| ILMN_21728 | NM_033131.2 | WNT3A | 17017978 | 5.606 | 5.399 | 8.010 | 7.964 | 2.485 |
| ILMN_10126 | NM_000527.2 | LDLR | 8051613 | 9.982 | 9.340 | 11.759 | 12.524 | 2.481 |
| ILMN_2247 | NM_000584.2 | IL8 | 28610153 | 5.527 | 5.162 | 7.451 | 8.184 | 2.474 |
| ILMN_1375 | NM_152594.1 | SPRED1 | 22749220 | 7.360 | 7.465 | 10.260 | 9.492 | 2.463 |
| ILMN_19411 | NM_021972.2 | SPHK1 | 21361087 | 5.044 | 5.545 | 7.873 | 7.637 | 2.460 |
| ILMN_20677 | NM_016575.1 | NT5DC3 | 7706748 | 8.748 | 8.952 | 11.192 | 11.427 | 2.459 |

| Table 5, continued | | | | | | | | |
|---|---|---|---|---|---|---|---|---|
| ILMN_10458 | NM_013246.2 | CLCF1 | 50726992 | 5.585 | 5.897 | 8.156 | 8.219 | 2.446 |
| ILMN_15078 | NM_181555.1 | CMTM3 | 32130529 | 6.238 | 5.322 | 8.334 | 8.112 | 2.443 |
| ILMN_16900 | NM_012485.1 | HMMR | 7108350 | 6.589 | 5.980 | 8.344 | 9.078 | 2.427 |
| ILMN_6399 | NM_001025247.1 | TAF5L | 69122930 | 6.909 | 6.835 | 9.318 | 9.273 | 2.423 |
| ILMN_14702 | NM_001827.1 | CKS2 | 4502858 | 8.280 | 8.504 | 10.938 | 10.676 | 2.414 |
| ILMN_25450 | NM_001965.1 | EGR4 | 4503494 | 5.766 | 5.548 | 7.844 | 8.293 | 2.412 |
| ILMN_24329 | NM_005647.2 | TBL1X | 19913359 | 6.119 | 5.878 | 8.402 | 8.413 | 2.409 |
| ILMN_19849 | NM_001067.2 | TOP2A | 19913405 | 6.874 | 6.580 | 9.031 | 9.242 | 2.409 |
| ILMN_19983 | NM_001252.2 | TNFSF7 | 24119161 | 7.573 | 7.670 | 10.117 | 9.912 | 2.393 |
| ILMN_29273 | NM_023016.2 | C2orf26 | 54607076 | 9.608 | 9.577 | 12.081 | 11.875 | 2.386 |
| ILMN_33325 | XM_937579.1 | LOC648526 | 89028961 | 8.027 | 8.467 | 10.415 | 10.826 | 2.373 |
| ILMN_25781 | NM_003504.3 | CDC45L | 34335230 | 4.755 | 3.818 | 6.803 | 6.508 | 2.369 |
| ILMN_28170 | NM_004040.2 | RHOB | 42716309 | 7.450 | 7.413 | 10.164 | 9.429 | 2.365 |
| ILMN_7620 | NM_001031684.1 | SFRS7 | 72534659 | 8.493 | 8.529 | 10.793 | 10.959 | 2.365 |
| ILMN_9334 | NM_003290.1 | TPM4 | 4507650 | 6.835 | 6.637 | 9.017 | 9.185 | 2.365 |
| ILMN_16372 | NM_006291.2 | TNFAIP2 | 26051239 | 6.508 | 6.976 | 9.439 | 8.764 | 2.359 |
| ILMN_13774 | NM_012323.2 | MAFF | 23111001 | 5.588 | 5.678 | 7.967 | 8.013 | 2.357 |
| ILMN_30782 | XM_938320.1 | LOC401317 | 89025876 | 4.912 | 4.797 | 6.819 | 7.560 | 2.335 |
| ILMN_12434 | NM_032918.1 | RERG | 14249703 | 4.186 | 4.828 | 6.891 | 6.789 | 2.333 |
| ILMN_9482 | NM_138371.1 | FAM113B | 19923900 | 5.935 | 5.984 | 8.436 | 8.145 | 2.331 |
| ILMN_3057 | NM_080668.2 | CDCA5 | 34147481 | 6.641 | 6.648 | 8.910 | 9.038 | 2.330 |
| ILMN_9405 | NM_016445.1 | PLEK2 | 7706642 | 6.318 | 6.498 | 8.861 | 8.573 | 2.308 |
| ILMN_4880 | NM_014750.3 | DLG7 | 21361644 | 5.984 | 5.489 | 7.809 | 8.269 | 2.303 |
| ILMN_25964 | NM_002405.2 | MFNG | 21536460 | 5.692 | 5.399 | 8.133 | 7.562 | 2.302 |
| ILMN_3766 | NM_021603.2 | FXYD2 | 27754766 | 5.970 | 5.182 | 7.768 | 7.974 | 2.295 |
| ILMN_1092 | NM_000228.2 | LAMB3 | 62868214 | 7.477 | 7.737 | 10.138 | 9.654 | 2.289 |
| ILMN_12662 | NM_002203.2 | ITGA2 | 6006008 | 7.382 | 7.517 | 9.643 | 9.834 | 2.289 |
| ILMN_1023 | NM_032270.2 | LRRC8C | 19923728 | 5.612 | 5.049 | 7.943 | 7.293 | 2.287 |
| ILMN_12131 | NM_181784.1 | SPRED2 | 32401444 | 6.322 | 6.664 | 8.997 | 8.524 | 2.268 |
| ILMN_6572 | NM_152339.2 | MGC26885 | 31377584 | 7.772 | 7.525 | 9.971 | 9.843 | 2.258 |
| ILMN_18797 | NM_198282.1 | LOC340061 | 38093658 | 7.098 | 6.940 | 9.327 | 9.203 | 2.246 |
| ILMN_17789 | NM_000418.2 | IL4R | 56788409 | 10.006 | 10.235 | 12.281 | 12.447 | 2.243 |
| ILMN_23984 | NM_001338.3 | CXADR | 45827793 | 8.317 | 8.588 | 10.654 | 10.718 | 2.234 |
| ILMN_9096 | NM_005168.3 | RND3 | 56676394 | 8.762 | 8.978 | 10.978 | 11.222 | 2.230 |
| ILMN_1802 | NM_005618.2 | DLL1 | 10518496 | 5.711 | 6.102 | 8.368 | 7.898 | 2.226 |
| ILMN_23044 | NM_052972.2 | LRG1 | 49574519 | 5.485 | 5.233 | 7.720 | 7.450 | 2.226 |
| ILMN_2466 | NM_005655.1 | KLF10 | 5032176 | 6.960 | 7.286 | 9.319 | 9.365 | 2.219 |
| ILMN_915 | NM_020675.3 | SPBC25 | 23510353 | 3.700 | 4.217 | 6.240 | 6.104 | 2.213 |
| ILMN_3781 | NM_001012632.1 | IL32 | 61658631 | 6.131 | 6.651 | 8.542 | 8.652 | 2.206 |
| ILMN_15358 | NM_001839.2 | CNN3 | 47080096 | 8.562 | 8.707 | 11.029 | 10.637 | 2.198 |
| ILMN_21296 | NM_000782.3 | CYP24A1 | 55770849 | 5.739 | 5.092 | 7.864 | 7.347 | 2.190 |
| ILMN_25434 | NM_000676.2 | ADORA2B | 22907046 | 8.087 | 8.159 | 10.629 | 9.983 | 2.183 |
| ILMN_25630 | NM_005911.4 | MAT2A | 46852159 | 12.211 | 12.206 | 14.408 | 14.359 | 2.175 |
| ILMN_22286 | NM_005950.1 | MT1G | 10835229 | 6.498 | 6.564 | 9.124 | 8.287 | 2.174 |
| ILMN_26449 | NM_152319.2 | C12orf54 | 34303924 | 5.495 | 5.508 | 7.721 | 7.607 | 2.162 |
| ILMN_26612 | NM_001216.1 | CA9 | 9955947 | 5.750 | 5.664 | 8.386 | 7.326 | 2.149 |
| ILMN_10287 | NM_032744.1 | C6orf105 | 14249371 | 6.699 | 6.855 | 9.073 | 8.775 | 2.147 |
| ILMN_12691 | NM_014951.1 | ZNF365 | 7662331 | 5.121 | 5.382 | 7.201 | 7.592 | 2.145 |
| ILMN_20932 | NM_001964.2 | EGR1 | 31317226 | 8.573 | 8.618 | 10.221 | 11.237 | 2.134 |
| ILMN_138267 | NM_000211.1 | ITGB2 | 4557885 | 5.644 | 5.624 | 8.120 | 7.401 | 2.127 |
| ILMN_25451 | NM_004078.1 | CSRP1 | 4758085 | 9.540 | 9.598 | 11.579 | 11.810 | 2.125 |
| ILMN_21287 | NM_003823.2 | TNFRSF6B | 14790166 | 5.924 | 5.895 | 7.720 | 8.343 | 2.123 |
| ILMN_2236 | NM_031453.2 | FAM107B | 40254981 | 5.588 | 5.555 | 7.944 | 7.434 | 2.117 |
| ILMN_2026 | NM_014736.4 | KIAA0101 | 71773764 | 8.634 | 7.657 | 10.421 | 10.098 | 2.114 |
| ILMN_36990 | XM_930914.1 | LOC653108 | 89058118 | 5.909 | 5.664 | 7.691 | 8.106 | 2.112 |
| ILMN_9309 | NM_001552.2 | IGFBP4 | 62243289 | 4.609 | 4.492 | 6.696 | 6.621 | 2.108 |
| ILMN_10005 | NM_031966.2 | CCNB1 | 34304372 | 6.759 | 6.498 | 8.531 | 8.925 | 2.100 |
| ILMN_3001 | NM_080591.1 | PTGS1 | 18104968 | 7.776 | 7.715 | 9.951 | 9.723 | 2.092 |
| ILMN_26712 | NM_003373.3 | VCL | 50593538 | 10.721 | 10.406 | 12.522 | 12.781 | 2.088 |

| Table 5, continued | | | | | | | | |
|---|---|---|---|---|---|---|---|---|
| ILMN_4419 | NM_015508.2 | TIPARP | 38524593 | 9.549 | 9.543 | 11.778 | 11.478 | 2.082 |
| ILMN_15254 | NM_004701.2 | CCNB2 | 10938017 | 8.128 | 7.113 | 9.694 | 9.701 | 2.077 |
| ILMN_22999 | NM_022127.1 | SLC28A3 | 11545852 | 5.409 | 4.935 | 7.132 | 7.363 | 2.075 |
| ILMN_20465 | NM_003981.2 | PRC1 | 40807441 | 7.796 | 7.132 | 9.388 | 9.684 | 2.071 |
| ILMN_138186 | XM_945237.1 | DNAJB5 | 89030236 | 6.131 | 6.225 | 8.174 | 8.325 | 2.071 |
| ILMN_21209 | NM_145057.2 | CDC42EP5 | 30089965 | 5.326 | 5.781 | 7.792 | 7.445 | 2.065 |
| ILMN_2941 | NM_170695.2 | TGIF | 28178842 | 9.161 | 9.287 | 11.347 | 11.227 | 2.063 |
| ILMN_2921 | NM_001856.2 | COL16A1 | 18641351 | 7.056 | 7.696 | 9.373 | 9.505 | 2.063 |
| ILMN_10592 | NM_000149.1 | FUT3 | 4503808 | 6.123 | 6.178 | 8.420 | 8.003 | 2.061 |
| ILMN_8937 | NM_003151.2 | STAT4 | 21618332 | 6.077 | 6.250 | 8.814 | 7.624 | 2.056 |
| ILMN_30361 | NM_003896.2 | ST3GAL5 | 28373079 | 4.986 | 5.079 | 7.181 | 6.990 | 2.053 |
| ILMN_3827 | NM_004093.2 | EFNB2 | 33359689 | 9.158 | 8.944 | 11.177 | 11.024 | 2.049 |
| ILMN_18538 | NR_002196.1 | H19 | 57862814 | 6.448 | 5.714 | 8.616 | 7.635 | 2.045 |
| ILMN_6528 | NM_006868.2 | RAB31 | 33589860 | 6.396 | 6.458 | 8.503 | 8.438 | 2.044 |
| ILMN_20816 | NM_002343.2 | LTF | 54607119 | 4.977 | 5.982 | 7.026 | 8.016 | 2.041 |
| ILMN_5918 | NM_016081.2 | PALLD | 21361584 | 9.868 | 9.904 | 11.906 | 11.948 | 2.041 |
| ILMN_138577 | NM_031311.2 | CPVL | 22027517 | 8.522 | 7.918 | 10.453 | 10.064 | 2.039 |
| ILMN_18673 | NM_002346.1 | LY6E | 4505048 | 10.127 | 9.887 | 12.104 | 11.984 | 2.037 |
| ILMN_12486 | NM_005556.3 | KRT7 | 67782364 | 9.058 | 8.459 | 11.028 | 10.557 | 2.034 |
| ILMN_34806 | XM_940575.1 | LOC651423 | 89061974 | 7.410 | 7.662 | 9.785 | 9.350 | 2.031 |
| ILMN_6876 | NM_003632.1 | CNTNAP1 | 4505462 | 6.127 | 5.825 | 7.929 | 8.080 | 2.028 |
| ILMN_13615 | NM_004433.3 | ELF3 | 40255034 | 6.426 | 6.732 | 8.320 | 8.865 | 2.013 |
| ILMN_26866 | NM_030938.2 | TMEM49 | 20070348 | 8.056 | 8.117 | 9.802 | 10.395 | 2.012 |
| ILMN_37936 | XM_939919.1 | LOC650832 | 89042512 | 7.237 | 7.387 | 9.368 | 9.275 | 2.009 |
| ILMN_18957 | NM_032047.3 | B3GNT5 | 44680131 | 7.182 | 6.768 | 9.028 | 8.938 | 2.008 |
| ILMN_28190 | NM_005449.3 | FAIM3 | 34147517 | 6.497 | 6.574 | 8.683 | 8.397 | 2.005 |
| ILMN_17143 | NM_000379.2 | XDH | 9257259 | 5.792 | 5.603 | 7.718 | 7.680 | 2.002 |
| ILMN_10095 | NM_002350.1 | LYN | 4505054 | 8.736 | 8.631 | 10.871 | 10.499 | 2.001 |
| ILMN_22378 | NM_031439.2 | SOX7 | 30581119 | 8.414 | 8.813 | 10.463 | 10.741 | 1.989 |
| ILMN_12381 | NM_001008490.1 | KLF6 | 56550082 | 8.355 | 8.634 | 10.304 | 10.657 | 1.986 |
| ILMN_5645 | NM_182972.1 | IRF2BP2 | 33667027 | 7.906 | 8.523 | 9.937 | 10.443 | 1.975 |
| ILMN_1557 | NM_003407.1 | ZFP36 | 4507960 | 10.396 | 10.302 | 11.945 | 12.702 | 1.974 |
| ILMN_6550 | NM_153256.2 | C10orf47 | 31377559 | 6.750 | 7.212 | 9.190 | 8.716 | 1.972 |
| ILMN_1946 | NM_006216.2 | SERPINE2 | 34147323 | 6.717 | 6.451 | 8.719 | 8.382 | 1.966 |
| ILMN_19827 | NM_001011666.1 | CREB5 | 59938775 | 4.492 | 5.057 | 6.682 | 6.791 | 1.962 |
| ILMN_2939 | NM_004572.2 | PKP2 | 52630430 | 6.272 | 5.900 | 7.953 | 8.141 | 1.961 |
| ILMN_25878 | NM_022817.1 | PER2 | 12707561 | 9.079 | 9.269 | 10.792 | 11.470 | 1.957 |
| ILMN_408 | NM_018136.2 | ASPM | 24211028 | 7.031 | 6.674 | 8.803 | 8.814 | 1.956 |
| ILMN_25449 | NM_002579.1 | PALM | 4557041 | 5.146 | 4.536 | 6.773 | 6.809 | 1.950 |
| ILMN_13834 | NM_199169.1 | TMEPAI | 40317615 | 8.041 | 8.518 | 10.791 | 9.666 | 1.949 |
| ILMN_23854 | NM_014467.1 | SRPX2 | 7657618 | 6.123 | 5.453 | 7.832 | 7.629 | 1.943 |
| ILMN_8968 | NM_004073.2 | PLK3 | 41872373 | 4.650 | 5.511 | 6.736 | 7.309 | 1.942 |
| ILMN_3335 | NM_006779.2 | CDC42EP2 | 30089963 | 5.883 | 5.624 | 7.353 | 8.034 | 1.940 |
| ILMN_17949 | NM_181427.2 | GABPB2 | 68215703 | 6.714 | 6.771 | 8.685 | 8.665 | 1.933 |
| ILMN_26025 | NM_024554.2 | PGBD5 | 25777747 | 6.271 | 6.347 | 7.645 | 8.831 | 1.929 |
| ILMN_3596 | NM_178865.3 | SERINC2 | 71834871 | 8.589 | 8.448 | 10.693 | 10.201 | 1.928 |
| ILMN_3836 | NM_018367.3 | PHCA | 31543398 | 5.973 | 6.085 | 8.105 | 7.792 | 1.920 |
| ILMN_10445 | NM_015062.3 | PPRC1 | 40807451 | 8.893 | 8.956 | 10.861 | 10.822 | 1.917 |
| ILMN_37820 | XM_939893.1 | LOC650803 | 89042509 | 8.575 | 8.640 | 10.748 | 10.300 | 1.916 |
| ILMN_21964 | NM_002648.2 | PIM1 | 31543400 | 8.511 | 8.510 | 9.956 | 10.889 | 1.912 |
| ILMN_138005 | NM_175617.2 | MT1E | 31581520 | 7.097 | 6.771 | 9.107 | 8.583 | 1.911 |
| ILMN_12005 | NM_013282.2 | UHRF1 | 16507203 | 7.110 | 6.997 | 9.006 | 8.922 | 1.911 |
| ILMN_14503 | NM_003749.2 | IRS2 | 38683859 | 8.157 | 8.487 | 10.233 | 10.227 | 1.909 |
| ILMN_17263 | NM_006795.2 | EHD1 | 30240931 | 9.824 | 9.669 | 11.693 | 11.609 | 1.905 |
| ILMN_30018 | NM_003236.1 | TGFA | 4507460 | 6.891 | 6.839 | 8.651 | 8.884 | 1.902 |
| ILMN_8340 | NM_001020820.1 | MYADM | 66932926 | 7.443 | 7.177 | 9.124 | 9.291 | 1.897 |
| ILMN_9368 | NM_201277.1 | CNN2 | 41327729 | 10.398 | 10.287 | 12.244 | 12.212 | 1.886 |
| ILMN_26720 | NM_006022.2 | TSC22D1 | 31543826 | 8.248 | 8.947 | 10.568 | 10.390 | 1.881 |
| ILMN_16273 | NM_203434.1 | IER5L | 44681485 | 6.062 | 6.336 | 8.403 | 7.755 | 1.880 |

| Table 5, continued | | | | | | | | |
|---|---|---|---|---|---|---|---|---|
| ILMN_9308 | NM_003244.2 | TGIF | 28178841 | 5.703 | 5.524 | 7.390 | 7.582 | 1.872 |
| ILMN_13727 | NM_001062.2 | TCN1 | 21071007 | 5.420 | 5.588 | 7.280 | 7.467 | 1.870 |
| ILMN_26276 | NM_032525.1 | TUBB6 | 14210535 | 7.940 | 8.009 | 9.723 | 9.965 | 1.869 |
| ILMN_8058 | NM_134268.3 | CYGB | 38454323 | 6.985 | 7.234 | 9.233 | 8.696 | 1.855 |
| ILMN_7092 | NM_003686.3 | EXO1 | 39995068 | 6.300 | 6.235 | 8.135 | 8.095 | 1.848 |
| ILMN_40918 | XM_291277.4 | DKFZp761P042 | 89027874 | 8.045 | 8.329 | 10.135 | 9.927 | 1.844 |
| ILMN_12475 | NM_003567.2 | BCAR3 | 62243893 | 9.400 | 9.531 | 11.653 | 10.962 | 1.842 |
| ILMN_19577 | NM_178868.3 | CMTM8 | 32130535 | 6.505 | 6.717 | 8.706 | 8.198 | 1.841 |
| ILMN_30154 | NM_003258.1 | TK1 | 4507518 | 5.916 | 5.459 | 7.607 | 7.440 | 1.836 |
| ILMN_652 | NM_007105.1 | SLC22A18AS | 6005877 | 5.667 | 5.392 | 6.926 | 7.788 | 1.827 |
| ILMN_26362 | NM_153840.2 | GPR110 | 61743939 | 6.146 | 6.242 | 8.308 | 7.732 | 1.826 |
| ILMN_137805 | NM_004217.1 | AURKB | 4759177 | 6.036 | 6.106 | 7.818 | 7.970 | 1.823 |
| ILMN_12816 | NM_015703.3 | CGI-96 | 62751922 | 7.840 | 7.673 | 9.590 | 9.569 | 1.823 |
| ILMN_5708 | NM_005238.2 | ETS1 | 41393580 | 7.549 | 8.287 | 9.834 | 9.636 | 1.817 |
| ILMN_25474 | NM_178229.3 | IQGAP3 | 39753960 | 7.216 | 7.113 | 8.584 | 9.368 | 1.812 |
| ILMN_18457 | NM_024667.1 | VPS37B | 13375925 | 7.151 | 7.485 | 9.150 | 9.107 | 1.811 |
| ILMN_18617 | NM_031426.2 | C9orf58 | 50428929 | 9.093 | 8.994 | 11.009 | 10.693 | 1.808 |
| ILMN_85344 | Hs.300262 | 0 | 51477606 | 4.358 | 5.213 | 6.235 | 6.946 | 1.805 |
| ILMN_15421 | NM_002068.1 | GNA15 | 4504038 | 9.330 | 8.921 | 10.843 | 11.017 | 1.805 |
| ILMN_138827 | NM_145810.1 | CDCA7 | 22027513 | 7.436 | 7.393 | 9.218 | 9.212 | 1.800 |
| ILMN_26148 | NM_018154.2 | ASF1B | 67782340 | 5.350 | 5.347 | 7.042 | 7.254 | 1.799 |
| ILMN_20107 | NM_006739.2 | MCM5 | 23510447 | 5.890 | 5.928 | 7.719 | 7.676 | 1.788 |
| ILMN_534 | NM_002754.3 | MAPK13 | 20986527 | 7.938 | 7.220 | 9.034 | 9.692 | 1.784 |
| ILMN_2570 | NM_000591.1 | CD14 | 4557416 | 7.468 | 8.057 | 9.941 | 9.150 | 1.783 |
| ILMN_4328 | NM_018948.2 | ERRFI1 | 21314673 | 11.387 | 11.417 | 13.250 | 13.114 | 1.780 |
| ILMN_15973 | NM_012116.2 | CBLC | 20149595 | 6.850 | 6.711 | 8.562 | 8.556 | 1.778 |
| ILMN_80817 | Hs.184721 | 0 | 8143882 | 6.387 | 6.430 | 7.839 | 8.527 | 1.775 |
| ILMN_25778 | NM_004385.2 | CSPG2 | 21361115 | 6.011 | 5.426 | 7.828 | 7.159 | 1.775 |
| ILMN_28602 | NM_001007538.1 | TMEM46 | 56090522 | 5.340 | 5.773 | 7.281 | 7.372 | 1.770 |
| ILMN_5835 | NM_014777.1 | KIAA0133 | 7661931 | 6.345 | 6.202 | 8.182 | 7.901 | 1.768 |
| ILMN_9112 | NM_003378.2 | VGF | 17136077 | 5.044 | 5.585 | 7.213 | 6.952 | 1.768 |
| ILMN_16821 | NM_020859.1 | SHRM | 18699721 | 6.438 | 5.863 | 8.087 | 7.750 | 1.768 |
| ILMN_20921 | NM_018685.2 | ANLN | 31657093 | 6.370 | 6.125 | 7.810 | 8.219 | 1.767 |
| ILMN_18397 | NM_021960.3 | MCL1 | 33519459 | 7.740 | 7.981 | 9.522 | 9.732 | 1.767 |
| ILMN_35907 | XM_931068.1 | C13orf25 | 89036826 | 7.186 | 6.798 | 8.512 | 8.994 | 1.761 |
| ILMN_1770 | NM_006342.1 | TACC3 | 5454101 | 5.858 | 5.966 | 7.814 | 7.527 | 1.758 |
| ILMN_6736 | NM_003975.2 | SH2D2A | 31543620 | 6.906 | 6.655 | 8.667 | 8.406 | 1.756 |
| ILMN_4070 | NM_002354.1 | TACSTD1 | 4505058 | 8.284 | 7.637 | 10.018 | 9.413 | 1.755 |
| ILMN_28483 | NM_152515.2 | FLJ40629 | 32526889 | 5.980 | 5.385 | 7.246 | 7.622 | 1.752 |
| ILMN_99306 | Hs.517692 | 0 | 20364037 | 5.129 | 5.221 | 7.048 | 6.803 | 1.750 |
| ILMN_20349 | NM_004508.2 | IDI1 | 40018632 | 7.130 | 6.915 | 8.591 | 8.948 | 1.747 |
| ILMN_3329 | NM_003820.2 | TNFRSF14 | 23200040 | 6.430 | 7.139 | 8.573 | 8.487 | 1.746 |
| ILMN_29529 | NM_014575.1 | SCHIP1 | 7657539 | 6.576 | 6.435 | 8.333 | 8.164 | 1.744 |
| ILMN_4868 | NM_003885.2 | CDK5R1 | 34304373 | 6.920 | 6.888 | 8.540 | 8.749 | 1.741 |
| ILMN_14470 | NM_033504.2 | TMEM54 | 34147466 | 6.509 | 6.336 | 7.924 | 8.372 | 1.725 |
| ILMN_10261 | NM_012137.2 | DDAH1 | 31881756 | 5.100 | 5.240 | 7.153 | 6.619 | 1.716 |
| ILMN_9854 | NM_020179.1 | FN5 | 9910225 | 7.044 | 7.105 | 9.073 | 8.502 | 1.713 |
| ILMN_23200 | NM_017816.1 | LYAR | 8923397 | 8.372 | 8.409 | 10.039 | 10.159 | 1.709 |
| ILMN_14069 | NM_000147.2 | FUCA1 | 24475878 | 7.250 | 6.843 | 8.819 | 8.658 | 1.692 |
| ILMN_5608 | NM_182826.1 | SCARA3 | 33598921 | 5.326 | 5.057 | 6.864 | 6.902 | 1.692 |
| ILMN_29852 | NM_001008218.1 | AMY1B | 56549661 | 7.188 | 6.759 | 8.832 | 8.496 | 1.691 |
| ILMN_1387 | NM_020799.2 | STAMBPL1 | 52694663 | 6.999 | 6.433 | 8.268 | 8.543 | 1.690 |
| ILMN_11282 | NM_020796.2 | SEMA6A | 47132510 | 8.032 | 8.441 | 9.843 | 10.004 | 1.687 |
| ILMN_3628 | NM_024094.1 | DCC1 | 13129095 | 5.766 | 5.830 | 7.652 | 7.314 | 1.685 |
| ILMN_28160 | NM_001102.2 | ACTN1 | 12025669 | 10.343 | 9.873 | 11.923 | 11.661 | 1.684 |
| ILMN_3414 | NM_021149.2 | COTL1 | 23510452 | 7.302 | 6.431 | 8.746 | 8.348 | 1.680 |
| ILMN_10290 | NM_013314.2 | BLNK | 40353774 | 6.190 | 6.119 | 7.755 | 7.905 | 1.676 |
| ILMN_28413 | NM_002053.1 | GBP1 | 4503938 | 6.548 | 6.839 | 8.386 | 8.350 | 1.674 |
| ILMN_30168 | NM_018004.1 | TMEM45A | 8922242 | 6.508 | 6.282 | 7.752 | 8.380 | 1.671 |

| Table 5, continued | | | | | | | | |
|---|---|---|---|---|---|---|---|---|
| ILMN_3104 | NM_006047.4 | RBM12 | 33469952 | 6.538 | 6.835 | 8.407 | 8.305 | 1.669 |
| ILMN_17961 | NM_001300.4 | KLF6 | 56550115 | 11.453 | 11.734 | 13.122 | 13.403 | 1.669 |
| ILMN_17288 | NM_005491.1 | CXorf6 | 4885170 | 6.361 | 7.047 | 8.731 | 8.014 | 1.669 |
| ILMN_8225 | NM_016343.3 | CENPF | 55770833 | 5.805 | 5.615 | 7.291 | 7.449 | 1.660 |
| ILMN_4806 | NM_003921.2 | BCL10 | 20336470 | 7.200 | 7.038 | 8.748 | 8.807 | 1.659 |
| ILMN_24075 | NM_000428.2 | LTBP2 | 46389563 | 5.835 | 6.235 | 7.750 | 7.637 | 1.658 |
| ILMN_6472 | NM_177401.4 | MIDN | 58761507 | 8.346 | 8.014 | 9.952 | 9.718 | 1.655 |
| ILMN_29986 | NM_000963.1 | PTGS2 | 4506264 | 5.695 | 5.776 | 7.011 | 7.764 | 1.652 |
| ILMN_14714 | NM_024599.2 | RHBDF2 | 24432005 | 9.135 | 9.086 | 10.833 | 10.689 | 1.651 |
| ILMN_15317 | NM_012081.3 | ELL2 | 34222159 | 8.242 | 8.193 | 9.912 | 9.820 | 1.649 |
| ILMN_14586 | NM_002309.2 | LIF | 6006018 | 5.282 | 4.591 | 6.750 | 6.420 | 1.648 |
| ILMN_26237 | NM_006082.2 | K-ALPHA-1 | 57013275 | 12.733 | 12.304 | 14.099 | 14.217 | 1.639 |
| ILMN_139141 | NM_053056.1 | CCND1 | 16950654 | 9.907 | 10.377 | 12.054 | 11.506 | 1.638 |
| ILMN_18895 | NM_030928.2 | CDT1 | 19923847 | 6.759 | 6.711 | 8.433 | 8.281 | 1.622 |
| ILMN_25046 | NM_006479.2 | RAD51AP1 | 19923778 | 5.463 | 5.888 | 7.105 | 7.486 | 1.621 |
| ILMN_29649 | NM_003017.3 | SFRS3 | 31377552 | 7.938 | 7.541 | 9.327 | 9.393 | 1.620 |
| ILMN_12806 | NM_014840.2 | NUAK1 | 48374438 | 7.081 | 7.463 | 8.580 | 9.195 | 1.615 |
| ILMN_29566 | NM_014344.2 | FJX1 | 18765710 | 9.089 | 9.303 | 10.834 | 10.780 | 1.611 |
| ILMN_11103 | NM_013390.1 | TMEM2 | 7019554 | 7.149 | 7.418 | 9.022 | 8.760 | 1.608 |
| ILMN_33245 | XM_035299.7 | ZSWIM6 | 88983661 | 6.910 | 7.543 | 8.985 | 8.682 | 1.607 |
| ILMN_15847 | NM_203418.1 | DSCR1 | 44680109 | 5.350 | 5.318 | 6.756 | 7.116 | 1.602 |
| ILMN_5694 | NM_153322.1 | PMP22 | 24430164 | 5.307 | 5.650 | 7.028 | 7.121 | 1.596 |
| ILMN_76952 | Hs.130313 | 0 | 10938922 | 6.644 | 6.684 | 8.315 | 8.203 | 1.595 |
| ILMN_7921 | NM_031476.1 | CRISPLD2 | 13899331 | 6.477 | 6.621 | 8.317 | 7.970 | 1.594 |
| ILMN_8015 | NM_003078.3 | SMARCD3 | 51477705 | 7.645 | 7.807 | 9.753 | 8.882 | 1.591 |
| ILMN_752 | NM_183049.2 | TMSL3 | 72255572 | 12.668 | 12.406 | 13.927 | 14.328 | 1.591 |
| ILMN_12497 | NM_002970.1 | SAT | 4506788 | 11.435 | 11.431 | 12.956 | 13.091 | 1.590 |
| ILMN_23836 | NM_005418.3 | ST5 | 47132528 | 5.840 | 6.087 | 7.557 | 7.545 | 1.587 |
| ILMN_21257 | NM_021158.3 | TRIB3 | 41327717 | 8.098 | 8.031 | 9.296 | 10.007 | 1.587 |
| ILMN_23486 | NM_173354.2 | SNF1LK | 48762713 | 9.456 | 9.405 | 10.879 | 11.151 | 1.584 |
| ILMN_5933 | NM_021194.2 | SLC30A1 | 52352802 | 8.095 | 7.888 | 9.650 | 9.495 | 1.581 |
| ILMN_11844 | NM_001018115.1 | FANCD2 | 66528887 | 5.853 | 5.567 | 7.252 | 7.328 | 1.580 |
| ILMN_121747 | Hs.569566 | 0 | 5363671 | 6.811 | 7.120 | 8.737 | 8.354 | 1.580 |
| ILMN_18885 | NM_006932.3 | SMTN | 19913393 | 6.038 | 5.916 | 7.601 | 7.510 | 1.579 |
| ILMN_8268 | NM_025135.2 | FHOD3 | 58331241 | 6.492 | 6.665 | 8.530 | 7.777 | 1.575 |
| ILMN_25780 | NM_002589.2 | PCDH7 | 14589930 | 6.208 | 6.073 | 7.881 | 7.545 | 1.573 |
| ILMN_23081 | NM_016274.3 | PLEKHO1 | 21361610 | 6.133 | 5.828 | 7.707 | 7.396 | 1.571 |
| ILMN_43594 | XM_498969.2 | LOC441019 | 88974818 | 9.553 | 9.414 | 11.161 | 10.942 | 1.568 |
| ILMN_29325 | NM_005354.2 | JUND | 10938013 | 12.026 | 12.027 | 13.512 | 13.676 | 1.568 |
| ILMN_12351 | NM_001002876.1 | C22orf18 | 50845413 | 6.629 | 5.995 | 7.835 | 7.923 | 1.567 |
| ILMN_7455 | NM_024871.1 | MAP6D1 | 13376305 | 6.539 | 6.858 | 8.424 | 8.102 | 1.564 |
| ILMN_13393 | NM_016498.3 | MTP18 | 51243054 | 8.811 | 8.960 | 10.693 | 10.200 | 1.561 |
| ILMN_14271 | NM_033267.2 | IRX2 | 52138574 | 10.364 | 10.137 | 11.941 | 11.675 | 1.558 |
| ILMN_5047 | NM_152308.1 | MGC24665 | 24308244 | 6.079 | 6.096 | 7.588 | 7.696 | 1.554 |
| ILMN_23585 | NM_002105.2 | H2AFX | 52630339 | 7.128 | 7.241 | 8.828 | 8.642 | 1.551 |
| ILMN_22527 | NM_001031628.1 | LOC57228 | 76496484 | 5.787 | 6.135 | 7.580 | 7.442 | 1.550 |
| ILMN_23238 | NM_058187.3 | C21orf63 | 38372914 | 9.735 | 9.773 | 11.513 | 11.094 | 1.550 |
| ILMN_11038 | NM_145018.2 | FLJ25416 | 25072198 | 5.498 | 5.875 | 7.161 | 7.298 | 1.543 |
| ILMN_103797 | Hs.538259 | 0 | 23273338 | 6.794 | 6.579 | 8.208 | 8.243 | 1.539 |
| ILMN_27083 | NM_032265.1 | ZMYND15 | 14149998 | 6.257 | 6.358 | 7.553 | 8.132 | 1.535 |
| ILMN_21172 | NM_139131.2 | NUP98 | 56549641 | 5.615 | 5.436 | 6.986 | 7.128 | 1.532 |
| ILMN_552 | NM_003582.2 | DYRK3 | 51702239 | 8.691 | 8.478 | 10.307 | 9.920 | 1.529 |
| ILMN_23474 | NM_144626.1 | TMEM125 | 21389442 | 6.192 | 5.961 | 7.764 | 7.440 | 1.525 |
| ILMN_26898 | NM_004368.2 | CNN2 | 41327728 | 5.706 | 6.005 | 7.407 | 7.345 | 1.521 |
| ILMN_2839 | NM_007174.1 | CIT | 32698687 | 5.508 | 5.206 | 6.787 | 6.950 | 1.511 |
| ILMN_26899 | NM_001071.1 | TYMS | 4507750 | 7.812 | 7.778 | 9.512 | 9.095 | 1.509 |
| ILMN_11869 | NM_004232.2 | SOCS6 | 21450784 | 4.982 | 5.485 | 6.746 | 6.737 | 1.508 |
| ILMN_28470 | NM_006372.3 | SYNCRIP | 23397426 | 9.622 | 9.276 | 10.846 | 11.065 | 1.507 |
| ILMN_124127 | Hs.571946 | 0 | 68294565 | 7.136 | 7.194 | 8.553 | 8.781 | 1.502 |

| Table 5, continued | | | | | | | | |
|---|---|---|---|---|---|---|---|---|
| ILMN_3918 | NM_145253.1 | FAM100A | 21687061 | 6.148 | 6.366 | 7.817 | 7.696 | 1.500 |
| ILMN_137303 | NM_006888.2 | CALM1 | 31377794 | 8.580 | 8.694 | 10.032 | 10.231 | 1.494 |
| ILMN_17339 | NM_001013652.1 | LOC389791 | 61966750 | 6.324 | 6.413 | 7.758 | 7.966 | 1.494 |
| ILMN_18637 | NM_001034.1 | RRM2 | 4557844 | 5.807 | 5.890 | 7.335 | 7.350 | 1.494 |
| ILMN_2565 | NM_001101.2 | ACTB | 5016088 | 11.871 | 11.467 | 13.097 | 13.226 | 1.493 |
| ILMN_16427 | NM_001237.2 | CCNA2 | 16950653 | 6.477 | 6.651 | 7.942 | 8.170 | 1.492 |
| ILMN_12401 | NM_022767.2 | ISG20L1 | 21362093 | 8.749 | 8.839 | 10.360 | 10.210 | 1.491 |
| ILMN_5126 | NM_020904.1 | PLEKHA4 | 10190743 | 6.013 | 6.466 | 7.732 | 7.725 | 1.489 |
| ILMN_14281 | NM_016359.2 | NUSAP1 | 59710089 | 7.704 | 7.807 | 9.220 | 9.259 | 1.484 |
| ILMN_20105 | NM_152341.2 | PAQR4 | 31542755 | 6.492 | 6.634 | 7.880 | 8.210 | 1.482 |
| ILMN_22933 | NM_024923.2 | NUP210 | 27477133 | 5.784 | 5.933 | 7.476 | 7.186 | 1.472 |
| ILMN_2137 | NM_003461.4 | ZYX | 58530843 | 10.419 | 10.500 | 12.055 | 11.807 | 1.471 |
| ILMN_5766 | NM_153752.1 | C21orf84 | 24371253 | 5.304 | 5.278 | 6.837 | 6.682 | 1.469 |
| ILMN_11272 | NM_032412.2 | ORF1-FL49 | 31543361 | 8.431 | 8.484 | 9.852 | 9.995 | 1.466 |
| ILMN_23731 | NM_002201.4 | ISG20 | 34147571 | 7.322 | 7.957 | 8.961 | 9.235 | 1.459 |
| ILMN_14280 | NM_017491.3 | WDR1 | 53729350 | 10.474 | 10.274 | 11.751 | 11.914 | 1.459 |
| ILMN_15226 | NM_000785.3 | CYP27B1 | 74099700 | 7.480 | 7.361 | 8.907 | 8.847 | 1.457 |
| ILMN_20208 | NM_012112.4 | TPX2 | 40354199 | 6.306 | 6.117 | 7.543 | 7.783 | 1.452 |
| ILMN_3481 | NM_033661.3 | WDR4 | 40217837 | 8.034 | 7.739 | 9.336 | 9.327 | 1.445 |
| ILMN_8372 | NM_005139.1 | ANXA3 | 4826642 | 7.700 | 7.697 | 9.234 | 9.038 | 1.438 |
| ILMN_24887 | NM_178448.2 | C9orf140 | 31341967 | 5.902 | 5.450 | 7.150 | 7.065 | 1.432 |
| ILMN_23620 | NM_022346.3 | HCAP-G | 50658080 | 7.019 | 6.695 | 8.103 | 8.473 | 1.431 |
| ILMN_9514 | NM_181054.1 | HIF1A | 31077210 | 7.296 | 7.403 | 8.852 | 8.704 | 1.429 |
| ILMN_21065 | NM_002539.1 | ODC1 | 4505488 | 9.445 | 9.270 | 10.859 | 10.691 | 1.417 |
| ILMN_30043 | NM_003542.3 | HIST1H4C | 21071024 | 11.812 | 11.860 | 13.199 | 13.297 | 1.412 |
| ILMN_9920 | NM_021732.1 | AVPI1 | 11119427 | 12.564 | 12.686 | 14.190 | 13.881 | 1.411 |
| ILMN_14823 | NM_014882.2 | ARHGAP25 | 55770896 | 5.213 | 5.382 | 6.807 | 6.607 | 1.410 |
| ILMN_121356 | Hs.569175 | 0 | 80848489 | 5.174 | 5.221 | 6.490 | 6.713 | 1.404 |
| ILMN_3601 | NM_003059.2 | SLC22A4 | 24497489 | 5.982 | 6.254 | 7.494 | 7.548 | 1.404 |
| ILMN_26865 | NM_013248.2 | NXT1 | 20127526 | 9.147 | 9.397 | 10.710 | 10.633 | 1.400 |
| ILMN_24353 | NM_001614.2 | ACTG1 | 11038618 | 12.178 | 11.604 | 13.330 | 13.241 | 1.394 |
| ILMN_14011 | NM_004666.1 | VNN1 | 4759311 | 8.661 | 8.619 | 9.874 | 10.193 | 1.393 |
| ILMN_7283 | NM_014793.3 | LCMT2 | 32455233 | 7.436 | 7.164 | 8.709 | 8.671 | 1.390 |
| ILMN_2730 | NM_012118.2 | CCRN4L | 31083027 | 6.739 | 6.425 | 7.887 | 8.047 | 1.385 |
| ILMN_24570 | NM_176814.3 | LOC168850 | 39753952 | 7.314 | 7.475 | 8.861 | 8.685 | 1.379 |
| ILMN_12915 | NM_004458.1 | ACSL4 | 4758331 | 9.547 | 9.357 | 10.889 | 10.756 | 1.371 |
| ILMN_11802 | NM_004856.4 | KIF23 | 20143965 | 6.576 | 6.459 | 7.765 | 8.006 | 1.368 |
| ILMN_28900 | NM_014316.1 | CARHSP1 | 7656994 | 10.060 | 9.934 | 11.554 | 11.176 | 1.368 |
| ILMN_27331 | NM_020412.3 | CHMP1B | 42734391 | 10.160 | 10.239 | 11.643 | 11.488 | 1.366 |
| ILMN_789 | NM_017801.2 | CMTM6 | 32130534 | 8.426 | 8.362 | 9.904 | 9.610 | 1.363 |
| ILMN_28588 | NM_003455.2 | ZNF202 | 56699474 | 5.873 | 5.924 | 7.238 | 7.274 | 1.358 |
| ILMN_3091 | NM_014888.1 | FAM3C | 7661713 | 7.208 | 7.475 | 8.777 | 8.620 | 1.358 |
| ILMN_7414 | NM_002296.2 | LBR | 37595749 | 9.496 | 9.259 | 10.954 | 10.507 | 1.353 |
| ILMN_28300 | NM_016101.3 | NIP7 | 59710091 | 9.582 | 9.466 | 10.803 | 10.927 | 1.341 |
| ILMN_3629 | NM_182507.1 | LOC144501 | 32698852 | 6.198 | 6.468 | 7.686 | 7.660 | 1.340 |
| ILMN_11198 | NM_005953.2 | MT2A | 31543214 | 13.935 | 13.691 | 15.263 | 15.015 | 1.326 |
| ILMN_25462 | NM_024708.2 | ASB7 | 30089993 | 5.498 | 5.274 | 6.772 | 6.641 | 1.320 |
| ILMN_11340 | NM_024090.1 | ELOVL6 | 13129087 | 6.953 | 6.823 | 8.135 | 8.259 | 1.309 |
| ILMN_12210 | NM_199329.1 | SLC43A3 | 41056258 | 6.868 | 7.175 | 8.309 | 8.350 | 1.308 |
| ILMN_28002 | NM_181353.1 | ID1 | 31317296 | 11.104 | 11.119 | 12.557 | 12.282 | 1.308 |
| ILMN_18209 | NM_013328.2 | PYCR2 | 21361453 | 8.544 | 8.816 | 9.915 | 10.060 | 1.308 |
| ILMN_74675 | Hs.100261 | 0 | 34526785 | 7.505 | 7.385 | 8.751 | 8.747 | 1.304 |
| ILMN_11616 | NM_002915.2 | RFC3 | 31795536 | 6.075 | 6.236 | 7.319 | 7.589 | 1.299 |
| ILMN_2930 | NM_052842.2 | BCL2L12 | 20336331 | 7.779 | 7.712 | 8.983 | 9.096 | 1.294 |
| ILMN_12352 | NM_198434.1 | STK6 | 38327565 | 7.036 | 6.707 | 8.197 | 8.132 | 1.293 |
| ILMN_6890 | NM_021034.1 | IFITM3 | 11995467 | 12.872 | 12.732 | 14.032 | 14.153 | 1.291 |
| ILMN_29766 | NM_021934.3 | C12orf44 | 34222337 | 8.413 | 8.700 | 9.821 | 9.868 | 1.288 |
| ILMN_7342 | NM_004736.2 | XPR1 | 19923271 | 9.849 | 9.745 | 11.265 | 10.902 | 1.287 |
| ILMN_18194 | NM_021805.1 | SIGIRR | 11141876 | 6.154 | 6.064 | 7.459 | 7.330 | 1.285 |

| Table 5, continued | | | | | | | | |
|---|---|---|---|---|---|---|---|---|
| ILMN_27595 | NM_022338.2 | C11orf24 | 52851412 | 6.318 | 6.356 | 7.595 | 7.646 | 1.283 |
| ILMN_138674 | NM_014521.1 | SH3BP4 | 7657561 | 9.693 | 9.845 | 11.117 | 10.986 | 1.283 |
| ILMN_28859 | NM_014887.1 | PFAAP5 | 7656970 | 7.162 | 7.207 | 8.442 | 8.486 | 1.280 |
| ILMN_17550 | NM_006963.3 | ZNF22 | 55775473 | 7.059 | 7.238 | 8.456 | 8.389 | 1.274 |
| ILMN_19508 | NM_014878.3 | KIAA0020 | 33620772 | 9.754 | 9.548 | 10.895 | 10.952 | 1.273 |
| ILMN_21821 | NM_019063.2 | EML4 | 19923496 | 8.293 | 8.247 | 9.671 | 9.406 | 1.268 |
| ILMN_15154 | NM_003999.1 | OSMR | 4557039 | 6.625 | 6.307 | 7.738 | 7.731 | 1.268 |
| ILMN_138016 | XM_940079.1 | TUBB6 | 89047322 | 9.669 | 9.783 | 10.816 | 11.170 | 1.267 |
| ILMN_9420 | NM_004281.3 | BAG3 | 62530382 | 9.750 | 9.975 | 11.152 | 11.103 | 1.265 |
| ILMN_10665 | NM_018455.3 | C16orf60 | 39725678 | 7.754 | 7.451 | 8.957 | 8.775 | 1.263 |
| ILMN_9627 | NM_015169.3 | RRS1 | 46094056 | 8.813 | 8.736 | 10.067 | 10.001 | 1.260 |
| ILMN_28955 | NM_006170.2 | NOL1 | 76150622 | 10.195 | 10.072 | 11.382 | 11.347 | 1.231 |
| ILMN_13273 | NM_024329.4 | EFHD2 | 42734435 | 10.862 | 10.823 | 12.057 | 12.075 | 1.224 |
| ILMN_8253 | NM_002473.3 | MYH9 | 51317362 | 10.963 | 11.085 | 12.230 | 12.235 | 1.209 |
| ILMN_12133 | NM_003088.2 | FSCN1 | 49472815 | 12.073 | 11.877 | 13.184 | 13.180 | 1.207 |
| ILMN_11901 | NM_012302.2 | LPHN2 | 57165356 | 8.921 | 8.751 | 9.979 | 10.095 | 1.201 |
| ILMN_26638 | NM_203290.1 | POLR1C | 42560245 | 10.199 | 10.086 | 11.351 | 11.311 | 1.189 |
| ILMN_12854 | NM_016289.2 | CAB39 | 19745179 | 11.445 | 11.439 | 12.647 | 12.549 | 1.156 |
| ILMN_24124 | NM_003384.2 | VRK1 | 71164882 | 7.246 | 7.211 | 8.369 | 8.367 | 1.139 |
| ILMN_14159 | NM_000837.1 | GRINA | 57165372 | 11.612 | 11.718 | 10.478 | 10.524 | -1.164 |
| ILMN_10669 | NM_005077.3 | TLE1 | 34147712 | 9.069 | 9.083 | 7.825 | 7.924 | -1.202 |
| ILMN_7322 | NM_002291.1 | LAMB1 | 4504950 | 10.746 | 10.689 | 9.544 | 9.453 | -1.219 |
| ILMN_1454 | NM_024815.2 | NUDT18 | 40254968 | 8.461 | 8.482 | 7.307 | 7.193 | -1.222 |
| ILMN_10067 | NM_014883.2 | FAM13A1 | 56119109 | 8.070 | 8.211 | 6.775 | 7.042 | -1.232 |
| ILMN_29930 | NM_022106.1 | C20orf177 | 32698751 | 8.062 | 8.143 | 6.874 | 6.827 | -1.252 |
| ILMN_2205 | NM_020531.2 | C20orf3 | 41327713 | 10.953 | 10.945 | 9.682 | 9.708 | -1.253 |
| ILMN_126912 | Hs.574731 | 0 | 13342530 | 6.213 | 6.098 | 4.873 | 4.912 | -1.263 |
| ILMN_16625 | NM_024537.1 | FLJ12118 | 13375694 | 9.632 | 9.652 | 8.326 | 8.427 | -1.265 |
| ILMN_2097 | NM_022905.3 | TTC23 | 63253299 | 8.796 | 8.687 | 7.468 | 7.473 | -1.271 |
| ILMN_10987 | NM_000247.1 | MICA | 4557750 | 9.779 | 9.780 | 8.400 | 8.612 | -1.273 |
| ILMN_20088 | NM_001150.1 | ANPEP | 4502094 | 9.312 | 8.990 | 7.916 | 7.825 | -1.280 |
| ILMN_6132 | NM_004064.2 | CDKN1B | 17978497 | 8.697 | 8.651 | 7.383 | 7.402 | -1.282 |
| ILMN_13301 | NM_013320.1 | HCFC2 | 7019404 | 6.921 | 6.954 | 5.524 | 5.779 | -1.287 |
| ILMN_27088 | NM_020141.3 | C1orf119 | 52851428 | 8.253 | 8.149 | 6.945 | 6.874 | -1.291 |
| ILMN_11918 | NM_006821.3 | ACOT2 | 34147581 | 6.682 | 6.966 | 5.632 | 5.416 | -1.300 |
| ILMN_15035 | NM_000877.2 | IL1R1 | 27894331 | 7.984 | 7.679 | 6.644 | 6.391 | -1.314 |
| ILMN_26003 | NM_012385.1 | P8 | 6912569 | 10.980 | 11.022 | 9.632 | 9.736 | -1.317 |
| ILMN_135987 | Hs.583806 | 0 | 21177747 | 11.509 | 11.625 | 10.376 | 10.105 | -1.326 |
| ILMN_112484 | Hs.556082 | 0 | 19116194 | 8.357 | 8.073 | 6.811 | 6.939 | -1.340 |
| ILMN_15434 | NM_012464.3 | TLL1 | 22547220 | 7.141 | 7.258 | 5.744 | 5.966 | -1.344 |
| ILMN_11368 | NM_005928.1 | MFGE8 | 5174556 | 13.464 | 13.532 | 12.106 | 12.195 | -1.347 |
| ILMN_137328 | NM_006736.4 | DNAJB2 | 34222304 | 10.416 | 10.436 | 9.281 | 8.872 | -1.350 |
| ILMN_85308 | Hs.298873 | 0 | 27824249 | 7.256 | 7.102 | 5.573 | 6.085 | -1.350 |
| ILMN_5224 | NM_031412.2 | GABARAPL1 | 56676368 | 11.233 | 10.953 | 9.793 | 9.672 | -1.361 |
| ILMN_11871 | NM_003739.4 | AKR1C3 | 24497582 | 13.929 | 13.528 | 12.553 | 12.173 | -1.365 |
| ILMN_30002 | NM_012427.3 | KLK5 | 22208993 | 7.372 | 7.526 | 6.079 | 6.068 | -1.375 |
| ILMN_15545 | NM_138452.1 | DHRS1 | 19923982 | 10.933 | 10.931 | 9.278 | 9.835 | -1.375 |
| ILMN_9590 | NM_017875.1 | FLJ20551 | 8923519 | 8.362 | 8.518 | 7.131 | 6.986 | -1.381 |
| ILMN_4218 | NM_005399.3 | PRKAB2 | 46877069 | 8.818 | 8.735 | 7.589 | 7.178 | -1.393 |
| ILMN_1735 | NM_006829.2 | C10orf116 | 47078273 | 12.519 | 12.355 | 11.060 | 11.025 | -1.394 |
| ILMN_27027 | NM_032409.1 | PINK1 | 14165271 | 9.815 | 9.805 | 8.418 | 8.395 | -1.403 |
| ILMN_13955 | NM_003204.1 | NFE2L1 | 4505378 | 9.837 | 9.733 | 8.273 | 8.452 | -1.422 |
| ILMN_29690 | NM_022740.2 | HIPK2 | 46852175 | 9.858 | 9.894 | 8.611 | 8.294 | -1.424 |
| ILMN_1226 | NM_199513.1 | C20orf44 | 41327688 | 10.616 | 10.303 | 9.050 | 9.003 | -1.433 |
| ILMN_39597 | XM_928729.1 | LOC645719 | 88942498 | 8.343 | 8.379 | 6.927 | 6.901 | -1.447 |
| ILMN_25836 | NM_024042.2 | METRN | 34147349 | 7.937 | 8.218 | 6.571 | 6.678 | -1.453 |
| ILMN_17578 | NM_003944.2 | SELENBP1 | 16306549 | 8.677 | 8.752 | 7.039 | 7.477 | -1.456 |
| ILMN_139087 | XM_938742.1 | SGPP2 | 88959174 | 11.649 | 11.751 | 10.242 | 10.242 | -1.458 |
| ILMN_10039 | NM_024661.2 | CCDC51 | 21362023 | 10.555 | 10.475 | 9.104 | 9.001 | -1.463 |

| Table 5, continued | | | | | | | | |
|---|---|---|---|---|---|---|---|---|
| ILMN_18038 | NM_001731.1 | BTG1 | 4502472 | 13.245 | 13.044 | 11.514 | 11.817 | -1.479 |
| ILMN_2416 | NM_006877.2 | GMPR | 31542848 | 7.535 | 7.719 | 5.933 | 6.352 | -1.484 |
| ILMN_114974 | Hs.561603 | 0 | 23066233 | 6.747 | 6.835 | 5.236 | 5.375 | -1.485 |
| ILMN_6779 | NM_020896.2 | OSBPL5 | 22035607 | 10.481 | 10.609 | 9.105 | 9.006 | -1.490 |
| ILMN_20958 | NM_016339.1 | RAPGEFL1 | 7705938 | 10.109 | 10.047 | 8.436 | 8.733 | -1.493 |
| ILMN_74694 | Hs.101003 | 0 | 27838294 | 6.845 | 6.773 | 5.057 | 5.570 | -1.496 |
| ILMN_102192 | Hs.534279 | 0 | 21955385 | 9.192 | 9.422 | 7.693 | 7.899 | -1.511 |
| ILMN_27164 | NM_005410.2 | SEPP1 | 62530390 | 10.930 | 11.118 | 9.555 | 9.459 | -1.517 |
| ILMN_7361 | NM_007288.1 | MME | 6042201 | 9.557 | 9.855 | 7.965 | 8.407 | -1.520 |
| ILMN_828 | NM_080878.2 | ITLN2 | 37622351 | 6.689 | 6.812 | 5.482 | 4.977 | -1.521 |
| ILMN_13399 | NM_001032278.1 | MMP28 | 73808270 | 9.191 | 9.401 | 7.770 | 7.743 | -1.539 |
| ILMN_1908 | NM_018398.2 | CACNA2D3 | 54112396 | 7.021 | 6.840 | 5.217 | 5.552 | -1.546 |
| ILMN_17837 | NM_014007.2 | ZNF297B | 45267833 | 10.229 | 9.900 | 8.356 | 8.671 | -1.550 |
| ILMN_27069 | NM_006665.2 | HPSE | 19923365 | 6.574 | 6.918 | 5.221 | 5.170 | -1.551 |
| ILMN_19750 | NM_001005404.3 | YPEL2 | 56550087 | 6.681 | 7.232 | 5.399 | 5.406 | -1.554 |
| ILMN_26811 | NM_174902.2 | LDLRAD3 | 31341355 | 8.797 | 8.990 | 7.408 | 7.268 | -1.556 |
| ILMN_26434 | NM_030806.3 | C1orf21 | 58761542 | 8.427 | 8.725 | 6.931 | 7.099 | -1.561 |
| ILMN_42462 | XM_932354.1 | LOC644760 | 88984918 | 6.891 | 6.874 | 5.446 | 5.190 | -1.565 |
| ILMN_18735 | NM_153046.1 | TDRD9 | 42734387 | 6.670 | 6.436 | 4.977 | 4.991 | -1.569 |
| ILMN_24736 | NM_152466.1 | C17orf69 | 22748982 | 7.119 | 7.133 | 5.271 | 5.838 | -1.572 |
| ILMN_3053 | NM_170744.2 | UNC5B | 32261317 | 6.361 | 6.421 | 4.878 | 4.750 | -1.578 |
| ILMN_14320 | NM_004428.2 | EFNA1 | 33359681 | 10.630 | 10.646 | 8.629 | 9.489 | -1.579 |
| ILMN_37098 | XM_942586.1 | LOC651309 | 89036309 | 7.068 | 6.988 | 5.358 | 5.527 | -1.586 |
| ILMN_32329 | XM_937528.1 | C10orf73 | 89031946 | 6.776 | 6.910 | 5.350 | 5.146 | -1.595 |
| ILMN_28123 | NM_001547.3 | IFIT2 | 34222091 | 7.505 | 7.928 | 5.938 | 6.285 | -1.605 |
| ILMN_39623 | XM_937048.1 | LOC647993 | 89033514 | 7.122 | 7.127 | 5.113 | 5.912 | -1.612 |
| ILMN_115186 | Hs.561940 | 0 | 16549932 | 7.509 | 7.604 | 5.687 | 6.190 | -1.619 |
| ILMN_92093 | Hs.438937 | 0 | 34529519 | 7.149 | 7.578 | 5.684 | 5.805 | -1.619 |
| ILMN_2924 | NM_005271.1 | GLUD1 | 4885280 | 12.611 | 12.759 | 11.066 | 11.033 | -1.635 |
| ILMN_16562 | NM_004117.2 | FKBP5 | 17149847 | 12.582 | 12.486 | 10.824 | 10.961 | -1.641 |
| ILMN_8954 | NM_001072.2 | UGT1A6 | 45827764 | 7.604 | 7.731 | 6.018 | 6.020 | -1.648 |
| ILMN_11805 | NM_003408.1 | ZFP37 | 4507962 | 6.955 | 6.833 | 5.600 | 4.863 | -1.663 |
| ILMN_9078 | NM_020152.2 | C21orf7 | 31542267 | 8.254 | 8.549 | 6.594 | 6.842 | -1.684 |
| ILMN_19900 | NM_020747.1 | ZNF608 | 55741877 | 7.184 | 7.238 | 5.456 | 5.594 | -1.686 |
| ILMN_16923 | NM_000396.2 | CTSK | 23110958 | 6.677 | 7.050 | 5.087 | 5.248 | -1.696 |
| ILMN_40266 | XM_928461.1 | LOC653626 | 89035446 | 9.696 | 9.691 | 7.739 | 8.227 | -1.710 |
| ILMN_28493 | NM_023944.1 | CYP4F12 | 13184045 | 8.332 | 7.791 | 5.989 | 6.700 | -1.717 |
| ILMN_1491 | NM_024650.2 | FLJ22531 | 31542734 | 10.465 | 10.511 | 8.647 | 8.881 | -1.724 |
| ILMN_76686 | Hs.128753 | 0 | 7021073 | 6.558 | 6.833 | 4.963 | 4.977 | -1.725 |
| ILMN_8703 | NM_170600.1 | SH2D3C | 41281820 | 6.827 | 7.364 | 5.492 | 5.244 | -1.727 |
| ILMN_16293 | NM_153377.3 | LRIG3 | 40255156 | 9.228 | 9.482 | 7.264 | 7.988 | -1.729 |
| ILMN_33860 | XM_926530.1 | LOC643161 | 89031545 | 6.468 | 7.027 | 4.802 | 5.182 | -1.755 |
| ILMN_13193 | NM_020431.1 | TMEM63C | 55742804 | 6.918 | 6.902 | 5.517 | 4.787 | -1.758 |
| ILMN_27758 | NM_022751.1 | FAM59A | 12232414 | 8.289 | 8.022 | 6.081 | 6.707 | -1.761 |
| ILMN_26240 | NM_001257.3 | CDH13 | 61676095 | 9.924 | 9.931 | 8.130 | 8.196 | -1.764 |
| ILMN_15043 | NM_017791.1 | C14orf58 | 8923349 | 7.435 | 7.426 | 5.561 | 5.766 | -1.768 |
| ILMN_25095 | NM_005971.2 | FXYD3 | 11612675 | 10.448 | 10.394 | 8.568 | 8.728 | -1.773 |
| ILMN_15496 | NM_001024668.1 | LETMD1 | 67089166 | 9.429 | 9.604 | 7.696 | 7.789 | -1.774 |
| ILMN_71632 | Hs.20255 | 0 | 9873865 | 7.258 | 7.533 | 5.206 | 6.036 | -1.775 |
| ILMN_40428 | XM_942885.1 | LOC440928 | 88958963 | 8.025 | 7.859 | 5.928 | 6.382 | -1.787 |
| ILMN_20716 | NM_173653.1 | SLC9A9 | 27734934 | 7.948 | 8.290 | 6.520 | 6.121 | -1.798 |
| ILMN_4567 | NM_178008.1 | STARD13 | 41281901 | 6.693 | 6.811 | 4.498 | 5.403 | -1.802 |
| ILMN_11581 | NM_017570.1 | OPLAH | 48314819 | 10.168 | 10.104 | 7.996 | 8.628 | -1.824 |
| ILMN_27652 | NM_004071.2 | CLK1 | 67551260 | 8.115 | 8.298 | 6.394 | 6.365 | -1.827 |
| ILMN_92725 | Hs.444329 | 0 | 34365191 | 10.075 | 9.594 | 7.918 | 8.064 | -1.843 |
| ILMN_4989 | NM_017622.1 | C17orf59 | 8923020 | 9.581 | 9.584 | 7.649 | 7.826 | -1.845 |
| ILMN_26717 | NM_006308.1 | HSPB3 | 5453687 | 6.670 | 7.335 | 4.921 | 5.347 | -1.868 |
| ILMN_12567 | NM_019005.2 | FLJ20323 | 46358341 | 10.147 | 10.193 | 8.331 | 8.264 | -1.873 |
| ILMN_18486 | NM_032160.2 | C18orf4 | 59938787 | 7.028 | 7.385 | 5.453 | 5.213 | -1.874 |

| Table 5, continued | | | | | | | | |
|---|---|---|---|---|---|---|---|---|
| ILMN_7083 | NM_014751.2 | MTSS1 | 30023852 | 8.063 | 8.347 | 6.194 | 6.445 | -1.886 |
| ILMN_20035 | NM_058229.2 | FBXO32 | 22547142 | 8.836 | 9.274 | 7.405 | 6.909 | -1.898 |
| ILMN_16107 | NM_001085.4 | SERPINA3 | 73858562 | 14.258 | 14.644 | 12.751 | 12.278 | -1.936 |
| ILMN_25965 | NM_002202.1 | ISL1 | 4504736 | 7.464 | 7.408 | 5.450 | 5.545 | -1.938 |
| ILMN_29543 | NM_022165.2 | LIN7B | 56676320 | 7.506 | 7.491 | 5.731 | 5.379 | -1.944 |
| ILMN_8744 | NM_153607.1 | LOC153222 | 23957697 | 8.135 | 8.499 | 6.135 | 6.597 | -1.951 |
| ILMN_10249 | NM_205862.1 | UGT1A6 | 45827766 | 8.645 | 8.804 | 6.988 | 6.531 | -1.965 |
| ILMN_6288 | NM_000196.2 | HSD11B2 | 31542940 | 7.591 | 7.375 | 5.463 | 5.558 | -1.973 |
| ILMN_14880 | NM_005384.2 | NFIL3 | 52630428 | 10.442 | 10.244 | 8.315 | 8.377 | -1.997 |
| ILMN_28225 | NM_207397.1 | CD164L2 | 46409425 | 7.431 | 6.968 | 5.194 | 5.190 | -2.008 |
| ILMN_15343 | NM_153034.2 | ZNF488 | 40255102 | 8.810 | 9.439 | 7.324 | 6.870 | -2.028 |
| ILMN_3809 | NM_148177.1 | FBXO32 | 22547143 | 10.809 | 11.028 | 9.204 | 8.565 | -2.034 |
| ILMN_27286 | NM_001024646.1 | CLK1 | 67551262 | 10.400 | 10.406 | 8.287 | 8.444 | -2.038 |
| ILMN_22366 | NM_024617.2 | ZCCHC6 | 58331271 | 11.512 | 11.524 | 9.387 | 9.564 | -2.043 |
| ILMN_3567 | NM_005012.1 | ROR1 | 4826867 | 6.889 | 7.482 | 4.722 | 5.517 | -2.066 |
| ILMN_137281 | NM_005738.2 | ARL4 | 47078225 | 9.756 | 9.742 | 7.700 | 7.633 | -2.083 |
| ILMN_19665 | NM_198061.1 | CES2 | 37622886 | 12.511 | 12.583 | 10.300 | 10.586 | -2.104 |
| ILMN_22390 | NM_006113.3 | VAV3 | 21614495 | 9.169 | 9.482 | 6.868 | 7.484 | -2.150 |
| ILMN_11566 | NM_000240.2 | MAOA | 33469954 | 13.362 | 13.122 | 10.654 | 11.435 | -2.198 |
| ILMN_5404 | NM_014454.1 | SESN1 | 7657436 | 9.607 | 9.431 | 7.400 | 7.209 | -2.214 |
| ILMN_540 | NM_001706.2 | BCL6 | 21040323 | 11.273 | 11.211 | 8.932 | 9.065 | -2.244 |
| ILMN_25981 | NM_005823.4 | MSLN | 68303642 | 13.222 | 13.410 | 11.322 | 10.811 | -2.249 |
| ILMN_18558 | NM_001512.2 | GSTA4 | 23065568 | 11.286 | 11.093 | 8.691 | 9.070 | -2.309 |
| ILMN_8842 | NM_002944.2 | ROS1 | 19924164 | 8.290 | 8.296 | 5.959 | 5.998 | -2.314 |
| ILMN_10722 | NM_004062.2 | CDH16 | 16507958 | 7.513 | 6.944 | 4.792 | 5.036 | -2.315 |
| ILMN_11739 | NM_002198.1 | IRF1 | 4504720 | 11.063 | 11.357 | 9.111 | 8.645 | -2.332 |
| ILMN_22942 | NM_006393.1 | NEBL | 5453757 | 8.105 | 8.262 | 6.106 | 5.594 | -2.333 |
| ILMN_1890 | NM_000421.2 | KRT10 | 40354191 | 12.224 | 13.005 | 9.907 | 10.583 | -2.369 |
| ILMN_30616 | XM_940680.1 | LOC648517 | 89061897 | 12.827 | 12.382 | 10.476 | 9.944 | -2.395 |
| ILMN_9057 | NM_006472.1 | TXNIP | 5454161 | 13.652 | 13.890 | 11.181 | 11.549 | -2.406 |
| ILMN_26458 | NM_025165.2 | ELL3 | 76781448 | 9.264 | 8.850 | 6.276 | 7.019 | -2.409 |
| ILMN_123332 | Hs.571151 | 0 | 10722614 | 8.843 | 8.656 | 6.219 | 6.392 | -2.444 |
| ILMN_11770 | NM_005309.1 | GPT | 4885350 | 6.582 | 6.343 | 3.070 | 4.883 | -2.486 |
| ILMN_3663 | NM_005461.3 | MAFB | 31652256 | 11.926 | 11.898 | 8.726 | 9.990 | -2.554 |
| ILMN_16362 | NM_001005474.1 | NFKBIZ | 53832023 | 9.372 | 9.450 | 6.146 | 7.485 | -2.596 |
| ILMN_17486 | NM_016335.2 | PRODH | 19924110 | 9.562 | 9.769 | 6.541 | 7.575 | -2.608 |
| ILMN_35558 | XM_379623.2 | FLJ41200 | 89029186 | 6.901 | 8.179 | 4.706 | 5.150 | -2.612 |
| ILMN_139156 | NM_001001669.1 | FLJ41603 | 48717281 | 9.598 | 10.022 | 7.013 | 7.381 | -2.613 |
| ILMN_41814 | XM_290629.6 | C14orf78 | 89037518 | 13.288 | 13.494 | 10.541 | 10.967 | -2.637 |
| ILMN_24488 | NM_024320.2 | ATAD4 | 34147376 | 9.089 | 8.451 | 5.858 | 6.331 | -2.676 |
| ILMN_4286 | NM_173462.2 | PAPLN | 50083294 | 8.530 | 9.280 | 5.895 | 6.497 | -2.709 |
| ILMN_34738 | XM_945010.1 | LOC651913 | 89057548 | 7.941 | 8.120 | 5.501 | 4.968 | -2.796 |
| ILMN_23990 | NM_001039.2 | SCNN1G | 42476332 | 10.500 | 10.366 | 7.464 | 7.801 | -2.801 |
| ILMN_137748 | XM_930820.1 | LRRK2 | 89035472 | 6.231 | 6.760 | 4.053 | 3.186 | -2.876 |
| ILMN_82165 | Hs.210390 | 0 | 10435476 | 7.970 | 8.391 | 5.083 | 5.520 | -2.879 |
| ILMN_20483 | NM_001005340.1 | GPNMB | 52694751 | 9.470 | 11.604 | 7.652 | 7.594 | -2.914 |
| ILMN_71591 | Hs.19339 | 0 | 34191392 | 9.050 | 9.362 | 6.304 | 6.274 | -2.917 |
| ILMN_6827 | NM_001885.1 | CRYAB | 4503056 | 8.985 | 9.125 | 5.880 | 6.345 | -2.942 |
| ILMN_13696 | NM_001011709.1 | PNLIPRP3 | 58743370 | 10.037 | 9.918 | 6.727 | 7.262 | -2.983 |
| ILMN_19114 | NM_139072.2 | DNER | 31542542 | 9.781 | 9.646 | 6.307 | 7.131 | -2.994 |
| ILMN_12568 | NM_013281.2 | FLRT3 | 38202220 | 11.298 | 11.262 | 8.007 | 8.384 | -3.084 |
| ILMN_4993 | NM_018208.1 | ETNK2 | 8922649 | 8.173 | 8.641 | 5.709 | 4.931 | -3.087 |
| ILMN_20221 | NM_000896.1 | CYP4F3 | 4503240 | 9.989 | 9.289 | 6.064 | 6.722 | -3.246 |
| ILMN_71322 | Hs.13291 | 0 | 21751275 | 7.150 | 7.358 | 4.096 | 3.459 | -3.476 |
| ILMN_3297 | NM_000777.2 | CYP3A5 | 15147331 | 7.764 | 8.019 | 3.926 | 4.744 | -3.556 |
| ILMN_28619 | NM_000336.1 | SCNN1B | 4506816 | 8.376 | 8.553 | 4.505 | 4.760 | -3.832 |
| ILMN_9188 | NM_002423.3 | MMP7 | 75709180 | 8.380 | 9.317 | 5.013 | 4.365 | -4.159 |
| ILMN_5569 | NM_206857.1 | RTN1 | 45827777 | 9.067 | 8.498 | 4.358 | 4.863 | -4.172 |
| ILMN_9893 | NM_004089.3 | TSC22D3 | 62865622 | 12.668 | 12.570 | 8.145 | 8.436 | -4.328 |

**Table 6: Affymetrix probe sets corresponding to the GAB2-signature and their Pearson correlation with sensitivity (GI-50) to Resveratrol, Piceatannol and SD-1029 in the NCI-60 cell line panel.**

| Affymetrix Probe Set | Gene Symbol | Pearson with GI50 to Resve-ratrol | Pearson with GI50 to Picea-tannol | Pearson with GI50 to SD-1029 |
|---|---|---|---|---|
| 204343_at | ABCA3 | -0.169 | -0.367 | -0.113 |
| 208161_s_at | ABCC3 | -0.023 | 0.334 | 0.133 |
| 209641_s_at | ABCC3 | -0.015 | 0.271 | 0.169 |
| 214979_at | ABCC3 | -0.004 | 0.094 | -0.052 |
| 230682_x_at | ABCC3 | 0.037 | 0.172 | 0.213 |
| 239217_x_at | ABCC3 | -0.023 | 0.225 | 0.102 |
| 242553_at | ABCC3 | 0.097 | 0.222 | 0.212 |
| 228132_at | ABLIM2 | 0.084 | 0.180 | -0.152 |
| 236087_at | ABLIM2 | -0.005 | 0.094 | 0.041 |
| 242624_at | ABLIM2 | 0.067 | 0.111 | 0.182 |
| 224882_at | ACSS1 | -0.243 | -0.110 | -0.063 |
| 234483_at | ACSS1 | 0.081 | -0.022 | 0.065 |
| 234484_s_at | ACSS1 | -0.056 | -0.037 | -0.012 |
| 234801_s_at | ACSS1 | 0.034 | 0.041 | 0.104 |
| 235724_at | ACSS1 | -0.171 | -0.275 | -0.245 |
| 200974_at | ACTA2 | 0.155 | 0.205 | 0.192 |
| 215787_at | ACTA2 | -0.031 | -0.029 | -0.266 |
| 243140_at | ACTA2 | 0.065 | -0.045 | 0.071 |
| 206262_at | ADH1A | 0.058 | 0.034 | -0.528 |
| 207820_at | ADH1A | -0.220 | 0.005 | -0.206 |
| 209160_at | AKR1C3 | 0.072 | 0.325 | 0.036 |
| 205623_at | ALDH3A1 | 0.061 | 0.186 | -0.029 |
| 203747_at | AQP3 | -0.196 | -0.022 | 0.071 |
| 39248_at | AQP3 | -0.187 | -0.170 | -0.052 |
| 39249_at | AQP3 | -0.198 | -0.023 | -0.006 |
| 201288_at | ARHGDIB | -0.266 | -0.327 | -0.100 |
| 212614_at | ARID5B | 0.298 | 0.114 | 0.213 |
| 235404_at | ARID5B | -0.105 | -0.334 | -0.107 |
| 241969_at | ARID5B | -0.001 | -0.339 | -0.099 |
| 219918_s_at | ASPM | 0.080 | 0.032 | 0.177 |
| 232238_at | ASPM | 0.245 | 0.081 | 0.209 |
| 239002_at | ASPM | 0.145 | -0.163 | 0.187 |
| 214070_s_at | ATP10B | 0.138 | 0.340 | -0.122 |
| 220920_at | ATP10B | 0.107 | 0.003 | -0.103 |
| 205473_at | ATP6V1B1 | 0.035 | 0.076 | -0.126 |
| 209464_at | AURKB | 0.247 | 0.043 | 0.236 |
| 239219_at | AURKB | 0.014 | -0.053 | 0.208 |
| 209309_at | AZGP1 | -0.175 | -0.041 | -0.110 |
| 217014_s_at | AZGP1 | -0.185 | -0.066 | -0.006 |
| 219476_at | C1orf116 | -0.120 | 0.195 | 0.045 |
| 219856_at | C1orf116 | -0.022 | 0.074 | 0.035 |
| 228865_at | C1orf116 | -0.061 | 0.234 | -0.088 |
| 241233_x_at | C21orf81 | -0.411 | -0.174 | 0.007 |
| 206707_x_at | C6orf32 | 0.175 | 0.102 | 0.141 |
| 209829_at | C6orf32 | 0.177 | 0.219 | 0.177 |
| 220150_s_at | C6orf60 | 0.130 | -0.274 | -0.118 |
| 223194_s_at | C6orf85 | -0.245 | 0.249 | -0.088 |
| 233206_at | C6orf85 | 0.062 | 0.133 | 0.017 |
| 212848_s_at | C9orf3 | 0.211 | 0.225 | 0.257 |
| 232270_at | C9orf3 | 0.226 | 0.161 | 0.105 |
| 232000_at | C9orf52 | -0.137 | 0.106 | -0.026 |
| 236826_at | C9orf52 | -0.062 | 0.053 | -0.042 |
| 242477_at | C9orf52 | 0.107 | 0.017 | -0.024 |
| 223074_s_at | C9orf58 | -0.010 | -0.002 | -0.004 |
| 223075_s_at | C9orf58 | 0.175 | 0.017 | -0.053 |

Table 6, continued

| | | | | |
|---|---|---|---|---|
| 203963_at | CA12 | -0.134 | 0.068 | 0.009 |
| 204508_s_at | CA12 | -0.142 | 0.082 | 0.063 |
| 204509_at | CA12 | -0.125 | -0.089 | -0.319 |
| 210735_s_at | CA12 | -0.172 | 0.102 | 0.022 |
| 214164_x_at | CA12 | -0.111 | 0.057 | 0.055 |
| 215867_x_at | CA12 | -0.130 | 0.037 | 0.052 |
| 209956_s_at | CAMK2B | 0.073 | -0.013 | -0.269 |
| 210404_x_at | CAMK2B | -0.028 | -0.052 | -0.259 |
| 211483_x_at | CAMK2B | 0.004 | -0.028 | -0.257 |
| 213276_at | CAMK2B | -0.168 | -0.114 | 0.121 |
| 34846_at | CAMK2B | 0.014 | -0.041 | -0.223 |
| 218309_at | CAMK2N1 | 0.108 | 0.268 | 0.255 |
| 228302_x_at | CAMK2N1 | -0.150 | 0.200 | 0.035 |
| 229163_at | CAMK2N1 | -0.061 | 0.180 | 0.115 |
| 201432_at | CAT | -0.235 | -0.204 | -0.125 |
| 211922_s_at | CAT | -0.324 | -0.245 | -0.204 |
| 215573_at | CAT | 0.044 | -0.008 | -0.248 |
| 238363_at | CAT | -0.211 | -0.287 | -0.244 |
| 212886_at | CCDC69 | -0.248 | -0.117 | 0.003 |
| 242430_at | CCDC69 | 0.045 | 0.155 | 0.185 |
| 216598_s_at | CCL2 | 0.016 | 0.124 | 0.220 |
| 203418_at | CCNA2 | -0.084 | -0.132 | -0.065 |
| 213226_at | CCNA2 | -0.049 | -0.153 | -0.029 |
| 214710_s_at | CCNB1 | 0.241 | 0.084 | 0.119 |
| 228729_at | CCNB1 | 0.301 | 0.036 | -0.008 |
| 202705_at | CCNB2 | -0.060 | -0.021 | 0.145 |
| 232764_at | CCNB2 | -0.380 | -0.154 | -0.029 |
| 232768_at | CCNB2 | 0.208 | -0.011 | 0.198 |
| 206488_s_at | CD36 | 0.117 | 0.227 | 0.041 |
| 209554_at | CD36 | -0.128 | -0.138 | -0.037 |
| 209555_s_at | CD36 | 0.059 | -0.009 | -0.253 |
| 228766_at | CD36 | 0.016 | -0.037 | 0.031 |
| 242197_x_at | CD36 | -0.072 | -0.136 | -0.056 |
| 209850_s_at | CDC42EP2 | 0.052 | 0.022 | 0.033 |
| 214014_at | CDC42EP2 | 0.088 | 0.106 | 0.081 |
| 204126_s_at | CDC45L | -0.017 | -0.044 | 0.107 |
| 224753_at | CDCA5 | -0.025 | -0.173 | -0.246 |
| 224428_s_at | CDCA7 | -0.050 | -0.302 | -0.174 |
| 230060_at | CDCA7 | -0.176 | -0.175 | -0.039 |
| 204726_at | CDH13 | 0.133 | -0.018 | 0.154 |
| 209832_s_at | CDT1 | -0.389 | -0.121 | -0.237 |
| 228868_x_at | CDT1 | -0.332 | -0.134 | -0.298 |
| 207828_s_at | CENPF | 0.151 | -0.040 | 0.477 |
| 209172_s_at | CENPF | 0.201 | 0.055 | 0.405 |
| 209667_at | CES2 | -0.074 | 0.199 | 0.034 |
| 209668_x_at | CES2 | -0.075 | 0.254 | -0.056 |
| 213509_x_at | CES2 | -0.058 | 0.167 | 0.005 |
| 203854_at | CFI | 0.174 | 0.184 | 0.065 |
| 218182_s_at | CLDN1 | -0.035 | 0.293 | -0.081 |
| 222549_at | CLDN1 | -0.050 | 0.302 | -0.061 |
| 201445_at | CNN3 | 0.372 | 0.076 | 0.381 |
| 219400_at | CNTNAP1 | -0.057 | 0.011 | 0.160 |
| 208146_s_at | CPVL | 0.127 | 0.151 | 0.195 |
| 216365_x_at | CPVL | 0.073 | 0.019 | -0.201 |
| 217239_x_at | CPVL | -0.043 | -0.174 | -0.221 |

| Table 6, continued | | | | |
|---|---|---|---|---|
| 205843_x_at | CRAT | -0.276 | 0.124 | 0.214 |
| 209522_s_at | CRAT | 0.027 | 0.184 | 0.223 |
| 209283_at | CRYAB | 0.170 | 0.132 | 0.062 |
| 203917_at | CXADR | 0.118 | 0.185 | -0.013 |
| 209201_x_at | CXCR4 | -0.581 | -0.342 | -0.278 |
| 211919_s_at | CXCR4 | -0.580 | -0.364 | -0.294 |
| 217028_at | CXCR4 | -0.575 | -0.375 | -0.284 |
| 202434_s_at | CYP1B1 | -0.025 | 0.090 | -0.131 |
| 202435_s_at | CYP1B1 | -0.033 | 0.212 | 0.141 |
| 202436_s_at | CYP1B1 | -0.055 | 0.196 | 0.163 |
| 202437_s_at | CYP1B1 | -0.097 | 0.150 | 0.140 |
| 206539_s_at | CYP4F12 | 0.022 | 0.146 | 0.025 |
| 206515_at | CYP4F3 | 0.016 | 0.182 | -0.062 |
| 216646_at | DCC1 | -0.009 | 0.008 | -0.240 |
| 219000_s_at | DCC1 | -0.012 | -0.144 | -0.099 |
| 209094_at | DDAH1 | 0.060 | -0.066 | 0.063 |
| 229456_s_at | DDAH1 | 0.166 | -0.070 | -0.127 |
| 243711_at | DDAH1 | 0.136 | -0.088 | 0.137 |
| 221081_s_at | DENND2D | -0.574 | -0.150 | -0.318 |
| 215151_at | DOCK10 | 0.156 | 0.078 | 0.072 |
| 219279_at | DOCK10 | -0.058 | 0.134 | 0.337 |
| 218585_s_at | DTL | -0.102 | -0.068 | 0.082 |
| 222680_s_at | DTL | -0.172 | -0.050 | -0.098 |
| 223402_at | DUSP23 | -0.254 | 0.318 | -0.043 |
| 207042_at | E2F2 | -0.128 | -0.108 | -0.284 |
| 228361_at | E2F2 | -0.184 | -0.172 | -0.239 |
| 235582_at | E2F2 | -0.251 | -0.250 | -0.019 |
| 204540_at | EEF1A2 | -0.145 | 0.192 | 0.018 |
| 208427_s_at | ELAVL2 | -0.050 | -0.060 | -0.157 |
| 228260_at | ELAVL2 | 0.077 | 0.115 | 0.090 |
| 201510_at | ELF3 | -0.050 | 0.269 | -0.015 |
| 210827_s_at | ELF3 | -0.008 | 0.115 | -0.163 |
| 203729_at | EMP3 | 0.096 | 0.005 | 0.304 |
| 203499_at | EPHA2 | 0.325 | 0.219 | 0.253 |
| 203348_s_at | ETV5 | 0.215 | 0.044 | 0.401 |
| 203349_s_at | ETV5 | 0.270 | 0.032 | 0.437 |
| 216375_s_at | ETV5 | 0.260 | 0.132 | 0.349 |
| 230102_at | ETV5 | 0.283 | 0.033 | 0.334 |
| 204603_at | EXO1 | -0.128 | -0.059 | 0.140 |
| 209955_s_at | FAP | -0.064 | -0.028 | 0.091 |
| 201910_at | FARP1 | 0.166 | 0.253 | 0.274 |
| 201911_s_at | FARP1 | 0.223 | 0.336 | 0.431 |
| 227996_at | FARP1 | 0.053 | 0.175 | 0.090 |
| 237767_at | FARP1 | 0.069 | 0.020 | 0.070 |
| 239246_at | FARP1 | 0.244 | 0.118 | 0.222 |
| 205014_at | FGFBP1 | 0.032 | 0.171 | -0.081 |
| 227717_at | FLJ41603 | 0.016 | 0.152 | 0.009 |
| 241380_at | FLJ41603 | 0.071 | 0.139 | -0.009 |
| 219250_s_at | FLRT3 | 0.129 | 0.106 | 0.106 |
| 222853_at | FLRT3 | 0.124 | 0.036 | 0.091 |
| 227475_at | FOXQ1 | 0.114 | 0.093 | -0.127 |
| 206774_at | FRMPD1 | -0.005 | -0.073 | -0.243 |
| 202838_at | FUCA1 | 0.206 | 0.261 | 0.112 |
| 229137_at | FUCA1 | -0.055 | -0.007 | 0.061 |
| 214088_s_at | FUT3 | -0.052 | 0.141 | -0.180 |
| 216010_x_at | FUT3 | 0.038 | 0.130 | -0.233 |
| 203397_s_at | GALNT3 | 0.106 | 0.258 | -0.079 |
| 203398_s_at | GALNT3 | 0.043 | -0.010 | -0.220 |
| 204836_at | GLDC | 0.086 | 0.121 | 0.039 |
| 201141_at | GPNMB | 0.123 | 0.128 | 0.265 |
| 206709_x_at | GPT | 0.056 | -0.009 | -0.246 |
| 202967_at | GSTA4 | 0.197 | -0.040 | 0.115 |
| 235405_at | GSTA4 | 0.322 | -0.078 | 0.137 |
| 207165_at | HMMR | 0.204 | -0.051 | -0.011 |
| 209709_s_at | HMMR | 0.104 | -0.125 | 0.021 |

| Table 6, continued | | | | |
|---|---|---|---|---|
| 206864_s_at | HRK | 0.197 | 0.227 | 0.144 |
| 206865_at | HRK | 0.059 | 0.015 | -0.209 |
| 201841_s_at | HSPB1 | 0.088 | 0.348 | 0.120 |
| 206375_s_at | HSPB3 | 0.118 | 0.008 | 0.069 |
| 204002_s_at | ICA1 | -0.104 | 0.061 | -0.194 |
| 207949_s_at | ICA1 | -0.361 | -0.024 | -0.462 |
| 210547_x_at | ICA1 | -0.243 | 0.013 | -0.468 |
| 211740_at | ICA1 | 0.022 | -0.056 | -0.245 |
| 214191_at | ICA1 | -0.065 | -0.048 | -0.262 |
| 208937_s_at | ID1 | 0.197 | 0.076 | 0.033 |
| 201565_s_at | ID2 | 0.135 | 0.005 | -0.176 |
| 201566_x_at | ID2 | 0.146 | -0.176 | -0.152 |
| 213931_at | ID2 | 0.091 | -0.224 | -0.114 |
| 207826_s_at | ID3 | 0.205 | 0.119 | 0.069 |
| 201601_x_at | IFITM1 | -0.193 | -0.301 | -0.184 |
| 214022_s_at | IFITM1 | -0.193 | -0.274 | -0.239 |
| 212203_x_at | IFITM3 | 0.287 | 0.070 | 0.356 |
| 203424_s_at | IGFBP5 | -0.355 | -0.051 | -0.057 |
| 203425_s_at | IGFBP5 | -0.105 | 0.041 | 0.195 |
| 203426_s_at | IGFBP5 | -0.272 | -0.106 | -0.044 |
| 211958_at | IGFBP5 | -0.187 | 0.019 | 0.098 |
| 211959_at | IGFBP5 | 0.025 | 0.047 | 0.179 |
| 231179_at | IHPK3 | 0.050 | -0.207 | -0.231 |
| 203126_at | IMPA2 | 0.124 | 0.114 | -0.196 |
| 229538_s_at | IQGAP3 | 0.335 | 0.189 | 0.311 |
| 241939_at | IQGAP3 | -0.001 | 0.028 | 0.015 |
| 231779_at | IRAK2 | -0.022 | 0.076 | 0.152 |
| 206104_at | ISL1 | -0.165 | -0.281 | -0.140 |
| 206766_at | ITGA10 | 0.154 | 0.074 | 0.145 |
| 202803_s_at | ITGB2 | -0.303 | -0.425 | -0.080 |
| 236988_x_at | ITGB2 | -0.239 | -0.328 | -0.231 |
| 209408_at | KIF2C | 0.287 | -0.122 | 0.220 |
| 211519_s_at | KIF2C | 0.323 | -0.125 | 0.150 |
| 205778_at | KLK7 | 0.153 | -0.194 | 0.078 |
| 239381_at | KLK7 | 0.160 | -0.086 | 0.117 |
| 207023_x_at | KRT10 | -0.040 | 0.187 | 0.364 |
| 210633_x_at | KRT10 | 0.018 | 0.204 | 0.371 |
| 213287_s_at | KRT10 | 0.004 | 0.219 | 0.357 |
| 207935_s_at | KRT13 | -0.069 | 0.159 | 0.130 |
| 209016_s_at | KRT7 | -0.021 | 0.251 | 0.171 |
| 214031_s_at | KRT7 | 0.003 | 0.090 | 0.077 |
| 201720_s_at | LAPTM5 | -0.377 | -0.255 | -0.262 |
| 201721_s_at | LAPTM5 | -0.318 | -0.291 | -0.232 |
| 212531_at | LCN2 | 0.101 | 0.188 | -0.092 |
| 202067_s_at | LDLR | -0.089 | -0.167 | 0.114 |
| 202068_s_at | LDLR | 0.055 | 0.029 | 0.378 |
| 217005_at | LDLR | 0.023 | -0.038 | -0.299 |
| 217103_at | LDLR | 0.024 | -0.056 | -0.256 |
| 217173_s_at | LDLR | -0.111 | -0.206 | 0.019 |
| 217183_at | LDLR | 0.055 | -0.009 | -0.248 |
| 209179_s_at | LENG4 | 0.368 | 0.367 | 0.166 |
| 211037_s_at | LENG4 | 0.135 | 0.234 | -0.081 |
| 215270_at | LFNG | 0.041 | 0.000 | -0.268 |
| 228762_at | LFNG | -0.009 | 0.129 | -0.150 |
| 219760_at | LIN7B | 0.017 | -0.010 | 0.130 |
| 241957_x_at | LIN7B | 0.051 | -0.170 | 0.059 |
| 239155_at | LOC653108 | 0.134 | 0.010 | -0.305 |
| 228648_at | LRG1 | -0.073 | -0.021 | -0.123 |
| 202145_at | LY6E | -0.218 | 0.138 | 0.141 |
| 205458_at | MC1R | 0.091 | 0.186 | 0.050 |
| 213476_x_at | MC1R | 0.356 | 0.284 | 0.173 |
| 232092_at | MCART1 | 0.194 | 0.029 | -0.053 |
| 238574_at | MCART1 | 0.028 | 0.257 | 0.066 |
| 201755_at | MCM5 | -0.200 | -0.229 | -0.091 |
| 216237_s_at | MCM5 | -0.165 | -0.182 | 0.028 |

Table 6, continued

| | | | | |
|---|---|---|---|---|
| 208795_s_at | MCM7 | -0.019 | -0.258 | -0.080 |
| 210983_s_at | MCM7 | 0.018 | -0.196 | -0.090 |
| 202291_s_at | MGP | -0.137 | -0.184 | 0.104 |
| 238481_at | MGP | -0.366 | -0.284 | -0.116 |
| 219909_at | MMP28 | 0.023 | -0.027 | -0.259 |
| 222937_s_at | MMP28 | -0.089 | -0.071 | -0.036 |
| 224207_x_at | MMP28 | -0.212 | 0.081 | -0.108 |
| 239272_at | MMP28 | 0.023 | 0.164 | 0.111 |
| 239273_s_at | MMP28 | 0.002 | 0.220 | 0.069 |
| 204745_x_at | MT1G | 0.094 | 0.038 | 0.207 |
| 210472_at | MT1G | 0.078 | 0.046 | 0.080 |
| 212185_x_at | MT2A | 0.303 | 0.269 | 0.406 |
| 218966_at | MYO5C | -0.181 | 0.008 | -0.171 |
| 218039_at | NUSAP1 | 0.173 | 0.017 | 0.206 |
| 219978_s_at | NUSAP1 | 0.040 | -0.112 | 0.152 |
| 214607_at | PAK3 | -0.040 | 0.042 | -0.011 |
| 218952_at | PCSK1N | -0.025 | -0.016 | 0.060 |
| 205960_at | PDK4 | -0.089 | -0.026 | 0.103 |
| 225207_at | PDK4 | 0.094 | 0.181 | 0.190 |
| 222687_s_at | PHCA | 0.179 | 0.266 | 0.116 |
| 222688_at | PHCA | 0.231 | 0.276 | 0.126 |
| 222689_at | PHCA | 0.088 | 0.215 | 0.078 |
| 231321_s_at | PHCA | 0.116 | -0.088 | 0.054 |
| 225533_at | PHF19 | 0.115 | -0.088 | 0.122 |
| 227211_at | PHF19 | -0.346 | -0.168 | -0.166 |
| 227212_s_at | PHF19 | -0.362 | -0.105 | -0.158 |
| 201397_at | PHGDH | 0.136 | -0.062 | 0.159 |
| 207469_s_at | PIR | 0.188 | 0.340 | 0.304 |
| 207717_s_at | PKP2 | 0.106 | 0.074 | 0.073 |
| 214154_s_at | PKP2 | -0.018 | 0.042 | -0.109 |
| 235958_at | PLA2G4F | -0.328 | 0.003 | 0.064 |
| 218644_at | PLEK2 | -0.059 | -0.005 | -0.190 |
| 210139_s_at | PMP22 | 0.359 | 0.087 | 0.481 |
| 218009_s_at | PRC1 | 0.166 | 0.273 | 0.295 |
| 205880_at | PRKD1 | 0.102 | 0.112 | 0.342 |
| 217705_at | PRKD1 | -0.070 | -0.197 | -0.124 |
| 205319_at | PSCA | 0.157 | 0.445 | 0.093 |
| 236939_at | PTPLAD2 | -0.053 | -0.170 | 0.087 |
| 244050_at | PTPLAD2 | -0.021 | 0.111 | -0.035 |
| 204146_at | RAD51AP1 | 0.047 | -0.140 | 0.044 |
| 210051_at | RAPGEF3 | 0.019 | 0.086 | 0.030 |
| 206391_at | RARRES1 | 0.043 | 0.124 | 0.057 |
| 206392_s_at | RARRES1 | 0.008 | 0.184 | 0.062 |
| 221872_at | RARRES1 | 0.077 | 0.203 | 0.096 |
| 227758_at | RERG | -0.186 | 0.037 | -0.118 |
| 244745_at | RERG | -0.311 | -0.214 | -0.098 |
| 202975_s_at | RHOBTB3 | 0.391 | 0.284 | 0.343 |
| 202976_s_at | RHOBTB3 | 0.408 | 0.269 | 0.311 |
| 216048_s_at | RHOBTB3 | 0.301 | 0.203 | 0.311 |
| 216049_at | RHOBTB3 | 0.122 | 0.036 | 0.006 |
| 225202_at | RHOBTB3 | 0.450 | 0.253 | 0.266 |
| 240111_at | RHOBTB3 | 0.187 | 0.170 | 0.124 |
| 205211_s_at | RIN1 | -0.058 | -0.037 | 0.273 |
| 209443_at | SERPINA5 | 0.180 | -0.134 | 0.104 |
| 212268_at | SERPINB1 | 0.036 | 0.102 | -0.113 |
| 213572_s_at | SERPINB1 | 0.047 | 0.081 | -0.078 |
| 228726_at | SERPINB1 | -0.010 | 0.080 | -0.049 |
| 239213_at | SERPINB1 | 0.100 | 0.176 | 0.097 |
| 205075_at | SERPINF2 | 0.006 | -0.059 | -0.319 |
| 218921_at | SIGIRR | -0.213 | -0.099 | -0.119 |
| 52940_at | SIGIRR | -0.169 | -0.121 | -0.101 |
| 219795_at | SLC6A14 | 0.041 | -0.021 | -0.249 |
| 204368_at | SLCO2A1 | -0.026 | -0.106 | -0.018 |
| 226837_at | SPRED1 | 0.211 | 0.119 | 0.180 |
| 235074_at | SPRED1 | 0.118 | 0.148 | 0.155 |

Table 6, continued

| | | | | |
|---|---|---|---|---|
| 244439_at | SPRED1 | 0.015 | 0.005 | 0.104 |
| 212558_at | SPRY1 | 0.239 | -0.047 | 0.014 |
| 203217_s_at | ST3GAL5 | 0.249 | 0.257 | 0.305 |
| 239755_at | ST3GAL5 | 0.190 | -0.090 | 0.220 |
| 204542_at | ST6GALNAC2 | 0.059 | 0.281 | 0.196 |
| 204595_s_at | STC1 | 0.159 | 0.054 | 0.144 |
| 204596_s_at | STC1 | 0.143 | 0.108 | 0.132 |
| 204597_x_at | STC1 | 0.129 | 0.048 | 0.138 |
| 230746_s_at | STC1 | 0.116 | 0.040 | 0.120 |
| 218207_s_at | STMN3 | -0.003 | -0.147 | -0.151 |
| 222557_at | STMN3 | 0.011 | -0.181 | -0.097 |
| 202289_s_at | TACC2 | 0.097 | -0.043 | 0.011 |
| 211382_s_at | TACC2 | 0.045 | -0.012 | 0.022 |
| 201839_s_at | TACSTD1 | -0.103 | -0.013 | -0.324 |
| 227279_at | TCEAL3 | 0.272 | 0.021 | 0.345 |
| 204106_at | TESK1 | 0.136 | 0.124 | 0.298 |
| 201107_s_at | THBS1 | 0.144 | 0.066 | 0.205 |
| 201108_s_at | THBS1 | 0.311 | 0.130 | 0.322 |
| 201109_s_at | THBS1 | 0.285 | 0.083 | 0.381 |
| 201110_s_at | THBS1 | 0.269 | 0.065 | 0.379 |
| 215775_at | THBS1 | 0.134 | 0.014 | -0.058 |
| 235086_at | THBS1 | 0.219 | 0.081 | 0.176 |
| 239336_at | THBS1 | 0.275 | -0.062 | 0.179 |
| 206415_at | TLL1 | 0.048 | 0.066 | -0.081 |
| 221908_at | TMEM118 | -0.109 | 0.024 | 0.166 |
| 221909_at | TMEM118 | -0.137 | 0.060 | 0.171 |
| 225822_at | TMEM125 | -0.023 | 0.145 | -0.152 |
| 205611_at | TNFSF12 | 0.130 | 0.093 | 0.204 |
| 206393_at | TNNI2 | -0.320 | -0.048 | -0.249 |
| 201291_s_at | TOP2A | 0.172 | -0.046 | 0.183 |
| 201292_at | TOP2A | 0.201 | -0.051 | 0.144 |
| 237469_at | TOP2A | 0.237 | -0.097 | 0.181 |
| 204649_at | TROAP | 0.091 | -0.074 | 0.261 |
| 209114_at | TSPAN1 | -0.012 | 0.196 | 0.036 |
| 202154_x_at | TUBB3 | 0.301 | 0.181 | 0.072 |
| 203894_at | TUBG2 | -0.107 | 0.011 | 0.055 |
| 205807_s_at | TUFT1 | 0.081 | 0.346 | 0.195 |
| 221490_at | UBAP1 | 0.093 | 0.177 | 0.118 |
| 46270_at | UBAP1 | 0.094 | 0.092 | 0.148 |
| 202954_at | UBE2C | 0.409 | 0.120 | 0.308 |
| 232654_s_at | UGT1A6 | 0.036 | 0.163 | -0.398 |
| 232655_at | UGT1A6 | 0.090 | 0.014 | 0.051 |
| 225655_at | UHRF1 | -0.140 | -0.241 | 0.040 |
| 203026_at | ZBTB5 | -0.032 | -0.304 | -0.064 |
| 220933_s_at | ZCCHC6 | 0.019 | 0.025 | 0.309 |
| 236155_at | ZCCHC6 | 0.051 | 0.113 | 0.099 |
| 236243_at | ZCCHC6 | 0.107 | -0.122 | 0.228 |
| 238800_s_at | ZCCHC6 | 0.076 | 0.010 | 0.119 |
| 242776_at | ZCCHC6 | 0.063 | 0.130 | 0.053 |
| 229901_at | ZNF488 | 0.132 | 0.085 | 0.262 |
| 242463_x_at | ZNF600 | 0.117 | -0.189 | -0.134 |

**Table 7: Affymetrix probe sets corresponding to the GAB2-signature and their differential expression between dasatinib-sensitive and resistant cells, expressed as Signal-to-Noise Ratio (SNR).**

| Affymetrix Probe Set | Gene Symbol | SNR |
|---|---|---|
| 204343_at | ABCA3 | -1.2917 |
| 208161_s_at | ABCC3 | -0.0133 |
| 209641_s_at | ABCC3 | 0.0650 |
| 214979_at | ABCC3 | -0.1119 |
| 230682_x_at | ABCC3 | 0.1751 |
| 239217_x_at | ABCC3 | 0.0813 |
| 242553_at | ABCC3 | 0.0016 |
| 228132_at | ABLIM2 | 0.0503 |
| 236087_at | ABLIM2 | -0.1627 |
| 242624_at | ABLIM2 | -0.0219 |
| 224882_at | ACSS1 | -0.3192 |
| 234483_at | ACSS1 | 0.1142 |
| 234484_s_at | ACSS1 | -0.3009 |
| 234801_s_at | ACSS1 | -0.0503 |
| 235724_at | ACSS1 | -0.5018 |
| 200974_at | ACTA2 | 0.2398 |
| 215787_at | ACTA2 | 0.0256 |
| 243140_at | ACTA2 | -0.3125 |
| 206262_at | ADH1A | -0.0249 |
| 207820_at | ADH1A | 0.0013 |
| 209160_at | AKR1C3 | 1.1867 |
| 205623_at | ALDH3A1 | 0.4305 |
| 203747_at | AQP3 | -0.1151 |
| 39248_at | AQP3 | 0.0890 |
| 39249_at | AQP3 | -0.0056 |
| 201288_at | ARHGDIB | 0.1788 |
| 212614_at | ARID5B | -0.0984 |
| 235404_at | ARID5B | -0.2819 |
| 241969_at | ARID5B | -0.0437 |
| 219918_s_at | ASPM | 0.3880 |
| 232238_at | ASPM | -0.0606 |
| 239002_at | ASPM | -0.1005 |
| 214070_s_at | ATP10B | -0.1916 |
| 220920_at | ATP10B | -0.2310 |
| 205473_at | ATP6V1B1 | -0.2273 |
| 209464_at | AURKB | 0.5817 |
| 239219_at | AURKB | 0.2544 |
| 209309_at | AZGP1 | -0.2565 |
| 217014_s_at | AZGP1 | -0.2509 |
| 219476_at | C1orf116 | 0.3344 |
| 219856_at | C1orf116 | 0.4266 |
| 228865_at | C1orf116 | 0.1427 |
| 241233_x_at | C21orf81 | -0.0234 |
| 206707_x_at | C6orf32 | 0.1807 |
| 209829_at | C6orf32 | 0.1513 |
| 220150_s_at | C6orf60 | -0.2357 |
| 223194_s_at | C6orf85 | -0.0356 |
| 233206_at | C6orf85 | 0.1986 |
| 212848_s_at | C9orf3 | 0.2988 |
| 232270_at | C9orf3 | 0.3266 |
| 232000_at | C9orf52 | 0.2623 |
| 236826_at | C9orf52 | 0.0964 |
| 242477_at | C9orf52 | 0.2371 |
| 223074_s_at | C9orf58 | -0.0917 |
| 223075_s_at | C9orf58 | -0.2530 |
| 203963_at | CA12 | -0.8093 |
| 204508_s_at | CA12 | -0.9347 |
| 204509_at | CA12 | -0.2344 |
| 210735_s_at | CA12 | -0.8612 |
| 214164_x_at | CA12 | -0.7568 |
| 215867_x_at | CA12 | -0.8985 |
| 209956_s_at | CAMK2B | -0.4969 |
| 210404_x_at | CAMK2B | -0.0402 |
| 211483_x_at | CAMK2B | 0.2953 |
| 213276_at | CAMK2B | -0.1196 |
| 34846_at | CAMK2B | 0.0163 |
| 218309_at | CAMK2N1 | 0.1456 |
| 228302_x_at | CAMK2N1 | 0.1640 |
| 229163_at | CAMK2N1 | 0.2860 |
| 201432_at | CAT | 0.0267 |
| 211922_s_at | CAT | 0.1285 |
| 215573_at | CAT | -0.2897 |
| 238363_at | CAT | -0.0192 |
| 212886_at | CCDC69 | 0.3816 |
| 242430_at | CCDC69 | -0.3356 |
| 216598_s_at | CCL2 | 0.3672 |
| 203418_at | CCNA2 | 0.3400 |
| 213226_at | CCNA2 | 0.3368 |
| 214710_s_at | CCNB1 | 0.3786 |
| 228729_at | CCNB1 | 0.0412 |
| 202705_at | CCNB2 | 0.3987 |
| 232764_at | CCNB2 | 0.1416 |
| 232768_at | CCNB2 | -0.2503 |
| 206488_s_at | CD36 | 0.0626 |
| 209554_at | CD36 | -0.1329 |
| 209555_s_at | CD36 | 0.1412 |
| 228766_at | CD36 | 0.1413 |
| 242197_x_at | CD36 | 0.7499 |
| 209850_s_at | CDC42EP2 | 0.1384 |
| 214014_at | CDC42EP2 | 0.1493 |
| 204126_s_at | CDC45L | 0.1430 |
| 224753_at | CDCA5 | 0.3386 |
| 224428_s_at | CDCA7 | 0.2473 |
| 230060_at | CDCA7 | 0.1252 |
| 204726_at | CDH13 | 0.1874 |
| 209832_s_at | CDT1 | -0.2648 |
| 228868_x_at | CDT1 | 0.1835 |
| 207828_s_at | CENPF | 0.3854 |
| 209172_s_at | CENPF | 0.1835 |
| 209667_at | CES2 | 0.0164 |
| 209668_x_at | CES2 | 0.0935 |
| 213509_x_at | CES2 | 0.1442 |
| 203854_at | CFI | 0.6272 |
| 218182_s_at | CLDN1 | 0.1980 |
| 222549_at | CLDN1 | 0.3482 |
| 201445_at | CNN3 | 0.3720 |
| 219400_at | CNTNAP1 | 0.0908 |
| 208146_s_at | CPVL | -0.0417 |
| 216365_x_at | CPVL | 0.1075 |
| 217239_x_at | CPVL | -0.1267 |
| 205843_x_at | CRAT | -0.3951 |
| 209522_s_at | CRAT | -0.5555 |
| 209283_at | CRYAB | 0.0510 |
| 203917_at | CXADR | 0.0597 |
| 209201_x_at | CXCR4 | -0.2549 |
| 211919_s_at | CXCR4 | -0.3531 |
| 217028_at | CXCR4 | -0.1512 |
| 202434_s_at | CYP1B1 | -0.0671 |
| 202435_s_at | CYP1B1 | 0.1428 |
| 202436_s_at | CYP1B1 | 0.2140 |
| 202437_s_at | CYP1B1 | 0.2173 |
| 206539_s_at | CYP4F12 | 0.4284 |
| 206515_at | CYP4F3 | 0.0897 |
| 216646_at | DCC1 | -0.4188 |
| 219000_s_at | DCC1 | 0.0925 |
| 209094_at | DDAH1 | 0.1613 |
| 229456_s_at | DDAH1 | 0.0988 |
| 243711_at | DDAH1 | 0.2452 |
| 221081_s_at | DENND2D | -0.2729 |
| 215151_at | DOCK10 | 0.0573 |
| 219279_at | DOCK10 | 0.0004 |
| 218585_s_at | DTL | -0.1413 |
| 222680_s_at | DTL | 0.2449 |
| 223402_at | DUSP23 | -0.1764 |
| 207042_at | E2F2 | -0.1420 |
| 228361_at | E2F2 | 0.0565 |
| 235582_at | E2F2 | 0.1751 |
| 204540_at | EEF1A2 | -0.1896 |
| 208427_s_at | ELAVL2 | 0.1634 |
| 228260_at | ELAVL2 | 0.3036 |
| 201510_at | ELF3 | -0.0282 |
| 210827_s_at | ELF3 | -0.1838 |
| 203729_at | EMP3 | 0.3474 |
| 203499_at | EPHA2 | 0.9949 |
| 203348_s_at | ETV5 | 0.2261 |
| 203349_s_at | ETV5 | 0.5569 |
| 216375_s_at | ETV5 | 0.4304 |
| 230102_at | ETV5 | 0.5101 |
| 204603_at | EXO1 | 0.2681 |
| 209955_s_at | FAP | 0.0377 |
| 201910_at | FARP1 | -0.0588 |
| 201911_s_at | FARP1 | -0.2407 |
| 227996_at | FARP1 | 0.0715 |
| 237767_at | FARP1 | -0.0924 |
| 239246_at | FARP1 | -0.1677 |
| 205014_at | FGFBP1 | 0.3498 |

| Table 7, continued | | |
|---|---|---|
| 227717_at | FLJ41603 | -0.0237 |
| 241380_at | FLJ41603 | 0.1083 |
| 219250_s_at | FLRT3 | 0.3552 |
| 222853_at | FLRT3 | 0.4135 |
| 227475_at | FOXQ1 | 0.6437 |
| 206774_at | FRMPD1 | 0.0773 |
| 202838_at | FUCA1 | 0.2997 |
| 229137_at | FUCA1 | -0.2080 |
| 214088_s_at | FUT3 | 0.2703 |
| 216010_x_at | FUT3 | 0.2436 |
| 203397_s_at | GALNT3 | -0.0281 |
| 203398_s_at | GALNT3 | 0.0226 |
| 204836_at | GLDC | -0.4364 |
| 201141_at | GPNMB | 0.0807 |
| 206709_x_at | GPT | -0.0163 |
| 202967_at | GSTA4 | 0.1563 |
| 235405_at | GSTA4 | 0.2410 |
| 207165_at | HMMR | 0.0572 |
| 209709_s_at | HMMR | 0.0853 |
| 206864_s_at | HRK | 0.0784 |
| 206865_at | HRK | -0.0996 |
| 201841_s_at | HSPB1 | -0.1601 |
| 206375_s_at | HSPB3 | -0.0306 |
| 204002_s_at | ICA1 | -0.4092 |
| 207949_s_at | ICA1 | -0.9633 |
| 210547_x_at | ICA1 | -0.8523 |
| 211740_at | ICA1 | -0.6783 |
| 214191_at | ICA1 | 0.1783 |
| 208937_s_at | ID1 | 0.3430 |
| 201565_s_at | ID2 | -0.5049 |
| 201566_x_at | ID2 | -0.4726 |
| 213931_at | ID2 | -0.1667 |
| 207826_s_at | ID3 | 0.2689 |
| 201601_x_at | IFITM1 | 0.6328 |
| 214022_s_at | IFITM1 | 0.5733 |
| 212203_x_at | IFITM3 | 0.6513 |
| 203424_s_at | IGFBP5 | -0.3914 |
| 203425_s_at | IGFBP5 | -0.4747 |
| 203426_s_at | IGFBP5 | -0.2139 |
| 211958_at | IGFBP5 | -0.2989 |
| 211959_at | IGFBP5 | -0.4112 |
| 231179_at | IHPK3 | -0.1870 |
| 203126_at | IMPA2 | -0.3208 |
| 229538_s_at | IQGAP3 | 0.1753 |
| 241939_at | IQGAP3 | 0.0851 |
| 231779_at | IRAK2 | 0.3498 |
| 206104_at | ISL1 | 0.1669 |
| 206766_at | ITGA10 | 0.1811 |
| 202803_s_at | ITGB2 | 0.2992 |
| 236988_x_at | ITGB2 | -0.1698 |
| 209408_at | KIF2C | 0.4707 |
| 211519_s_at | KIF2C | 0.4824 |
| 205778_at | KLK7 | 0.3250 |
| 239381_at | KLK7 | 0.3196 |
| 207023_x_at | KRT10 | 0.2529 |
| 210633_x_at | KRT10 | 0.3828 |
| 213287_s_at | KRT10 | 0.5596 |
| 207935_s_at | KRT13 | 0.1074 |

| Table 7, continued | | |
|---|---|---|
| 209016_s_at | KRT7 | 0.1193 |
| 214031_s_at | KRT7 | 0.2079 |
| 201720_s_at | LAPTM5 | 0.0981 |
| 201721_s_at | LAPTM5 | 0.5006 |
| 212531_at | LCN2 | 0.3741 |
| 202067_s_at | LDLR | -0.0216 |
| 202068_s_at | LDLR | 0.1907 |
| 217005_at | LDLR | 0.0121 |
| 217103_at | LDLR | -0.0265 |
| 217173_s_at | LDLR | -0.1375 |
| 217183_at | LDLR | -0.2507 |
| 209179_s_at | LENG4 | 0.7025 |
| 211037_s_at | LENG4 | 0.1078 |
| 215270_at | LFNG | -0.8127 |
| 228762_at | LFNG | -0.1513 |
| 219760_at | LIN7B | -0.1251 |
| 241957_x_at | LIN7B | -0.0530 |
| 239155_at | LOC653108 | 0.0828 |
| 228648_at | LRG1 | 0.2809 |
| 202145_at | LY6E | -0.0463 |
| 205458_at | MC1R | 0.1631 |
| 213476_x_at | MC1R | 0.1376 |
| 232092_at | MCART1 | 0.4259 |
| 238574_at | MCART1 | 0.0635 |
| 201755_at | MCM5 | 0.1099 |
| 216237_s_at | MCM5 | 0.0816 |
| 208795_s_at | MCM7 | -0.1668 |
| 210983_s_at | MCM7 | -0.1753 |
| 202291_s_at | MGP | -0.1521 |
| 238481_at | MGP | -0.0215 |
| 219909_at | MMP28 | -0.0629 |
| 222937_s_at | MMP28 | -0.2078 |
| 224207_x_at | MMP28 | 0.1944 |
| 239272_at | MMP28 | 0.0924 |
| 239273_s_at | MMP28 | 0.3107 |
| 204745_x_at | MT1G | 0.5408 |
| 210472_at | MT1G | -0.1444 |
| 212185_x_at | MT2A | 0.3611 |
| 218966_at | MYO5C | -0.4062 |
| 218039_at | NUSAP1 | 0.7152 |
| 219978_s_at | NUSAP1 | 0.5114 |
| 214607_at | PAK3 | -0.3567 |
| 218952_at | PCSK1N | -0.2453 |
| 205960_at | PDK4 | 0.0754 |
| 225207_at | PDK4 | 0.1803 |
| 222687_s_at | PHCA | -0.0311 |
| 222688_at | PHCA | 0.0834 |
| 222689_at | PHCA | 0.0563 |
| 231321_s_at | PHCA | -0.1356 |
| 225533_at | PHF19 | 0.6055 |
| 227211_at | PHF19 | 0.3203 |
| 227212_s_at | PHF19 | 0.1859 |
| 201397_at | PHGDH | 0.0473 |
| 207469_s_at | PIR | -0.2290 |
| 207717_s_at | PKP2 | 0.2378 |
| 214154_s_at | PKP2 | -0.1900 |
| 235958_at | PLA2G4F | -0.5375 |
| 218644_at | PLEK2 | 0.1881 |

| Table 7, continued | | |
|---|---|---|
| 210139_s_at | PMP22 | 0.1274 |
| 218009_s_at | PRC1 | 0.2819 |
| 205880_at | PRKD1 | 0.1444 |
| 217705_at | PRKD1 | 0.2954 |
| 205319_at | PSCA | -0.0597 |
| 236939_at | PTPLAD2 | -0.2552 |
| 244050_at | PTPLAD2 | 0.1434 |
| 204146_at | RAD51AP1 | 0.0724 |
| 210051_at | RAPGEF3 | -0.2167 |
| 206391_at | RARRES1 | 0.3354 |
| 206392_s_at | RARRES1 | 0.2153 |
| 221872_at | RARRES1 | 0.2271 |
| 227758_at | RERG | -0.4985 |
| 244745_at | RERG | -0.2456 |
| 202975_s_at | RHOBTB3 | 0.5507 |
| 202976_s_at | RHOBTB3 | 0.5981 |
| 216048_s_at | RHOBTB3 | 0.4641 |
| 216049_at | RHOBTB3 | 0.0948 |
| 225202_at | RHOBTB3 | 0.7685 |
| 240111_at | RHOBTB3 | 0.3935 |
| 205211_s_at | RIN1 | 0.2119 |
| 209443_at | SERPINA5 | 0.0393 |
| 212268_at | SERPINB1 | 0.7204 |
| 213572_s_at | SERPINB1 | 0.5011 |
| 228726_at | SERPINB1 | 0.3225 |
| 239213_at | SERPINB1 | 0.2244 |
| 205075_at | SERPINF2 | 0.2460 |
| 218921_at | SIGIRR | -0.3994 |
| 52940_at | SIGIRR | -0.3177 |
| 219795_at | SLC6A14 | 0.0233 |
| 204368_at | SLCO2A1 | 0.1363 |
| 226837_at | SPRED1 | 0.4914 |
| 235074_at | SPRED1 | 0.2638 |
| 244439_at | SPRED1 | 0.6733 |
| 212558_at | SPRY1 | 0.2549 |
| 203217_s_at | ST3GAL5 | -0.1949 |
| 239755_at | ST3GAL5 | 0.0269 |
| 204542_at | ST6GALNAC2 | -0.4321 |
| 204595_s_at | STC1 | -0.1292 |
| 204596_s_at | STC1 | -0.1987 |
| 204597_x_at | STC1 | -0.1196 |
| 230746_s_at | STC1 | -0.0028 |
| 218207_s_at | STMN3 | -0.2173 |
| 222557_at | STMN3 | -0.2538 |
| 202289_s_at | TACC2 | -0.0011 |
| 211382_s_at | TACC2 | 0.0393 |
| 201839_s_at | TACSTD1 | -0.2499 |
| 227279_at | TCEAL3 | -0.1189 |
| 204106_at | TESK1 | -0.4211 |
| 201107_s_at | THBS1 | 0.2892 |
| 201108_s_at | THBS1 | 0.3508 |
| 201109_s_at | THBS1 | 0.2165 |
| 201110_s_at | THBS1 | 0.2028 |
| 215775_at | THBS1 | -0.2847 |
| 235086_at | THBS1 | 0.1593 |
| 239336_at | THBS1 | 0.1047 |
| 206415_at | TLL1 | 0.2815 |
| 221908_at | TMEM118 | -0.4085 |

| Table 7, continued | | |
|---|---|---|
| 221909_at | TMEM118 | -0.6264 |
| 225822_at | TMEM125 | -0.2078 |
| 205611_at | TNFSF12 | 0.1025 |
| 206393_at | TNNI2 | 0.1896 |
| 201291_s_at | TOP2A | 0.2640 |
| 201292_at | TOP2A | 0.4519 |
| 237469_at | TOP2A | -0.0908 |
| 204649_at | TROAP | -0.4803 |
| 209114_at | TSPAN1 | 0.0340 |
| 202154_x_at | TUBB3 | 0.3144 |
| 203894_at | TUBG2 | 0.0822 |
| 205807_s_at | TUFT1 | -0.2774 |
| 221490_at | UBAP1 | 0.2669 |
| 46270_at | UBAP1 | 0.2421 |
| 202954_at | UBE2C | 0.2767 |
| 232654_s_at | UGT1A6 | 0.5998 |
| 232655_at | UGT1A6 | -0.1915 |
| 225655_at | UHRF1 | 0.5735 |
| 203026_at | ZBTB5 | 0.1349 |
| 220933_s_at | ZCCHC6 | 0.1230 |
| 236155_at | ZCCHC6 | -0.3686 |
| 236243_at | ZCCHC6 | -0.2179 |
| 238800_s_at | ZCCHC6 | -0.0419 |
| 242776_at | ZCCHC6 | -0.5296 |
| 229901_at | ZNF488 | 0.2833 |
| 242463_x_at | ZNF600 | 0.0176 |

**Table 8: Genomic classifier based on the the GAB2-signature discriminating breast cancer patients with good and poor prognosis**

| Gene Symbol | Gene Bank Accession | NKI dataset Systematic name | Affymetrix Probe Set (mapped via MAQC) | Average expression in poor prognosis samples | Average expression in good prognosis samples |
|---|---|---|---|---|---|
| ABCA3 | NM_001089 | NM_001089 | 204343_at | -0.0973175675675676 | -0.0574555145625030 |
| ABCC3 | NM_003786 | NM_003786 | 208161_s_at | -0.1132837837837840 | -0.1358186839080460 |
| ABLIM2 | AI240129 | Contig53510_RC | 228132_at | 0.0075135135135135 | -0.0006188103448276 |
| ACTA2 | NM_001613 | NM_001613 | | -0.0851013513513514 | -0.0676449022988506 |
| ADH1A | NM_000667 | NM_000667 | 207820_at | -0.1229729729729730 | -0.0620641436781609 |
| AKR1C3 | NM_003739 | NM_003739 | | -0.0303851351351351 | 0.0022494310344828 |
| AQP3 | NM_004925 | NM_004925 | 39248_at | 0.0052847222222222 | 0.0024003141063592 |
| ARHGDIB | L20688 | L20688 | 201288_at | -0.0114864864864865 | 0.0153505172413793 |
| ARHGDIB | NM_001175 | NM_001175 | | -0.0200945945945946 | -0.0066353793103448 |
| ARID5B | AL049471 | AL049471 | 212614_at | -0.0810945945945946 | -0.0155751724137931 |
| ARID5B | AA169339 | Contig10363_RC | | -0.0575202702702703 | 0.0045479252873563 |
| ASPM | AA748494 | Contig33814_RC | 219918_s_at | 0.0725135135135135 | -0.0232848620689655 |
| ASPM | NM_018136 | NM_018136 | | -0.0293445945945946 | -0.1333095928841940 |
| ATP6V1B1 | NM_001692 | NM_001692 | | -0.2727972972972970 | -0.2627616896551720 |
| AURKB | AW139028 | Contig34729_RC | | 0.0417723554033486 | -0.1094642251171650 |
| AURKB | NM_004217 | NM_004217 | | 0.0388986486486486 | 0.0172058548037448 |
| AZGP1 | NM_001185 | NM_001185 | 209309_at | -0.2488310810810810 | -0.0724386206896552 |
| C1orf116 | AW138165 | Contig54612_RC | 219476_at | -0.0571554054054054 | -0.0721187816091954 |
| C9orf3 | AF043897 | AF043897 | 212848_s_at | 0.0030810810810811 | -0.0158670517241379 |
| C9orf3 | AL137535 | AL137535 | | -0.0065472972972973 | -0.0192644712643678 |
| C9orf52 | AI796221 | Contig42253_RC | | -0.0308986486486486 | -0.0145442873563218 |
| C9orf58 | AA205873 | Contig53698_RC | 223075_s_at | 0.0337364864864865 | -0.0049932621244575 |
| CA12 | NM_001218 | NM_001218 | 215867_x_at | -0.1706216216216220 | -0.0703468563218391 |
| CAMK2B | AF131776 | AF131776 | 211483_x_at | 0.0436013513513513 | 0.0283393923427177 |
| CAMK2N1 | NM_018584 | NM_018584 | | -0.0645675675675676 | -0.0409414942528736 |
| CAT | NM_001752 | NM_001752 | 201432_at | -0.0014594594594595 | 0.0005220229885057 |
| CCDC69 | AL080169 | AL080169 | 212886_at | -0.0431554054054054 | 0.0036758908045977 |
| CCL2 | NM_002982 | NM_002982 | | -0.0216418918918919 | -0.0442826896551724 |
| CCNA2 | NM_001237 | NM_001237 | 203418_at | 0.0621418918918919 | -0.0439983569862468 |
| CCNB1 | AA632161 | Contig56843_RC | 228729_at | 0.0484594594594595 | -0.1131970574712640 |
| CCNB2 | NM_004701 | NM_004701 | 202705_at | 0.0322027027027027 | -0.1844693160919540 |
| CD36 | NM_000072 | NM_000072 | | -0.1236554054054050 | -0.0762945172413793 |
| CDC45L | NM_003504 | NM_003504 | 204126_s_at | 0.0530675675675676 | -0.0993011034482760 |
| CDCA7 | AI992158 | Contig55725_RC | 224428_s_at | -0.0896756756756757 | -0.3275271666666670 |
| CDH13 | NM_001257 | NM_001257 | | -0.0166148648648649 | -0.0496801321839080 |
| CDT1 | AF070552 | AF070552 | 209832_s_at | 0.0413513513513514 | -0.0432771421500233 |
| CES2 | NM_003869 | NM_003869 | 209667_at | 0.0078205859969559 | 0.0015881429881949 |
| CFI | NM_000204 | NM_000204 | 203854_at | -0.0630337837837838 | 0.0043407758620690 |
| CLDN1 | AF101051 | AF101051 | 218182_s_at | -0.0645878378378378 | -0.0752664540229885 |
| CNN3 | NM_001839 | NM_001839 | 201445_at | -0.0435945945945946 | -0.0158344195402299 |
| CPVL | AF217508 | AF217508 | | -0.0542027027027027 | -0.0582470862068966 |
| CRAT | NM_000755 | NM_000755 | 209522_s_at | -0.1332770270270270 | -0.0569630229885057 |
| CRAT | NM_004003 | NM_004003 | | 0.0070675675675676 | 0.0310594367816092 |
| CRYAB | NM_001885 | NM_001885 | 209283_at | -0.1935337837837840 | -0.2234344712643680 |
| CXADR | NM_001338 | NM_001338 | | -0.0733648648648650 | -0.0642962413793104 |
| CXCR4 | NM_003467 | NM_003467 | 217028_at | -0.0311283783783784 | -0.0797674597701150 |
| CYP1B1 | NM_000104 | NM_000104 | 202437_s_at | -0.0799932432432433 | -0.0942721233140655 |
| DENND2D | AI494568 | Contig53439_RC | 221081_s_at | -0.0625878378378378 | -0.0287088735632184 |
| DTL | NM_016448 | NM_016448 | 218585_s_at | 0.0650743243243243 | -0.0679427694505348 |
| DUSP23 | NM_017823 | NM_017823 | 223402_at | 0.0329722222222222 | -0.0142847143736101 |
| E2F2 | AW137640 | Contig48913_RC | 228361_at | 0.0434932432432432 | -0.1274577528735630 |

| Table 8, continued | | | | | |
|---|---|---|---|---|---|
| EEF1A2 | NM_001958 | NM_001958 | 204540_at | -0.1831891891891890 | -0.1868675344827590 |
| ELF3 | AA527180 | Contig46868_RC | | 0.0019256756756757 | -0.0134318160919540 |
| ELF3 | NM_004433 | NM_004433 | | -0.0443513513513514 | -0.0308428448275862 |
| EMP3 | NM_001425 | NM_001425 | 203729_at | 0.0213040540540541 | 0.0108019310344828 |
| EPHA2 | NM_004431 | NM_004431 | 203499_at | -0.0065000000000000 | -0.0480073793103448 |
| EXO1 | NM_003686 | NM_003686 | 204603_at | 0.0866891891891892 | -0.0611460172413793 |
| EXO1 | NM_006027 | NM_006027 | | 0.0791824324324324 | -0.0515690229885057 |
| FAP | NM_004460 | NM_004460 | 209955_s_at | -0.1578175675675680 | -0.0817100402298850 |
| FARP1 | AI028516 | Contig38580_RC | | -0.1318513513513510 | -0.0394333620689655 |
| FARP1 | NM_005766 | NM_005766 | | -0.0182770270270270 | -0.0042042068965517 |
| FGFBP1 | NM_005130 | NM_005130 | 205014_at | -0.1678310810810810 | -0.1534052586206900 |
| FLRT3 | NM_013281 | NM_013281 | | -0.1194189189189190 | -0.0331315402298851 |
| FOXQ1 | AI676059 | Contig39891_RC | 227475_at | -0.0511824324324324 | -0.1024194942528740 |
| FRMPD1 | NM_014907 | NM_014907 | 206774_at | 0.0443581081081081 | 0.0398352068965517 |
| FUCA1 | NM_000147 | NM_000147 | 202838_at | -0.0887567567567568 | -0.0416350459770115 |
| FUT3 | NM_000149 | NM_000149 | 214088_s_at | 0.0331148648648649 | 0.0027814540229885 |
| GALNT3 | NM_004482 | NM_004482 | 203398_s_at | -0.0458986486486486 | -0.0472084942528736 |
| GPNMB | NM_002510 | NM_002510 | 201141_at | -0.0562297297297297 | -0.0943240804597701 |
| GSTA4 | NM_001512 | NM_001512 | 202967_at | 0.0128175675675676 | 0.0053533160919540 |
| HMMR | NM_012484 | NM_012484 | 207165_at | 0.0034594594594595 | -0.0466654425287356 |
| HRK | NM_003806 | NM_003806 | 206864_s_at | -0.0023783783783784 | -0.0562851321839080 |
| HSPB1 | NM_001540 | NM_001540 | 201841_s_at | -0.0331283783783784 | -0.0830411379310345 |
| ICA1 | NM_004968 | NM_004968 | | -0.0242229729729730 | 0.0057655689655172 |
| ID1 | NM_002165 | NM_002165 | 208937_s_at | -0.0161180555555556 | 0.0013991565057539 |
| ID2 | NM_002166 | NM_002166 | 201565_s_at | 0.0121301369863014 | 0.0175744335354725 |
| ID3 | NM_002167 | NM_002167 | 207826_s_at | 0.0124594594594595 | -0.0092958160919540 |
| ID3 | X69111 | X69111 | | 0.0408958333333333 | 0.0421523709852773 |
| IGFBP5 | AF055033 | AF055033 | 211959_at | -0.0024729729729730 | -0.1353204367816090 |
| IGFBP5 | L27560 | L27560 | | -0.0688445945945946 | -0.1995905747126440 |
| IGFBP5 | NM_000599 | NM_000599 | | -0.0897027027027027 | -0.2114060114942530 |
| IMPA2 | NM_014214 | NM_014214 | 203126_at | -0.0269189189189189 | -0.1519694195402300 |
| ITGA10 | NM_003637 | NM_003637 | 206766_at | 0.0594662162162162 | 0.0529058724267722 |
| ITGB2 | NM_000211 | NM_000211 | 202803_s_at | 0.0017702702702703 | -0.0427479367816092 |
| KIF2C | NM_006845 | NM_006845 | | 0.0355675675675676 | -0.1442553448275860 |
| KLK7 | NM_005046 | NM_005046 | 239381_at | -0.4061148648648650 | -0.3655788103448280 |
| KRT10 | NM_000421 | NM_000421 | | -0.1534027777777780 | -0.0947164485767666 |
| KRT13 | NM_002274 | NM_002274 | | -0.4402364864864870 | -0.3557130747126440 |
| KRT7 | NM_005556 | NM_005556 | 209016_s_at | -0.0429662162162162 | -0.0293865689655172 |
| LAPTM5 | NM_006762 | NM_006762 | 201721_s_at | 0.0028243243243243 | -0.0458129029632583 |
| LFNG | AA583350 | Contig29647_RC | | -0.0780608108108108 | -0.0635260057471264 |
| LY6E | NM_002346 | NM_002346 | 202145_at | 0.0308648648648649 | -0.0759872758620690 |
| MC1R | AI123000 | Contig61366_RC | 205458_at | 0.0074729729729730 | 0.0170421845539120 |
| MC1R | NM_002386 | NM_002386 | | 0.0333851351351351 | 0.0235363908045977 |
| MCART1 | AI268054 | Contig30784_RC | | 0.0808581081081081 | 0.0715398333333333 |
| MCM5 | NM_006739 | NM_006739 | 216237_s_at | 0.0238175675675676 | -0.0611690919540230 |
| MCM7 | D55716 | D55716 | 208795_s_at | 0.0414054054054054 | -0.0577164890704937 |
| MGP | NM_000900 | NM_000900 | 202291_s_at | -0.2841901408450700 | -0.1432557313177860 |
| MT1G | N53454 | Contig66143_RC | | -0.1178108108108110 | -0.1612321724137930 |
| MT1G | NM_005950 | NM_005950 | | -0.1064729729729730 | -0.1455453735632180 |
| MT2A | NM_005953 | NM_005953 | | 0.0116013513513514 | -0.0226894712643678 |
| MYO5C | NM_018728 | NM_018728 | 218966_at | -0.1136824324324320 | -0.0231488275862069 |
| NUSAP1 | NM_016359 | NM_016359 | 218039_at | 0.0681013513513513 | -0.1180766264367820 |
| NUSAP1 | NM_018454 | NM_018454 | | 0.0949324324324324 | -0.0202723656899874 |
| PHF19 | AL117477 | AL117477 | 225533_at | 0.0283648648648649 | -0.0268998218390805 |
| PHGDH | AI004352 | Contig6114_RC | 201397_at | -0.0049797297297297 | -0.1646724712643680 |
| PHGDH | NM_006623 | NM_006623 | | 0.0197027027027027 | 0.0126551140787988 |
| PIR | NM_003662 | NM_003662 | 207469_s_at | 0.0593108108108108 | -0.0872385977011494 |
| PKP2 | NM_004572 | NM_004572 | | -0.0057291666666667 | -0.0006870497076967 |

| Table 8, continued | | | | | |
|---|---|---|---|---|---|
| PLEK2 | NM_016445 | NM_016445 | 218644_at | 0.0353986486486487 | -0.0101067281908179 |
| PMP22 | NM_000304 | NM_000304 | 210139_s_at | -0.0613377092846271 | -0.0210373879940791 |
| PRC1 | NM_003981 | NM_003981 | | 0.0666689189189189 | -0.1365778563218390 |
| PRKD1 | NM_002742 | NM_002742 | | -0.0631216216216216 | -0.0312609080459770 |
| PSCA | NM_005672 | NM_005672 | | -0.2390405405405410 | -0.2753426724137930 |
| RARRES1 | NM_002888 | NM_002888 | 206391_at | -0.1311283783783780 | -0.1249915919540230 |
| RERG | AW294092 | Contig50719_RC | 227758_at | -0.1991081081081080 | -0.0631513563218391 |
| RHOBTB3 | AI040030 | Contig4539 | 202976_s_at | -0.0708986486486486 | -0.0674772420769384 |
| RHOBTB3 | NM_014899 | NM_014899 | | -0.0737034817351598 | -0.0712184792811748 |
| RIN1 | NM_004292 | NM_004292 | 205211_s_at | 0.0263581081081081 | 0.0170924885057471 |
| SERPINA5 | J02639 | J02639 | | -0.1432297297297300 | -0.0634124085775032 |
| SERPINA5 | NM_000624 | NM_000624 | | -0.2503310810810810 | -0.1589570459770110 |
| SERPINB1 | M93056 | M93056 | 212268_at | -0.0471283783783784 | -0.0057291321839081 |
| SERPINF2 | D00174 | D00174 | 205075_at | -0.0568513513513513 | -0.0423329270812571 |
| SIGIRR | AA085764 | Contig974_RC | | 0.0293040540540541 | 0.0121208563218391 |
| SLC6A14 | NM_007231 | NM_007231 | 219795_at | -0.1205675675675680 | -0.2001074942528740 |
| SLCO2A1 | NM_005630 | NM_005630 | 204368_at | -0.0233310810810811 | -0.0274570517241379 |
| SPRED1 | AI742347 | Contig34355_RC | | -0.0298648648648649 | -0.0145794885057471 |
| SPRY1 | AF041037 | AF041037 | 212558_at | -0.0420619292237443 | -0.0065434269589658 |
| ST3GAL5 | NM_003896 | NM_003896 | 203217_s_at | -0.0006824324324324 | 0.0038459425287356 |
| ST6GALNAC2 | NM_006456 | NM_006456 | 204542_at | -0.0478918918918919 | -0.0592792528735632 |
| STC1 | NM_003155 | NM_003155 | 204597_x_at | -0.2473783783783780 | -0.2237332236396250 |
| TACC2 | AF176646 | AF176646 | 202289_s_at | -0.0198918918918919 | -0.0041489310344828 |
| TACSTD1 | NM_002354 | NM_002354 | 201839_s_at | -0.0593310810810811 | -0.0975506896551724 |
| TCEAL3 | AI340029 | Contig52641_RC | | -0.0344797297297297 | 0.0002885689655172 |
| TESK1 | NM_006285 | NM_006285 | 204106_at | 0.0150675675675676 | -0.0040065977011494 |
| THBS1 | AW139567 | Contig42410_RC | 201110_s_at | 0.0263243243243243 | -0.0142456225167763 |
| THBS1 | NM_003246 | NM_003246 | | -0.0611756756756757 | -0.0697565147166301 |
| TLL1 | NM_012464 | NM_012464 | | 0.0223716216216216 | 0.0555686034482759 |
| TMEM125 | AI628756 | Contig54290_RC | 225822_at | -0.0395270270270270 | -0.0313580172413793 |
| TROAP | NM_005480 | NM_005480 | 204649_at | 0.0690270270270270 | -0.0155351770314265 |
| TSPAN1 | NM_005727 | NM_005727 | | -0.2038851351351350 | -0.1900224080459770 |
| TUBB3 | NM_006086 | NM_006086 | | -0.0994189189189190 | -0.2448362377250680 |
| TUBG2 | NM_016437 | NM_016437 | | -0.0381351351351351 | 0.0057381264367816 |
| TUFT1 | NM_020127 | NM_020127 | 205807_s_at | -0.0080878378378378 | -0.0239102298850575 |
| UBAP1 | NM_016525 | NM_016525 | 46270_at | 0.0070675675675676 | 0.0024964597701149 |
| UBE2C | NM_007019 | NM_007019 | | 0.0946148648648650 | -0.0788783115407614 |
| UGT1A6 | NM_000463 | NM_000463 | | 0.0541701221769715 | 0.0664383202213250 |
| UHRF1 | NM_013282 | NM_013282 | 225655_at | 0.0543108108108108 | 0.0008945114942529 |
| ZBTB5 | NM_014872 | NM_014872 | 203026_at | -0.0020137012012012 | -0.0031744330545327 |
| ZCCHC6 | AI800829 | Contig41991_RC | 220933_s_at | -0.0145472972972973 | 0.0054469827586207 |

**Table 10: Univariate and multivariate Cox regression analyses, comparing the GAB2 signature with existing clinical and genomic predictors in the 198-sample dataset**

| Univariate analyses | p | HR | lower .95 | upper .95 |
|---|---|---|---|---|
| Adjuvant!Online | 0.03200 | 3.09008 | 1.10129 | 8.67038 |
| GAB2-Signature | 0.00170 | 23.81942 | 3.27349 | 173.32089 |
| Veridex Index | 0.00420 | 5.56595 | 1.71764 | 18.03627 |
| MammaPrint | 0.00170 | 23.84934 | 3.27744 | 173.54720 |
| Genomic Grade Index | 0.00005 | 5.99948 | 2.52165 | 14.27390 |
| **Pairwise Multivariate 1** | **p** | **HR** | **lower .95** | **upper .95** |
| GAB2-Signature | 0.003 | 20.947 | 2.843 | 154.350 |
| Adjuvant!Online | 0.330 | 1.676 | 0.593 | 4.733 |
| **Pairwise Multivariate 2** | **p** | **HR** | **lower .95** | **upper .95** |
| GAB2-Signature | 0.005 | 17.65819 | 2.38999 | 130.46544 |
| Veridex Index | 0.078 | 2.89930 | 0.88643 | 9.48289 |
| **Pairwise Multivariate 3** | **p** | **HR** | **lower .95** | **upper .95** |
| GAB2-Signature | 0.053 | 7.91200 | 0.97100 | 64.44500 |
| MammaPrint | 0.053 | 7.93600 | 0.97400 | 64.64900 |
| **Pairwise Multivariate 4** | **p** | **HR** | **lower .95** | **upper .95** |
| GAB2-Signature | 0.010 | 13.66311 | 1.61679 | 115.46353 |
| Genomic Grade Index | 0.220 | 1.99342 | 0.78514 | 5.06119 |
| **Triple Multivariate 1** | **p** | **HR** | **lower .95** | **upper .95** |
| GAB2-Signature | 0.031 | 10.510 | 1.236 | 89.375 |
| Veridex Index | 0.086 | 2.825 | 0.864 | 9.245 |
| Ggi | 0.165 | 1.931 | 0.762 | 4.892 |
| **Triple Multivariate 2** | **p** | **HR** | **lower .95** | **upper .95** |
| GAB2-Signature | 0.093 | 6.725 | 0.729 | 62.040 |
| MammaPrint | 0.079 | 7.035 | 0.800 | 61.859 |
| Genomic Grade Index | 0.626 | 1.269 | 0.487 | 3.310 |
| **Triple Multivariate 3** | **p** | **HR** | **lower .95** | **upper .95** |
| GAB2-Signature | 0.087 | 6.267 | 0.766 | 51.258 |
| MammaPrint | 0.059 | 7.501 | 0.926 | 60.790 |
| Veridex Index | 0.094 | 2.750 | 0.842 | 8.981 |
| **Quadruple Multivariate** | **p** | **HR** | **lower .95** | **upper .95** |
| GAB2-Signature | 0.140 | 5.28400 | 0.57000 | 49.00400 |
| Veridex Index | 0.093 | 2.75700 | 0.84400 | 9.00400 |
| MammaPrint | 0.086 | 6.65800 | 0.76600 | 57.88600 |
| Genomic Grade Index | 0.610 | 1.28000 | 0.49200 | 3.32900 |

Table 9: Two gene functional modules extracted from the GAB2-signature are differentially expressed in breast cancer patients with good and poor prognosis

| Module | Gene Symbol | Functional Module | Functional annotation |
|---|---|---|---|
| High in good prognosis | FAP | Regulation of cell-matrix interaction, migration and invasion | Stromal expression of fibroblast activation protein/seprase, a cell membrane serine proteinase and gelatinase, is associated with longer survival in patients with invasive ductal carcinoma of breast. |
| High in good prognosis | SERPINB1 | Regulation of cell-matrix interaction, migration and invasion | Inhibitor of elastase and other matrix-degrading proteases. SERPINB1 is one of the most efficient inhibitor of the neutrophil granule proteases, which include neutrophil elastase, proteinase-3 (PR3), and cathepsin G (CatG). |
| High in good prognosis | FUCA1 | Regulation of cell-matrix interaction, migration and invasion | Alpha-L-fucosidase, removes fucose from ECM glycans. Fucose-containing glycans were found widely distributed on the cell surface of breast cancer cells and could be effectively removed by alpha-L: -fase treatment. This decreased fucosylation, in turn, was seen to impair the interaction between tumor cells and extracellular matrices, and thus affected key cell functions modulating tumor invasion. |
| High in good prognosis | PMP22 | Regulation of cell-matrix interaction, migration and invasion | Integral membrane protein (4-spanning), widely expressed at apical junctions of epithelial cells, and also a major component of myelin in the peripheral nervous system. Expression of human PMP22 (hPMP22) slows cell growth and increases transepithelial electrical resistance. Subsequent to wounding, epithelial monolayers expressing hPMP22 fail to migrate normally. |
| High in good prognosis | ARHGDIB | Regulation of cell-matrix interaction, migration and invasion | Rho-GDI beta suppresses tumor progression by inhibiting Rho and migration. |
| High in good prognosis | SPRY1 | Regulation of cell-matrix interaction, migration and invasion | Sprouty1 inhibits events downstream of multiple receptor tyrosine kinases and regulates both cell proliferation and differentiation. In particular, Sprouty1 specifically inhibits the Ras/Raf/MAP kinase pathway by preventing Ras activation. |
| High in poor prognosis | CCNA2 | Positive role in cell proliferation | This cyclin binds and activates CDC2 or CDK2 kinases, and thus promotes both cell cycle G1/S and G2/M transitions. |
| High in poor prognosis | CCNB1 | Positive role in cell proliferation | The protein encoded by this gene is a regulatory protein involved in mitosis. The gene product complexes with p34(cdc2) to form the maturation-promoting factor (MPF). Two alternative transcripts have been found, a constitutively expressed transcript and a cell cycle-regulated transcript, that is expressed predominantly during G2/M phase. The different transcripts result from the use of alternate transcription initiation sites. |
| High in poor prognosis | CCNB2 | Positive role in cell proliferation | Cyclin B2 is a member of the cyclin family, specifically the B-type cyclins. The B-type cyclins, B1 and B2, associate with p34cdc2 and are essential components of the cell cycle regulatory machinery. B1 and B2 differ in their subcellular localization. Cyclin B1 co-localizes with microtubules, whereas cyclin B2 is primarily associated with the Golgi region. Cyclin B2 also binds to transforming growth factor beta RII and thus cyclin B2/cdc2 may play a key role in transforming growth factor beta-mediated cell cycle control. |
| High in poor prognosis | CDC45L | Positive role in cell proliferation | This protein has been shown to interact with MCM7 and DNA polymerase alpha. Studies of the similar gene in Xenopus suggested that this protein play a pivotal role in the loading of DNA polymerase alpha onto chromatin |
| High in poor prognosis | DTL | Positive role in cell proliferation | Nuclear protein with centrosome targeting in mitosis, plays important roles in DNA synthesis, cell cycle progression, cytokinesis, proliferation, and differentiation. |
| High in poor prognosis | EXO1 | Positive role in cell proliferation | Exo1 is a nuclease involved in mismatch repair, DSB repair, stalled replication fork processing and in the DNA damage response triggered by dysfunctional telomeres. |
| High in poor prognosis | CDT1 | Positive role in cell proliferation | human CDT1 is essential for DNA replication and chromatin licensing Cdt1 overexpression contributes to tumorigenecity by causing genomic instability in transgenic p53 knockout mice. |
| High in poor prognosis | MCM5 | Positive role in cell proliferation | The encoded protein is upregulated in the transition from the G0 to G1/S phase of the cell cycle and may actively participate in cell cycle regulation. |
| High in poor prognosis | MCM7 | Positive role in cell proliferation | The protein encoded by this gene is one of the highly conserved mini-chromosome maintenance proteins (MCM) that are essential for the initiation of eukaryotic genome replication. |
| High in poor prognosis | E2F2 | Positive role in cell proliferation | The protein encoded by this gene is a member of the E2F family of transcription factors. The E2F family plays a crucial role in the control of cell cycle and action of tumor suppressor proteins and is also a target of the transforming proteins of small DNA tumor viruses |
| High in poor prognosis | UHRF1 | Positive role in cell proliferation | Member of a subfamily of RING-finger type E3 ubiquitin ligases. Binds to specific DNA sequences, and recruits a histone deacetylase to regulate gene expression. Its expression peaks at late G1 phase and continues during G2 and M phases of the cell cycle. It plays a major role in the G1/S transition. |
| High in poor prognosis | NUSAP1 | Positive role in cell proliferation | nucleolar and spindle associated protein 1 |
| High in poor prognosis | ASPM | Positive role in cell proliferation | The ASPM gene is the human ortholog of the Drosophila melanogaster 'abnormal spindle' gene (asp), which is essential for normal mitotic spindle function in embryonic neuroblasts . |
| High in poor prognosis | HMMR | Positive role in cell proliferation | Receptor for hyaluronan-mediated motility (RHAMM), an acidic coiled coil protein previously characterized as a cell surface receptor for hyaluronan, and a microtubule-associated intracellular hyaluronan binding protein. A subset of cellular RHAMM localizes to the centrosome and functions in the maintenance of spindle integrity. |
| High in poor prognosis | TROAP | Positive role in cell proliferation | The major function of tastin during mitosis is to maintain the structural and dynamic features of centrosomes, thereby contributing to spindle bipolarity. |

**Definitions**

The present invention relates to identification of GAB2-signature genes and their association with diagnosis, prognosis, metastasis, metastatic relapse and prediction of treatment response.
The GAB2-signature genes of the present invention are listed in Tables 1, 2, 3, 4 and 5.

By claiming expression of at least two of GAB2-signature genes, it is meant that these two genes can be either from the same table or one each from different tables in a given scenario.

By 'metastatic potential', it is meant that the ability of a cancer cell to invade and to spread of cancer cells to other parts of the body.

By 'metastatic relapse', it is meant that the relapse occurs when a person is affected again by a condition of metastasis that affected him in the past.
By "prognosing", it is meant the ability to predict the potential course and outcome of a particular patient's cancer including potential for metastasis, growth and response to treatment

"predicting response to treatment" shall mean the ability to determine ahead of a treatment the probability that a particular type of treatment could be fully/partially effective or be fully/partially be ineffective in a particular patient and such treatments shall include, but not limited to chemotherapy, targeted drug therapy, radiation therapy, other cytotoxic drug therapies, alternate therapies or any other therapies other cytotoxic drug therapies, alternate therapies or any other therapies used in the treatment of cancer or one or more combinations thereof.

'Cancer treatment' as meant in the current specification includes but not limited to targeted drug therapy, chemotherapy, radiation therapy other cytotoxic drug therapies, alternate therapies or any other therapies used in the treatment of cancer or one or more combinations thereof.

'Grading of tumor' is a system used to classify cancer cells in terms of how abnormal they look under a microscope and how quickly the tumor is likely to grow and spread and includes defining different stages of cancer as per histology or other parameters as defined by a pathologist and physician.

The 'cancer' as mentioned in the specification includes all types (solid, liquid, and lymphatic origin), and not limited to breast cancer, metastatic malignant melanoma, lymphomas (Hodgkins and non-Hodgkins), sarcomas (Ewing's sarcoma), carcinomas, brain tumors, central nervous system (CNS) metastases, gliomas, , prostate cancer, lung cancer (small cell and non-small cell), colon cancer, pancreatic cancer, Head and Neck cancers, oropharyngeal squamous cell carcinoma. The cancer cell may be originated from any part of the body, and not limited to any organ of human body such as brain, lung, adrenal glands, pituitary gland, breast, prostate, pancreas, ovaries, Gastro Intestinal Tract, kidneys, Liver, spleen, testicles, cervix, upper, lower, or middle esophagus either primary or secondary tumors of all types.

***Innovative aspects of the invention***

To ensure successful metastatic dissemination, malignant cells must acquire the ability to grow in the absence of their environment of origin. In fact, the capacity of cells to survive and proliferate in vitro in the absence of integrin-mediated adhesion strongly correlates with tumorigenesis in-vivo and may enable tumor cells to metastasize and grow at inappropriate sites in the body (Danen and Yamada 2001, J Cell Physiol, 189, 1-13). We hereby describe a key role in anchorage-independent growth for Gab2, a multiadaptor protein devoid of enzymatic activity. The role of Gab2 in anchorage-independent growth emerged within the context of a high-throughput selective functional screening, in which this protein competed with several thousand others. Apart from GAB2, the analysis revealed a reproducible enrichment also for a well-known transforming gene, NTRK3, previously found to play a key role in anoikis resistance (Geiger and Peeper 2007, Cancer Res, 67, 6221-6229) and useful as an internal control of the screening effectiveness. Gab2 is a member of the Grb2-associated binding protein (GAB) gene family (Gu et al. 1998, Mol Cell, 2, 729-740). They are so called "scaffolding" or "docking" proteins because of the presence of multiple functional motifs mediating interactions with many other signaling molecules (Nishida et al. 1999). GAB proteins are involved in signaling events

triggered by a variety of stimuli, including GFs, cytokines, G-coupled receptors and T- and B-lymphocyte antigens, ultimately regulating cell growth, differentiation and transformation (Bouscary et al. 2001; Liu et al. 2001, Mol Cell Biol, 21, 3047-3056; Sattler et al. 2002, Cancer Cell, 1, 479-492). Among the Gab2 direct interactors are proteins with key roles in human cancer when mutated, such as PI3K and the tyrosine phosphatase Ptpn11/Shp2. Recent work suggested that the oncogenic properties of Ptpn11 mutant proteins require signal enhancement by Gab2 (Zatkova et al. 2006, Cancer, 45, 798

807). Interestingly, Gab2 maps to a chromosomal region (11q13) amplified in 10-15% of breast cancers, and its overexpression was confirmed in several breast cancer cell lines (Daly et al. 2002, Oncogene, 21, 5175-5181). The role of Gab2 in mammary tumor metastasis was also explored and confirmed in mouse models (Ke et al. 2007, Oncogene, 26, 4951-4960). More recently, a key role for GAB2 in motility/invasion of melanoma cells and metastatic progression of melanoma was also highlighted (Horst et al. 2009). We now show that Gab2 also promotes anchorage-independent growth of breast cancer and melanoma cells. This information extends the previously described growth-promoting activity of Gab2 in adherent cells (Brummer et al. 2006, J Biol Chem, 281, 626-637). We also found that Gab2-driven anchorage independence is not due to a protection from cell death upon detachment. This finding was unexpected, given the fact that Gab2 potentiates the PI3k/Akt and Ras/Erk pathways, but it is in line with previous reports indicating that Gab2 does not prevent apoptosis of luminal cells during morphogenesis of MCF10A cells (tires-Alj et al. 2006, Nat Med, 12, 114-121). Our experiments using small molecule inhibitors showed that, while the PI3k/Akt and Ras/Erk pathways are required independently of the adhesion status and of Gab2 expression, Src inhibition had no effect on wild-type cells in suspension, but strongly impaired their adherent growth, confirming that Src conveys the proliferative consensus provided by integrin engagement (Playford and Schaller 2004). Moreover, Gab2-expressing cells required Src activity also in suspension, providing a strong rationale for Src involvement in Gab2-driven anchorage-independence. The biochemical link between Gab2 and Src can be provided by Ptpn11, previously described to directly bind Gab2 (Kong et al. 2003) and to activate Src (Zhang et al. 2004, Mol Cell, 13, 341-355). It is of particular interest that Gab2sustained growth in suspension was impaired when cells were cultured in the absence of EGF, indicating that Gab2 can only overcome the lack of adhesive consensus in the presence of an

upstream signal from GFs. Recently, Gab2 was found to promote GF independence in cooperation with oncogenic Src (Bennett et al. 2007, Oncogene, 27, 2693-2704). Therefore, Gab2 can rescue cells from the need of two concomitant proliferative stimuli - activated GF receptors and activated Src when at least one of the two is present at sufficiently high levels. Therefore, Gab2 can be a key rheostat and integrator, allowing for a "spillover" of the signal across the two pathways, in the context of a network containing points of reciprocal influence and cross-talk (ffrench-Constant and Colognato 2004, Trends Cell Biol, 14, 678-686). In this view, proliferation of non-adherent cells could be promoted by a GF-driven direct activation of the Erk and Akt pathways and indirect, Gab2mediated activation of Src and of its downstream signaling molecules, in particular Stat3. Indeed, Stat3 has been already involved in Src and Jak1-driven proliferation of human breast carcinoma cells (Garcia et al. 2001, Oncogene, 20, 2499-2502) and in anchorage-independent growth of cancer cells (Zhang et al. 2006, Mol Cell Biol, 26, 413-424). Moreover, Gab2 was found to contain a functional Stat3 binding motif promoting its recruitment and activation (Ni et al. 2007, Mol Cell Biol, 27, 3708-3715). Our biochemical data confirmed the contribution of Src and Stat3 to Gab2-mediated anchorage-independent growth: Gab2 expression increased Src and Stat3 phosphorylation both basally and after prolonged suspension culture, and Gab2 downregulation by RNAi led to reduction of Src and Stat3 activation not only in MCF10A cells constitutively expressing exogenous Gab2, but also in neoplastic cells loosing anchorage independence as a consequence of endogenous Gab2 silencing. In line with this, our gene expression analysis showed that a significant fraction of the genes whose expression is regulated by Gab2 are also differentially expressed in cancer cells resistant or sensitive to small molecule inhibitors of the Src/Jak1-STAT3 signaling axis. Finally, it is of particular significance that the Gab2 transcriptional signature yields a robust classifier for metastatic relapse of human breast cancer. Of the two key functional modules found in the signature, the proliferation module, positively correlated with metastasis, adds further informative genes to the already described core of proliferation genes associated to breast cancer progression (Wirapati et al. 2008, Breast Cancer Res, 10, R65). More distinctive is the module of genes negatively correlated with metastasis, among which particularly interesting are: (i) two extracellular proteins that, respectively, inhibit matrix-degrading proteases (SERPINB1 (Cooley et al. 2001, Biochemistry, 40, 15762-15770)) and remove fucose from ECM glycans (FUCA1), thereby impairing ECM

binding and invasion by cancer cells (Yuan et al. 2008, Pathol Oncol Res, 14, 145-156); (ii) the FAP gene, encoding an integral membrane protease whose expression is negatively correlated with metastatic progression (See, Ariga et al., 2001, Int J Cancer, 95, 67-72); (iii) PMP22, that encodes a 4-spanning integral membrane protein widely expressed at apical junctions of epithelial cells, increasing transepithelial electrical resistance and decreasing migration (Roux et al. 2005, Mol Biol Cell, 16, 1142-1151); (iv) the intracellular products of the ARHGDIB and SPRY1 genes, negative regulators of, respectively, Rho-family GTPases (DerMardirossian and Bokoch 2005, Trends Cell Biol, 15, 356-363) and tyrosine kinase receptors like EGFR and FGFR (Mason et al. 2006, Trends Cell Biol, 16, 45-54). These two functional modules, within the context of the GAB2-signature, generate a prognostic classifier predicting metastatic progression with high accuracy, independently from ER status and from other existing genomic signatures, and greatly outperforming the clinical-pathological prognostic parameters currently integrated into the Adjuvant!Online web tool (Hess 2008). Altogether, we demonstrated a key role for Gab2 in anchorage-independent growth of neoplastic cells and, as an example of the diagnostic potential of the signatures described herein, we validated the transcriptional GAB2-signature as a new, strong and independent prognostic and predictive classifier for breast cancer. This confirms that the signatures described in tables 1 to 5, or other signatures obtained in cellular models of GAB2-driven processes and anchorage independence, can be successfully used as prognostic and predictive classifiers of human cancers, and contain novel therapeutical targets for cancer treatment. Furthermore, we have also demonstrated that GAB2 driven signatures are also predictive of drug response as demonstrated by the unique signatures identified in presence of anti-cancer drugs like resveratrol, dasatinib and Piceatannol. Hence the method can be used to identify GAB2 associated signatures which could predict sensitivity or resistance to any anti-cancer drug or combination of drugs and its dose or even to radiotherapy by identifying the GAB2 associated signature in presence of these drugs or cytotoxic or biologic modifiers in cell lines or primary cells derived from the tumor biopsy of a patient thereby providing a power tool to pre-determine which treatment a particular patient will respond to or not thus improving the efficacy of treatment and reducing unwanted side effect and cost of treatment. Since GAB-2 signature also can be correlated with the aggressiveness of the tumor cells, it could also be used as a method for assigning grades to the tumor, which is currently done by less accurate histochemical grading methods.

## Methods

### Cell Culture and Reagents

MCF10A cells were obtained from ATCC and cultured as described (Reginato et al. 2003, Nat Cell Biol, 5, 733-740). MDA-MB-231 and MDA-MB-435 cells were obtained from ATCC and cultured in DMEM (Gibco) supplemented with 10% fetal bovine serum (Sigma). The antibodies used were: antiGab2 (Upstate Biotechnology), anti- Tyr416-phosphorylated Src (Cell Signaling), anti-total Src (Cell Signaling), anti-Tyr705-phosphorylated Stat3 (Cell Signaling), anti-total Stat3 (Cell Signaling), goat anti-actin (Santa Cruz). Retroviral expression library and pFB-hrGFP retroviral supernatant, packaged in the VSV envelope, were purchased from Stratagene (ViraPort, Cat n. 972300) and used to infect $1.5x10^5$ MCF10A cells in 60mm tissue culture plates using 10 µg/ml DEAE-dextran (Amersham Bioscence). GFP expression analysis was performed after 48 hours using a FACS Calibur flow cytometer (Becton Dickinson). Retroviral expression vector for GAB2 in pMIG (also known as pMSCV-IRES-GFP) was a gift of R. Daly. Virus production and transduction were performed as described (Brummer et al. 2006).

### Anchorage-independent growth selection

Polyhema-coated 10cm Petri dishes were prepared by applying 4ml of a 12mg/ml solution of poly-hydroxy-ethyl-methacrylate (polyhema; Sigma) in ethanol, drying under tissue culture hood, repeating the application once and incubating the plates overnight at 37°C. For the selection, $3 \times 10^6$ cells were plated onto polyhema-coated plates in complete growth medium. Cells were cultured in suspension for 48h then were let to recover on regular plates for 24h before repeating the selection cycle.

### Western Blot

Cell lysates from $2–5\times10^6$ cells were prepared in RIPA buffer (150 mM NaCl, 1% NP40, 0.5% DOC, 50 mM TrisHCL at pH 8, 0.1% SDS, 10% glycerol, 5 Mm EDTA, 20 mM NaF and 1 mM Na3VO4) supplemented with 1 µg /ml each of pepstatin, leupeptin, aprotinin, and 200 µg/ml phenyl methylsulphonyl fluoride (PMSF). Lysates were cleared by centrifugation at 12,000 rpm for 20 min at 4°C and normalized with the BCA Protein Assay Reagent Kit (Pierce). Extracts were run on SDS-polyacrylamide gels, transferred onto nitrocellulose membranes (Hybond; GE Healthcare) and incubated with different

antibodies overnight at 4°C. Nitrocellulose-bound antibodies were detected by the ECL system (GE Healthcare).

Real-time PCR.

Two micrograms of total RNA were reverse transcribed with the High Capacity cDNA Reverse Transcription Kit (Applied Biosystems, Foster City, CA). Quantitative Real-time PCR with Sybr Green was performed on the ABI Prism 7900HT Sequence Detection System (Applied Biosystems, Oak Brook, IL). Details on PCR primer design are available in Supplementary Methods.

**Cell-based assays**

For MTT cell growth assays, $10^3$ cells were seeded in regular or polyhema-coated 96-well plates. Cells were cultured in growth medium containing all supplements or in starving medium (serum reduced to 2%, no EGF). At the indicated times, a tetrazolium salt–based reagent (CellTiter96 Aqueous One Solution, Promega) was added to each well according to the instructions provided by the manufacturer. After an incubation of 2 h, absorbance was read at 490 nm on a DTX 880 plate reader (Beckman Coulter). A control measurement after 4h from plating was used as a reference to adjust subsequent acquisitions of each cell line. For soft agar growth, $3x10^4$ cells were resuspended in 2ml of 0.5% top agar (SeaPlaque Agarose from Cambrex) in growth medium and seeded in 6-well plates previously filled with 3ml of 1% basal agar in growth medium. The assay was performed in duplicate. After 3 weeks, phase-contrast pictures were captured by a BD Pathway microscopic station (BD biosciences). Image analysis and quantification of single colonies number and size were performed by the Attovision 1.5 software (BD biosciences). For detachment-induced cell death analysis, $3x10^5$ cells were plated on regular or polyhemacoated 35mm plates for 48 hours. Cell death was then measured by assessing the number of hypodiploid nuclei with the DNAcon3 kit (ConsulTS, Rivalta, Italy), according to the manufacturer's protocol and with cytofluorimetric analysis using a FACSCalibur (Becton Dickinson, San Diego, CA). Hypodiploid, subG0/G1 nuclei were defined as those displaying a PI staining value lower than that of cells in the G0/G1 cell cycle phase (diploid DNA peak).

**Xenoarray and gene expression analysis**

RNA was extracted using the Trizol Plus purification Kit (Invitrogen, cat.no.12183555),

according to the manufacturer's protocol. Quantification and quality analysis of RNA was performed on a Bioanalyzer 2100 (Agilent). Synthesis of cDNA and biotinylated cRNA were performed using the Illumina TotalPrep RNA Amplification Kit (Ambion Cat. n. IL1791), according to the manufacturer's protocol, with previously reported variations in the case of Xenoarray analysis (Martelli et al. 2008, BMC Genomics, 9, 254), for which hybridization was carried out on Illumina Mouse6_V1 arrays. For standard microarray analysis of the Gab-2 signature, 1500 nanograms of cRNAs were hybridized on Illumina Beadarrays (Human_6_V2). Array washing was performed using Illumina High-stringency wash buffer for 10 min at 55°C, and followed by staining and scanning according to standard Illumina protocols. Probe intensity data were obtained using the Illumina BeadStudio software, and further processed with R-Bioconductor (Gentleman et al. 2004, Genome Biol. 5, R80) and Excel software.

**Definition of transcriptional signatures associated to GAB2 and anchorage independence in MCF10A cells**

**Preliminary data treatment**

Data were rank-invariant normalized and filtered to remove probes for which the detection score was lower than 0.99 in the sample with higher signal. Filtered data were scaled by adding the arbitrary value of 40 to remove negative expression values from the analysis. As an additional filter, genes differentially regulated between the two controls, i.e. WT and GFP-transduced cells, were removed from the analysis. Such genes were defined according to Illumina Custom statistic, with a fold-change threshold of 2 and a differential score of 20 (corresponding to a p-value of 0.01).

**Selection of differentially expressed genes**

To identify genes differentially expressed between GAB2-SEL and GFP-SEL samples we employed the Dunnett's T-test (Dunnett et al. 1964, Biometrics 20, 482-491), an inferential parametric test designed to compare the mean of each of several experimental groups with the mean of a control group. A simple description of the properties of the Dunnett's T-test can be found at

http://davidmlane.com/hyperstat/B112114.html

The formula of the test is the following:

$$\frac{\left|\overline{E}-\overline{C}\right|-m}{\sqrt{\frac{2*MSE_{wg}}{Nh}}}=t$$

Where: E = average of the experimental group to test

C = average of the control condition

m = minimal difference threshold (optional)

$MSE_{wg}$= mean square error within group, calculated from all experimental conditions like in ANOVA

t: the ratio of the test

Nh= harmonic mean of sample replicates for the two conditions tested

The test evaluates the hypothesis, in our case the change of log2 expression values, by means of an estimation of the mean square error within groups, corrected by the harmonic mean of the sample numbers. The test was performed on log2-scaled values, with m = 1. To increase accuracy of the $MSE_{wg}$ estimation, we calculated it from all experimental conditions, i.e. GAB2-selectet, GFP-selected, GAB2-unselected, GFP-unselected and Lib selected. In the standard Dunnett's test the m threshold is absent and the t threshold for significance can be derived from the Dunnett's t tables, available for example at http://davidmlane.com/hyperstat/table_Dunnett.html. In our case, with m different from zero, we had to estimate the correct t value by running the test iteratively on permutations of experiments, thereby estimating the False Discovery Rate (FDR; Tucher et al.2001, Proc Natl Acad Sci U S A. 98, 5116-21). Indeed, our FDR analysis showed that the Dunnett's test with m different from zero is more powerful, and much more reliable than classical T-test. To prioritize differentially regulated genes, we choose t = 2, with an estimated alpha (FDR) of <0.05 according to the median distribution of 5000 randomly permutated datasets. The list of selected genes and their expression in control and Gab2-transduced cells is reported in Table 1. The same procedure was applied for the other signatures illustrated in Tables 2 to 5.

The following examples provide illustrative embodiments of the invention. A person skilled in the art will readily recognize the various modifications and variations that may be performed without altering the scope of the present invention. Such modifications and

variations are encompassed within the scope of the invention and the examples do not in any way limit the scope of the invention.

**Examples**

**Example 1 - Analysis of GAB2-signature enrichment in genes correlated to cancer aggressiveness and response to treatment**

***Enrichment in genes correlated with cell response to drugs***

To verify if expression of GAB2-signature genes is correlated to responsiveness of cell lines to inhibitors of the Src/STAT3 signaling axis, we used two sets of data built on the NCI-60 panel of cell lines: (i) a gene expression dataset (Shankavaram et al. 2007) generated using Affymetrix HGU133 arrays and downloaded from the NCBI Gene Expression Omnibus (GEO, GSE5720); (ii) the database of Developmental Therapeutics Program NCI/NIH (http://dtp.nci.nih.gov/index.html), reporting for each cell line the GI50 (concentrations required to inhibit growth by 50%) for over 50.000 different compounds. In particular, we focused on 3 drugs (Resveratrol, Piceatannol, and SD-1029) targeting STAT3 activation by Src- or Jak-family kinases, and calculated the Pearson correlation, across all cell lines, between the GI50 and the expression of each gene of the Affy dataset. To assess the enrichment of the GAB2-signature in genes with high correlation with the GI50 of the above drugs, Gene Symbols corresponding to the signature were mapped on the dataset, resulting in 356 Affymetrix probe sets (Supplementary Table 2). Subsequently, the number of signature genes with correlation values falling in the top 5% of all the dataset was counted. Significance of the difference between expected and observed probe sets with high correlation was calculated by hypergeometric distribution analysis as illustrated in the following table:

| Compound name | Total Number of probe sets | Number of GAB2-signature probe sets | 95th percentile correlation threshold | Number of GAB2signature genes above the threshold | Observed/ Expected | Hypergeometric p.value |
|---|---|---|---|---|---|---|
| Resveratrol | 44928 | 356 | 0.21531873 | 38 | 2.13 | 0.00001043 |
| Piceatannol | 44928 | 356 | 0.243598545 | 32 | 1.80 | 0.00107 |
| Sd-1029 | 44928 | 356 | 0.26522899 | 35 | 1.97 | 0.000121304 |

To assess enrichment of the GAB2-signatures for predictive markers of response to

Dasatinib, we exploited a gene expression dataset obtained by Huang and colleagues using Affymetrix HGU133 arrays on a panel of 23 breast cancer cell lines, either resistant (16 lines) or sensitive (7 lines) to Dasatinib (Huang et al., 2007). The resulting dataset was downloaded from the NCBI Gene Expression Omnibus (GEO, GSE6569). For each probe in the array, the differential expression between Dasatinib-sensitive and resistant cells was calculated using the Signal to Noise ratio (Golub et al., 1999, Science 286, 531-537). To assess the enrichment of the GAB2-signature in genes with high SNR, Gene Symbols corresponding to the signature were mapped on the dataset, resulting in 356 Affymetrix probe sets. Subsequently, the number of signature genes with absolute SNR values falling in the top 5% of all the dataset was counted. Significance of the difference between expected (18) and observed (30) probe sets with high SNR was calculated by hypergeometric distribution analysis.

**Example 2**

***Enrichment in genes discriminating good and poor prognosis breast cancer***

For meta-analysis on breast cancer microarray data, two public available data sets from the Netherlands Cancer Institute (van't., Veer et al 2002, Nature, 415, 530-536; van de Vijver et al. 2002, N Engl J Med, 347, 1999-2009) (NKI; http://www.rii.com/publications/2002/default.html) were used and merged into a unique 311sample dataset (NKI-311). The data were filtered to remove probes whose signal never reached the 50$^{th}$ percentile in any sample. Further filtering was applied on probes for which more than 99% of the expression values were missing. The probes were annotated with gene symbols obtained via Unigene (release Hs # 204), and for each of them the Signal-to-Noise Ratio (SNR; Golub et al.1999) between poor- and good -prognosis samples (presence or absence of metastatic relapse within 5 years) was calculated in the NKI-311 dataset, according to the following formula:

$$SNR = \frac{AVG_{PP} - AVG_{GP}}{STDEV_{PP} + STDEV_{GP}}$$

Where $AVG_{PP}$ and $AVG_{GP}$ are the average expression values in poor-prognosis and good-prognosis samples, respectively, and $STDEV_{PP}$ and $STDEV_{GP}$ are the standard deviations in poor-prognosis and good-prognosis samples, respectively. After mapping the GAB2-

signature on this dataset via Gene Symbols, its enrichment in genes with high SNR was calculated as described above.

The results are displayed in the following table:

| Metric | Total Number of probes | Number of GAB2-signature probe sets | 5th percentile correlation threshold | Number of GAB2-signature genes above the threshold | Observed/ Expected | Hypergeometric p.value |
|---|---|---|---|---|---|---|
| Signal to noise ratio for metastatic recurrence whitin 5 years | 12018 | 150 | -0.21 | 28 | 3.73 | 1.21E-009 |

**Example 3 - Construction and validation of a Breast cancer classifier based on the GAB2-signature**

***Classifier construction***

To generate a classifier for breast cancer patients, we applied a modification of the nearest mean classifier approach (Wessels 2005). Briefly, we calculated for each gene of the GAB2Signature the median expression in the good and poor prognosis subgroups of the NKI-311 dataset. For a more accurate calculation of the median expression, the data were bootstrapped (1000 bootstraps each including a random selection of 80% of subgroup samples). The classifier is therefore composed of the list of the GAB2-signature genes mapped on the NKI dataset and, for each gene, the median expression values (means) for the good and poor prognosis groups (Supplementary Table 3). To classify samples, a "Metastasis Score" (MS) is then calculated, based on the GAB2-signature genes, according to the following formula:

$$MS = k + Pearson_{PP} - Pearson_{GP}$$

Where k is a scaling factor, $Pearson_{PP}$ is the correlation of the sample with the poor prognosis centroid, and $Pearson_{GP}$ is the correlation of the sample with the good prognosis centroid. The MS is therefore directly proportional to the risk of metastatic relapse within five years, and if it is greater than zero, patients are classified as poor prognosis, otherwise they are classified as good prognosis. We found that a k value of 0.16

minimizes the rate of false negatives (patients classified as "good prognosis" that instead developed metastasis within 5 years) in the NKI-311 dataset.

*Classifier validation*

To map the GAB2-signature on independent breast cancer datasets obtained on different microarray platforms, we used a univocal cross-mapping table generated by the Microarray Quality Control (MAQC) consortium (Maqc consortium, 2006, Nat Biotechnol. 24, 1151-1161) and applied it to five independent datasets of 198, 236, 286, 289 and 134 samples (Desmedt et al 2007, Clin Cancer Res, 13, 3207-3214; Miller et al. 2005, Proc Natl Acad Sci U S A, 102, 13550-13555; Wang et al. 2005, Lancet, 365, 671-679; Ivshina et al. 2006, Cancer Res, 66, 10292-10; Hess et al. 2006, J Clin Oncol, 24, 4236-4244). To reach homogeneity in data structure and to properly apply the NMC obtained in the NKI-311 dataset, Affymetrix log2 expression signals were converted, for each dataset, into log2 ratios against median expression in that dataset. Univariate and multivariate analyses were conducted in the 198sample dataset using R-Bioconductor.

**Example 4 – Neutralization of Gab-2 function using a short hairpin RNA vector as a method for treating breast cancer and other epithelial cancers**

Lentiviral shRNA expression vectors against murine or human GAB2 can be purchased from Sigma (MISSION™ TRC shRNA Target Set), together with the pLKO.1-puro Control Vector. Viral supernatants are obtained according to the manufacturer's protocol. Infected cells are selected by puromycin treatment (2ug/ml for one week). Specific shRNA sequences which efficiently downregulate Gab2 protein, as assessed in Western blot, are the following:

(i) Murine: CCGGCCGACACAATACAGAATTCAACTCGAGTTGAATTC-TGTATTGTGTCG-GTTTTTG;

(ii) Human: CCGGCAGCCAACTCTGTTCACGTTTCTC-GAGAAACGTGAACAGAGTTGGCTGTTTTTTG. Neutralization of GAB2 by the shRNA leads to inhibition of proliferation in adherence, as measured by MTT cell growth assays or $^{3}$H-thymidine uptake and in suspension, as measured by soft agar growth assay. In a preferred embodiment, the shRNA vector would be replaced with an artificial molecule targeting the GAB2 mRNA, such as a peptide-nucleic acid (PNA) or other nuceleotide-based reagent. In another preferred embodiment, one would use a small

molecule inhibitor against Gab2 selected using combinatorial chemistry, rational design or other methods. Such drugs would be properly formulated and administered parenterally, orally or as an injection. In fact, one could use any agent that has the ability to neutralize fully or partially the function of Gab2 or its interaction with other proteins by neutralizing either the gene, its mRNA or the protein itself. In a further embodiment of the invention, one would use the same strategies described above to inhibit the function of the transcriptional targets of GAB2 and/or of anchorage independence as described in Tables 1 to 5, or contained other signatures obtained in cellular models of GAB2-driven processes and anchorage independence.

**Example 5 – A real-time PCR-based classifier for predicting metastasis, prognosis and sensitivity to chemotherapy in breast cancer patients**

We analyzed RNAs extracted from 32 breast cancer samples, and measured gene expression using Illumina microarrays or realtime PCR as described in Methods, for 15 genes of the GAB2 signature (list of genes/TaqMan Inventoried Assay ID: EEF1A2/Hs00157325_m1; PHGDH/Hs00198333_m1; C9orf58/Hs00230107_m1; IGFBP5/Hs00181213_m1; CDCA7/Hs00230589_m1; CCNB2/Hs00270424_m1; EXO1/Hs00243513_m1; TROAP/Hs00193896_m1; CCNA2/Hs00153138_m1; CDT1/Hs00368864_m1; ASPM/Hs00250800_m1; CYP1B1/Hs00164383_m1; NUSAP1/Hs00251213_m1; CDC45L/Hs00185895_m1; ARHGDIB/Hs00171288_m1). We then calculated for each sample the Metastasis-Score with the procedure described in Example 3, using the 15 genes measured either with microarrays or with realtime PCR. The dot plot in **Figure 10** shows that the two platforms for gene expression analysis generate highly correlated scores ($R^2 = 0.70$), confirming the possibility of using genes of the GAB2 signatures for cancer diagnosis independently of the measurement technique.

**Example 6 – Application of the GAB2-signature to malignant melanoma**

We have verified whether genes of the GAB2-signature show expression changes during the progression of human melanoma, from normal skin to nevus to primary malignant melanoma to metastatic melanoma. To this aim, we acquired publicly available DNA

microarray gene expression data (Affymetrix) from two papers, including in total over 100 melanomas, primary and metastatic, 18 nevi and seven samples of healthy skin (Talantov et al. 2005, Clin Cancer Res, 11, 7234-7242; Xu et al. 2008, Mol Cancer Res, 6, 760-769). Genes of the GAB2-signature were mapped onto this dataset via gene symbols, resulting in 83 Affymetrix probesets. For each gene, the log2ratio between each sample's signal and the median signal for that gene in all samples was then calculated. Expression data were then Fuzzy SOM-clustered using the GEDAS software (Fu and Medico, 2007, BMC Bioinformatics, 8, 3), with cosine correlation as the similarity metric. The result of this procedure is illustrated in Figure 11, clearly showing the the GAB2 signautre discriminates benign lesions from melanomas, with some of the primary melanomas displaying a profile similar to nevi, and others more similar to metastatic melanoma, which show the highest divergence from benign tissues. Subdivision of primary melanomas in two subgroups, one similar to nevi and the other similar to metastases, highlights possible differences in the aggressiveness of the primary lesion which could guide therapeutic decisions. Is it of particular relevance to the present invention that the GAB2-signature, obtained *in vitro* on breast cells, without any further selection or training, displays such a strong discriminating capacity on such a different type of neoplastic lesion. It is likely that, similar properties will be displayed also on other cancer types, and also by genes of the other GAB-2 signatures presented here.

It will be evident to those skilled in the art that the invention is not limited to the details of the foregoing illustrative examples and that the present invention may be embodied in other specific forms without departing from the essential attributes thereof, and it is therefore desired that the present embodiments and examples be considered in all respects as illustrative and not restrictive, reference being made to the appended claims, rather than to the foregoing description, and all changes which come within the meaning and range of equivalency of the claims are therefore intended to be embraced therein.

**We Claim:**

1) A method of diagnosing or prognosing cancer in subjects comprising detecting expression of GAB2 and/or of its transcriptional target genes in the tumor tissue and/or in tumor cells isolated from the subject.
2) A method of diagnosing or prognosing cancer in subjects comprising detecting in the tumor tissue and/or in tumor cells isolated from the subject expression of at least two of GAB2-signature genes listed in Table 1, 2, 3, 4 or 5, either from a single list or across the lists.
3) The method of diagnosing or prognosing cancer in subjects as in claim 2, wherein the cancer is breast cancer, comprising detecting in the subject expression of at least 2 of GAB2-signature genes listed in Table 1.
4) The method of diagnosing or prognosing cancer in subjects as in claim 2, wherein the cancer is melanoma, comprising detecting in the subject expression of at least 2 of GAB2-signature genes listed in Table 1, 2, 3, 4 or 5, either from a single list or across the lists.
5) A method of predicting metastasis or metastatic relapse or metastatic potential or response to treatment in cancer patients comprising detecting the expression of GAB2 and or its transcriptional target genes in the tumor tissue and/or in tumor cells isolated from the subject.
6) The method of predicting metastasis in cancer patients as in claim 5, comprising detecting the expression of at least two of GAB2-signature genes listed in Table 1, 2, 3, 4 or 5 either from a single list or across the lists.
7) The method of predicting metastasis in cancer patients as in claim 5, wherein the cancer is breast cancer, comprising detecting the expression of at least two of GAB2-signature genes listed in Table 1.
8) The method of predicting metastasis in cancer patients as in claim 5, wherein the cancer is melanoma, comprising detecting the expression of at least two of GAB2-signature genes listed in Table 1, 2, 3, 4 or 5 either from a single list or across the lists.
9) The method of predicting metastatic relapse or metastatic potential in cancer patients as in claim 5, comprising detecting the expression of at least two of

GAB2-signature genes listed in Table 1, 2, 3, 4 or 5 either from a single list or across the lists.

10) The method of predicting metastatic relapse or metastatic potential in cancer patients as in claim 5, wherein the cancer is breast cancer, comprising detecting the expression of at least two of GAB2-signature genes listed in Table 8 or 9.

11) The method of predicting metastatic relapse or metastatic potential in cancer patients as in claim 5, wherein the cancer is melanoma, comprising detecting the expression of at least two of GAB2-signature genes listed in Table 1, 2, 3, 4 or 5 either from a single list or across the lists.

12) The method of predicting response to treatment in cancer patients as in claim 5, wherein the cancer treatment is targeted drug therapy, chemotherapy, radiation therapy or a combination thereof, comprising detecting the expression of at least two of GAB2-signature genes listed in Table 1, 2, 3, 4 or 5 either from a single list or across the lists.

13) The method of predicting response to treatment in cancer patients as in claim 12, wherein the cancer is breast cancer, comprising detecting the expression of at least 2 of GAB2-signature genes listed in Table 1.

14) The method of predicting response to treatment in cancer patients as in claim 12, wherein the cancer is melanoma, comprising detecting the expression of at least 2 of GAB2-signature genes listed in Table 1, 2, 3, 4 or 5 either from a single list or across the lists.

15) A method of treating a subject with cancer comprising the steps of:

a) obtaining blood or tissue sample from the subject with cancer;

b) screening said sample for the expression of a polypeptide encoded by a polynucleotide selected from a group consisting of GAB2-signature genes listed in Table 1, 2, 3, 4 and 5;

c) providing an antibody that reacts immunologically against said polypeptide; and

d) administering an effective amount of said antibody to the subject with cancer.

16) A method of treating a subject suffering from cancer comprising the steps of:

a) obtaining a sample of tissue from a subject suffering from cancer;

b) screening said sample for the expression of a polypeptide encoded by a polynucleotide selected from a group consisting of GAB2-signature genes listed in Table 1, 2, 3, 4 and 5;

c) providing an antisense DNA molecule that encodes an RNA molecule that binds to said polynucleotide;

d) providing said antisense DNA molecule in the form of a human vector containing appropriate regulatory elements for the production of said RNA molecule; and

e) administering an effective amount of said vector to the subject with cancer.

17) A method of using *in vitro* anchorage independence model for deriving gene signature, the said signature comprising a set of genes associated with diagnosis, prognosis, metastasis and predicting response to treatment in cancer.

18) The method of claim 17 wherein the said gene signature is GAB2-signature comprising at least two GAB2 and or its transcriptional target genes listed in Tables 1, 2, 3, 4 or 5 either from a single list or across the lists.

19) A method of predicting the grade of a tumor in a cancer patient, comprising detecting the expression of GAB2 and/or its transcriptional target genes in the tumor tissue and/or in tumor cells isolated from the subject.

20) The method of predicting the grade of a tumor in a cancer patient as in claim 19, comprising detecting the expression of at least two of GAB2-signature genes listed in Table 1, 2, 3, 4 or 5 either from a single list or across the lists.

21) A GAB2-signature for diagnosing or prognosing cancer in subjects comprising GAB2 and/or its transcriptional target genes in the tumor tissue and/or in tumor cells isolated from the subject as diagnostic or prognostic markers.

22) The GAB2-signature comprising GAB2 and or its transcriptional target genes as diagnostic or prognostic markers for diagnosing or prognosing cancer in subjects as in claim 21, wherein the diagnosis or prognosis comprises detecting in the tumor tissue and/or in tumor cells isolated from the subject expression of at least two of GAB2-signature genes listed in Tables 1, 2, 3, 4 or 5 either from a single list or across the lists.

23) The GAB2-signature comprising GAB2 and or its transcriptional target genes as diagnostic or prognostic markers for diagnosing or prognosing breast cancer in

subjects as in claim 21, wherein the diagnosis or prognosis comprises detecting in the tumor tissue and/or in tumor cells isolated from the subject expression of at least two of GAB2-signature genes listed in Table 1.

24) A GAB2-signature for predicting
metastasis; or
metastatic relapse; or
metastatic potential; or
response to treatment
in cancer patients comprising GAB2 and or its transcriptional target genes.

25) The GAB2-signature comprising GAB2 and or its transcriptional target genes as markers for predicting metastasis in cancer patients as in claim 24, wherein the prediction of metastasis comprises detecting in tumor tissue and/or in tumor cells isolated from the patient expression of at least two of GAB2-signature genes listed in Tables 1, 2, 3, 4 or 5 either from a single list or across the lists.

26) The GAB2-signature comprising GAB2 and or its transcriptional target genes as markers for predicting metastasis in cancer patients as in claim 24, wherein the cancer is breast cancer and wherein the prediction of metastasis comprises detecting in tumor tissue and/or in tumor cells isolated from the patient expression of at least two of GAB2-signature genes listed in Table 1.

27) The GAB2-signature comprising GAB2 and or its transcriptional target genes as markers for predicting metastasis in cancer patients as in claim 24, wherein the cancer is melanoma and wherein the prediction of metastasis comprises detecting in tumor tissue and/or in tumor cells isolated from the patient expression of at least two of GAB2-signature genes listed in Table 1, 2, 3, 4 or 5 either from a single list or across the lists.

28) The GAB2-signature comprising GAB2 and or its transcriptional target genes as markers for predicting metastatic relapse in cancer patients as in claim 24, wherein the prediction of metastatic relapse comprises detecting in tumor tissue and/or in tumor cells isolated from the patient expression of at least two of GAB2-signature genes listed in Table 1, 2, 3, 4 or 5 either from a single list or across the lists.

29) A GAB2-signature comprising GAB2 and or its transcriptional target genes as markers for predicting metastatic relapse in cancer patients as in claim 24, wherein the cancer is breast cancer and wherein the prediction of metastatic relapse comprises detecting in tumor tissue and/or in tumor cells isolated from the patient expression of at least two of GAB2-signature genes listed in Table 1.

30) The GAB2-signature comprising GAB2 and or its transcriptional target genes as markers for predicting metastatic relapse in cancer patients as in claim 24, wherein the cancer is breast cancer and wherein the prediction of metastatic relapse comprises detecting in tumor tissue and/or in tumor cells isolated from the patient expression of at least two of GAB2-signature genes listed in Table 8 or 9.

31) The GAB2-signature comprising GAB2 and or its transcriptional target genes as markers for predicting metastatic relapse in cancer patients as in claim 24, wherein the cancer is melanoma and wherein the prediction of metastatic relapse comprises detecting in tumor tissue and/or in tumor cells isolated from the patient expression of at least two of GAB2-signature genes listed in Table 1, 2, 3, 4 or 5 either from a single list or across the lists.

32) The GAB2-signature comprising GAB2 and or its transcriptional target genes as markers for predicting response to treatment in cancer patients as in claim 24, wherein the treatment is targeted drug therapy, chemotherapy, radiation therapy or a combination thereof and wherein predicting response to the treatment comprises detecting in tumor tissue and/or in tumor cells isolated from the patient expression of at least two of GAB2-signature genes listed in Table 1, 2, 3, 4 or 5 either from a single list or across the lists.

33) The GAB2-signature comprising GAB2 and or its transcriptional target genes as markers for predicting response to treatment in cancer patients as in claim 24, wherein the treatment is targeted drug therapy, chemotherapy, radiation therapy or a combination thereof and wherein the cancer is breast cancer and wherein predicting response to the treatment comprises detecting in tumor tissue and/or in tumor cells isolated from the patient expression of at least two of GAB2-signature genes listed in Table 1.

34) The GAB2-signature comprising GAB2 and or its transcriptional target genes as markers for predicting response to treatment in cancer patients as in claim 24, wherein the treatment is targeted drug therapy, chemotherapy, radiation therapy or

a combination thereof and wherein the cancer is myeloma and wherein predicting response to the treatment comprises detecting in tumor tissue and/or in tumor cells isolated from the patient expression of at least two of GAB2-signature genes listed in Table 1, 2, 3, 4 or 5 either from a single list or across the lists.

35) An array comprising polynucleotides capable of specifically hybridizing to at least two genes listed in Table 1, 2, 3, 4 or 5 either from a single list or across the lists.

36) A kit comprising the array of claim 34 for diagnosing or prognosing cancer or predicting metastasis or metastatic relapse or metastatic potential of cancer cells in a subject by determining the expression of at least 2 genes listed in Table 1, 2, 3, 4 or 5 either from a single list or across the lists.

37) A kit for diagnosing or prognosing cancer cells or predicting metastasis or metastatic relapse or metastatic potential of cancer cells in a biological sample comprising a primer pair for amplifying a nucleic acid sequence selected from a group consisting of GAB2-signature genes listed in Table 1, 2, 3, 4 and 5 and containers for the primers.

38) A kit for diagnosing or prognosing cancer cells or predicting metastasis or metastatic relapse or metastatic potential of cancer cells in a biological sample comprising an oligonucleotide probe that binds under high stringency conditions to an isolated nucleic acid sequence selected from a group consisting of GAB2-signature genes listed in Table 1, 2, 3, 4 and 5 and a container for the probe.

39) A kit for diagnosing or prognosing cancer cells or predicting metastasis or metastatic relapse or metastatic potential of cancer cells in a biological sample comprising an antibody which binds immunologically to a protein having an amino acid sequence encoded by a polynucleotide selected from a group consisting of GAB2-signature genes listed in Table 1, 2, 3, 4 and 5 and a container for the probe.

40) A kit for diagnosing or prognosing cancer cells or predicting metastasis or metastatic relapse or metastatic potential of cancer cells in a biological sample comprising an array of probes selected from a group consisting of GAB2-signature genes listed in Table 1, 2, 3, 4 and 5 and a container for the probe and the expression of the genes is determined by Real-time PCR or other quantitative PCR assay.

# FIGURE I/IX

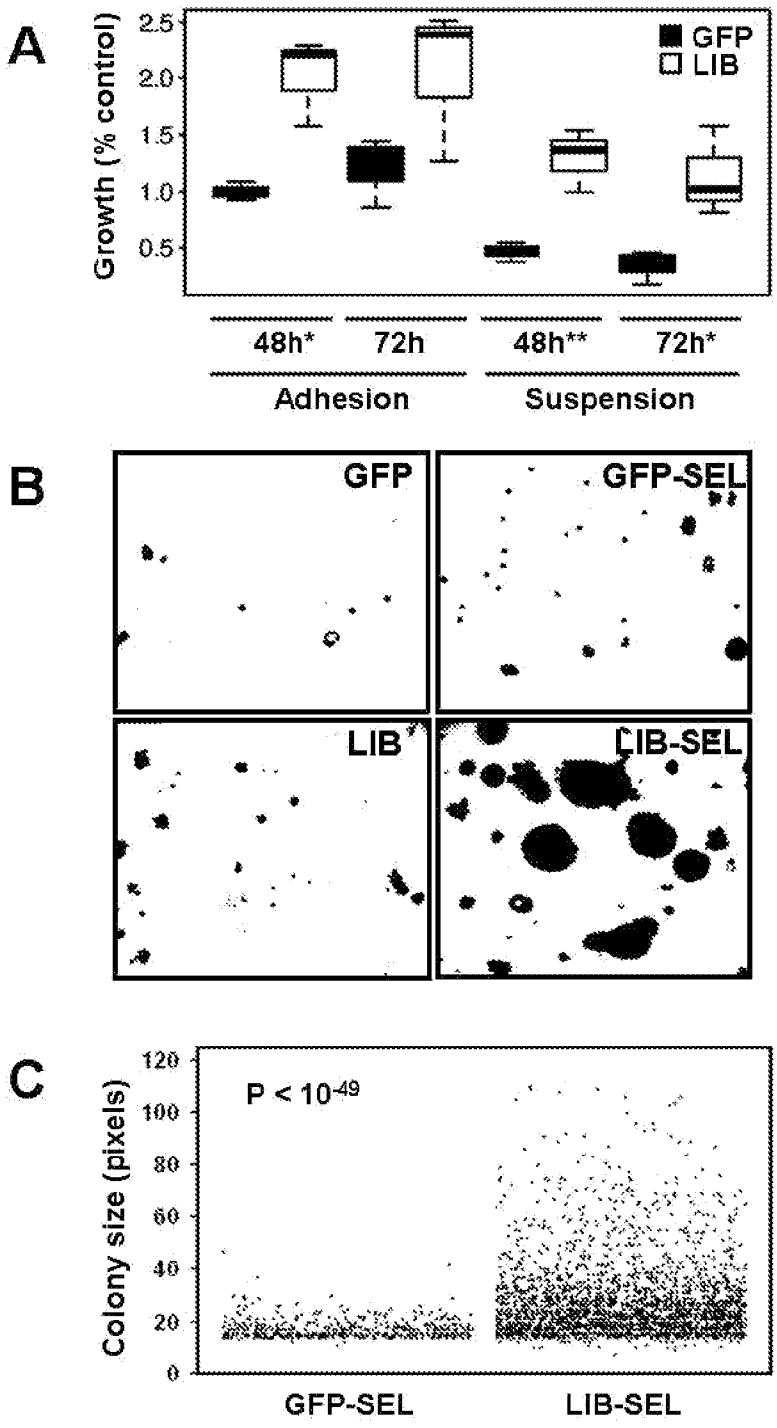
A
Growth (% control)
2.5
2.0
1.5
1.0
0.5
GFP
LIB
48h*
72h
48h**
72h*
Adhesion
Suspension
B
GFP
GFP-SEL
LIB
LIB-SEL
C
Colony size (pixels)
120
100
80
60
40
20
0
P < 10-49
GFP-SEL
LIB-SEL

# FIGURE II/IX

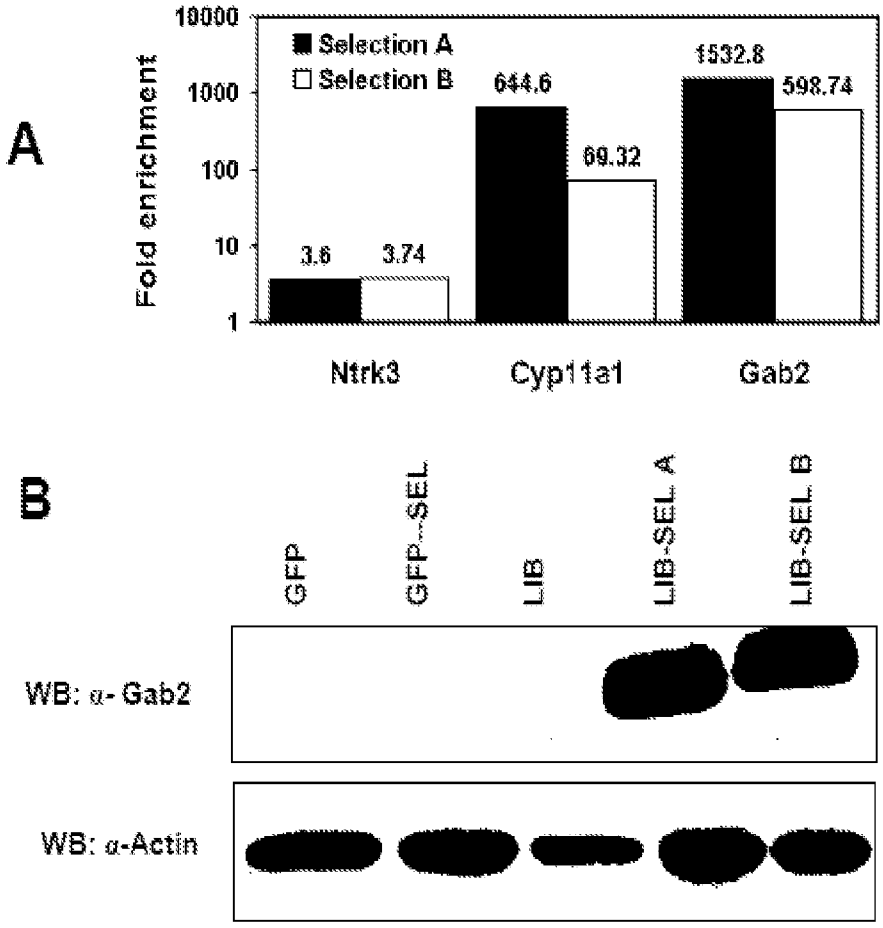
A
Fold enrichment
10000
1000
100
10
1
Selection A
Selection B
3.6
3.74
644.6
69.32
1532.8
598.74
Ntrk3
Cyp11a1
Gab2
B
GFP
GFP--SEL
LIB
LIB-SEL A
LIB-SEL B
WB: α- Gab2
WB: α-Actin

# FIGURE III/IX

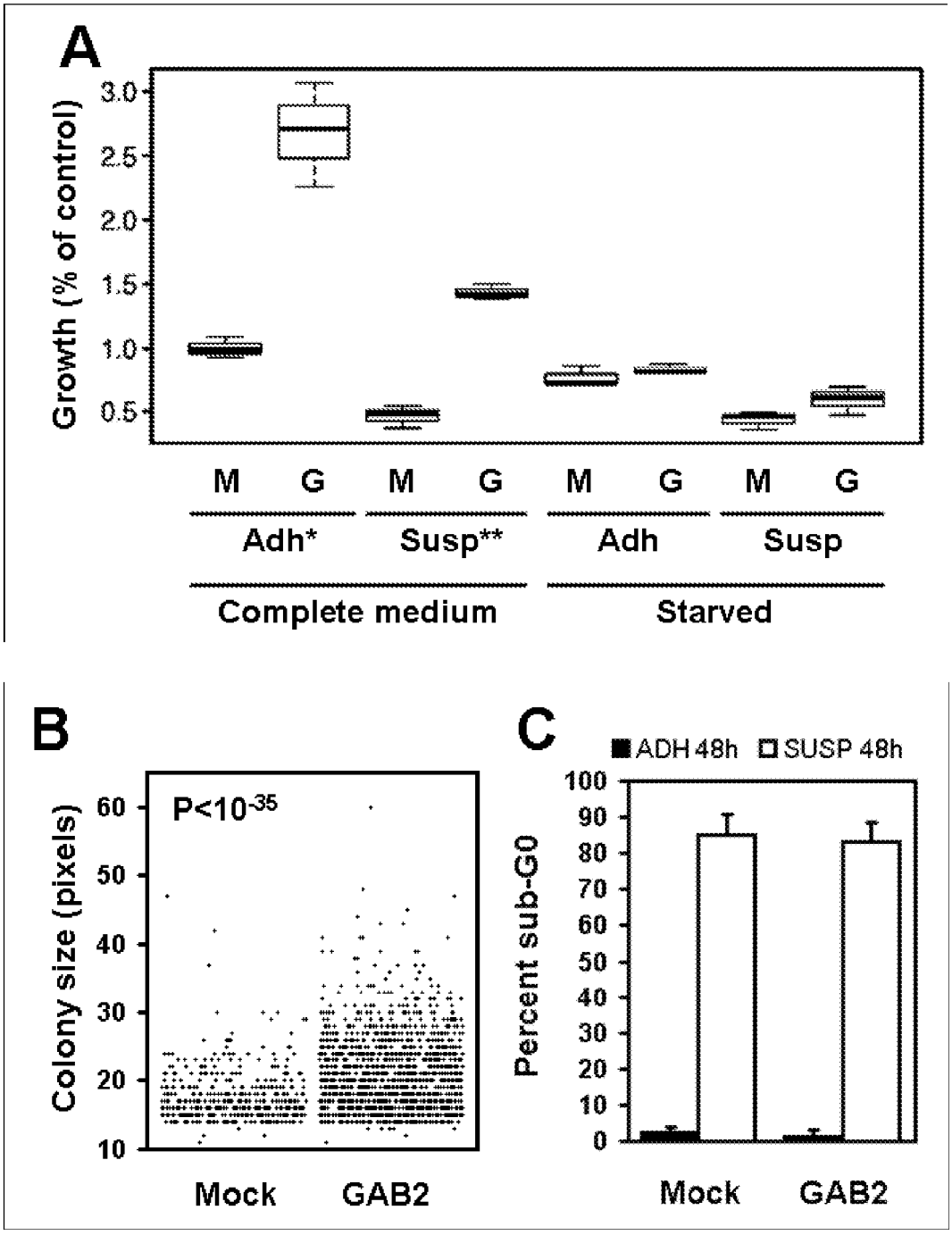

# FIGURE IV/IX

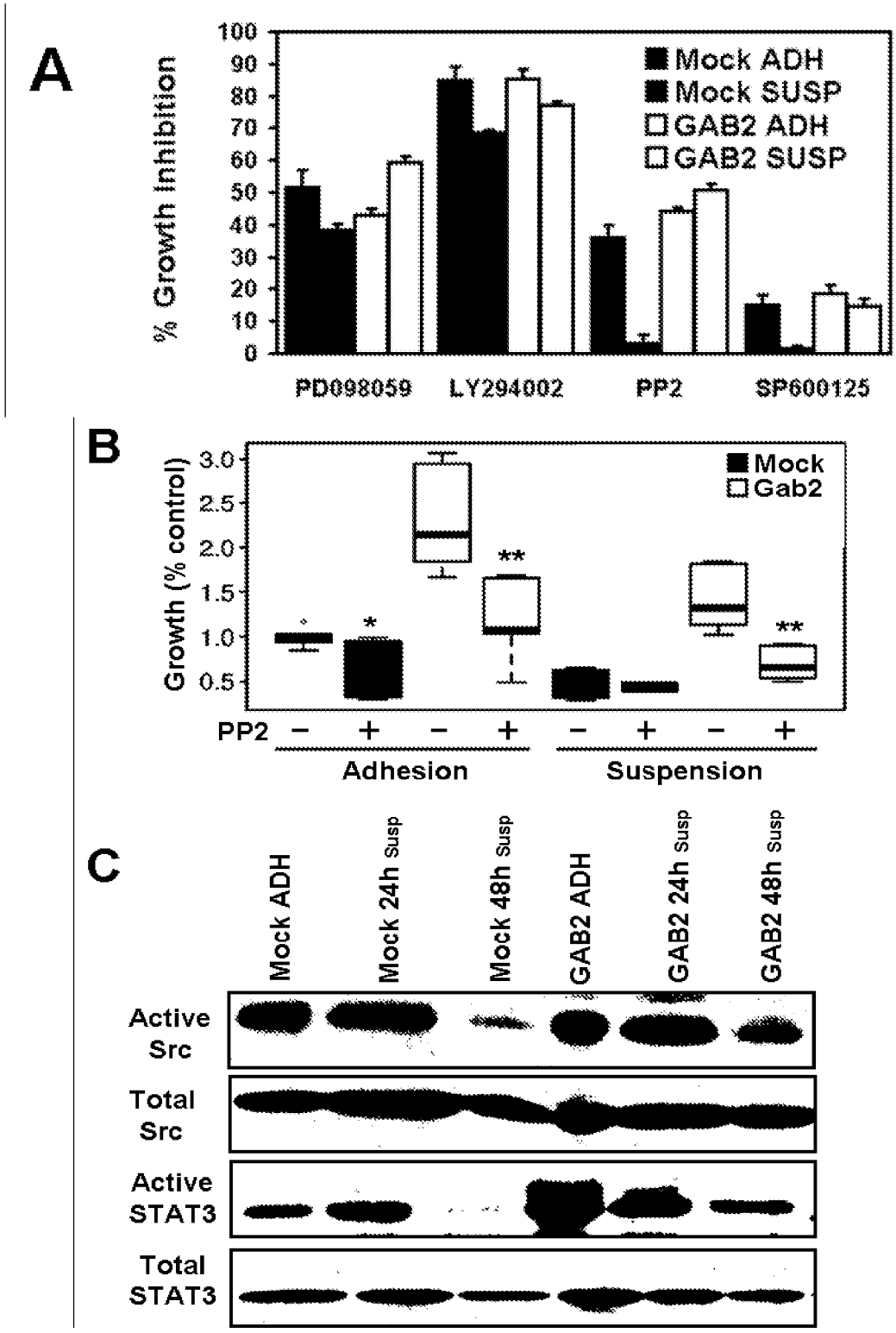
A
% Growth inhibition
100
90
80
70
60
50
40
30
20
10
0
Mock ADH
Mock SUSP
GAB2 ADH
GAB2 SUSP
PD098059
LY294002
PP2
SP600125
B
Growth (% control)
3.0
2.5
2.0
1.5
1.0
0.5
Mock
Gab2
*
**
**
PP2 − + − + − + − +
Adhesion
Suspension
C
Mock ADH
Mock 24h Susp
Mock 48h Susp
GAB2 ADH
GAB2 24h Susp
GAB2 48h Susp
Active Src
Total Src
Active STAT3
Total STAT3

# FIGURE V/IX

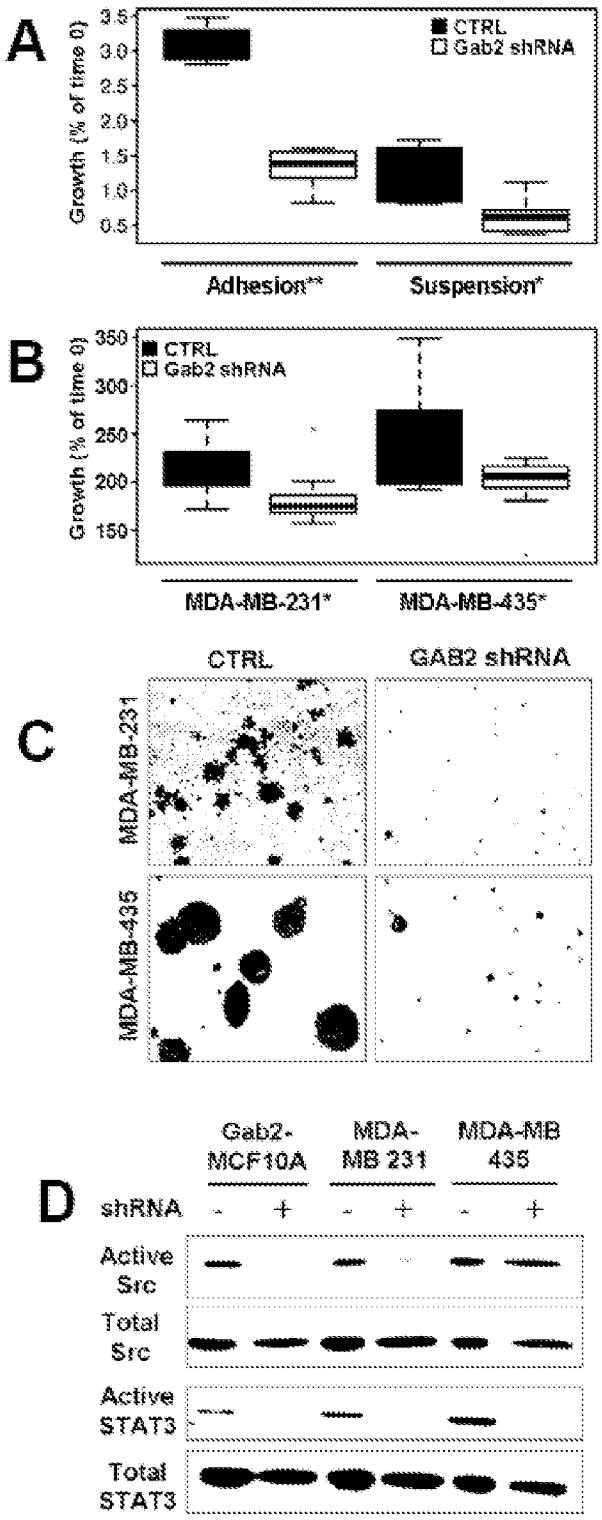
A
Growth (% of time 0)
3.5
3.0
2.5
2.0
1.5
1.0
0.5
CTRL
Gab2 shRNA
Adhesion**
Suspension*
B
Growth (% of time 0)
350
300
250
200
150
CTRL
Gab2 shRNA
MDA-MB-231*
MDA-MB-435*
C
CTRL
GAB2 shRNA
MDA-MB-231
MDA-MB-435
D
Gab2-MCF10A
MDA-MB 231
MDA-MB 435
shRNA - + - + - +
Active Src
Total Src
Active STAT3
Total STAT3

# FIGURE VI/IX

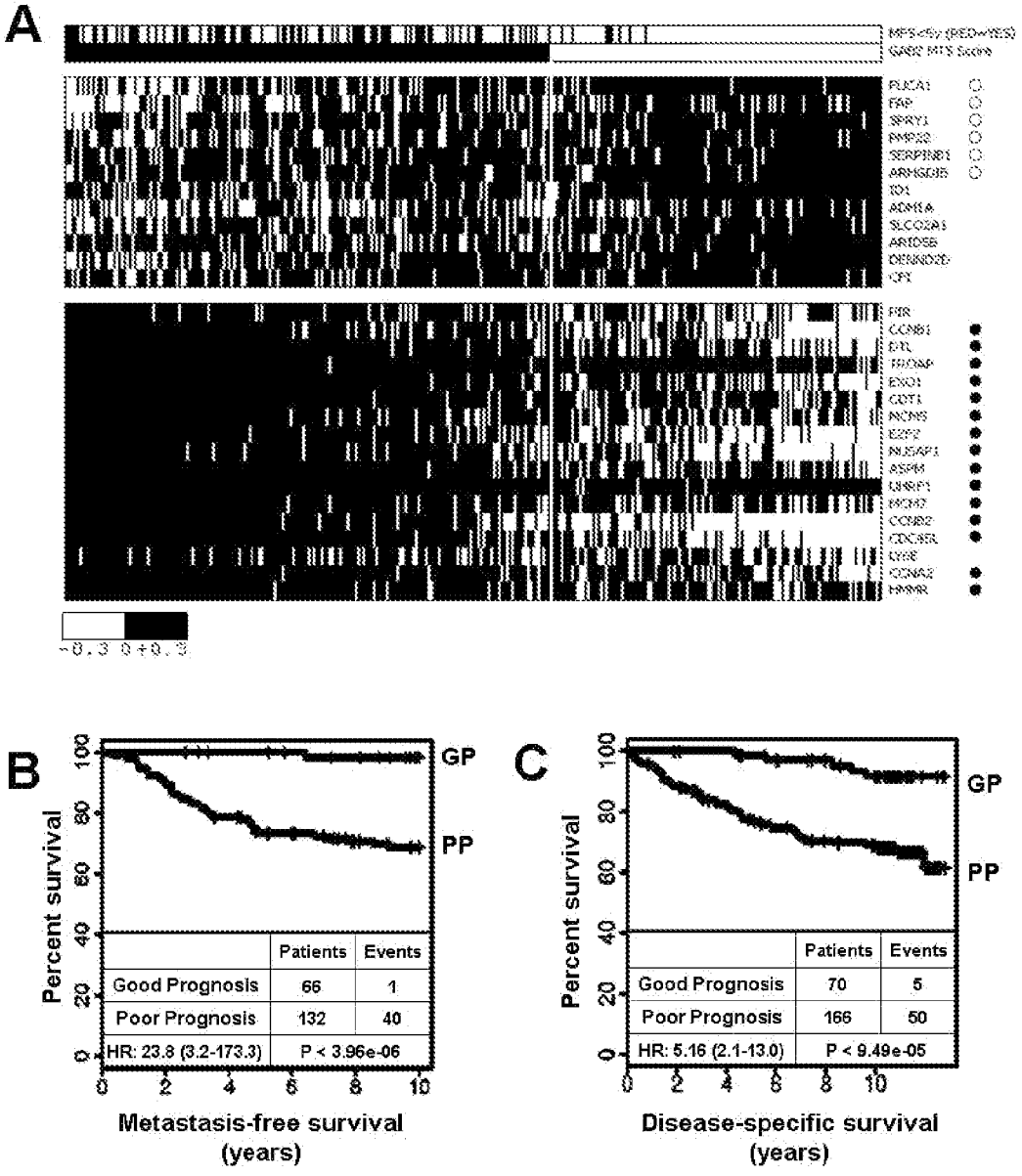
A
B
Percent survival
GP
PP
Patients
Events
Good Prognosis
66
1
Poor Prognosis
132
40
HR: 23.8 (3.2-173.3)
P < 3.96e-06
Metastasis-free survival
(years)
C
Percent survival
GP
PP
Patients
Events
Good Prognosis
70
5
Poor Prognosis
166
50
HR: 5.16 (2.1-13.0)
P < 9.49e-05
Disease-specific survival
(years)

# FIGURE VII/IX

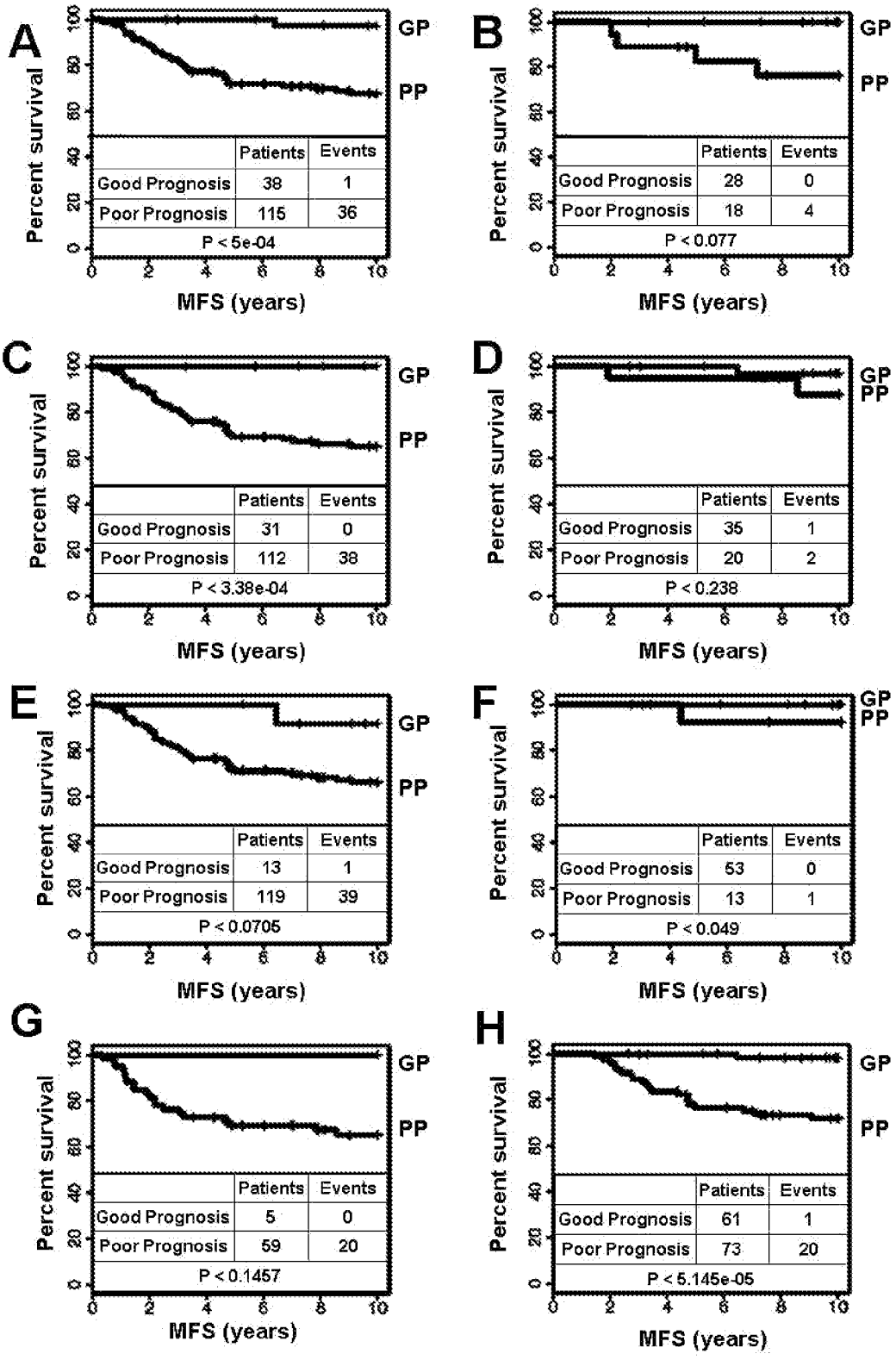

**FIGURE VIII/IX**

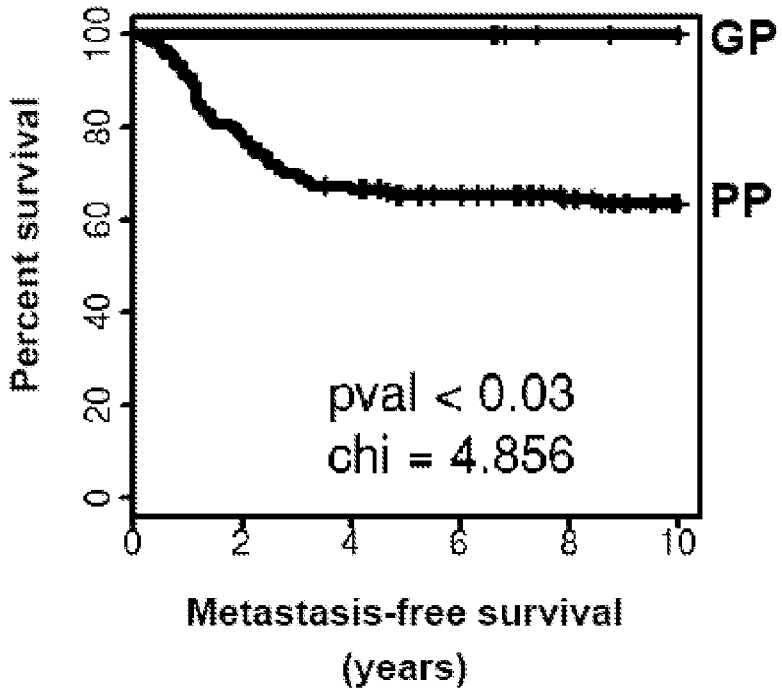

# FIGURE IX/IX

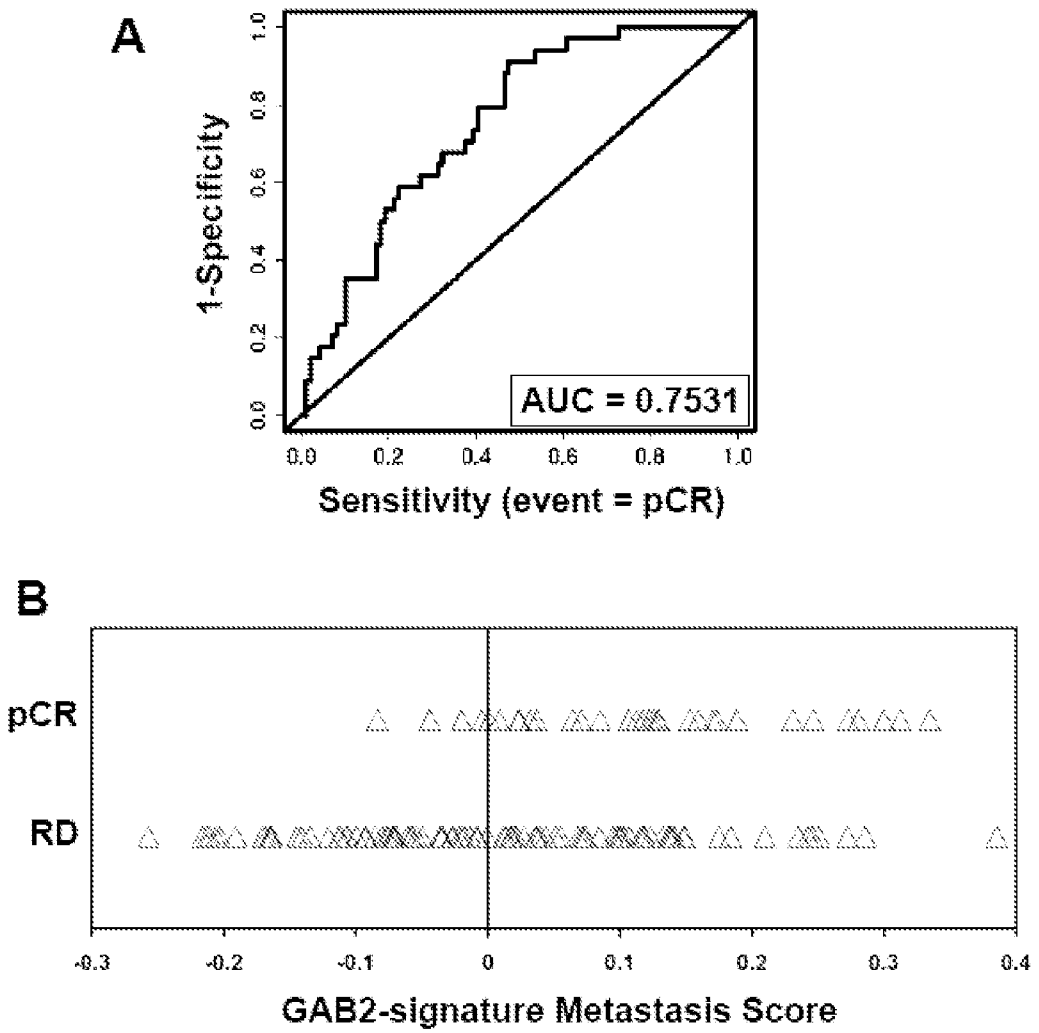
A
1-Specificity
0.0
0.2
0.4
0.6
0.8
1.0
AUC = 0.7531
Sensitivity (event = pCR)
B
pCR
RD
-0.3
-0.2
-0.1
0
0.1
0.2
0.3
0.4
GAB2-signature Metastasis Score